

JOURNAL OF

CHROMATOGRAPHY A

INCLUDING ELECTROPHORESIS AND OTHER SEPARATION METHODS

EDITORS

U.A.Th. Brinkman (Amsterdam)

R.W. Giese (Boston, MA)

J.K. Haken (Kensington, N.S.W.)

L.R. Snyder (Orinda, CA)

EDITORS, SYMPOSIUM VOLUMES.

E. Heftmann (Orinda, CA), Z. Deyl (Prague)

EDITORIAL BOARD

D.W. Armstrong (Rolla, MO)

W.A. Aue (Halifax)

P. Bocek (Brno)

A.A. Boulton (Saskatoon)

P.W. Carr (Minneapolis, MN)

N.H.C. Cooke (San Ramon, CA)

V.A. Davankov (Moscow)

G.J. de Jong (Weesp)

Z. Deyl (Prague)

S. Dilli (Kensington, N.S.W.)

Z. El Rassi (Stillwater, OK)

H. Engelhardt (Saarbrücken)

F. Erni (Basle)

M.B. Evans (Hatfield)

J.L. Glajch (N. Billerica, MA)

G.A. Guiochon (Knoxville, TN)

P.R. Haddad (Hobart, Tasmania)

I.M. Hais (Hradec Králové)

W.S. Hancock (Palo Alto, CA)

S. Hjerten (Uppsala)

S. Honda (Higashi-Osaka)

Cs. Horváth (New Haven, CT)

J.F.K. Huber (Vienna)

K.-P. Hupe (Waldbrunn)

J. Janák (Brno)

P. Jandera (Pardubice)

B.L. Karger (Boston, MA)

J.J. Kirkland (Newport, DE)

E. sz. Kováts (Lausanne)

K. Macek (Prague)

A.J.P. Martin (Cambridge)

L.W. McLaughlin (Chestnut Hill, MA)

E.D. Morgan (Keele)

J.D. Pearson (Kalamazoo, MI)

H. Poppe (Amsterdam)

F.E. Regnier (West Lafayette, IN)

P.G. Righetti (Milan)

P. Schoenmakers (Amsterdam)

R. Schwarzenbach (Dübendorf)

R.E. Shoup (West Lafayette, IN)

R.P. Singhal (Wichita, KS)

A.M. Siouffi (Marseille)

D.J. Strydom (Boston, MA)

N. Tanaka (Kyoto)

S. Terabe (Hyogo)

K.K. Unger (Mainz)

R. Verpoorte (Leiden)

Gy. Vigh (College Station, TX)

J.T. Watson (East Lansing, MI)

B.D. Westerlund (Uppsala)

EDITORS, BIBLIOGRAPHY SECTION

Z. Deyl (Prague), J. Janák (Brno), V. Schwarz (Prague)

ELSEVIER

JOURNAL OF CHROMATOGRAPHY A

INCLUDING ELECTROPHORESIS AND OTHER SEPARATION METHODS

Scope. The *Journal of Chromatography A* publishes papers on all aspects of **chromatography, electrophoresis** and related methods. Contributions consist mainly of research papers dealing with chromatographic theory, instrumental developments and their applications. In the *Symposium volumes*, which are under separate editorship, proceedings of symposia on chromatography, electrophoresis and related methods are published. *Journal of Chromatography B: Biomedical Applications*—This journal, which is under separate editorship, deals with the following aspects: developments in and applications of chromatographic and electrophoretic techniques related to clinical diagnosis or alterations during medical treatment; screening and profiling of body fluids or tissues related to the analysis of active substances and to metabolic disorders; drug level monitoring and pharmacokinetic studies; clinical toxicology; forensic medicine; veterinary medicine; occupational medicine; results from basic medical research with direct consequences in clinical practice.

Submission of Papers. The preferred medium of submission is on disk with accompanying manuscript (see *Electronic manuscripts* in the Instructions to Authors, which can be obtained from the publisher, Elsevier Science B.V., P.O. Box 330, 1000 AH Amsterdam, Netherlands). Manuscripts (in English; *four* copies are required) should be submitted to: Editorial Office of *Journal of Chromatography A*, P.O. Box 681, 1000 AR Amsterdam, Netherlands, Telefax (+31-20) 5862 304, or to: The Editor of *Journal of Chromatography B: Biomedical Applications*, P.O. Box 681, 1000 AR Amsterdam, Netherlands. Review articles are invited or proposed in writing to the Editors who welcome suggestions for subjects. An outline of the proposed review should first be forwarded to the Editors for preliminary discussion prior to preparation. Submission of an article is understood to imply that the article is original and unpublished and is not being considered for publication elsewhere. For copyright regulations, see below.

Publication information. *Journal of Chromatography A* (ISSN 0021-9673): for 1994 Vols. 652–682 are scheduled for publication. *Journal of Chromatography B: Biomedical Applications* (ISSN 0378-4347): for 1994 Vols. 652–662 are scheduled for publication. Subscription prices for *Journal of Chromatography A*, *Journal of Chromatography B: Biomedical Applications* or a combined subscription are available upon request from the publisher. Subscriptions are accepted on a prepaid basis only and are entered on a calendar year basis. Issues are sent by surface mail except to the following countries where air delivery via SAL is ensured: Argentina, Australia, Brazil, Canada, China, Hong Kong, India, Israel, Japan, Malaysia, Mexico, New Zealand, Pakistan, Singapore, South Africa, South Korea, Taiwan, Thailand, USA. For all other countries airmail rates are available upon request. Claims for missing issues must be made within six months of our publication (mailing) date. Please address all your requests regarding orders and subscription queries to: Elsevier Science B.V., Journal Department, P.O. Box 211, 1000 AE Amsterdam, Netherlands. Tel.: (+31-20) 5803 642; Fax: (+31-20) 5803 598. Customers in the USA and Canada wishing information on this and other Elsevier journals, please contact Journal Information Center, Elsevier Science Inc., 655 Avenue of the Americas, New York, NY 10010, USA, Tel. (+1-212) 633 3750, Telefax (+1-212) 633 3764.

Abstracts/Contents Lists published in Analytical Abstracts, Biochemical Abstracts, Biological Abstracts, Chemical Abstracts, Chemical Titles, Chromatography Abstracts, Current Awareness in Biological Sciences (CABS), Current Contents/Life Sciences, Current Contents/Physical, Chemical & Earth Sciences, Deep-Sea Research/Part B: Oceanographic Literature Review, Excerpta Medica, Index Medicus, Mass Spectrometry Bulletin, PASCAL-CNRS, Referativnyi Zhurnal, Research Alert and Science Citation Index.

US Mailing Notice. *Journal of Chromatography A* (ISSN 0021-9673) is published weekly (total 52 issues) by Elsevier Science B.V., (Sara Burgerhartstraat 25, P.O. Box 211, 1000 AE Amsterdam, Netherlands). Annual subscription price in the USA US\$ 4994.00 (US\$ price valid in North, Central and South America only) including air speed delivery. Second class postage paid at Jamaica, NY 11431. **USA POSTMASTERS:** Send address changes to *Journal of Chromatography A*, Publications Expediting, Inc., 200 Meacham Avenue, Elmont, NY 11003. Airfreight and mailing in the USA by Publications Expediting.

See inside back cover for Publication Schedule, Information for Authors and information on Advertisements.

© 1994 ELSEVIER SCIENCE B.V. All rights reserved.

0021-9673/94/\$07.00

No part of this publication may be reproduced, stored in a retrieval system or transmitted in any form or by any means, electronic, mechanical, photocopying, recording or otherwise, without the prior written permission of the publisher, Elsevier Science B.V., Copyright and Permissions Department, P.O. Box 521, 1000 AM Amsterdam, Netherlands.

Upon acceptance of an article by the journal, the author(s) will be asked to transfer copyright of the article to the publisher. The transfer will ensure the widest possible dissemination of information.

Special regulations for readers in the USA – This journal has been registered with the Copyright Clearance Center, Inc. Consent is given for copying of articles for personal or internal use, or for the personal use of specific clients. This consent is given on the condition that the copier pays through the Center the per-copy fee stated in the code on the first page of each article for copying beyond that permitted by Sections 107 or 108 of the US Copyright Law. The appropriate fee should be forwarded with a copy of the first page of the article to the Copyright Clearance Center, Inc., 27 Congress Street, Salem, MA 01970, USA. If no code appears in an article, the author has not given broad consent to copy and permission to copy must be obtained directly from the author. The fee indicated on the first page of an article in this issue will apply retroactively to all articles published in the journal, regardless of the year of publication. This consent does not extend to other kinds of copying, such as for general distribution, resale, advertising and promotion purposes, or for creating new collective works. Special written permission must be obtained from the publisher for such copying.

No responsibility is assumed by the Publisher for any injury and/or damage to persons or property as a matter of products liability, negligence or otherwise, or from any use or operation of any methods, products, instructions or ideas contained in the materials herein. Because of rapid advances in the medical sciences, the Publisher recommends that independent verification of diagnoses and drug dosages should be made.

Although all advertising material is expected to conform to ethical (medical) standards, inclusion in this publication does not constitute a guarantee or endorsement of the quality or value of such product or of the claims made of it by its manufacturer.

Ⓢ The paper used in this publication meets the requirements of ANSI/NISO Z39.48-1992 (Permanence of Paper).

Printed in the Netherlands

CONTENTS

(Abstracts/Contents Lists published in *Analytical Abstracts*, *Biochemical Abstracts*, *Biological Abstracts*, *Chemical Abstracts*, *Chemical Titles*, *Chromatography Abstracts*, *Current Awareness in Biological Sciences (CABS)*, *Current Contents/Life Sciences*, *Current Contents/Physical, Chemical & Earth Sciences*, *Deep-Sea Research/Part B: Oceanographic Literature Review*, *Excerpta Medica*, *Index Medicus*, *Mass Spectrometry Bulletin*, *PASCAL-CNRS*, *Referativnyi Zhurnal*, *Research Alert* and *Science Citation Index*)

REGULAR PAPERS

Column Liquid Chromatography

- Limitation of the ET(30) solvent strength scale in reversed-phase liquid chromatography
by J.H. Park, A.J. Dallas, P. Chau and P.W. Carr (Minneapolis, MN, USA) (Received 6 April 1994) 1
- 3,5-Dimethylphenylcarbamates of cellulose and amylose regioselectively bonded to silica gel as chiral stationary phases for high-performance liquid chromatography
by E. Yashima, H. Fukaya and Y. Okamoto (Nagoya, Japan) (Received 22 February 1994) 11
- Characterization of synthetic resins by gel permeation chromatography with a multi-angle laser light scattering detector
by Š. Podzimek (Düsseldorf, Germany) (Received 5 April 1994) 21
- Qualitative and quantitative reversed-phase high-performance liquid chromatography of flavonoids in *Crataegus* leaves and flowers
by A. Rehwald (Zürich, Switzerland), B. Meier (Romanshorn, Switzerland) and O. Sticher (Zürich, Switzerland) (Received 5 April 1994) 25
- Highly sensitive high-performance liquid chromatographic method for the determination of the absolute configuration and the optical purity of di-O-acylglycerols using a chiral derivatizing agent, (*S*)-(+)-2-*tert*-butyl-2-methyl-1,3-benzodioxole-4-carboxylic acid
by J.-H. Kim, H. Uzawa, Y. Nishida, H. Ohruai and H. Meguro (Sendai, Japan) (Received 19 April 1994) 35
- Novel DNA-Sepharose purification of the FadR transcription factor
by C. DiRusso, R.P. Rogers and H.W. Jarrett (Memphis, TN, USA) (Received 14 February 1994) 45
- High-performance liquid chromatography in stability studies of an organophosphorus insecticide in free form and after formulation as emulsifiable concentrate. Response surface design correlation of kinetic data and parameters
by Y.L. Loukas, E. Antoniadou-Vyza and A. Papadaki-Valiraki (Athens, Greece) (Received 15 February 1994) 53
- Determination of phenoxyalkanoic acids and other acidic herbicides at the low ppt level in water applying solid-phase extraction with RP-C₁₈ material
by S. Butz, Th. Heberer and H.-J. Stan (Berlin, Germany) (Received 1 March 1994) 63
- Reversed-phase high-performance liquid chromatographic method using a pentafluorophenyl bonded phase for analysis of tocopherols
by S.L. Richeimer, M.C. Kent and M.W. Bernart (Boulder, CO, USA) (Received 19 April 1994) 75
- Simultaneous high-performance liquid chromatographic determination of residual sulphamonomethoxine, sulphadimethoxine and their N⁴-acetyl metabolites in foods of animal origin
by N. Furusawa and T. Mukai (Towada, Japan) (Received 27 April 1994) 81
- High-performance liquid chromatographic stability-indicating determination of zopiclone in tablets
by J.P. Bounine, B. Tardif, P. Beltran and D.J. Mazzo (Antony, France) (Received 7 March 1994) 87
- Gas Chromatography*
- Theoretical calculation of gas hold-up time in capillary gas chromatography. Influence of column, instrument parameters and analysis conditions and comparison of different methods of dead time determination
by G. Castello, S. Vezzani and P. Moretti (Genova, Italy) (Received 15 March 1994) 95

Contents (continued)

- Gas chromatographic-mass spectrometric determination of nitro polycyclic aromatic hydrocarbons in airborne particulate matter from workplace atmospheres contaminated with diesel exhaust
by P.T.J. Scheepers, D.D. Velders, M.H.J. Martens, J. Noordhoek and R.P. Bos (Nijmegen, Netherlands) (Received 14 April 1994) 107
- Automated in situ gas chromatographic-mass spectrometric analysis of ppt level volatile organic trace gases using multistage solid-adsorbent trapping
by D. Helmig and J.P. Greenberg (Boulder, CO, USA) (Received 28 March 1994) 123
- Gas chromatographic separation of the enantiomers of volatile fluoroether anesthetics by derivatized cyclodextrins. III. Preparative-scale separations for enflurane
by D.U. Staerk, A. Shitangkoon and G. Vigh (College Station, TX, USA) (Received 12 April 1994) 133

Supercritical Fluid Chromatography

- Large-volume injection in packed-capillary supercritical fluid chromatography
by B.N. Zegers, H.-J. de Geus, S.H.J. Wildenburg, H. Lingeman and U.A.Th. Brinkman (Amsterdam, Netherlands) (Received 11 January 1994) 141

Electrophoresis

- In-line isotachophoretic focusing of very large injection volumes for capillary zone electrophoresis using a hydrodynamic counterflow
by M. Mazereeuw, U.R. Tjaden and J. van der Greef (Leiden, Netherlands) (Received 29 March 1994) 151
- Influence of sample injection time of ions on migration time in capillary zone electrophoresis
by H.-W. Zhang, X.-G. Chen and Z.-D. Hu (Gansu, China) (Received 16 March 1994) 159
- Polymerase chain reaction heteroduplex polymorphism analysis by entangled solution capillary electrophoresis
by J. Cheng, T. Kasuga, K.R. Mitchelson and E.R.T. Lightly (Aberdeen, UK), N.D. Watson (Glasgow, UK) and W.J. Martin and D. Atkinson (Aberdeen, UK) (Received 5 April 1994) 169
- Determination of sorbic acid in food products by capillary zone electrophoresis in a hydrodynamically closed separation compartment
by D. Kaniansky, M. Masár, V. Madajová and J. Marák (Bratislava, Slovak Republic) (Received 25 February 1994) 179

SHORT COMMUNICATIONS

Column Liquid Chromatography

- High-performance liquid chromatography of *cis-trans* isomers of proline-containing dipeptides. III. Comparative studies with different stationary phases
by A. Wutte and G. Gübitz (Graz, Austria) and S. Friebe and G.-J. Krauss (Halle, Austria) (Received 19 April 1994) 186

Column Liquid Chromatography and Gas Chromatography

- Separation of selenium analogues of sulphur-containing amino acids by high-performance liquid chromatography and high-resolution gas chromatography
by J. Janák (Brno, Czech Republic), H.A.H. Billiet, J. Frank and K.Ch.A.M. Luyben (Delft, Netherlands) and P. Hušek (Prague, Czech Republic) (Received 25 April 1994) 192

Gas Chromatography

- Highly selective liquid crystalline polysiloxane stationary phase for gas chromatographic separation of isomers
by G. Kraus and J.M. Thierfelder (Halle Saale, Germany) and L. Soják (Bratislava, Slovak Republic) (Received 22 March 1994) 197
- Analysis of the petroleum components benzene, toluene, ethyl benzene and the xylenes in water by commercially available solid-phase microextraction and carbon-layer open tubular capillary column gas chromatography
by L.P. Sarna, G.R.B. Webster, M.R. Friesen-Fischer and R. Sri Ranjan (Winnipeg, Canada) (Received 8 March 1994) 201

BOOK REVIEWS

Manual of Pesticide Residue Analysis (edited by H.-P. Thier and J. Kirchhoff), reviewed by K. Fodor-Csorba (Budapest, Hungary) 206

Applications of Supercritical Fluids in Industrial Analysis (edited by J.R. Dean), reviewed by M.E.P. McNally (Wilmington, DE, USA) 208

Announcement of a Special Issue on Chromatographic and Electrophoretic Analyses of Carbohydrates 209

JOURNAL OF CHROMATOGRAPHY A

VOL. 677 (1994)

JOURNAL OF CHROMATOGRAPHY A

INCLUDING ELECTROPHORESIS AND OTHER SEPARATION METHODS

EDITORS

U.A.Th. BRINKMAN (Amsterdam), R.W. GIESE (Boston, MA), J.K. HAKEN (Kensington, N.S.W.),
L.R. SNYDER (Orinda, CA)

EDITORS, SYMPOSIUM VOLUMES

E. HEFTMANN (Orinda, CA), Z. DEYL (Prague)

EDITORIAL BOARD

D.W. Armstrong (Rolla, MO), W.A. Aue (Halifax), P. Boček (Brno), A.A. Boulton (Saskatoon), P.W. Carr (Minneapolis, MN), N.H.C. Cooke (San Ramon, CA), V.A. Davankov (Moscow), G.J. de Jong (Weesp), Z. Deyl (Prague), S. Dilli (Kensington, N.S.W.), Z. El Rassi (Stillwater, OK), H. Engelhardt (Saarbrücken), F. Erni (Basle), M.B. Evans (Hatfield), J.L. Glajch (N. Billerica, MA), G.A. Guiochon (Knoxville, TN), P.R. Haddad (Hobart, Tasmania), I.M. Hais (Hradec Králové), W.S. Hancock (Palo Alto, CA), S. Hjertén (Uppsala), S. Honda (Higashi-Osaka), Cs. Horváth (New Haven, CT), J.F.K. Huber (Vienna), K.-P. Hupe (Waldbronn), J. Janák (Brno), P. Jandera (Pardubice), B.L. Karger (Boston, MA), J.J. Kirkland (Newport, DE), E. sz. Kováts (Lausanne), K. Macek (Prague), A.J.P. Martin (Cambridge), L.W. McLaughlin (Chestnut Hill, MA), E.D. Morgan (Keele), J.D. Pearson (Kalamazoo, MI), H. Poppe (Amsterdam), F.E. Regnier (West Lafayette, IN), P.G. Righetti (Milan), P. Schoenmakers (Amsterdam), R. Schwarzenbach (Dübendorf), R.E. Shoup (West Lafayette, IN), R.P. Singhal (Wichita, KS), A.M. Siouffi (Marseille), D.J. Strydom (Boston, MA), N. Tanaka (Kyoto), S. Terabe (Hyogo), K.K. Unger (Mainz), R. Verpoorte (Leiden), Gy. Vigh (College Station, TX), J.T. Watson (East Lansing, MI), B.D. Westerlund (Uppsala)

EDITORS, BIBLIOGRAPHY SECTION

Z. Deyl (Prague), J. Janák (Brno), V. Schwarz (Prague)



ELSEVIER

Amsterdam – Lausanne – New York – Oxford – Shannon – Tokyo

J. Chromatogr. A, Vol. 677 (1994)

ห้องสมุดกรมวิทยาศาสตร์บริการ

© 1994 ELSEVIER SCIENCE B.V. All rights reserved.

0021-9673/94/\$07.00

No part of this publication may be reproduced, stored in a retrieval system or transmitted in any form or by any means, electronic, mechanical, photocopying, recording or otherwise, without the prior written permission of the publisher, Elsevier Science B.V., Copyright and Permissions Department, P.O. Box 521, 1000 AM Amsterdam, Netherlands.

Upon acceptance of an article by the journal, the author(s) will be asked to transfer copyright of the article to the publisher. The transfer will ensure the widest possible dissemination of information.

Special regulations for readers in the USA – This journal has been registered with the Copyright Clearance Center, Inc. Consent is given for copying of articles for personal or internal use, or for the personal use of specific clients. This consent is given on the condition that the copier pays through the Center the per-copy fee stated in the code on the first page of each article for copying beyond that permitted by Sections 107 or 108 of the US Copyright Law. The appropriate fee should be forwarded with a copy of the first page of the article to the Copyright Clearance Center, Inc., 27 Congress Street, Salem, MA 01970, USA. If no code appears in an article, the author has not given broad consent to copy and permission to copy must be obtained directly from the author. The fee indicated on the first page of an article in this issue will apply retroactively to all articles published in the journal, regardless of the year of publication. This consent does not extend to other kinds of copying, such as for general distribution, resale, advertising and promotion purposes, or for creating new collective works. Special written permission must be obtained from the publisher for such copying.

No responsibility is assumed by the Publisher for any injury and/or damage to persons or property as a matter of products liability, negligence or otherwise, or from any use or operation of any methods, products, instructions or ideas contained in the materials herein. Because of rapid advances in the medical sciences, the Publisher recommends that independent verification of diagnoses and drug dosages should be made.

Although all advertising material is expected to conform to ethical (medical) standards, inclusion in this publication does not constitute a guarantee or endorsement of the quality or value of such product or of the claims made of it by its manufacturer.

Ⓢ The paper used in this publication meets the requirements of ANSI/NISO Z39.48-1992 (Permanence of Paper).

Printed in the Netherlands

Limitation of the $E_T(30)$ solvent strength scale in reversed-phase liquid chromatography

Jung Hag Park¹, Andrew J. Dallas², Phoebe Chau, Peter W. Carr*

Department of Chemistry, University of Minnesota, 207 Pleasant Street S.E., Minneapolis, MN 55455, USA

First received 8 February 1994; revised manuscript received 6 April 1994

Abstract

The transition energies (E_T) of the maximum absorption of the solvatochromic indicator denoted ET(33) [2,6-dichloro-4-(2,4,6-triphenyl-N-pyridino)-phenolate] in methanol-, acetonitrile-, isopropanol- and tetrahydrofuran-water mixtures over the full range in composition were measured. Its relationships with those for the closely related indicator ET(30) [2,6-diphenyl-(2,4,6-triphenyl-N-pyridino)-phenolate] were studied. Although the two indicators have very similar structures and hence we expected them to sense via their solvatochromic shifts the same intermolecular interactions exerted by the solvent in a similar way, plots of $E_T(33)$ vs. $E_T(30)$ are definitely non-linear. This and non-linearities in plots of $\ln k'$ vs. $E_T(30)$ and $\ln k'$ vs. $E_T(33)$ obviate the generality of a single-parameter solvent strength scale in RPLC.

1. Introduction

The “polarity” of the mobile phase is a major factor that influences solute retention in reversed-phase liquid chromatography (RPLC). For non-polar solutes retention in RPLC monotonically increases as the “polarity” of the mobile phase is increased upon addition of water. Many empirical scales of overall solvent strength and polarity have been proposed. These are typically based on either the effect of solvent on the rate of a chemical reaction or more commonly its influence on some spectroscopic property of a *single* indicator [1–10]. All the above-cited scales

have been proposed as single-parameter overall scales of solvent strength. In contrast, the Kamlet–Taft multi-parameter π^* , α and β solvent scales [11–13] although highly empirical are based on the differential evaluation of solvent dipolarity/polarizability (π^*), solvent hydrogen bond (HB) donating acidity (α), and solvent HB accepting basicity (β). Although empirical the Kamlet–Taft scales have the advantage of being fundamentally interpretable. That is, π^* is decoupled from solvent hydrogen bonding processes and similarly solvent α and β are not related to solvent dipolarity. The $E_T(30)$ scale [14–16] and Kamlet–Taft multi-parameter scales [17–20] have both been used to study retention in RPLC. $E_T(30)$ has been used to correlate the effect of mobile phase composition on solute retention in RPLC [14–16]. Extrapolation of $\ln k'$ vs. $E_T(30)$ to 100% water has been proposed

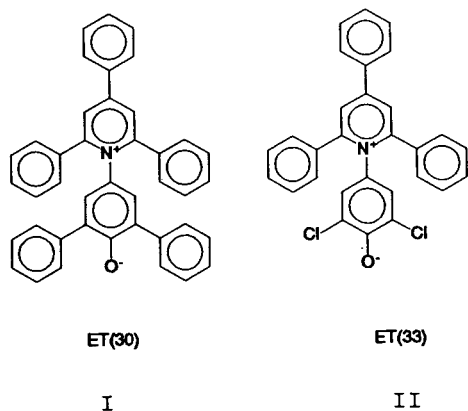
* Corresponding author.

¹ On leave from Yeungnam University, Department of Chemistry, Kyongsan 712-749, South Korea.

² Present address: Donaldson Co., Inc., 9250 W. Bloomington Freeway, Bloomington, MN 55431, USA.

as the basis of a universal method for estimating $\ln k'_w$, the capacity factor using pure water as the eluent, for use in correlating octanol–water partition coefficients [21,22]. $E_T(30)$ measurements in mixed aqueous–organic media have been used to study the effect of media on organic reactions [23,24].

Comparison of structures I and II below shows that ET(33), 2,6-dichloro-4-(2,4,6-triphenyl-N-pyridino)-phenolate [25], has the same structure as ET(30), 2,6-diphenyl-(2,4,6-triphenyl-N-pyridino)-phenolate, except that the two phenyl groups at the 2,6-positions on the phenoxide ring are replaced by two chlorine atoms, which makes the pK_a of ET(33) (4.38) lower than that of ET(30) (8.65) [25].



In addition the absorption maximum of ET(33) occurs at a shorter wavelength than ET(30) [25]. Since the structure of ET(33) is so very similar to that of ET(30) it should sense via its solvatochromic shift the same intermolecular interactions exerted by the solvent as does ET(30). Given this we expect that the transition energies (the so-called E_T value) of the maximum absorption for ET(33) should be linearly related to those for ET(30) in aqueous organic mixtures. In this work we measured the E_T values of the indicator ET(33) in methanol-, acetonitrile-, isopropanol- and tetrahydrofuran–water mixtures over the full composition range, and then examined the relationships between E_T values of ET(33) and ET(30) and relationships between RPLC $\ln k'$ and both $E_T(30)$ and $E_T(33)$ in these mixtures.

We observed that plots of $E_T(33)$ vs. $E_T(30)$ for the above four mixtures are non-linear and that plots of $\ln k'$ vs. $E_T(33)$ and vs. $E_T(30)$ are also non-linear when the full range of water–organic composition is considered.

The initial motivation for the present study was our concern that the greater pH sensitivity of the ET(30) dye in comparison to the analogous dichloro dye [ET(33)] could be the source of some experimental difficulties. Previously we noted [26] that a measurement of the hydrogen bond donor acidity of methanol–water mixtures based on $E_T(30)$ showed a minimum at intermediate compositions. This behavior was not observed with other hydro–organic mixtures [26] nor with a chemically distinct indicator [27]. Thus we felt that it might be due to a peculiar property of this indicator perhaps due to protonation of the phenoxide. Note that the chloro substituents weaken the Bronsted basicity of the phenoxide in ET(33) relative to that of the phenoxide in ET(30). Chloro groups are electron withdrawing whereas phenyl groups are electron donating thus the phenoxide group of ET(33) is a weaker Bronsted base than is the phenoxide group of ET(30). In the course of this work we discovered with surprise that plots of $E_T(33)$ vs. $E_T(30)$ are not linear as the mobile phase composition is varied even though both dyes are totally unprotonated under all conditions encountered in this study.

Johnson et al. [14] have shown that plots of $\ln k'$ vs. the mobile phases' $E_T(30)$ parameters are very often more linear than are plots of $\ln k'$ vs. volume fraction of organic modifier. These results were obtained with a large number of solutes, but did not encompass the entire range in mobile phase composition. Recently we have shown [28], based on the linear solvation energy relationship of Kamlet and Taft [13], that there can be no global single-parameter solvent polarity scale for RPLC except when the solute and solvent are incapable of forming hydrogen bonds and, in addition, the energy of cavity formation is either negligible compared to the strength of the solute–solvent interactions or is strictly proportional to the strength of such interactions. When relationships of $\ln k'$ were examined vs.

$E_T(30)$ for extended ranges of solvent composition, plots for such non-polar and non-hydrogen bonding solutes as alkylbenzenes were not linear and were not necessarily better than plots vs. volume fraction of organic modifier. Sometimes $\ln k'$ is more linear with volume fraction of organic modifier than with $E_T(30)$. Linearity in plots of $\ln k'$ vs. $E_T(30)$ was observed over a limited range in composition. We thus concluded that a single-parameter solvent strength scale may provide a set of plotting coordinates that linearizes the data for interpolation or other practical concerns, but one should avoid theoretical interpretation of the meaning of the regression coefficients. However, theoretical interpretation of the regression coefficients for plots of $\ln k'$ vs. $E_T(30)$ and extrapolation of the plot for $\ln k'$ vs. $E_T(30)$ for a limited range of mixture composition to 100% water have been reported [21,22,29]. Thus we felt that it is important to show the limitations of the linearity of $\ln k'$ vs. $E_T(30)$. This was done by examining relationships between RPLC $\ln k'$ values and a different solvent polarity scale based on the chemically similar indicator, ET(33), which is believed to sense via its solvatochromic shift the same intermolecular interactions exerted by the solvent in a similar fashion to ET(30).

2. Experimental

All solvents used here were HPLC grade and were used without further purification. The solvent mixtures were prepared by mixing a known volume of each liquid. ET(33) was prepared and purified using a procedure given in the literature [25]. All spectroscopic measurements were made using a Varian DMS 200 spectrophotometer using a slit width of 0.2 nm, 20 nm/min scan rate, a smoothing constant of 5 s, and 1-cm pathlength quartz cells. The wavelength of the spectrophotometer was calibrated daily using a holmium oxide filter and the stability of the instrument throughout this experiment is indicated by no more than a 0.10 nm change in any of the six holmium oxide peaks monitored. All samples were thermostatted at 25 (± 0.2)°C for

15 min before scans were made and this included the holmium oxide filter. Each of the samples were gently rocked after sitting for 10 min in order to ensure temperature equilibrium throughout the sample. Peak maxima were determined using the “9/10” method in order to minimize the effect of changes in band shape with solvent [30]. Triplicate measurements of peak maxima agreed with one another within less than 0.5 nm. The indicator concentration was adjusted so as to give an absorbance in the range of 0.5 to 0.8 absorbance units. At this concentration it was confirmed that the peak maxima are independent on solute self-association.

3. Results and discussion

3.1. Solvatochromic comparison of $E_T(30)$ and $E_T(33)$

Although the absorption bands of ET(33) are at shorter wavelengths than those of ET(30), it exhibits almost the same shift with solvent in its electronic transition energy as does ET(30) [25]. Since the structure of ET(33) is very similar to ET(30) and thus will sense via its solvatochromic shift the same intermolecular interactions exerted by the solvent in a similar way to that of ET(30), we expected that the absorption energies of ET(33) would differ from those of ET(30) but that they would be *linearly* related as the volume fraction of organic modifier is varied. Plots of $E_T(33)$ vs. $E_T(30)$ for four different water–organic mixtures are shown in Fig. 1. The error bars indicate the random experimental error associated with determination of E_T . These plots are clearly not linear.

There are two potential simple explanations for the lack of linearity in such plots. First, as Kamlet et al. [31] have shown, $E_T(30)$ is actually a composite solvent characteristic. It actually responds to changes in both a solvent's dipolarity/polarizability, that is π^* , and a solvent's hydrogen bond donor strength, α .

$$E_T(30) = 31.00 + 13.43\pi^* + 15.06\alpha$$

$$N = 40, \text{ S.D.} = 1.65, r = 0.984$$

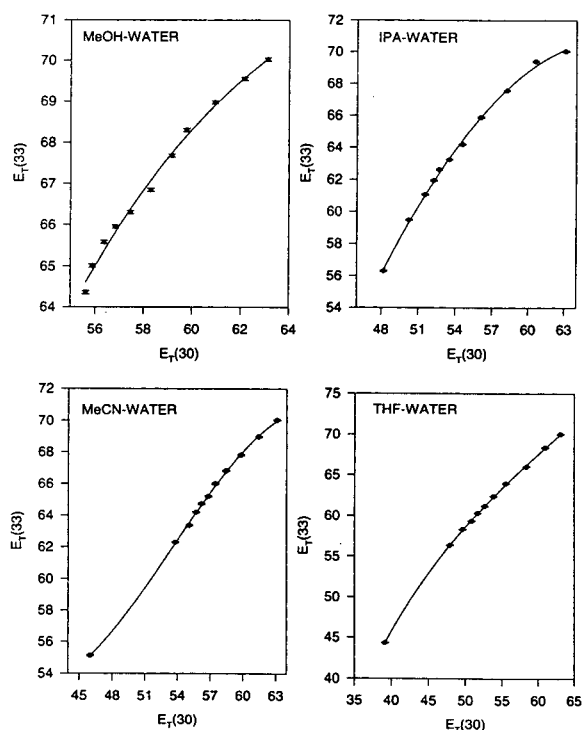


Fig. 1. Plots of $E_T(33)$ vs. $E_T(30)$ for aqueous mixtures of methanol (MeOH), acetonitrile (MeCN), isopropanol (IPA) and tetrahydrofuran (THF).

If ET(33) has a different blend of sensitivities to the solvent π^* and α then it would not respond linearly to plots of $E_T(30)$ vs. $E_T(33)$. In order to establish whether or not this is true we require a great deal of data on ET(33) in a series of pure solvents of known π^* and α . We will report on this elsewhere [32]. However, given the strong electron withdrawing effect of a chloro group it is quite possible that the sensitivities to π^* and α will be different for ET(30) and ET(33). Second, it is quite possible that the cybotactic region around the two dyes and especially at the O^- group could differ. It seems reasonable in view of the fact that a chloro group is a better electron acceptor than is a phenyl group that the relative amount of water in the solvent adjacent to the dye could differ for the two dyes. This results in a different effect on the solvatochromic shift of the two indicators.

In Fig. 2 normalized E_T values for ET(33),

$E_T^N(33)$, are plotted against corresponding $E_T^N(30)$ values for ET(30). The error bars indicate the size of the random experimental error. All the points in the plot lie below the 1:1 line. If solvation of the two dyes by the components in the aqueous mixture were to be the same all the points in the plot should fall on the 1:1 line. We believe that the deviations are probably due to preferential solvation, by which solvatochromic indicators are differentially solvated by one component of the hydro-organic mixtures. Preferential solvation has been widely reported [26,27,33–40]. A second possible explanation for the lack of agreement between the two indicators is microheterogeneity as discussed by Marcus and Migron [41–44]. Microheterogeneity refers to the state of incipient phase separation. That is the two components of the mixture on average prefer molecules of their own type. At this time we tentatively prefer to explain the systematic difference in behavior of the two indicators based on differential solvation. We do so because deviations from the 1:1 line (see Fig. 2) are least for the acetonitrile–water system which is the most non-ideal mixture and greatest for the two alcohol–water systems which are the more ideal mixtures. We will deal with the details of preferential solvation versus microheterogeneity elsewhere. As a consequence the polarity sensed by a single specific indicator in a water–organic mixture can not represent the average polarity which is sensed by various types of solutes.

The above data indicate that the theoretical interpretation of any single-parameter scale of solvent strength of hydro-organic mixtures is complex as is the interpretation of results based on such scales. Nonetheless single-parameter scales of solvent strength such as Snyder's S [48], the $E_T(30)$ scale or the $E_T(33)$ scale are undeniably very useful in practical chromatography.

3.2. Chromatographic comparison of $E_T(30)$ and $E_T(33)$

Table 1 lists the results of linear regressions for correlations between RPLC $\ln k'$ values and $E_T(30)$, $E_T(33)$ and volume fraction of organic

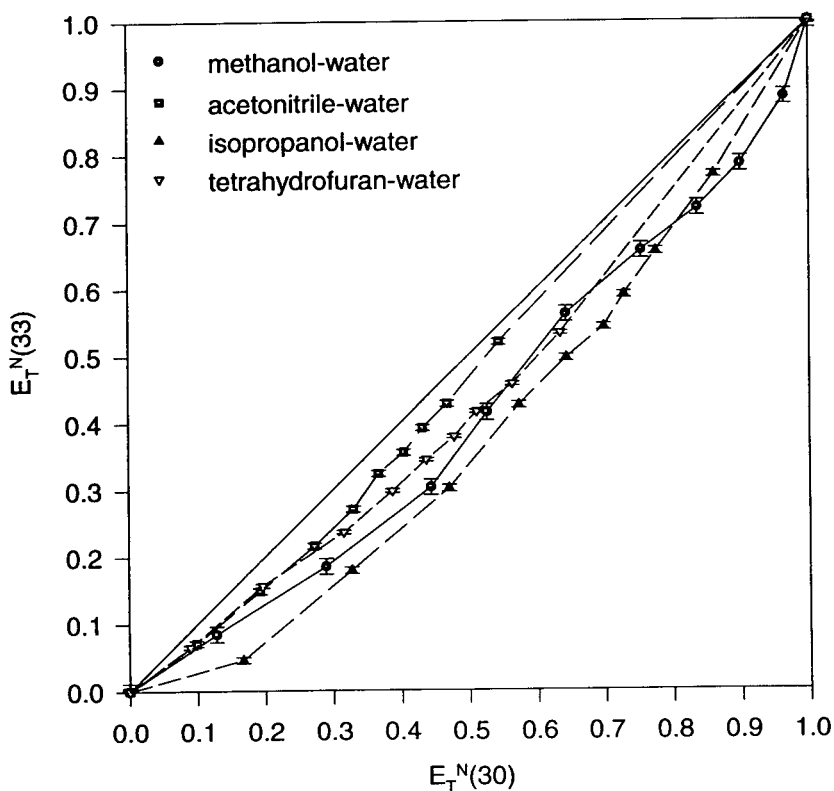


Fig. 2. Plot of $E_T^N(33)$ vs. $E_T^N(30)$ for aqueous mixtures of methanol, acetonitrile, isopropanol and tetrahydrofuran. E_T^N values are computed by the equation: $E_T^N = [E_T(\text{water}) - E_T(\phi_0)]/[E_T(\text{water}) - E_T(\text{pure organic})]$.

modifier (ϕ_0) for a number of solutes for an extended range of water–organic modifier compositions. In methanol–water mixtures correlations for non-polar solutes such as alkyl-benzenes and naphthalene vs. $E_T(33)$ and ϕ_0 are better than those vs. $E_T(30)$. In contrast, for the polar solutes correlations with $E_T(30)$ are better than with $E_T(33)$ and ϕ_0 . A similar trend is observed in acetonitrile–water mixtures. In isopropanol–water and tetrahydrofuran–water mixtures correlations with $E_T(30)$ are almost always better than with $E_T(33)$ and sometimes better than with ϕ_0 . For the 332 $\ln k'$ data set Johnson et al. [14] reported an average r^2 of 0.9910 and average standard deviation of much less than 0.1 for plotting $\log k'$ vs. the mobile phases' $E_T(30)$ parameter, compared to an average r^2 of 0.9783 for plotting vs. volume percent organic modifier. However, their results were obtained with $\ln k'$

data measured in mobile phases over a limited composition range. Only a few of the ranges were 70% and most were less than 50%. As can be seen in Table 1, r^2 values are much lower and standard deviations are much higher when the compositions of the mixtures are extended to the full range.

As expected from the non-linearity of plots of $E_T(33)$ vs. $E_T(30)$ (see Fig. 1) regression results with $E_T(33)$ are different from those with $E_T(30)$. Figs. 3 and 4 show plots of $\ln k'$ for a few selected solutes vs. $E_T(30)$ and $E_T(33)$, respectively. For a limited range in composition linearity is observed but curvature is evident if the entire range of the composition is examined. It can be argued that the curvature at low k' is an artifact due to an error in the void volume, but curvature is also observed in the range of high water content where retention is quite high.

Table 1
Linear regression results for correlation between $\ln k'$ and either volume fraction, $E_T(30)$ or $E_T(33)$

Solute	Solvent/ % range	$E_T(30)$		$E_T(33)$		ϕ_0		n
		r^2	S.D.	r^2	S.D.	r^2	S.D.	
Benzene	MeOH/10-100	0.9737	0.292	0.9927	0.154	0.9998	0.024	10
Toluene		0.9918	0.231	0.9951	0.179	0.9921	0.227	10
Ethylbenzene		0.9847	0.344	0.9955	0.187	0.9970	0.151	10
Naphthalene		0.9649	0.708	0.9893	0.173	0.9998	0.048	10
Anisole		0.9954	0.208	0.9701	0.530	0.9488	0.694	10
Benzophenone		0.9986	0.132	0.9853	0.429	0.9712	0.600	10
Benzonitrile		0.9975	0.088	0.9906	0.171	0.9808	0.244	10
Phenol		0.9963	0.086	0.9925	0.122	0.9847	0.174	10
Benzene	MeCN/10-90	0.9827	0.218	0.9825	0.219	0.9836	0.212	9
Toluene		0.9827	0.257	0.9823	0.260	0.9832	0.253	9
Ethylbenzene		0.9820	0.278	0.9842	0.260	0.9877	0.229	9
Naphthalene		0.9778	0.269	0.9861	0.213	0.9953	0.123	9
Anisole		0.9768	0.263	0.9730	0.284	0.9719	0.289	9
Benzophenone		0.9825	0.298	0.9785	0.331	0.9756	0.352	9
Benzonitrile		0.9822	0.203	0.9773	0.229	0.9735	0.247	9
Phenol		0.9720	0.221	0.9560	0.277	0.9415	0.320	9
Benzene	THF/10-90	0.9860	0.238	0.9857	0.240	0.9728	0.332	9
Toluene		0.9861	0.272	0.9849	0.284	0.9704	0.399	9
Ethylbenzene		0.9855	0.289	0.9870	0.274	0.9778	0.358	9
Naphthalene		0.9855	0.322	0.9814	0.365	0.9609	0.529	9
Anisole		0.9861	0.238	0.9836	0.258	0.9663	0.370	9
Benzophenone		0.9852	0.302	0.9805	0.347	0.9587	0.505	9
Benzonitrile		0.9861	0.190	0.9853	0.195	0.9716	0.272	9
Phenol		0.9861	0.192	0.9850	0.199	0.9704	0.280	9
Benzene	THF/30-90	0.9841	0.076	0.9766	0.093	0.9908	0.058	7
Toluene		0.9835	0.091	0.9755	0.110	0.9872	0.079	7
Ethylbenzene		0.9721	0.131	0.9617	0.153	0.9766	0.120	7
Propylbenzene		0.9692	0.154	0.9587	0.179	0.9720	0.147	7
Butylbenzene	THF/40-90	0.9496	0.169	0.9392	0.185	0.9819	0.101	6
Benzene	IPA/30-100	0.9139	0.171	0.8464	0.229	0.9665	0.107	8
Toluene		0.9216	0.190	0.8550	0.259	0.9657	0.126	8
Ethylbenzene		0.9225	0.214	0.8559	0.292	0.9617	0.150	8
Propylbenzene		0.9213	0.244	0.8537	0.333	0.9568	0.181	8
Butylbenzene		0.9207	0.272	0.8526	0.371	0.9528	0.210	8

Capacity factor data are from refs. [45-47].

It is also observed that the amount of curvature in the correlations varies systematically with the test solutes. Systematic failure for such non-polar and non-hydrogen bonding solutes as alkylben-

zenes and naphthalene is a strong indication that any single-parameter solvent scale should not be used for correlation of RPLC retention data for the full range of composition and subsequent

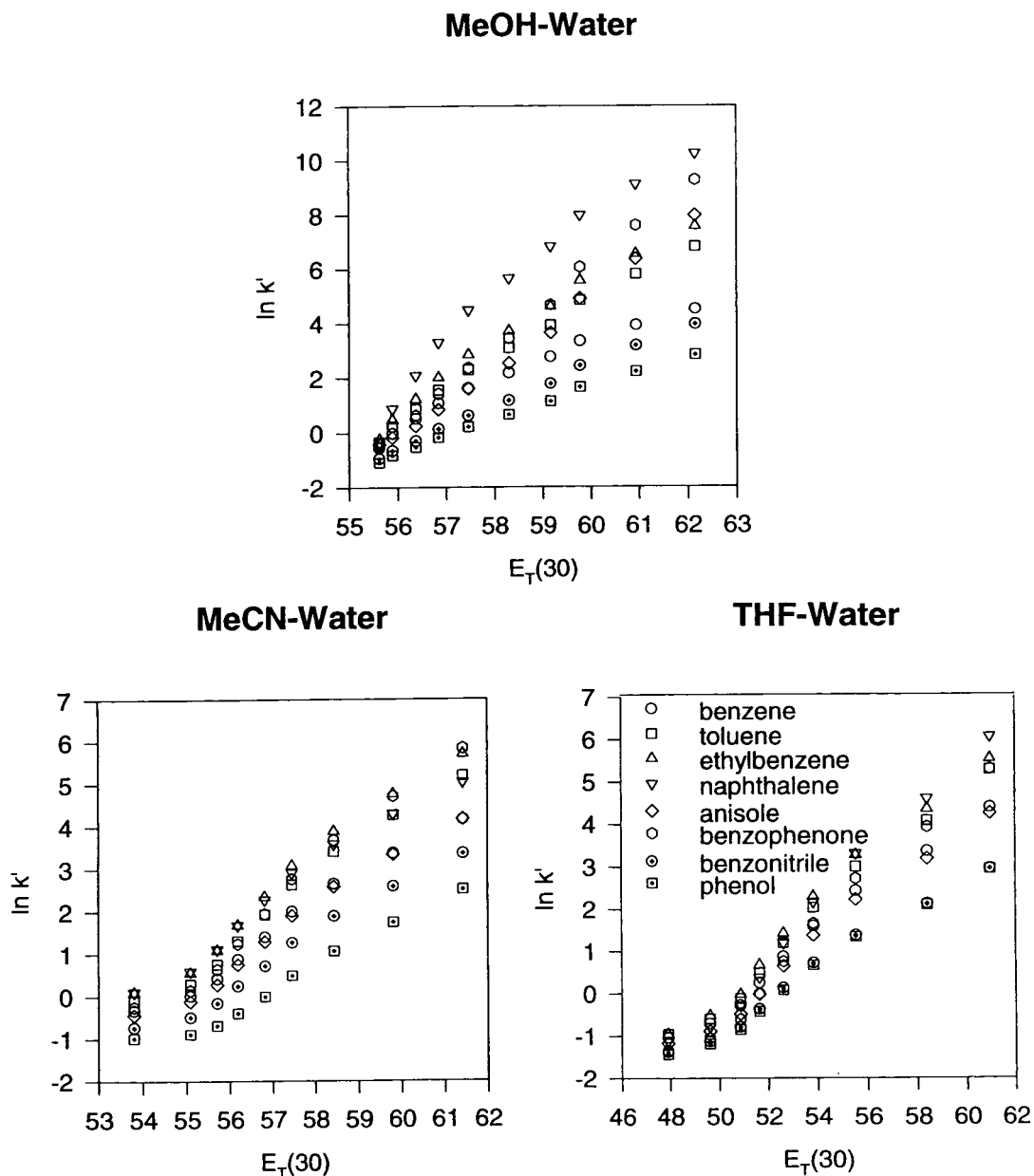


Fig. 3. Plots of logarithmic capacity factor vs. $E_T(30)$ for aqueous mixtures of methanol, acetonitrile and tetrahydrofuran. Symbols are shown in the THF-water plot.

theoretical interpretation of the meaning of the regression coefficients based on those regressions.

Although no specific results are given here we examined the effect of using the $E_T(33)$ scale as a basis for extrapolation to pure water eluent to

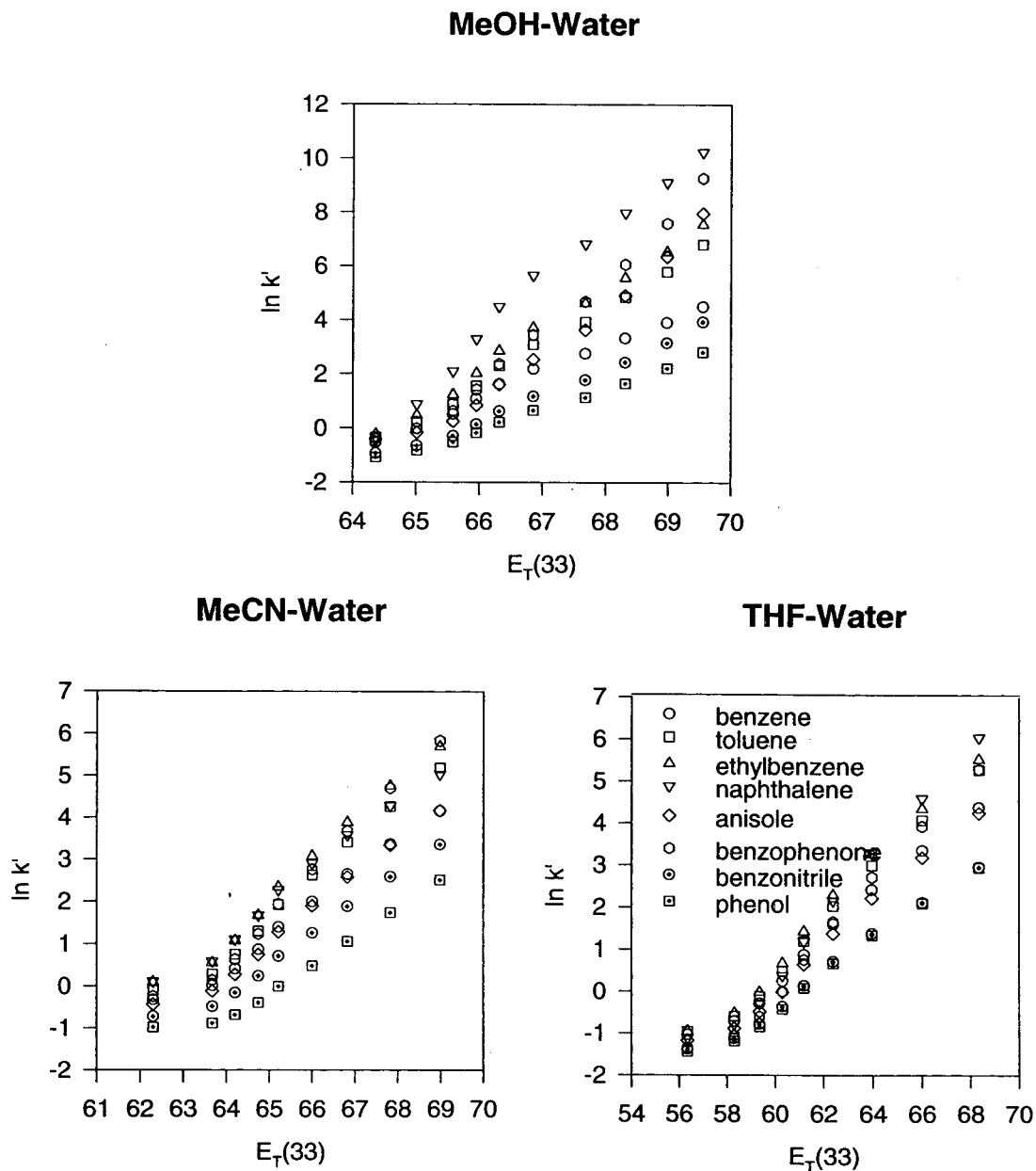


Fig. 4. Plots of logarithmic capacity factor vs. $E_T(33)$ for aqueous mixtures of methanol, acetonitrile and tetrahydrofuran. Symbols are shown in the THF-water plot.

obtain $\log k'_w$ values. As expected in many cases we observed that statistically different $\log k'_w$ values are obtained depending on whether the $E_T(30)$ or $E_T(33)$ scales are used. Thus we again

caution against the use of any single-parameter scale for the elucidation of either thermodynamic or kinetic studies [23,24] in mixed aqueous organic media.

Acknowledgement

This work was supported in part by a grant from the National Science Foundation.

References

- [1] E. Grunwald and S. Winstein, *J. Am. Chem. Soc.*, 70 (1948) 846.
- [2] S. Winstein, E. Grunwald and H.W. Jones, *J. Am. Chem. Soc.*, 73 (1951) 2700.
- [3] A.H. Finberg and S. Winstein, *J. Am. Chem. Soc.*, 78 (1956) 2770.
- [4] M. Gielen and J. Nasielski, *J. Organomet. Chem.*, 1 (1964) 173.
- [5] A. Benson, Z. Hamlet and W.A. Muller, *J. Am. Chem. Soc.*, 84 (1962) 297.
- [6] E.M. Kosower, *J. Am. Chem. Soc.*, 80 (1958) 3253.
- [7] E.M. Kosower, *Molecular Biochemistry*, McGraw-Hill, London, 1962, p. 180.
- [8] S. Brownstein, *Can. J. Chem.*, 38 (1960) 1590.
- [9] K. Dimroth, C. Reichardt, T. Siepmann and F. Bohlmann, *Liebigs Ann. Chem.*, 661 (1963) 1.
- [10] K. Dimroth, C. Reichardt and A. Schweig, *Liebigs Ann. Chem.*, 669 (1963) 95.
- [11] M.J. Kamlet, J.L.M. Abboud and R.W. Taft, *Prog. Phys. Org. Chem.*, 13 (1981) 591.
- [12] M.J. Kamlet, J.L.M. Abboud, M.H. Abraham and R.W. Taft, *J. Org. Chem.*, 48 (1983) 2877.
- [13] M.J. Kamlet and R.W. Taft, *Acta Chem. Scand.*, B39 (1985) 611.
- [14] B.P. Johnson, M.G. Khaledi and J.G. Dorsey, *Anal. Chem.*, 58 (1986) 2354.
- [15] J.G. Dorsey and B.P. Johnson, *J. Liq. Chromatogr.*, 10 (1987) 2695.
- [16] B.P. Johnson, M.G. Khaledi and J.G. Dorsey, *J. Chromatogr.*, 384 (1987) 221.
- [17] P.C. Sadek, P.W. Carr, R.M. Doherty, M.J. Kamlet, R.W. Taft and M.H. Abraham, *Anal. Chem.*, 57 (1985) 2971.
- [18] P.W. Carr, R.M. Doherty, M.J. Kamlet, R.W. Taft, W. Melander and Cs. Horváth, *Anal. Chem.*, 58 (1986) 2674.
- [19] J.H. Park, P.W. Carr, M.H. Abraham, R.W. Taft, R.M. Doherty and M.J. Kamlet, *Chromatographia*, 25 (1988) 373.
- [20] J.H. Park, M.D. Jang and S.T. Kim, *Bull. Korean Chem. Soc.*, 11 (1990) 297.
- [21] J.J. Michels and J.G. Dorsey, *J. Chromatogr.*, 499 (1990) 435.
- [22] P.T. Ying and J.G. Dorsey, *Talanta*, 38 (1991) 237.
- [23] C. Catiuela, J.I. Garcia, J.A. Mayoral, A. Avenoza, J.M. Pregrine and M.A. Roy, *J. Phys. Org. Chem.*, 4 (1991) 48.
- [24] I. Hunt and C.D. Johnson, *J. Chem. Soc., Perkin Trans. 2*, (1991) 1051.
- [25] M.A. Kessler and O.S. Wolfbeis, *Chem. Phys. Lipids*, 50 (1989) 51.
- [26] W.J. Cheong and P.W. Carr, *Anal. Chem.*, 60 (1988) 820.
- [27] J.H. Park, M.D. Jang, D.S. Kim and P.W. Carr, *J. Chromatogr.*, 513 (1990) 107.
- [28] W.J. Cheong and P.W. Carr, *Anal. Chem.*, 61 (1989) 1524.
- [29] M.M. Hsieh and J.G. Dorsey, *J. Chromatogr.*, 631 (1993) 63.
- [30] J.E. Brady and P.W. Carr, *J. Phys. Chem.*, 89 (1985) 1813.
- [31] M.J. Kamlet, J.L.M. Abboud and R.W. Taft, *Prog. Phys. Org. Chem.*, 13 (1983) 485.
- [32] A.J. Dallas, *Ph.D. Thesis*, University of Minnesota, Minneapolis, MN, 1994.
- [33] J.G. Dawber, J. Ward and R.A. Williams, *J. Chem. Soc., Faraday Trans. 1*, 84 (1988) 713.
- [34] J.G. Dawber, *J. Chem. Soc., Faraday Trans.*, 86 (1990) 287.
- [35] M.J. Kamlet, E.G. Kayser, M.E. Jones, J.L.M. Abboud, J.W. Eastes and R.W. Taft, *J. Phys. Chem.*, 82 (1978) 2477.
- [36] K.S. Nitsche and P. Suppan, *Chimia*, 36 (1982) 346.
- [37] C. Lerf and P. Suppan, *J. Chem. Soc., Faraday Trans.*, 84 (1992) 963.
- [38] E. Dutkiewicz, A. Jakubowska and M. Dutkiewicz, *Spectrochim. Acta*, 48A (1992) 1409.
- [39] P. Chatterjee and S. Bagchi, *J. Chem. Soc., Faraday Trans.*, 86 (1990) 1785.
- [40] W.P. Zurawsky and S.F. Scarlata, *J. Phys. Chem.*, 96 (1992) 6012.
- [41] Y. Migron and Y. Marcus, *J. Chem. Soc., Faraday Trans.*, 87 (1991) 1339.
- [42] Y. Marcus and Y. Migron, *J. Phys. Chem.*, 96 (1991) 400.
- [43] Y. Marcus, *J. Chem. Soc., Faraday Trans. 1*, 85 (1988) 381.
- [44] Y. Marcus, *J. Chem. Soc., Faraday Trans.*, 86 (1990) 2215.
- [45] P.J. Schoenmakers, H.A.H. Billiet and L. de Galan, *J. Chromatogr.*, 282 (1983) 107.
- [46] B.N. Barman, *Ph.D. Thesis*, Georgetown University, Washington, DC, 1985.
- [47] W.J. Cheong, *Ph.D. Thesis*, University of Minnesota, Minneapolis, MN, 1989.
- [48] L.R. Snyder, J.W. Dolan and J.R. Gant, *J. Chromatogr.*, 165 (1979) 3.



ELSEVIER

Journal of Chromatography A, 677 (1994) 11-19

JOURNAL OF
CHROMATOGRAPHY A

3,5-Dimethylphenylcarbamates of cellulose and amylose regioselectively bonded to silica gel as chiral stationary phases for high-performance liquid chromatography

Eiji Yashima, Hiroyasu Fukaya, Yoshio Okamoto*

Department of Applied Chemistry, School of Engineering, Nagoya University, Chikusa-ku, Nagoya 464-01, Japan

Received 22 February 1994

Abstract

3,5-Dimethylphenylcarbamates of amylose (ADMPC) (1) and cellulose (CDMPC) (2) chemically bonded to 3-aminopropylsilica gel were prepared with 4,4'-diphenylmethane diisocyanate as a spacer and their optical resolution abilities were evaluated as chiral stationary phases (CSPs) for high-performance liquid chromatography (HPLC). To investigate the influence of the position of the glucose unit in immobilization on chiral recognition, the polysaccharide derivatives were regioselectively bonded to the silica surface. ADMPC regioselectively bonded at the 6-position to silica gel possesses a higher optical resolving power than that bonded at the 2- or 3-position. The chiral recognition ability of the former CSP was almost comparable to that of ADMPC coated on silica gel. For CDMPC, the position of glucose in immobilization on silica gel hardly affected the chiral recognition. The enantioselectivities of these CSPs were also influenced by the amount of the diisocyanate used for immobilization. These chemically bonded-type CSPs were able to be used with eluents such as CHCl_3 in which the polysaccharide derivatives are soluble or swollen. A few racemates which were not or poorly separated on the coated-type CSP were more efficiently resolved on the chemically bonded-type CSP using CHCl_3 as a component of the mobile phase.

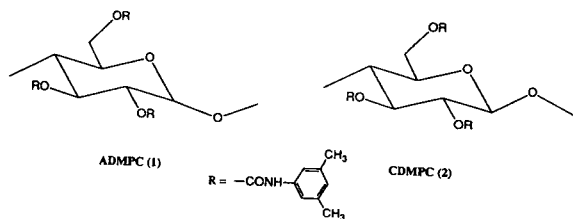
1. Introduction

Cellulose and amylose are the most accessible optically active polymers. These polysaccharides are known to show a chiral recognition which is not high enough for practical use. However, their benzoate [1,2] and phenylcarbamate derivatives [3-9] exhibit a high chiral recognition ability and afford practically useful chiral stationary phases (CSPs) for HPLC. We previously reported that twenty substituted trisphenylcarba-

mate derivatives of cellulose exhibited characteristic optical resolving powers as CSPs for HPLC when they were coated on silica gel [4]. Among them, tris(3,5-dimethylphenylcarbamate) (CDMPC) (2) and tris(3,5-dichlorophenylcarbamate) were the best derivatives with respect to chiral recognition. Of the derivatives of amylose, the tris(3,5-dimethylphenylcarbamate) (ADMPC) (1) was again the most efficient CSP for many racemates [5].

These CSPs have been prepared by coating the polysaccharide phenylcarbamate derivatives on silica gel and the tris(3,5-dimethylphenylcarbam-

* Corresponding author.



ate) phases possess a high durability when a hexane–2-propanol mixture is used as the eluent, whereas for the cellulose tris(3,5-dichlorophenylcarbamate) phase an eluent containing more than 10% of 2-propanol can not be used because of the high solubility. Some solvents such as tetrahydrofuran (THF) and CHCl_3 , in which the polysaccharide derivatives themselves are dissolved or swollen, are unable to be used as eluents. To improve these defects, the derivatives were chemically bonded to 3-aminopropylsilanized silica gel with diisocyanates as a spacer non-regioselectively through the hydroxy groups at the 2-, 3- or 6-position of the glucose units [10]. However, the chiral recognition ability was greatly changed by immobilization, usually showing a lower resolving ability than those of coated-type CSPs.

In this study, we prepared chemically bonded-type CSPs regioselectively linked to amino-propyl-functionalized silica gel with a diisocyanate, and their chiral recognition abilities were evaluated.

2. Experimental

2.1. Chemicals

Racemic solutes were obtained from different sources [11]. Amylose of guaranteed reagent grade was purchased from Nacalai Tesque (Kyoto, Japan) (M_r 16 000) or was a gift from Nakano Vinegar (Handa, Japan) (M_r 11 000). Cellulose (Avicel) was obtained from Merck (Darmstadt, Germany). Triphenylmethyl chloride, 4,4'-diphenylmethane diisocyanate and 3-aminopropyltriethoxysilane were of guaranteed reagent grade from Tokyo Kasei (Tokyo,

Japan). 3,5-Dimethylphenyl isocyanate was prepared from 3,5-dimethylaniline and triphosgene by a conventional method. Porous spherical silica gel with a mean particle size of $7\ \mu\text{m}$ and a mean pore diameter of 100 nm was kindly supplied by Daiso Chemical (Osaka, Japan). All solvents used in the preparation of CSPs were of analytical reagent grade, carefully dried and distilled before use. Solvents used in the chromatographic experiments were of HPLC grade.

2.2. Preparation of CSPs

The CSPs were prepared by the reaction of polysaccharide derivatives and 3-aminopropyl-functionalized silica gel with 4,4'-diphenylmethane diisocyanate. Polysaccharides were regioselectively bonded to silica gel on their glucose units. Fig. 1 shows the immobilization of ADMPC to macroporous silica gel at the 6-position of the glucose unit. Macroporous silica gel was treated with an excess of the silanizing reagent 3-aminopropyltriethoxysilane in dry benzene.

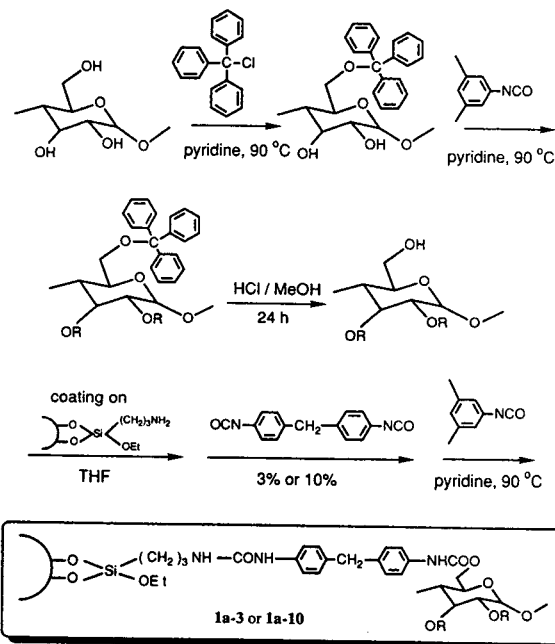


Fig. 1. Regioselective bonding of ADMPC at the 6-position.

Amylose (3.00 g) was allowed to react in pyridine (60 ml) at 80–90°C for 24 h with a large excess triphenylmethyl chloride (10.32 g), which can react only with the primary hydroxy group at the 6-position to form a trityl ether. After confirming the formation of the trityl ether by IR spectrometry, an excess of 3,5-dimethylphenyl isocyanate (9.55 g) was added to form carbamate residues with the hydroxy groups at the 2- and 3-positions. The 2,3-bis(3,5-dimethylphenylcarbamoyl)-6-O-trityl amylose obtained was suspended in a large excess of methanol containing a small amount of hydrochloric acid so as to remove the trityl group at room temperature. The amylose 2,3-bis(3,5-dimethylphenylcarbamate) (0.79 g) thus obtained was dissolved in THF, and the solution was coated on 3-amino-propylsilica gel (3.30 g) as described previously [4]. After THF had been removed *in vacuo*, the amylose derivative on silica gel was dispersed in a mixture of dry toluene (10 ml) containing 4,4'-diphenylmethane diisocyanate (3 or 10 mol-% based on the 6-position hydroxy groups of amylose) and dry pyridine (2 ml), and then the mixture was heated at 90–100°C for 24 h. The CSP (**1a-3** or **1a-10**) thus obtained was collected by filtration and washed with THF to remove free ADMPC derivative. The content of ADMPC derivative bonded to the silica surface was estimated by elemental analysis.

The ADMPC derivative (**1b-3** or **1b-10**) immobilized regioselectively via secondary hydroxy groups at the 2- and 3-positions of the glucose unit was also prepared according to Fig. 2 in order to investigate the influence of the positions of chemical bonding on enantioselectivity. For comparison, ADMPC non-regioselectively bonded to silica gel at the 2-, 3- and 6-positions (**1c-3**) was also synthesized directly from amylose on silica gel according to the previous report [10] for cellulose.

The CDMPC derivatives regioselectively bonded to the silica surface (**2a** and **2b**) were analogously prepared by the procedures for the CSPs of amylose derivatives described above.

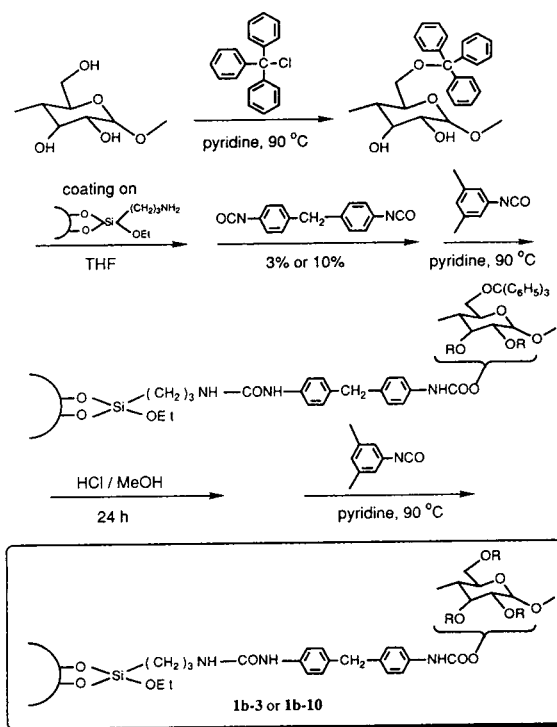


Fig. 2. Regioselective bonding of ADMPC at the 2- and 3-positions.

Regioselectivity in immobilization of amylose and cellulose derivatives is presumed to be more than 90% and 70%, respectively, judging from the results of the regioselective carbamoylation of amylose and cellulose with 3,5-dimethylphenyl and 3,5-dichlorophenyl isocyanates reported previously [12]. A regioselectivity of 90% for the amylose derivative means that, for instance, with **1a**, a chemical bond between amylose and silica gel is formed to the extent of 90% at the 6-position and 10% at the 2- or 3-position.

2.3. Apparatus and chromatography

The carbamoylated amylose and cellulose bonded to silica gel were packed into stainless-steel columns (250 × 4.6 mm I.D.) by the conventional high-pressure slurry-packing procedure [4]. Chromatographic experiments were performed on a Jasco BIP-I chromatograph equipped with a Jasco Model 875 UV detector

(254 nm), a Jasco DIP-181C polarimetric detector (mercury lamp, no filter, flow cell 50×3 mm I.D.) and a Jasco RC-228 recorder at room temperature. Separation was carried out with hexane–2-propanol (90:10) at a flow-rate of 0.5 ml/min. A racemate solution (1–10 μ l) was injected into the chromatographic system with a Rheodyne Model 7125 injector (20- μ l loop). The dead time (t_0) was determined with 1,3,5-tri-*tert.*-butylbenzene as a non-retained compound. Most columns exhibited theoretical plate numbers of 3000–5000 against benzene.

IR spectra were taken on a Jasco IR-810 spectrophotometer as KBr pellets. ^1H NMR spectra were measured with a Varian VXR500 spectrometer (500 MHz) using TMS as an internal standard.

3. Results and discussion

3.1. Preparation of CSPs

Fig. 3 shows the Fourier transform (FT) IR spectrum of ADMPC (**1a–3** in Fig. 1) immobilized at the 6-position on the silica surface with diisocyanate corresponding to 3 mol-% of the

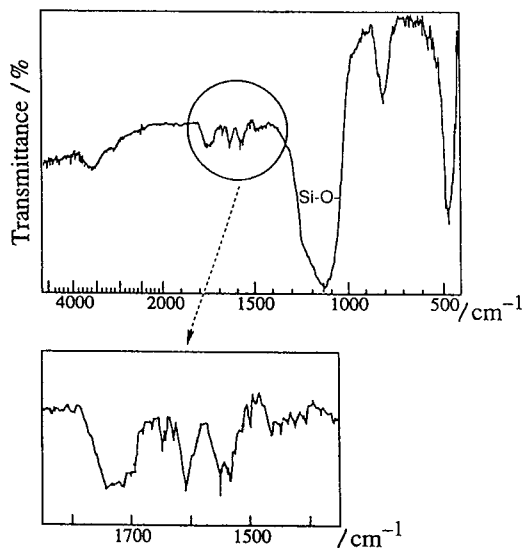


Fig. 3. FT-IR spectrum of ADMPC chemically bonded to silica gel at the 6-position (**1a–3**).

primary hydroxy group. Two peaks due to the carbonyl and phenyl groups were observed at around 1720 and 1620 cm^{-1} , respectively. This suggests that ADMPC was immobilized on the silica surface. The existence of the polysaccharide derivatives on the silica surface was also confirmed for other packing materials. The contents of ADMPC and CDMPC on the packing materials were estimated to be 7–23 mass-% by elemental analyses (Table 1). In most instances, the amount of the immobilized polysaccharide derivatives was greater in the reaction with 10% than in the reaction with 3% diisocyanate. When dichlorodiphenylsilanized silica gel was employed in place of 3-aminopropylsilica gel, only a small amount of the cellulose derivative was fixed on the silica surface, probably through cross-linking between cellulose chains [10]. This suggests that the immobilization of polysaccharides can be attributed mainly to bond formation between the amino group of 3-aminopropylsilanized silica gel and the hydroxy groups of the polysaccharides by the diisocyanate. Therefore, the methods illustrated in Figs. 1 and 2 seem suitable for the regioselective immobilization of the polysaccharide derivatives.

3.2. Optical resolution on amylose CSPs

Fig. 4 shows a chromatogram of the resolution of racemic 2,2'-dihydroxy-6,6'-dimethylbiphenyl (**c**) on a column packed with ADMPC (**1a–3**) bonded at the 6-position of glucose with 3 mol-% diisocyanate. The enantiomers eluted at retention times of t_1 and t_2 showing complete separation. The capacity factors (k'_1 and k'_2), which were evaluated as $(t_1 - t_0)/t_0$ and $(t_2 - t_0)/t_0$, were 0.67 and 1.40, respectively. The separation factor [$\alpha = k'_2/k'_1 = (t_2 - t_0)/(t_1 - t_0)$] and the resolution factor [$R_s = 2(t_2 - t_1)/(W_1 + W_2)$] were determined to be 2.10 and 4.42, respectively.

In Table 2 are summarized the results for the resolution of racemic compounds **a–i** on the five ADMPC phases which were fixed with different amounts of diisocyanate at different positions on the glucose unit. The results with the coated ADMPC phase, which was prepared by physical

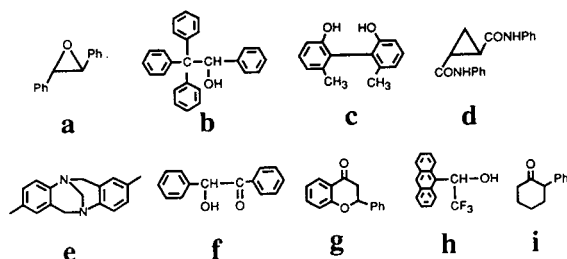
Table 1
Preparation of CSPs

No.	Polysaccharide	Positions	Diisocyanate ^a (mol-%)	Elemental analyses			Amount of polysaccharide ^b (mass-%)
				C (%)	H (%)	N (%)	
1a-3	ADMPC	6	3.0	5.33	0.53	0.64	7.7
1a-10		6	10.0	7.17	0.71	0.84	11.0
1b-3		2,3	3.0	5.89	0.62	0.68	8.8
1b-10		2,3	10.0	12.22	1.10	1.30	21.5
1c-3		2,3,6	3.0	12.87	1.27	1.39	23.0
2a-3	CDMPC	6	3.0	7.70	0.77	0.79	12.2
2a-10		6	10.0	10.51	0.71	1.03	17.7
2b-3		2,3	3.0	6.94	0.33	0.89	10.6
2b-10		2,3	10.0	12.15	0.70	1.35	21.3
2c-3		2,3,6	3.0	11.71	0.68	1.05	20.3
2c-10		2,3,6	10.0	11.92	0.45	1.27	20.8
Silica gel ^c	—	—	—	0.63	0.15	0.07	—

^a Diisocyanate used for the preparation of CSPs based on hydroxy groups of polysaccharide.

^b The amount of polysaccharide derivatives on silica gel calculated from C (%) of CSPs.

^c 3-Aminopropylsilica gel.



adsorption of ADMPC on silica gel, are also shown for comparison [7]. The results indicate that the chiral discrimination ability depends on both the position of the glucose unit immobilized and the amount of diisocyanate used. The chiral recognition ability tended to decrease as the degree of chemical bonding between the amylose derivatives and the silica surface increased, as reported previously [10]. However, it should be noted that the ADMPC phases (**1a**) immobilized at the 6-position show a higher resolving power than the other CSPs (**1b** and **1c**) immobilized irregularly at the 2- and 3-positions or at the 2-, 3- and 6-positions. In particular, **1a-3**, showed a high chiral recognition comparable to that of the coated-type phase.

The most important adsorbing site of

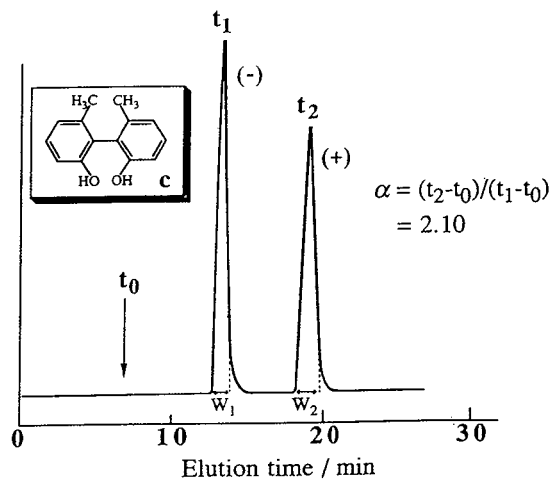


Fig. 4. Optical resolution of 2,2'-dihydroxy-6,6'-dimethylbiphenyl on **1a-3**. Eluent, hexane-2-propanol (90:10); flow-rate, 0.5 ml/min.

phenylcarbamate derivatives of polysaccharide for chiral recognition has been considered to be the carbamate residues [4]. The racemates probably interact with the carbamate residues through hydrogen bonding, as shown in Fig. 5. However, the enantioselectivities of these CSPs depended greatly on the kind of racemate. For example, in the resolution of **d** and **e**, these

Table 2
Optical resolution of racemates (a-i) on ADMPC-fixed phases (1a-3-1c-3)

Racemate	1a-10			1b-3			1b-10			1c-3			Coated-type ^a		
	k'_1	α	R_s	k'_1	α	R_s	k'_1	α	R_s	k'_1	α	R_s	k'_1	α	R_s
a	0.14(+)	2.53	2.27	0.20(+)	2.44	2.68	0.14(+)	2.08	2.00	0.42(+)	1.55	1.88	0.44(+)	1.99	4.22
b	0.70(+)	1.94	4.12	1.05(+)	1.85	3.71	0.60(+)	1.75	2.93	1.52(+)	1.58	3.14	1.79(+)	1.75	5.52
c	0.67(-)	2.10	4.42	0.97(-)	1.98	3.60	0.75(-)	1.63	2.29	1.96(-)	1.48	2.40	1.88(-)	1.89	4.47
d	0.84(+)	1.75	1.82	1.35(+)	1.68	1.64	0.87	1.0		2.45	1.0		3.59(+)	1.60	1.31
e	0.20(+)	1.37	0.62	0.31(+)	1.38	0.84	0.69(+)	ca.1		10.24	1.0		0.99(+)	ca.1	
f	1.04(-)	1.09	0.61	1.45(-)	1.05	0.32	1.14(+)	1.09		3.21(+)	1.14	1.47	3.62	1.0	
g	0.34(+)	ca.1		0.49(+)	1.10	0.61	0.46(+)	ca.1		1.30(+)	1.11		1.30(+)	1.16	1.19
h	0.45	1.0		0.58	1.0		0.49	ca.1		1.27	1.13		1.29	1.07	
i	0.65	1.0		0.80	1.0		0.30(-)	ca.1		0.85(-)	ca.1		2.04	1.0	

Eluent, hexane-2-propanol (90:10, v/v); flow-rate, 0.5 ml/min. The signs in parentheses represent the optical rotation of the first-eluted enantiomer.

^aData taken from ref. 7.

Table 3
Optical resolution of racemates (a-i) on CDMPC-fixed phases (2a-3-2c-10)

Racemate	2a-10			2b-3			2b-10			2c-3			2c-10			Coated-type ^a		
	k'_1	α	R_s	k'_1	α	R_s	k'_1	α	R_s	k'_1	α	R_s	k'_1	α	R_s	k'_1	α	R_s
a	0.32(-)	1.30	1.64	0.46(-)	1.24	1.10	0.23(-)	1.46	1.67	0.50(-)	ca.1		0.32(+)	ca.1	2.20	0.06(+)	ca.1	0.74(-)
b	0.79(-)	1.11		1.12(-)	1.25	1.32	0.52(+)	1.11		1.16(+)	ca.1		0.64(+)	1.14		0.16	1.0	1.37(+)
c	0.64(-)	3.47	5.55	0.93(-)	2.74	4.48	0.62(-)	2.76	4.34	1.10(-)	4.54	3.14	0.70(-)	2.63		0.17(-)	ca.1	2.36(-)
d	0.50(+)	1.40	2.06	0.74(+)	1.34	1.47	0.46(+)	1.46	1.60	0.96	1.0		0.79	1.0	1.09	0.19	1.0	0.83(+)
e	0.45(+)	1.40	2.30	0.52(+)	1.47	2.08	0.41(+)	1.32	1.03(+)	1.49			1.27	1.0	0.60	0.60	1.0	0.97(+)
f	1.17(+)	1.31	3.56	1.58(+)	1.28	2.97	0.93(+)	1.29	1.62	2.09(+)	1.19		1.51(+)	1.16	2.65	0.44	1.0	2.43(+)
g	0.70(+)	1.19	2.20	1.00(-)	1.17	1.48	0.51(-)	1.21	1.37	1.20(-)	ca.1		0.82(-)	ca.1	0.84	0.20	1.0	1.47(-)
h	0.77(-)	2.33	10.8	1.10(-)	2.32	8.93	0.68(-)	2.12	3.16	1.25(-)	1.87	1.80	0.92(-)	1.63	0.30	1.0	2.13(-)	2.59
i	0.55(-)	1.22	1.33	0.74(-)	1.22	1.25	0.41(-)	1.19	0.85(-)	1.28	0.91	0.60(-)	1.22	0.16(-)	ca.1	1.17(-)	1.15	

Eluent, hexane-2-propanol (90:10, v/v); flow-rate, 0.5 ml/min. The signs in parentheses represent the optical rotation of the first-eluted enantiomer.

^aData taken from ref. 4.

racemates were sufficiently separated on 6-position-fixed phases (**1a–3** and **1a–10**), but almost no chiral discrimination was attained on the 2- and 3-positions-fixed phases, **1b–3** and **1b–10**. This indicates that the enantiomers of **d** and **e** may be discriminated mainly on the carbamate groups at the 2- and 3-positions. This speculation was also supported by the results of the enantioseparation of a variety of racemates using regioselective carbamoylated amylose with 3,5-dimethylphenyl and 3,5-dichlorophenyl isocyanates [12]. Among the carbamate groups, those at the 2- and 3-positions seem to be responsible for efficient chiral recognition in the amylose derivatives; that is, the regular arrangement of carbamate groups at the 2- and 3-positions may be important for a high enantioseparation [12]. Moreover, the formation of a covalent bond through the primary hydroxy groups at the 6-position may be suitable for keeping the sterically preferred conformation of the main chain of amylose.

In the resolution of **f**, the (–)-isomer eluted first on **1a–3** and **1a–10**, whereas the (+)-isomer eluted first on **1b–3** and **1b–10**. This indicates that for **f** the mechanism of chiral recognition is different between **1a** and **1b**. The enantiomers of **f** may be discriminated mainly on the carbamate residues at the 2- or 3-position of **1a** and at the 6-position of **1b**. The former carbamate residues probably interact more strongly with the (+)-

isomer of **f** and the later carbamate with the (–)-isomer.

3.3. Optical resolution on cellulose CSPs

The results of the optical resolution of **a–i** on the six cellulose derivatives are listed in Table 3. The regioselectively fixed CSPs (**2a** and **2b**) showed obviously a higher enantioselectivity than the non-regioselectively fixed CSPs (**2c**), analogously to the case of the CSPs based on ADMPC. The lower degree of chemical bonding between cellulose and silica gel seems to be better. Although the 6-position-fixed phase had a higher optical resolving power with ADMPC-fixed CSPs, in the cellulose derivatives a significant difference in chiral recognition between the 6-position-bonded phase (**2a–3**) and the 2- and 3-positions-bonded phase (**2b–3**) was not observed. These results suggest that the mechanism of enantioseparation may be similar between on **2a–3** and **2b–3**; racemates are likely to interact simultaneously with multiple 3,5-dimethylphenylcarbamate residues at the 2- and 3-positions and 6-position of neighbouring glucose units [12]. In the case of the amylose derivatives, the carbamate groups at the 2- and 3-positions are often more important for the optical resolution than that at the 6-position, as mentioned above. The difference observed between the cellulose and amylose derivatives can be explained as follows.

The possible structures of the phenylcarbamates of cellulose [13] and amylose [14] have been reported on the basis of X-ray analysis by Vogt and Zugenmaier. The cellulose derivative possesses the conformation of a left-handed threefold (3/2) helix. Racemates can simultaneously interact with all the carbamate residues in a complicated manner, because the residues at the 2- and 3-positions of a glucose unit and the 6-position of neighbouring glucose units are located close to each other. In the cellulose derivatives, the carbamate residue at the 6-position may be as important for chiral recognition as those at the 2- and 3-positions, and therefore the CDMPC-bonded phases show little influence on chiral recognition with respect to the posi-

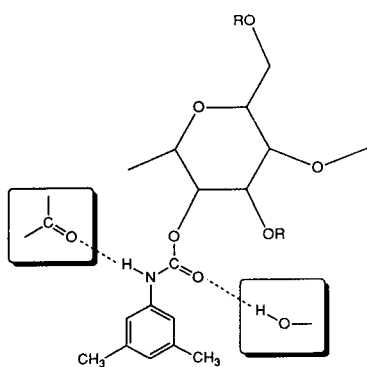


Fig. 5. Schematic interaction of the racemic compounds with the phenylcarbamoyl residue.

tions of chemical bonding. On the other hand, the conformation of the amylose derivative is proposed to be a left-handed fourfold (4/1) helix [14]. The racemates cannot interact simultaneously with the phenylcarbamate residues at the 2- and 3-positions of a glucose unit and the 6-position of the neighbouring glucose units, since these are remote from each other. In the amylose derivatives, the carbamate residues at the 2- and 3-positions seem to play a more important role than that isolated at the 6-position. Hence the 6-position-bonded ADMPC phases may show a high optical resolution ability without decreasing the chiral recognition ability of the carbamate residues at the 2- and 3-positions.

3.4. Separation of racemates under different chromatographic conditions

As mentioned above, the chemically bonded-type CSPs can be used with solvents such as CHCl_3 and THF which swell or dissolve ADMPC. Enantioseparation of some racemates using these eluents was studied preliminarily on column **1a–3** (Fig. 6). 2-Phenylcyclohexanone (**i**), which could not be separated on either the **1a–3** or the ADMPC-coated-type column under normal-phase conditions [hexane–2-propanol (90:10)], was almost completely separated into enantiomers when a small amount of CHCl_3 (5%) was added to the mobile phase. Similarly, flavanone (**g**) was completely resolved on the **1a–3** column using hexane– CHCl_3 –2-propanol (95:5:1) as the eluent. The enantioselectivity ($\alpha = 1.60$) of **g** on **1a–3** [eluent hexane– CHCl_3 –2-propanol (95:5:1)] was much greater than that on the ADMPC-coated phase ($\alpha = 1.12$) under normal-phase conditions. A similar result was obtained in the separation of **h** on **1a–3** by use of the eluent hexane– CHCl_3 –2-propanol (95:5:1) ($\alpha = 1.34$); the separation factor of **h** on the coated-type phase [eluent hexane–2-propanol (90:10)] was 1.15. The presence of a much smaller amount of 2-propanol may improve the chiral discrimination ability of the ADMPC phase, on which the hydrogen bonding between the CSP and racemates may play an important role. This

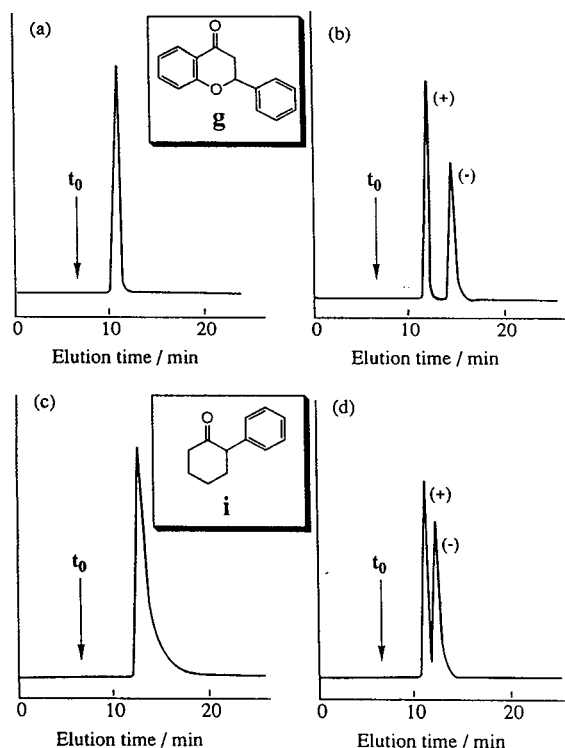


Fig. 6. Effect of eluent on optical resolution of (a and b) **g** and (c and d) **i**. Eluent: (a and c) hexane–2-propanol (90:10); (b) hexane– CHCl_3 –2-propanol (95:5:1); (d) hexane– CHCl_3 (95:5).

may also be ascribed to some conformational change of ADMPC because ADMPC is swollen in CHCl_3 . The selection of the composition of the eluent seems very important for achieving efficient optical resolution. Clearly, more studies must be done to investigate the influence of solvents on the chiral recognition and elucidate the separation mechanism.

4. Conclusions

ADMPC and CDMPC could be regioselectively immobilized on 3-aminopropylsilica gel with diisocyanate. The chiral recognition abilities of the amylose and cellulose derivatives bonded non-regioselectively at the 2-, 3- and 6-positions were also evaluated. In the amylose derivatives, the optical resolving ability of the 6-position-

bonded phase with a smaller extent of chemical bonding was higher than that of the 2- and 3-positions-bonded phase, but it was slightly lower than that of ADMPC-coated phase. On the other hand, for the cellulose derivatives, a clear dependence of enantioseparation on the position of the glucose unit for immobilization could not be observed. With both derivatives, regioselectively bonded phases had a superior chiral discrimination to non-regioselectively bonded phases. The optical resolving power of these CSPs was also influenced by the degree of immobilization by diisocyanate in the preparation of CSPs. Since these chemically bonded phases were not damaged by polar solvents such as CHCl_3 , a more efficient separation of racemates was attained by the use of an eluent containing a small amount of CHCl_3 , which could not be applied with the coated CSPs.

5. Acknowledgements

The authors thank Nakano Vinegar for providing amylose. Part of this work was supported by Grant-in-Aids for Scientific Research Nos. 05559009 and 05234213 from the Ministry of Education, Science and Culture and Sumitomo Foundation.

6. References

- [1] Y. Okamoto, M. Kawashima, K. Yamamoto and K. Hatada, *Chem. Lett.*, (1984) 739.
- [2] Y. Okamoto, R. Aburatani and K. Hatada, *J. Chromatogr.*, 389 (1987) 95.
- [3] Y. Okamoto, M. Kawashima and K. Hatada, *J. Am. Chem. Soc.*, 106 (1984) 5357.
- [4] Y. Okamoto, M. Kawashima and K. Hatada, *J. Chromatogr.*, 363 (1986) 173.
- [5] Y. Okamoto, R. Aburatani, T. Tukumoto and K. Hatada, *Chem. Lett.*, (1987) 1857.
- [6] Y. Okamoto and Y. Kaida, *J. High Resolut. Chromatogr.*, 13 (1990) 708.
- [7] Y. Okamoto, R. Aburatani and K. Hatada, *Bull. Chem. Soc. Jpn.*, 63 (1990) 955.
- [8] Y. Okamoto, Y. Kaida, R. Aburatani and K. Hatada, in S. Ahuja (Editor), *Chiral Separation of Liquid Chromatography (ACS Symposium Series, No. 471)*, American Chemical Society, Washington, DC, 1991, p. 101.
- [9] Y. Okamoto and Y. Kaida, *J. Chromatogr.*, 666 (1994) 403.
- [10] Y. Okamoto, R. Aburatani, S. Miura and K. Hatada, *J. Liq. Chromatogr.*, 10 (1987) 1613.
- [11] Y. Kaida and Y. Okamoto, *Bull. Chem. Soc. Jpn.*, 65 (1992) 2286.
- [12] Y. Kaida and Y. Okamoto, *Bull. Chem. Soc. Jpn.*, 66 (1993) 2225.
- [13] U. Vogt and P. Zugenmaier, *Ber. Bunsenges. Phys. Chem.*, 89 (1985) 1217.
- [14] U. Vogt and P. Zugenmaier, presented at the *European Science Foundation Workshop on Specific Interactions in Polysaccharide Systems, Uppsala, 1983*.

Characterization of synthetic resins by gel permeation chromatography with a multi-angle laser light scattering detector

Š. Podzimek¹

Institute for Organic and Macromolecular Chemistry, Heinrich Heine University, 40225 Düsseldorf, Germany

First received 27 December 1993; revised manuscript received 5 April 1994

Abstract

Gel permeation chromatography coupled with a multi-angle laser-light scattering detector was applied to the characterization of various kinds of synthetic resins (epoxy, phenoxy, novolac, unsaturated polyester, alkyd resins). The relations between molecular mass and elution volume of polystyrene and particular resins were investigated and the presence of branched molecules in the resins was proved by the root mean square radius vs. molecular mass plot. The possibilities and limitations of conventional gel permeation chromatography are discussed based on the obtained results.

1. Introduction

Synthetic resins are a specific group of synthetic polymers of a great technical importance. They are usually used as a component of lacquers, adhesives and graphite- or glass-reinforced construction materials. The major part of the molecules even in the higher-molecular-mass types of the resins has molecular masses up to several tens of thousands, but high-molecular-mass fractions with molecular masses of the order of magnitude 10^6 to 10^7 may be present in some resins.

The combination of gel permeation chroma-

graphy (GPC) with the molecular mass sensitive multi-angle laser-light scattering (MALLS) detector gives the absolute molecular mass and size distribution (providing sample chemical homogeneity). GPC–MALLS has been employed several times for the characterization of organic and water-soluble polymers [1–6], but the results concerning synthetic resins may not have been reported. The aim of this work is to show possibilities of the GPC–MALLS technique for the investigation of these materials.

The DAWN-F photometer measures the intensity of the light scattered from a flowing sample at 15 angular positions. A chromatography peak is divided into several hundreds of slices and the molecular mass and the root mean square (RMS) radius (also called the radius of gyration) are calculated for each slice. The reciprocal scattering function Kc/R_θ is plotted as

¹ Present address: SYNPO–Research Institute for Synthetic Resins and Lacquers, S.K. Neumann 1316, 532 07 Pardubice, Czech Republic.

a function of $\sin^2(\Theta/2)$. The intercept of this plot k_0 yields the molecular mass M_r :

$$M_r = (k_0 - 2A_2c)^{-1} \quad (1)$$

and the slope for $\Theta \rightarrow 0$ m_0 gives RMS radius $\langle r_g^2 \rangle^{1/2}$:

$$\langle r_g^2 \rangle^{1/2} = \frac{\sqrt{3}\lambda_0}{4\pi n_0} \sqrt{m_0 M_r} \quad (2)$$

where A_2 is the second virial coefficient, which often may be neglected, c is the concentration usually measured by a refractive index (RI) detector, λ_0 is the wavelength of the incident light in vacuo, n_0 is the refractive index of the solvent, K is a physical constant proportional to the square of the specific refractive index increment dn/dc and R_Θ is the excess Rayleigh ratio proportional to the intensity of scattered light.

2. Experimental

The GPC–MALLS instrument consisted of a Model 510 Waters pump, an Ultrastaygel Linear column (Waters), a DAWN-F photometer (Wyatt Technology) and a Wyatt Optilab 903 refractometer. Data collection and handling were carried out using ASTRA and EASI software (Wyatt Technology). Tetrahydrofuran (THF) served as the mobile phase at the flow-rate of 1 ml/min. Samples were prepared as solutions in THF: 0.15% polystyrene (PS), 0.6% epoxy and phenoxy resins, 0.75% novolacs, 0.9% unsaturated polyesters and alkyds. Unusually high concentrations of the resin samples were used to improve the signal-to-noise ratio of the light scattering and RI detectors at the edges of the chromatograms. As a major part of the molecules in the analysed samples has molecular mass of the order of magnitude 10^4 , the term $2A_2cM_r \ll 1$ and the concentrations do not significantly affect the results. The dn/dc calculation method was used for the data evaluation of PS, phenoxy and epoxy resins using the following values of dn/dc : 0.1845 ml/g (PS), 0.1773 ml/g (phenoxy resin) and 0.1869 ml/g (epoxy

resin) [7]. The mass calculation method was used for unsaturated polyesters, alkyds and novolacs.

All resins analysed were synthesized at SYNPO or obtained commercially. Broad PS was purchased from Aldrich.

3. Results and discussion

An example of GPC chromatograms of synthetic resin recorded by MALLS (90°) and RI detectors is presented in Fig. 1. The chromatograms do not overlap due to the different kind of response. The large volume difference between the peaks of light scattering and RI profiles gives evidence about very high polydispersity of the resin.

Molecular mass vs. elution volume plots (GPC calibration curves) of particular resins are compared with that of PS in Figs. 2–5. Fig. 2 shows that the molecular mass of epoxy resin is by about 40% lower than that of PS of the same elution volume. The plot of phenoxy resin approximately overlapped the epoxy resin curve. The molecular mass vs. elution volume plots of unsaturated polyester resin and PS (Fig. 3) cross at the molecular mass of about 20 000 and the difference between them becomes more pronounced towards high molecular masses. Calibration plots of novolac resins made using different phenol/formaldehyde ratios overlapped and the mutual course of novolac and PS curves (Fig.

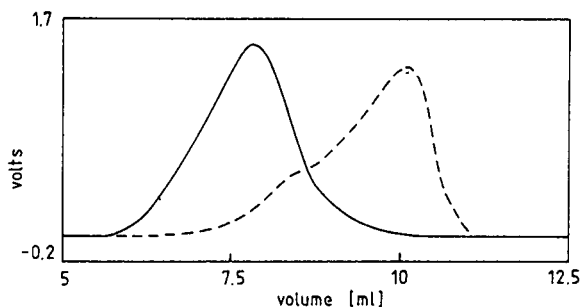


Fig. 1. RI (dashed line) and 90° light scattering (solid line) chromatograms of novolac resin (phenol–formaldehyde ratio 1:0.9). Column, Ultrastaygel Linear 300×7.8 mm; particle size, $7 \mu\text{m}$; mobile phase, THF; flow-rate, 1 ml/min; sample size, $100 \mu\text{l}$.

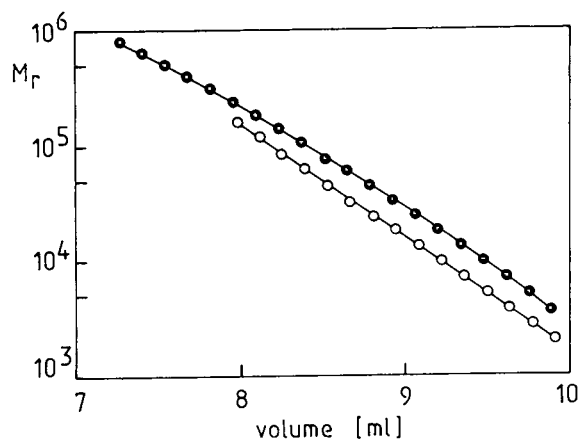


Fig. 2. Molecular mass vs. elution volume plots of PS (●) and epoxy resin (○).

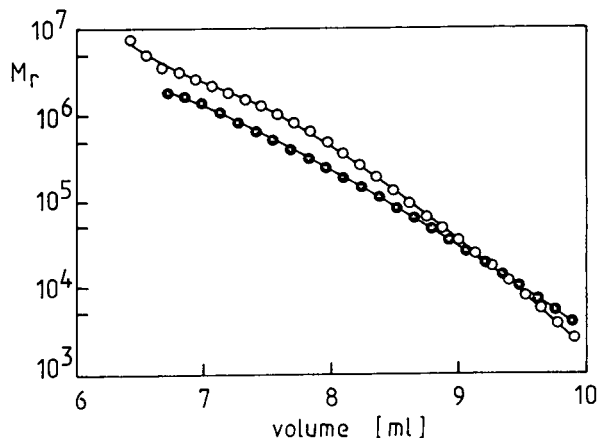


Fig. 4. Molecular mass vs. elution volume plots of PS (●) and novolac resin (○).

4) is similar as in the case of unsaturated polyester. Fig. 5 presents molecular mass vs. elution volume plots of PS and two different alkyd resins. The significant shift of calibration curves of both alkyds can be explained by different degree of branching.

RMS radius is the second important physical parameter that can be extracted from the MALLS measurement. The determination of the molecular mass and RMS radius at each volume slice provides the RMS radius vs. molecular mass plot. The plot gives information about the struc-

ture of polymer chain. In order to improve the accuracy of the measurement, high-molecular-mass fractions from unsaturated polyester, epoxy and novolac resins were isolated by the precipitation of THF solutions by hexane. An example of the RMS radius vs. molecular mass plot for a high-molecular-mass novolac fraction is shown in Fig. 6. The plot of PS is superimposed in Fig. 6. The slope of the PS plot is 0.56 which is a typical value for the linear random coils in a good solvent while all resins showed significantly lower values: 0.36 novolac, 0.36 unsaturated polyester,

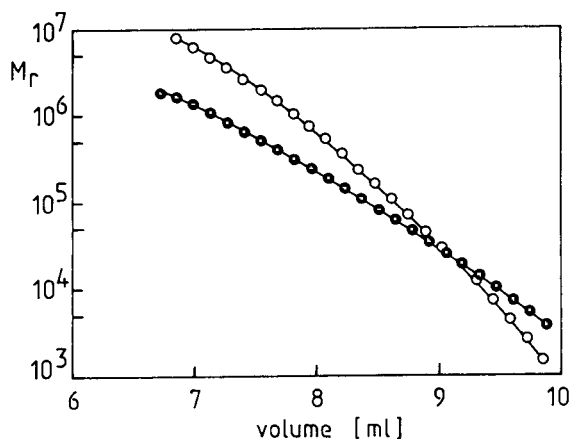


Fig. 3. Molecular mass vs. elution volume plots of PS (●) and unsaturated polyester resin (○).

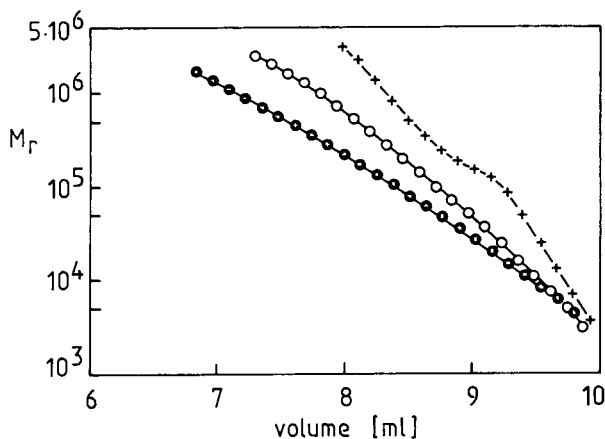


Fig. 5. Molecular mass vs. elution volume plots of PS (●) and two alkyd resins (○, +).

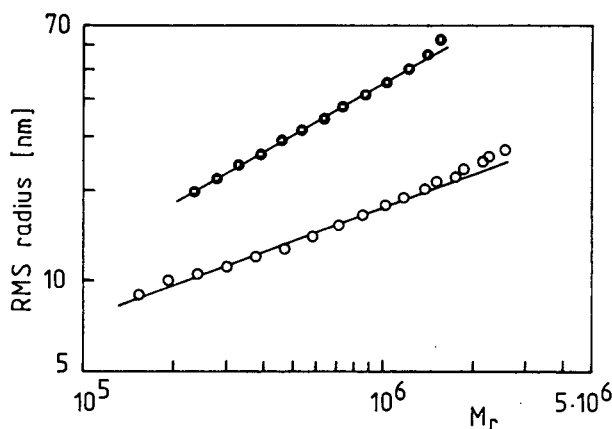


Fig. 6. RMS radius vs. molecular mass plots of high-molecular-mass novolac fraction (○) and PS (●); slopes: 0.56 (PS) and 0.36 (novolac).

0.37 epoxy resin, 0.38 alkyd. The lower slopes prove the presence of more compact branched molecules.

4. Conclusions

The following notes concerning conventional GPC can be drawn from the obtained results:

(1) Epoxy and phenoxy resins: the application of PS calibration gives higher values of number-average molecular mass (M_n) and mass-average molecular mass (M_w).

(2) Novolac and unsaturated polyester resins: calibration based on PS standards has tendency to overestimate M_n and, for samples containing high-molecular-mass fractions, underestimate M_w . The relation between molecular masses of novolac and styrene oligomers proposed in ref. [8] can be used only for low-molecular-mass novolacs and mainly for the determination of M_n . Its application to the determination of M_w values of high-molecular-mass novolac resins yields misleading results lower up to ten times.

(3) Alkyd resins: PS calibration underestimates M_n and mainly M_w . Alkyds are usually the most branched resins and consequently conven-

tional GPC may give even confusing results as shown in Fig. 5. The most useful application of conventional GPC in the production of alkyd resins may be following the course of polycondensation.

GPC-MALLS provides the absolute molecular mass distribution and very sensitive determination of high-molecular-mass fractions. The method can prove the presence of branched molecules and to characterize them. This capability seems very useful because the highly branched compact molecules may have reduced reactivity with respect to the curing agents due to the lack of reactive positions and their steric hindrance. The branched particles may affect as microscopic defects and influence unfavourably the properties of the cured resins.

Acknowledgements

GPC-MALLS measurements were carried out at the Institute for Organic and Macromolecular Chemistry of the University in Düsseldorf. The author is much indebted to Professor Dr. G. Wulff, head of the Institute, for his invitation to the Institute. Special thanks are due to Mrs. A. Králová from SYNPO for the preparation of fractions.

References

- [1] P.J. Wyatt, *Anal. Chim. Acta*, 272 (1993) 1.
- [2] P.J. Wyatt, *J. Liq. Chromatogr.*, 14 (1991) 2351.
- [3] C. Jackson, L.M. Nilsson and P.J. Wyatt, *J. Appl. Polym. Sci.: Appl. Polym. Symp.*, 43 (1989) 99.
- [4] C. Jackson, L.M. Nilsson and P.J. Wyatt, *J. Appl. Polym. Sci.: Appl. Polym. Symp.*, 45 (1990) 191.
- [5] B. Bednar and J.P. Hennessey, Jr., *Carbohydr. Res.*, 243 (1993) 115.
- [6] Š. Podzimek, *J. Appl. Polym. Sci.*, submitted for publication.
- [7] *Application Notes 1 and 2*, Chromatix, Sunnyvale, CA, 1976 and 1977.
- [8] Š. Podzimek and L. Hroch, *J. Appl. Polym. Sci.*, 47 (1993) 2005.



ELSEVIER

Journal of Chromatography A, 677 (1994) 25–33

JOURNAL OF
CHROMATOGRAPHY A

Qualitative and quantitative reversed-phase high-performance liquid chromatography of flavonoids in *Crataegus* leaves and flowers

A. Rehwald^a, B. Meier^b, O. Sticher^{a,*}

^aDepartment of Pharmacy, Swiss Federal Institute of Technology (ETH) Zurich, CH-8057 Zürich, Switzerland

^bZeller AG, CH-8590 Romanshorn, Switzerland

First received 27 December 1993; revised manuscript received 5 April 1994

Abstract

A qualitative and a quantitative reversed-phase HPLC method for the analysis of the flavonoids in *Crataegus* have been developed. The qualitative fingerprint method allows the separation of the main constituents vitexin-2"-O-rhamnoside, acetylvitexin-2"-O-rhamnoside, hyperoside, vitexin, rutin and chlorogenic acid. The quantitative determination contains acid hydrolysis of the flavonoid glycosides to vitexin as main C-glycoside and quercetin as aglycone in order to reduce the complex flavonoid pattern to two major compounds. This method, applied to the quantification of several commercial samples, revealed good accuracy and precision. Compared to other, well established methods (Ph. Helv. VII, DAB 10, Ph. Franç. X), the total flavonoid content, determined as vitexin and quercetin after acid hydrolysis, was twice as high as the results obtained by applying the pharmacopoeial methods. Collected plant material (*Crataegus monogyna* Jacq.) was investigated qualitatively and quantitatively on its seasonal variations.

The HPLC fingerprint analysis can be used for qualitative analysis, especially to control identity of plant material, extracts and preparations containing hawthorn, whereas the hydrolysis method is suitable for the quantitative determination of flavonol-O-glycosides and flavone-C-glycosides with commercially available reference standards.

1. Introduction

Crataegus (hawthorn) is widely used as medicinal plant both in official and traditional medicine. It shows numerous mild, but well documented pharmacological activities [1] and few side effects. Preparations of *Crataegus* improve the heart function, and their indications are cases of declining cardiac performance equiv-

alent to stages I and II of the NYHA (New York Heart Association) classification, deficiency of the coronary blood supply and mild forms of arrhythmias [2].

The flowering tops and flowers are harvested from *Crataegus monogyna* Jacq. emend. Lindm. or *Crataegus laevigata* (Poir.) D.C. (synonym: *Crataegus oxyacantha* L.) or, less frequently, from other European *Crataegus* species (Rosaceae). They contain flavonoids such as hyperoside, vitexin, vitexin-2"-O-rhamnoside and

* Corresponding author.

acetylvitexin-2''-O-rhamnoside as well as oligomeric procyanidins and (-)-epicatechin. These two groups are considered to be the main active constituents [1,3–5], and the standardization of *Crataegus* leaves, flowers and preparations aims at either the flavonoids or the oligomeric procyanidins or at both.

The quantitative determination of the flavonoids by spectrophotometric analysis of the aluminium chelate complexes after acid hydrolysis, as it is required by the German and Swiss pharmacopoeias, is not very suitable for *Crataegus* because at least half of the total flavonoid content are C-glycosides [6] which can not be hydrolyzed by acid and therefore are not extracted with ethyl acetate and not determined. By means of a HPLC fingerprint chromatogram it could be shown in our laboratory that all the vitexin derivatives remain to a large extent in the aqueous solution which is discarded. This confirmed the results of previous works [6,7]. Besides, the prescribed wavelength of 425 nm does not represent the absorption maximum of the vitexin derivatives that have partially passed into the ethyl acetate. Since this method comprises only the flavonol-O-glycosides and not the flavone-C-glycosides, it is not accurate and yields unsatisfactory results.

Nowadays reversed-phase high-performance liquid chromatography (RP-HPLC) is the commonly used analytical separation technique for polyphenolic compounds like flavonoids. Due to the variability of column filling materials and solvent systems, RP-HPLC exhibits a great potential in separating complex mixtures of flavonoids and other phenolic compounds. Several studies on correlations between structure and retention time values of flavonoids have been carried out [8–11], using isocratic or gradient elution technique. They demonstrate the influence of the pattern of hydroxylation, degree of unsaturation and glycosylation on the chromatographic behaviour of a large number of flavonoids.

The HPLC fingerprint analysis has become a useful and suitable method for quality control and standardization of plant material and preparations. It requires good separation and resolu-

tion of the complex mixture as well as peak purity control in order to prevent peak overlapping. Davis and Giddings [12] developed a method for the evaluation of the number of components in multicomponent chromatograms, which was applied to the analysis of plant extracts by Dondi *et al.* [13].

Several authors [6,14–17] described reversed-phase HPLC fingerprint chromatograms for the quantitative determination of the flavonoids in *Crataegus*. They used the internal or external standard method. The greatest disadvantage of these analyses is that not all compounds are commercially available reference standards.

Therefore a quantitative reversed-phase HPLC method was developed which is based on the reduction of the complex flavonoid glycoside pattern to one major aglycone and one C-glycoside by acid hydrolysis [18]. The main flavonol-O-glycosides hyperoside and rutin can be hydrolyzed to quercetin, while the principal flavone-C-glycosides vitexin-2''-O-rhamnoside and acetyl-vitexin-2''-O-rhamnoside react to vitexin. Quercetin and vitexin are commercially available standards which can be used for calibration curves for the standardization of *Crataegus* plant material and preparations. Beside this quantitative method a fingerprint chromatogram for quality control was elaborated.

2. Experimental

2.1. Plant material

The samples of *Crataegus* leaves and flowers (*Crataegi folium cum flore*) were purchased from different commercial sources (Dixa, St. Gallen, Switzerland; Hanseler, Herisau, Switzerland). Plant extracts were provided by Zeller (Romanshorn, Switzerland). For the investigation of the seasonal variations, leaves, flowers and fruits of *Crataegus monogyna* Jacq. were collected monthly in Buchs (Canton Zurich, Switzerland) from April to October, 1993. The plant material was identified by Dr. W. Lippert, Munchen, Germany, and voucher specimens are deposited in the Botanische Staatssammlung, Munchen,

Germany, and in the Herbarium ETH, Zürich, Switzerland. The collected plant material was immediately dried at 35°C in a Salvis TSK 2 HL dryer (Salvis, Emmenbrücke, Switzerland) for 48 h (leaves, flowers) and for 7 days (fruits).

2.2. Standards and solvents

Quercetin dihydrate (puriss.) was from Fluka (Buchs, Switzerland); vitexin, isovitexin and vitexin-2''-O-rhamnoside (Rotichrom HPLC grade) were from Roth (Basel, Switzerland). Methanol, acetonitrile, tetrahydrofuran and isopropanol were of HPLC quality (Romil Chemicals, Shepshed, U.K.). Orthophosphoric acid (analytical-reagent grade) was purchased from Siegfried (Zofingen, Switzerland) and hydrochloric acid (analytical-reagent grade) from Fluka. Water was obtained using a NANOpure Cartridge System (Skan, Basel-Allschwil, Switzerland). Bond Elut C₁₈ (500 mg) extraction columns used for sample clean-up were purchased from Analytichem International (ICT, Basel, Switzerland).

2.3. Instrumentation and column

All HPLC analyses were performed using a Hewlett-Packard instrument (Model 79994A analytical workstation, Model 1090 liquid chromatograph, Model 1040 diode-array detector). A Knauer (Berlin, Germany) prepacked column cartridge (100 × 4 mm I.D.) filled with Hypersil ODS 5 μm (Shandon, Runcorn, U.K.) was used for all chromatographic separations. A EF4 Modulyo (Edwards AG, West Sussex, U.K.) was used for freeze-drying the tea preparations.

2.4. Chromatographic conditions

Fingerprint

The mobile phase was optimized using the "PRISMA" system [19]. It consisted of solvent A [tetrahydrofuran–acetonitrile–methanol (92.4:3.4:4.2, v/v/v)] and solvent B (0.5% orthophosphoric acid). The elution profile was: 0–12 min 12% A in B, 12–25 min 12% to 18% A

in B (linear gradient), 25–30 min 18% A in B. The flow rate was 1.00 ml/min, the column temperature 25.0°C and the injection volume 10 μl. The UV detector was set at 370 nm, 336 nm and 260 nm.

Determination of vitexin after acid hydrolysis

The mobile phase consisted of solvent A [tetrahydrofuran–isopropanol–acetonitrile (10:8:3, v/v/v)] and solvent B (0.5% orthophosphoric acid). The separation was carried out using isocratic elution (0–13 min 12% A in B) with a flow rate of 1.00 ml/min and a column temperature of 25.0°C. The injection volume was 5 μl, and UV detection was effected at 336 nm and 260 nm.

Determination of quercetin after acid hydrolysis

The analyses were performed by gradient elution: 0–15 min 30% A (methanol) in B (0.5% orthophosphoric acid) to 55% A in B. The flow rate was 1.00 ml/min, the column temperature 25.0°C and the injection volume 10 μl. UV detection was performed at 370 nm and 260 nm.

2.5. Sample preparation

Qualitative analysis

Fingerprint

3 g of dried and pulverized plant material or 2 g of dried plant extract were refluxed with 60 ml of methanol 80% for 60 min, filtered and refluxed with 40 ml of methanol 80% for another 10 min. The filtered extract was evaporated under vacuum to about 20 ml and diluted to 25.0 ml with 80% methanol. 5.0 ml of this solution were filtered through a Bond Elut C₁₈ cartridge for sample clean-up and diluted to 10.0 ml with 80% methanol. A 10-μl volume of this solution was injected into the chromatographic system.

Quantitative analyses

Method 1. (acid hydrolysis)

8 g of dried and pulverized plant material or 6 g of dried plant extract were extracted in a Soxhlet apparatus with 150 ml of methanol for 5

h. The extract was evaporated under vacuum to about 80 ml and diluted to 100.0 ml with methanol. For the determination of vitexin, 25.0 ml of this solution and 10 ml of 25% hydrochloric acid were refluxed for 90 min. For the determination of quercetin, 25.0 ml of the extraction solution and 2 ml of 25% hydrochloric acid were refluxed for 60 min. After cooling the hydrolyzed extracts were diluted to 50.0 ml. 5.0 ml of these solutions were filtered through Bond Elut C₁₈ cartridges for sample clean-up and diluted to 10.0 ml with methanol. A 5- μ l (vitexin) and 10- μ l (quercetin) volume of these solutions were injected into the HPLC system.

Method 2 (quantitative fingerprint)

5.0 ml of the extraction solution of method 1 were filtered through a Bond Elut C₁₈ cartridge for sample clean-up and diluted to 10.0 ml with methanol. A 10- μ l volume of this solution was injected into the chromatographic system.

Method 3

This method was according to Ph. Franç. X.

Method 4

This method corresponded to Ph. Helv. VII.

Tea preparation

To 1.8 g of dried plant material 150 ml of boiling water were added and stirred from time to time. After 20 min the tea was filtered, and the filtrate was freeze-dried for further investigations. The quantitative determination was effected by applying method 1.

2.6. Determination and calibration

The determination of vitexin and quercetin for method 1 was performed using the external standard method and calculating the peak areas. The calibration curves were obtained with eight samples of various concentrations using linear regression analysis. Each sample was measured three times. Over the selected concentration range of 46 μ g/ml to 276 μ g/ml for vitexin and 27 μ g/ml to 176 μ g/ml for quercetin the calibration curves showed a linear detector re-

sponse. The correlation coefficients were 0.9995 for both vitexin and quercetin.

During the acid hydrolysis vitexin is partially converted into isovitexin [20] due to a Wessely–Moser rearrangement [21], and an equilibrium mixture of both isomers results. Under the conditions mentioned above, the hydrolysis mixture consists of mainly vitexin and approximately 6% isovitexin. Isovitexin was calculated as vitexin by summing the peak areas. There was no significant difference ($p < 0.001$) between this calculation and the determination with an additional calibration curve for isovitexin.

The quantitative determination of vitexin-2''-O-rhamnoside and hyperoside for method 2 was carried out with external standards (six-point calibration). The correlation coefficients were 0.9993 for vitexin-2''-O-rhamnoside and 0.9990 for hyperoside. Acetylvitexin-2''-O-rhamnoside was calculated as vitexin-2''-O-rhamnoside and rutin as hyperoside.

For method 3 the quantitative determination of vitexin-2''-O-rhamnoside and hyperoside was performed using external standards (one-point calibration).

2.7. Reproducibility

The reproducibility of the chromatographic separations was verified with columns from several batches. The fingerprint method and the determination of quercetin after acid hydrolysis were reproducible on five different column batches, the separation of vitexin, isovitexin and vitexin-2''-O-rhamnoside for the determination of vitexin after acid hydrolysis was reproducible on three columns. All chromatographic analyses were reproducible on a second HPLC instrument (Hewlett-Packard HPLC^{3D} ChemStation, 1090 LC Series II).

3. Results and discussion

3.1. Extraction and sample preparation

The preparation of the plant material was performed by continuous, exhausting extraction

in a Soxhlet apparatus. Other extraction methods like reflux or turbo extraction, which are proposed by various authors [6,14,18] were tested, but they revealed only incomplete extraction of the flavonoids, even if repeated several times. The resulting flavonoid content was at least 15% lower.

The hydrolytic conditions for the flavonoid glycosides were examined in a first step using reference standards (hyperoside and vitexin-2''-O-rhamnoside), subsequently transferred to the plant material and finally optimized. For the hydrolysis of hyperoside and other flavonol-O-glycosides mild hydrolytic conditions are sufficient. The vitexin derivatives vitexin-2''-O-rhamnoside and its acetate require more hydrochloric acid and a longer time of refluxing for a complete hydrolysis. These conditions again are too strong for the flavonol-O-glycosides and lead to a loss of 15–20% of quercetin. Similar results were found by other authors [22] who report a significant degradation of 10–20% of quercetin due to an increased acid concentration and an increased reaction period. The fact that quercetin is partially decomposed by the acid and by the heat might also explain the inferior recovery of quercetin and hyperoside compared to vitexin and vitexin-2''-O-rhamnoside (see below). Therefore these two groups of glycosides are hydrolyzed and analyzed separately.

3.2. Qualitative analysis

Five commercial samples (*Crataegi folium cum flore*) were examined for their flavonoid composition. They all showed rather uniform fingerprint chromatograms with vitexin-2''-O-rhamnoside, hyperoside and acetylvitexin-2''-O-rhamnoside as main peaks in similar relative concentrations. Beside little amounts of vitexin and rutin, chlorogenic acid was detected in all samples (see Fig. 1). In contrast to that the collected plant material (*Crataegus monogyna* Jacq.) contained no acetylated vitexin-2''-O-rhamnoside. Lamaison *et al.* [14] obtained contrary results. They found the acetylated vitexin-2''-O-rhamnoside only in the leaves of *Crataegus monogyna*, but not in *Crataegus laevigata*.

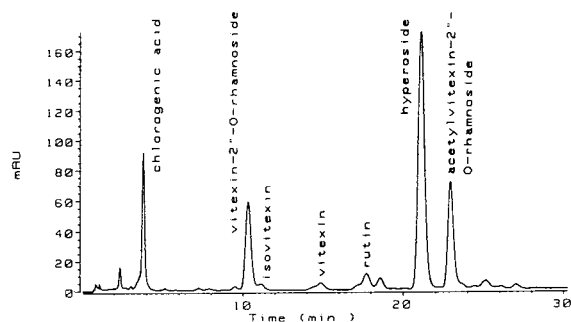


Fig. 1. Typical HPLC fingerprint chromatogram of hawthorn leaves with flowers. For conditions, see Experimental.

In all samples of collected plant material we could detect vitexin-2''-O-rhamnoside, hyperoside, vitexin, rutin and chlorogenic acid, but, however, considerable differences concerning the relative concentrations could be made out, depending on the part of the plant and on the stage of development. In the flowers (collected in the beginning of May) we found, corresponding to other authors [6,7,14], hyperoside as main constituent, whereas vitexin-2''-O-rhamnoside was predominant in the leaves over the whole collecting period. The wooden branches exhibited flavonoid patterns similar to the leaves, but at low concentrations and with relatively more hyperoside. The fruits (collected from August to October) revealed mainly hyperoside and notable amounts of rutin, but almost no vitexin-2''-O-rhamnoside. Also the flowers showed a remarkable amount of rutin, while in the leaves it was, as well as vitexin, present only in minor concentrations.

The drying of the collected plant material had no influence on the flavonoid composition. We found no qualitative differences and the same relative concentrations in the fingerprint chromatograms of dried and fresh plant material.

3.3. Quantitative analysis

Five commercial samples (*Crataegi folium cum flore*) were quantified by the hydrolysis method described above in order to obtain some information on its precision and accuracy. The relative standard deviations ($n = 3$ or 6) were

between 1% and 3% in all samples. The recoveries were determined by twice adding two different amounts of each vitexin and vitexin-2"-O-rhamnoside and two different amounts of quercetin and hyperoside at the beginning of the sample extraction. For vitexin-2"-O-rhamnoside and hyperoside the theoretically expected amounts of vitexin and quercetin, assuming a complete hydrolysis, were calculated. The recoveries were, on an average, 96.4% for vitexin and 91.5% for quercetin. This indicates almost complete hydrolysis and only little loss of compounds during the sample preparation.

Twelve batches of dried leaves, flowers and fruits of *Crataegus monogyna* Jacq. at different plant development stages were examined for their flavonoid content using method 1 (see Fig. 2). The highest amount of total flavonoids was found in the leaves during the pre-flowering time (April) and the flowering time (beginning of May). Afterwards the total flavonoid content in the leaves decreased and remained at a rather constant level, comparable with the flowers. The fruits, which contain mainly oligomeric and polymeric procyanidins [23], exhibited very low flavonoid concentrations, so that their flavonoid determination and standardization could be left out. The flowers and leaves revealed remarkable

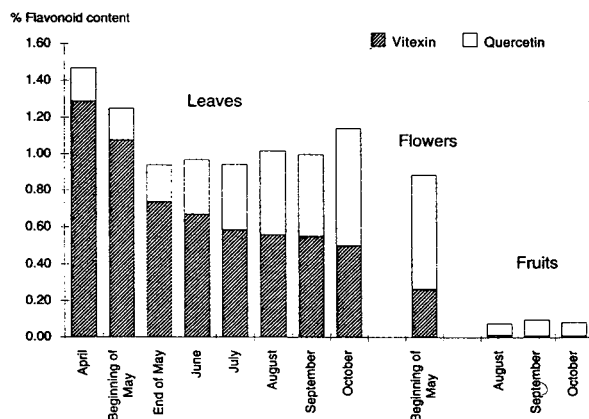


Fig. 2. Flavonoid determination by the hydrolysis method of *Crataegus monogyna* Jacq. at different stages of development.

differences concerning the ratio of vitexin and quercetin: the ratio was 0.4 in the flowers, but 7 in the leaves at the beginning of the collecting period, decreasing to 0.8 in October.

These results are in accordance with the results of other authors who report the maximal flavonoid content for the leaves during the pre-flowering and the flowering time in May [23,24], with an increasing amount of flavonol-O-glycosides towards the end of the vegetation period [24]. Taking into consideration the obtained results, it is recommendable to harvest both the leaves and flowers during the flowering time to get on the one hand the highest content of total flavonoids and, on the other hand, a well-balanced proportion of flavonol-O- and flavone-C-glycosides.

With the intention to get some information on the validity of the hydrolysis method, it was compared to three other quantitative methods (methods 2–4). Two commercial samples 1 and 2 (*Crataegi folium cum flore*) were quantified by these four methods. The results are represented in Table 1. Statistical calculations were carried out by means of the two-tailed Student's t-test.

In both samples the total flavonoid amount obtained by method 2 was 6–6.5% higher (significant; $p < 0.001$) than by method 1. We also found differences concerning the relative concentrations of flavonol-O-glycosides and flavone-C-glycosides: the ratio of vitexin-2"-O-rhamnoside to hyperoside was 1.9 with method 1, but 2.8 with method 2. These differences were significant ($p < 0.001$).

Methods 1 and 2 consider the whole spectrum of flavonoids, that is to say the flavonol-O-glycosides and the flavone-C-glycosides and yield similar amounts of total flavonoids. Nevertheless, method 1 should have priority, because after a simple hydrolysis procedure in order to reduce the flavonoid pattern to two compounds, it is possible to perform the quantitative determination with only two reference standards, whereas with a fingerprint method (like 2) more reference substances and calculating factors are needed.

The results obtained with method 3 were

Table 1
Quantitative flavonoid determination of two samples by four different methods

Method	Flavonoid content (% , dry weight)					
	Sample 1			Sample 2		
	VR ^a	H ^b	Σ ^c	VR ^a	H ^b	Σ ^c
Method 1 ^d (acid hydrolysis)	0.957 (1.9)	0.503 (2.3)	1.460 (1.9)	0.885 (3.2)	0.460 (2.0)	1.345 (2.4)
Method 2 (fingerprint)	1.130 (2.0)	0.415 (3.5)	1.545 (2.3)	1.065 (1.8)	0.372 (4.1)	1.436 (2.3)
Method 3 (Ph. Franç. X)	0.493 (8.2)	0.289 (4.1)	0.783 (6.0)	0.341 (2.0)	0.359 (3.5)	0.700 (1.6)
Method 4 (Ph. Helv. VII)			0.734 ^e (7.0)			0.721 ^e (7.3)

^a Mean ($n = 6$) content of vitexin-2''-O-rhamnoside (VR) with relative standard deviation (%) in parentheses.

^b Mean ($n = 6$) content of hyperoside (H) with relative standard deviation (%) in parentheses.

^c Total flavonoid content, obtained by summing vitexin-2''-O-rhamnoside and hyperoside.

^d To compare the results with those of methods 2 and 3, vitexin was calculated as vitexin-2''-O-rhamnoside and quercetin as hyperoside.

^e Mean ($n = 6$) of total flavonoid content with relative standard deviation (%) in parentheses.

clearly lower, although this method is, in principal, similar to method 2. The significant ($p < 0.001$) loss of about 30% of hyperoside compared to methods 1 and 2 is mostly due to the incomplete extraction of the plant material. The significant ($p < 0.001$) decrease of 50–60% of vitexin-2''-O-rhamnoside compared to methods 1 and 2 resulted from the non-consideration of the acetylated vitexin-2''-O-rhamnoside. Since this compound is not commercially available, an inserted hydrolysis step or summing the peak areas of vitexin-2''-O-rhamnoside and acetyl-vitexin-2''-O-rhamnoside could easily include it.

Method 4, which determines the total flavonoid content, calculated as hyperoside, revealed results in the range of those of method 3. It is, as criticized often [6,7,15,18], not specific and neglects the flavone-C-glycosides. It should not be applied to herbal drugs with a considerable content of flavone-C-glycosides.

The obtained results are in agreement with

those reported by other authors: Lamaison *et al.* [15] found in samples of *Crataegi folium cum flore* 1.74% of total flavonoid content by means of an HPLC fingerprint analysis, but only 0.91% with the spectrophotometric determination. Applying the method of Ph. Franç. X they obtained 0.56% of hyperoside and 0.54% of vitexin-2''-O-rhamnoside. Wagner *et al.* [6] determined 1.87% of total flavonoids in *Crataegi folium cum flore* by HPLC fingerprint analysis and 1.20% by spectrophotometric quantification.

A tea preparation, according to the prescription in the experimental part which is based on literature [25, 26], was quantified by method 1. From the given single dose of 1.8 g plant material (which is prescribed 2–3 times daily), 10–15 mg flavonoids, calculated as hyperoside, were extracted by hot water. This was only half as much as could be extracted by an exhausting extraction with methanol, but it is, already in a single dose, more than the required minimal

daily dose of 10 mg total flavonoids, calculated as hyperoside [2]. The tea preparation was additionally examined for the qualitative composition. It revealed exactly the same fingerprint chromatogram as an extract with 80% methanol.

4. Conclusions

The flavonol-O-glycosides and the flavone-C-glycosides seem to exhibit qualitatively and quantitatively different pharmacological activities [27]. Concerning the inhibition of the 3',5'-cyclic adenosine monophosphate phosphodiesterase, hyperoside as flavonol-O-glycoside showed a clearly higher potency than the flavone-C-glycosides vitexin, vitexin-2"-O-rhamnoside and acetylvitexin-2"-O-rhamnoside [28,29]. C-glycosides are generally considered to be poorer inhibitors than O-glycosides [29,30], and flavonols exhibit a higher inhibitor potency than flavones [31]. On the other hand, for various flavones and flavone-C-glycosides (among them vitexin) an antiarrhythmic and anti-schaemic activity was demonstrated [32]. A positive inotropic effect and an increase of the coronary blood flow was revealed by vitexin-2"-O-rhamnoside, but not by hyperoside [33]. Taking this aspect into consideration, it is certainly advantageous to have the possibility of determining flavonol-O-glycosides and flavone-C-glycosides separately. Therefore we consider acid hydrolysis of the flavonoids to quercetin and vitexin as the most convenient method nowadays for the quantitative analysis of flavonoids in hawthorn as well as for the standardization of hawthorn extracts and preparations.

Acknowledgements

Financial support from Ciba-Geigy OTC Pharma Schweiz, Gland, Switzerland is gratefully acknowledged. We also thank Dr. W. Lippert, München, Germany, for kindly identifying the collected plant material.

References

- [1] H.P.T. Ammon and M. Händel, *Planta Med.*, 43 (1981) 105, 209, 313.
- [2] *Bundesanzeiger*, Nr. 1, 3. 1. 1984.
- [3] A. Leukel, U. Fricke and J. Hölzl, *Planta Med.*, 52 (1986) 545.
- [4] A. Leukel-Lenz, *Thesis*, Philipps-Universität, Marburg, 1988.
- [5] C. Roddewig and H. Hensel, *Arzneimittel-Forsch.*, 27 (1977) 1407.
- [6] H. Wagner, G. Tittel and S. Bladt, *Dtsch. Apoth.-Ztg.*, 123 (1983) 515.
- [7] H. Glasl, *Fresenius' Z. Anal. Chem.*, 321 (1985) 325.
- [8] L.W. Wulf and C.W. Nagel, *J. Chromatogr.*, 116 (1976) 271.
- [9] K. Vande Castele, H. Geiger and C. Van Sumere, *J. Chromatogr.*, 240 (1982) 81.
- [10] D.J. Daigle and E.J. Conkerton, *J. Chromatogr.*, 240 (1982) 202.
- [11] M.C. Pietrogrande, P. Reschiglian, F. Dondi, Y.D. Kahie and V. Bertolasi, *J. Chromatogr.*, 592 (1992) 65.
- [12] J.M. Davis and J.C. Giddings, *Anal. Chem.*, 55 (1983) 418.
- [13] F. Dondi, Y.D. Kahie, G. Lodi, M. Remelli, P. Reschiglian and C. Bigghi, *Anal. Chim. Acta*, 191 (1986) 261.
- [14] J.L. Lamaison and A. Carnat, *Pharm. Acta Helv.*, 65 (1990) 315.
- [15] J.L. Lamaison, A. Carnat, C. Petitjean-Freytet and A.P. Carnat, *Plant. Med. Phytother.*, 25 (1991) 177.
- [16] P. Ficarra, R. Ficarra and A. Tommasini, *Farmaco Ed. Prat.*, 39 (1984) 148.
- [17] A. Hiermann and T. Kartnig, *Sci. Pharm.*, 52 (1984) 30.
- [18] A. Hasler, *Thesis*, No. 9353, ETH Zurich, 1990.
- [19] Sz. Nyiredy, B. Meier, C. Erdelmeier and O. Sticher, *J. High Resol. Chromatogr. Chromatogr. Commun.*, 8 (1985) 186.
- [20] J.B. Harborne, T.J. Mabry and H. Mabry, *The Flavonoids*, Chapman and Hall, London, 1975.
- [21] F. Wessely and G. Moser, *Monatsh. Chem.*, 56 (1930) 97.
- [22] M. Hertog, P. Hollman and D. Venema, *J. Agric. Food Chem.*, 40 (1992) 1591.
- [23] T. Kartnig, A. Hiermann and S. Azzam, *Sci. Pharm.*, 55 (1987) 95.
- [24] J.L. Lamaison and A. Carnat, *Plant. Med. Phytother.*, 25 (1991) 12.
- [25] *Standardzulassungen für Fertigarzneimittel (1986)*, Deutscher Apothekerverlag, Govi Verlag, Frankfurt, Monographie Stand 12, March 1986.
- [26] M. Wichtl, *Teedrogen*, Wissenschaftliche Verlagsgesellschaft mbH, Stuttgart, 1989.
- [27] M. Schüssler and J. Hölzl, *Dtsch. Apoth.-Ztg.*, 132 (1992) 1327.
- [28] M. Schüssler, U. Fricke, N. Nikolov and J. Hölzl, *Planta Med.*, 57, Suppl. Issue 2 (1991) A133.

- [29] T. Nikaïdo, T. Ohmoto, U. Sankawa, T. Tomimori, Y. Miyaichi and Y. Imoto, *Chem. Pharm. Bull.*, 36 (1988) 654.
- [30] E. Petkov, N. Nikolov and P. Uzunov, *Planta Med.*, 43 (1981) 183.
- [31] A. Beretz, R. Anton and J.C. Stoclet, *Experientia*, 34 (1978) 1054.
- [32] F. Occhiuto, G. Busa, S. Ragusa and A. De Pasquale, *Phytotherapy Research*, 5 (1991) 9.
- [33] F. Occhiuto, C. Circosta, R. Costa, F. Briguglio and A. Tommasini, *Plant. Med. Phytother.*, 20 (1986) 52.

Highly sensitive high-performance liquid chromatographic method for the determination of the absolute configuration and the optical purity of di-O-acylglycerols using a chiral derivatizing agent, (*S*)-(+)-2-*tert.*-butyl-2-methyl-1,3-benzodioxole-4-carboxylic acid

Jeong-Hwan Kim, Hirotaka Uzawa, Yoshihiro Nishida, Hiroshi Ohru, Hiroshi Meguro*

Department of Applied Biological Chemistry, Faculty of Agriculture, Tohoku University, 1-1 Tsutsumidori-Amamiyamachi, Aoba-ku, Sendai 981, Japan

First received 27 December 1993; revised manuscript received 19 April 1994

Abstract

A general method was developed to determine the optical purity of 1,2-(or 2,3)-di-O-acyl-*sn*-glycerol, which involves the chemical transformation to the key compound 3-(or 1)-O-*tert.*-butyldimethylsilyldi-O-(+)-TBMB-*sn*-glycerol (**4a** or **4b**). [TBMB = (*S*)-(+)-2-*tert.*-butyl-2-methyl-1,3-benzodioxole]. The chiral di-O-acylglycerols were first silylated and the acyl groups were removed by Grignard degradation to 3-(or 1)-O-*tert.*-butyldimethylsilyl-*sn*-glycerol. Subsequent fluorescent labelling by (+)-TBMB-COOH gave the key compound **4a** or **4b** without arising acyl migration. The diastereoisomers were separated by silica gel TLC or normal-phase silica column HPLC with fluorescence detection. This is an extremely sensitive method to determine the stereoselectivities of lipase reactions.

1. Introduction

Glycerol has a symmetrical plane centre at C-2, being achiral and optically inactive itself. 1,2-Di-O-acyl-*sn*-glycerol is, however, chiral with the enantiomer of 2,3-di-O-acyl-*sn*-glycerol. Although they may be generated by lipase-catalysed hydrolysis of triacylglycerols or esterification of monoacylglycerols, the stereoselectivities

of these lipase reactions have not been well established because of the difficulty of determining the optical purities of di-O-acylglycerols. The facile acyl migration may be another reason for the poor stereoselectivities observed in the previous lipase reaction.

Several methods have been reported to determine the optical purity of 1,2-(or 2,3)-di-O-acylglycerol [1–6]. Recently, Takagi and co-workers [3,4] and Sempore and Bezard [5] reported the enantiomeric separation of di-O-acylglycerols using either normal- or reversed-

* Corresponding author.

phase chiral columns after derivatization to the 3,5-dinitrophenylurethane (3,5-DNPU) derivatives. Another HPLC separation was also reported by Rogalska et al. [6] using diastereoisomeric carbamate derivatives on a normal-phase column. However, all the mentioned methods were less general and authentic samples with known configurations were necessary in each acyl group to determine the absolute configuration.

More recently, we have reported two methods for the determination of the optical purity and absolute configuration of 1,2-(or 2,3)-di-O-acylglycerol via the key compound 1,2-di-O-benzoyl-3-O-*tert.*-butyl-dimethylsilyl-*sn*-glycerol or its enantiomer either by a circular dichroism (CD) method or by chiral column HPLC using UV detection [7,8]. However, the former method needs CD equipment and the latter needs supplementary GC data for correction for the contaminated 1,3-isomer which overlaps the peak of the dibenzoyl derivative of 1,2-di-O-acyl-*sn*-glycerol in HPLC. Therefore, a simpler and more sensitive method is required to determine the absolute configuration and the optical purity of di-O-acylglycerols in order, for example, to determine the stereoselectivity of lipase hydrolysis in the early stages.

We have also developed (*S*)-(+)-2-*tert.*-butyl-2-methyl-1,3-benzodioxole-4-carboxylic acid [(*S*)-(+)-TBMB-COOH] as a fluorescent chiral derivatizing agent [9–11]. This reagent was designed to determine the absolute configuration and optical purity of amines and alcohols using HPLC, NMR and CD.

In this paper, we describe enantiomer separations of di-O-acylglycerols using this reagent. Di-O-acyl-*sn*-glycerols (**1a** and **1b**) were derivatized to *tert.*-butyldimethylsilylated 1,2-(and 2,3)-di-O-(+)-TBMB-*sn*-glycerols (**4a** and **4b**), and the diastereomers thus derived were well separated by normal-phase silica column HPLC. The sensitivity was greatly improved by using fluorescent detection, and possible all isomers of *sn*-1,2-, *sn*-2,3- and 1,3-di-O-acylglycerols were completely separated within 30 min.

2. Experimental

2.1. Chemicals

1,2-Di-O-palmitoyl-*sn*-glycerol [**1a**, ca. 100% enantiomeric excess (e.e.) as determined by HPLC of the (+)-TBMB derivative] and 1,3-di-O-palmitoyl-*sn*-glycerol (**1c**) were purchased from Sigma (St. Louis, MO, USA). D,L-1,2-Dipalmitin (**1**, racemate) was obtained from Nacalai Tesque (Kyoto, Japan). Triolein, substrate of lipase-catalysed hydrolysis, was also purchased from Sigma. Lipase (Amano AP, EC 3.1.1.3) from *Pseudomonas* sp. was purchased from Amano Pharmaceutical (Nagoya, Japan). (+)-TBMB-COOH (100% e.e. as determined by ¹H NMR of the (–)-cinchonidine salt) was synthesized according to our method [9].

2.2. Derivatizations of di-O-acyl glycerols

Preparation of 1,2-di-O-(+)-TBMB-3-O-tert.-butyldimethylsilyl-rac-glycerol (4) from 1,2-di-O-palmitoyl-rac-glycerol (1)

Silylation of 1,2-di-O-acyl-rac-glycerol. 1,2-Di-O-palmitoyl-*rac*-glycerol (**1**, 18.0 mg, 0.03 mM) in methylene chloride (10 ml) was added to *tert.*-butyldimethylsilyl chloride (TBDMS-Cl, 300 mg, 1.99 mM) in dry pyridine (10 ml) at room temperature. After 2 h, the reaction mixture was diluted with CH₂Cl₂ (20 ml) and washed with saturated NaHCO₃ solution (2 × 10 ml) and water (20 ml) to neutrality. The methylene chloride solution was dried over MgSO₄, the latter was removed by filtration and the solvent was evaporated in vacuo at 40°C to afford the monosilyl compound **2**, which was purified by column chromatography on silica gel [toluene–ethyl acetate (20:1, v/v)] before use in the next reaction (20.0 mg, yield 93%) [7].

Replacement of acyl groups of 2 with (+)-TBMB groups. The acyl groups were removed a Grignard reaction as described previously [7]. Methylmagnesium bromide in diethyl ether (0.1

ml, 0.3 mM) was added to the solution of **2** (20.0 mg, 0.03 mM) in dry diethyl ether (10 ml) under a nitrogen atmosphere. The mixture was stirred for a few minutes and saturated NH_4Cl solution (20 ml) was added carefully to decompose the excess of the Grignard reagent at 0°C . After 1 h, the usual work-up in a similar manner to that described previously [7] using ethyl acetate (3×20 ml) gave the deacylated derivative **3** (yield ca. 100%).

On the other hand, (+)-TBMB-COOH (71 mg, 100% e.e., 0.3 mM) in dry benzene (10 ml) was added into SOCl_2 (450 mg, 3.77 mM) and the mixture was kept at 60°C . After 10 min, excess of SOCl_2 and benzene were removed in vacuo to give (+)-TBMB-COCl. Then, dry pyridine (10 ml), 4-dimethylaminopyridine (DMAP, ca. 10 mg) and (+)-TBMB-COCl were added to the solution of **3** in dry CH_2Cl_2 (10 ml) at room temperature. After 4 h, the usual work-up gave optically active 1,2-di-O-(+)-TBMB-3-O-*tert.*-butyldimethylsilyl-*rac*-glycerol (**4**), which was purified by preparative TLC [*n*-hexane-ethyl acetate (20:1, v/v)] (18.2 mg, yield 97%).

1,2-Di-O-(+)-TBMB-3-O-TBDMS-*rac*-glycerol (**4**): $[\alpha]_D^{22} + 19.5^\circ$ ($c = 0.58$, MeOH); high-resolution electron impact (EI) MS, found 642.3199, calculated for $\text{C}_{35}\text{H}_{50}\text{O}_9\text{Si}$ [M^+] 642.3221; ^1H NMR (400 MHz, CDCl_3), δ 0.032–0.038 [12H, s $\times 2$, (Si–Me₂) $\times 2$], 0.869–0.870 [18H, s $\times 2$, (Si-*tert.*-Bu) $\times 2$], 0.999–1.046 [36H, s $\times 3$, (TBMB-*tert.*-Bu) $\times 4$], 1.485–1.568 [12H, s $\times 3$, (TBMB–Me) $\times 4$], 3.940–5.401 [10H, m, glycerol (*sn*-1, *sn*-2, *sn*-3) $\times 2$], 6.707–7.348 [12H, m, (TBMB-aromatic 3H) $\times 4$].

Preparation of 1,2-di-O-(+)-TBMB-3-O-tert.-butyldimethylsilyl-sn-glycerol (4a) from 1,2-di-O-palmitoyl-sn-glycerol (1a)

Silylation and subsequent di-O-(+)-TBMB derivatization of 1,2-di-O-palmitoyl-*sn*-glycerol [**1a**, ca. 100% e.e. as determined by HPLC of the (+)-TBMB derivative], conducted in the same manner as described above, gave optically active 1,2-di-O-(+)-TBMB-3-O-*tert.*-butyldimethylsilyl-*sn*-glycerol (**4a**, ca. 100% e.e., yield

92%). The HPLC analysis indicated that **4a** is optically pure.

1,2-Di-O-(+)-TBMB-3-O-TBDMS-*sn*-glycerol (**4a**, standard sample): $[\alpha]_D^{22} + 7.7^\circ$ ($c = 1.08$, MeOH); high-resolution EI-MS, found 642.3222, calculated for $\text{C}_{35}\text{H}_{50}\text{O}_9\text{Si}$ [M^+] 642.3221; ^1H NMR (400 MHz, CDCl_3), δ 0.032–0.038 (6H, s $\times 2$, Si–Me₂), 0.869 (9H, s, Si-*tert.*-Bu), 1.046 [18H, s, (TBMB-*tert.*-Bu) $\times 2$], 1.485 ([6H, s, (TBMB–Me) $\times 2$], 3.913–3.992 [2H, dd $\times 2$, glycerol (*sn*-3)], 4.553–4.622 [2H, dd $\times 2$, glycerol (*sn*-1)], 5.378–5.401 [1H, m, glycerol (*sn*-2)], 6.722–7.335 [6H, m, (TBMB-aromatic 3H) $\times 2$].

Preparation of 2,3-di-O-(+)-TBMB-1-O-tert.-butyldimethylsilyl-sn-glycerol (4b)

2,3-Di-O-(+)-TBMB-1-O-*tert.*-butyldimethylsilyl-*sn*-glycerol [**4b**, $R_F = 0.26$ on TLC, *n*-hexane-ethyl acetate (20:1, v/v)] was separated from 1,2-di-O-(+)-TBMB-3-O-*tert.*-butyldimethylsilyl-*rac*-glycerol (**4**) on a preparative TLC plate [*n*-hexane-ethyl acetate (20:1, v/v), developed five times]. The lower band on the preparative TLC plate corresponding to **4b** was carefully scraped off and dissolved in CH_2Cl_2 (10 ml). Then, silica gel was removed by filtration (CH_2Cl_2 , 3×10 ml) and the filtrate was evaporated to dryness at 40°C under reduced pressure to give **4b** (diastereomer of **4a**).

1,2-Di-O-(+)-TBMB-3-O-*tert.*-butyldimethylsilyl-*sn*-glycerol (**4a**, $R_F = 0.28$) was also separated on the preparative TLC plate from 1,2-di-O-(+)-TBMB-3-O-*tert.*-butyldimethylsilyl-*rac*-glycerol (**4**) in the same manner as described above.

2,3-Di-O-(+)-TBMB-1-O-TBDMS-*sn*-glycerol (**4b**): $[\alpha]_D^{22} + 32.3^\circ$ ($c = 0.67$, MeOH); high-resolution EI-MS, found 642.3223, calculated for $\text{C}_{35}\text{H}_{50}\text{O}_9\text{Si}$ [M^+] 642.3221; ^1H NMR (400 MHz, CDCl_3), δ 0.037 (6H, s, Si–Me₂), 0.870 (9H, s, Si-*tert.*-Bu), 0.999–1.011 [18H, s $\times 2$, (TBMB-*tert.*-Bu) $\times 2$], 1.562–1.568 [6H, s $\times 2$, (TBMB–Me) $\times 2$], 3.932–3.995 [2H, dd $\times 2$, glycerol (*sn*-1)], 4.525–4.631 [2H, dd $\times 2$, glycerol (*sn*-3)], 5.375–5.401

[1H, m, glycerol (*sn*-2)], 6.719–7.347 [6H, m, (TBMB–aromatic 3H) × 2].

1,2 - Di - O - (+) - TBMB - 3 - O - TBDMS-*sn*-glycerol (**4a**, scraped off from **4** on TLC plate): $[\alpha]_D^{22} + 7.7^\circ$ ($c = 0.94$, MeOH); high-resolution EI - MS, found: 642.3222, calculated for $C_{35}H_{50}O_9Si$ [M^+] 642.3221; 1H NMR (400 MHz, $CDCl_3$), δ 0.032–0.038 (6H, $s \times 2$, Si-Me₂), 0.869 (9H, s , Si-*tert*-Bu), 1.046 [18H, s , (TBMB-*tert*-Bu) × 2], 1.485 [6H, s , (TBMB-Me) × 2], 3.913–3.992 [2H, $dd \times 2$, glycerol (*sn*-3)], 4.553–4.622 [2H, $dd \times 2$, glycerol (*sn*-1)], 5.378–5.401 [1H, m , glycerol (*sn*-2)], 6.722–7.335 [6H, m , TBMB–aromatic 3H) × 2].

Preparation of 1,3-di-O-(+)-TBMB-2-O-tert.-butyldimethylsilyl-sn-glycerol (4c) from 1,3-di-O-palmitoyl-sn-glycerol (1c)

Silylation and subsequent di-O-(+)-TBMB derivatization of 1,3-di-O-palmitoyl-*sn*-glycerol (**1c**, achiral) were also conducted by the above method to give 1,3-di-O-(+)-TBMB-2-O-*tert*-butyldimethylsilyl-*sn*-glycerol (**4c**, yield 89%).

1,3 - Di - O-(+) - TBMB - 2 - O - TBDMS - *sn*-glycerol (**4c**): $R_F = 0.28$ on TLC [*n*-hexane–ethyl acetate 20:1, (v/v)]; high-resolution EI-MS, found 642.3197, calculated for $C_{35}H_{50}O_9Si$ [M^+] 642.3221; 1H NMR (400 MHz, $CDCl_3$), δ 0.087–0.093 (6H, $s \times 2$, Si-Me₂), 0.860 (9H, s , Si-*tert*-Bu), 1.063–1.066 [18H, $s \times 2$, (TBMB-*tert*-Bu) × 2], 1.587–1.600 [6H, $s \times 2$, (TBMB-Me) × 2], 4.264–4.291 [1H, m , glycerol (*sn*-2)], 4.390–4.500 [4H, m , glycerol (*sn*-1, *sn*-3)], 6.745–7.346 [6H, m , (TBMB–aromatic 3H) × 2].

2.3. Fluorescence spectra and HPLC separations

For measurement of the excitation and emission spectra of each derivative (**4a** or **4b**), a JASCO (Tokyo, Japan) Model FP-550A spectrofluorimeter with a 1-cm quartz cell was employed without spectral correction. Excitation and emission spectra of 6.86 μM of each derivative (**4a** or **4b**) were measured in the same solvent as the HPLC mobile phase [*n*-hexane–*n*-butanol

(750:1, w/w)]. The fluorescence intensities of the derivatives were determined at the maximum excitation and emission wavelengths.

HPLC separations were conducted with a Tosoh (Tokyo, Japan) CCPM instrument connected to an FS-8010 fluorescent detector monitoring at $\lambda_{ex} = 310$ nm and $\lambda_{em} = 370$ nm. Separations were achieved on a Deverosil 60-3 silica gel column (Nomura Chemical) (stainless steel, 5 cm × 4.6 mm I.D.). The analyses were carried out isocratically using a mixture of HPLC-grade *n*-hexane and *n*-butanol (750:1, w/w) at a flow-rate of 0.6 ml/min as the mobile phase at room temperature. For quantitative determination, peak areas were calculated using an 807-IT integrator (JASCO).

2.4. Applications to the determination of stereochemistry of lipase-catalysed reaction

Lipase-catalysed hydrolysis of triolein in the initial stages

A suspension of triolein (100 mg) in 4 ml of 1 M Tris–HCl buffer (pH 7.5) containing the enzyme (Amano AP, 25 mg) was incubated at 40°C with vigorous shaking. After the reaction had proceeded to the extent of *ca.* 5–10% (10 min), monitored by silica gel TLC [toluene–ethyl acetate (20:1, v/v)], the enzymatic hydrolysate was extracted with diethyl ether [7]. Silylation and subsequent di-O-(+)-TBMB derivatization were then conducted according to the above method.

Lipase-catalysed esterification of 2-O-benzoyl-glycerol

The substrate of lipase-catalysed esterification, 2-O-benzoylglycerol, was prepared according to the literature [12]. 2-O-Benzoyl-1,3-di-O-benzylglycerol (120 mg, 0.32 mM) in ethyl acetate (10 ml) was debenzylated with Pd–C under a hydrogen atmosphere at room temperature (yield *ca.* 100%). At the end of the reaction, the mixture was filtered off and concentrated under reduced pressure at 40°C.

2-O-Benzoylglycerol (60 mg) in diisopropyl

ether (5 ml) was mixed with palmitic acid (660 mg, 2.56 mM) and lipase (Amano AP, 15 mg), and the mixture was incubated at 40°C. After 20 h, the reaction mixture was filtered off, washed with ethyl acetate (3 × 10 ml) and concentrated under reduced pressure at 40°C. Silylation and subsequent di-O-(+)-TBMB derivatization were then conducted according to the above method.

3. Results and discussion

By di-O-TBMB derivatization, the chiral di-O-acylglycerols were subjected to the introduction of two new chiral centres, which led to the generation of eight kinds of diastereomers. Hence it is essential for the determination of the original optical purity of 1,2-(or 2,3)di-O-acyl-*sn*-glycerol (**1a** or **1b**) to use (+)-TBMB-COOH acid of 100% optical purity for the derivatization. (+)-TBMB-COOH [100% e.e. as determined by ¹H NMR of the (–)-cinchonidine salt] used in this study was synthesized according to our method, and its optical purity was confirmed in our previous studies [9–11]. Consequently, only two diastereomers can be derived from a mixture of 1,2- and 2,3-di-O-acylglycerols, as can be seen in Fig. 3.

The TBMB derivatization shown in Fig. 1 was detailed in the Experimental section. It proceeded to an overall yield of more than 90% and no acyl migration was observed during the reactions. The TBMB carboxylation of **3** (or **3a** or **3c**) was performed under the usual conditions using pyridine in CH₂Cl₂. The use of more than a fourfold excess of (+)-TBMB-COOH was necessary for the completion of the derivatization. The other reaction conditions from **1** to **2** and then to **3** had been optimized previously [7,8].

Fig. 1 represents all reactions starting from di-O-acylglycerol (racemate **1** or optically active **1a** or achiral **1c**) to obtain the corresponding TBMB derivative (**4** or **4a** or **4c**). Compound **4a** could be also obtained from **4** by the TLC separation. Compound **4b** (diastereomer of **4a**) was also obtainable in this way.

Fig. 2 shows a typical HPLC trace of the key

compounds (**4**) derived from di-O-acylglycerols. HPLC gave the 1,2-di-O-(+)-TBMB-3-O-TBDMS-*sn*-glycerol (**4a**) and 2,3-di-O-(+)-TBMB-1-O-TBDMS-*sn*-glycerol (**4b**, diastereomer of **4a**) as two symmetrical peaks in less than 30 min after injection with a separation factor (α) of 1.35. The *sn*-1,2-isomer (**4a**) was eluted first, followed by the *sn*-2,3-isomer (**4b**). In addition, the 1,3-di-O-(+)-TBMB-2-O-TBDMS-glycerol (**4c**) derivatized from 1,3-di-O-acylglycerol (**1c**, achiral), which may be contaminated in the lipase hydrolysate, was eluted in front of the *sn*-1,2-isomer (**4a**). Hence, all three regioisomers of di-O-acylglycerols were well separated using TBMB derivatization.

For the fluorescence spectra, the maximum excitation and emission wavelengths of 1,2-di-O-(+)-TBMB-3-O-TBDMS-*sn*-glycerol (**4a**) were approximately 315–317 and 358–361 nm [in *n*-hexane-*n*-butanol (750:1, w/w)], respectively. The same results were obtained in the fluorescence spectra of 2,3-di-O-(+)-TBMB-1-O-TBDMS-*sn*-glycerol (**4b**). Both of the excitation and emission fluorescence intensities were identical for **4a** and **4b**, confirming that the two diastereomers can be monitored quantitatively in HPLC analysis using a fixed single wavelength for fluorescence excitation and detection. The HPLC fluorescence detector was therefore, fixed at 310 and 370 nm for excitation and detection, respectively.

In order to confirm the reproducibility and the efficiency of the present method, the derivatization was carried out using di-O-acylglycerols of known optical purities to give the results summarized in Table 1 and Fig. 3. By using a series of standard solutions containing a mixture of di-O-acylglycerols (**1** and **1a**) with a known ratio, excellent agreement was obtained for the optical purities before and after the derivatization of di-O-acylglycerols within the usual limits of variation (S.D. = 0.91, *n* = 4).

Fig. 3 shows HPLC traces of di-O-TBMB-glycerol derivatives derived from four standard di-O-acylglycerols represented in Table 1. It should be noted that the chromatogram (iv) of the corresponding 1,2-di-O-(+)-TBMB-3-O-TBDMS-*sn*-glycerol derivative from commercial-

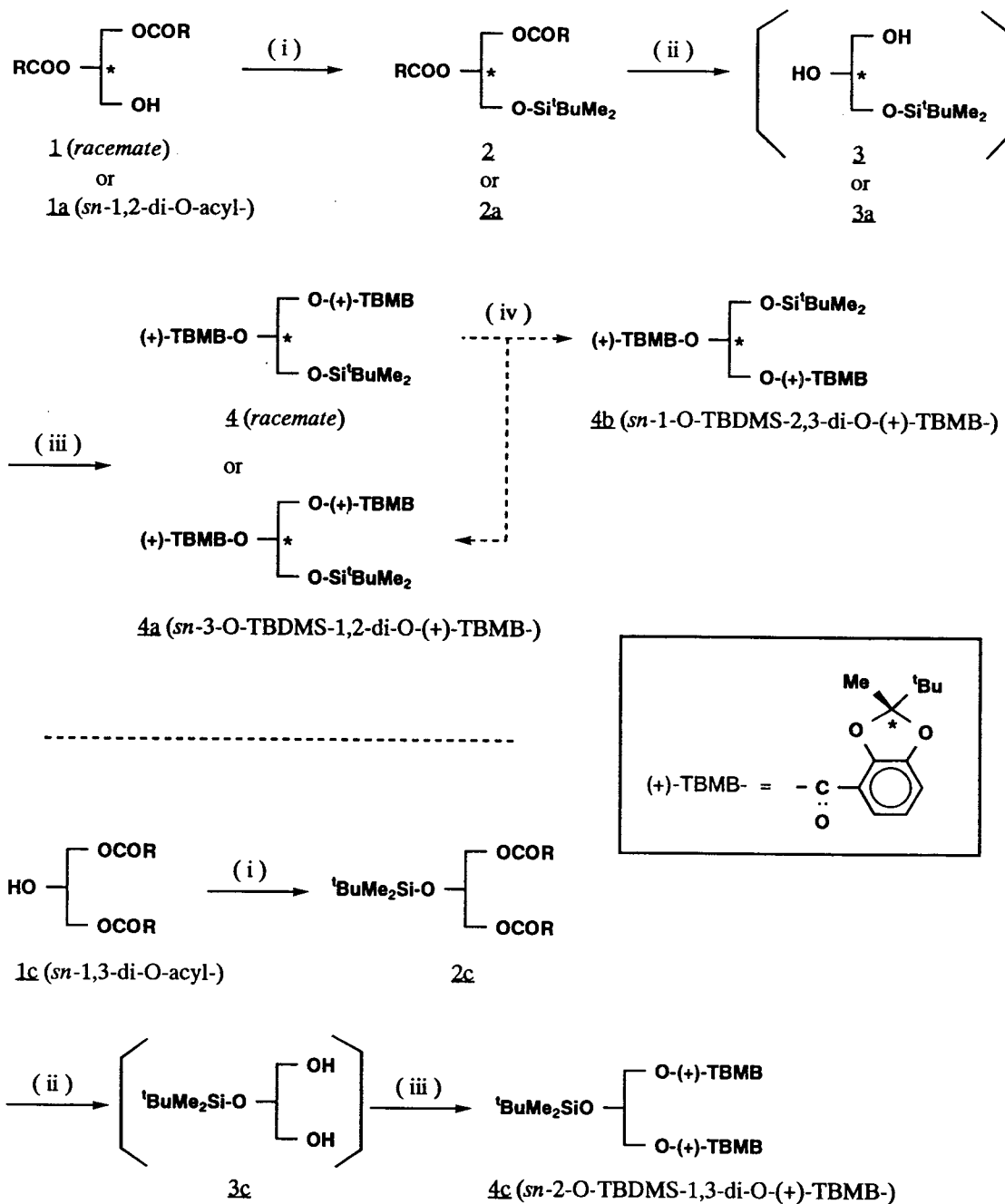


Fig. 1. Scheme for the derivatization to the di-O-(+)-TBMB-glycerol derivatives from di-O-acylglycerols. 1 = D,L-1,2-dipalmitin (racemate); 1a = 1,2-di-O-palmitoyl-*sn*-glycerol (*sn*-1,2-enantiomer); 1c = 1,3-di-O-palmitoyl-*sn*-glycerol, R = -(CH₂)₁₄CH₃. (i) Pyridine, *tert*-butyl-dimethylsilyl chloride (TBDMS-Cl), r.t.; (ii) methylmagnesium bromide, diethyl ether, r.t.; (iii) (+)-TBMB-COCl, pyridine, 4-dimethylaminopyridine (DMAP), r.t.; (iv) separation by TLC [*n*-hexane-ethyl acetate (20:1, v/v), developed five times] (r.t. = room temperature).

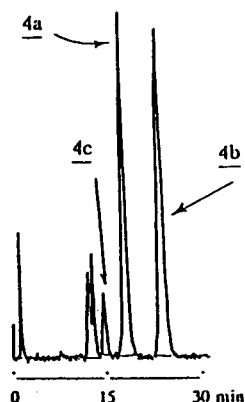


Fig. 2. Chromatogram of di-O-acylglycerols labelled with (+)-TBMB-COOH. **4a** = *sn*-3-O-TBDMS-1,2-di-O-(+)-TBMB-glycerol; **4b** = *sn*-1-O-TBDMS-2,3-di-O-(+)-TBMB-glycerol; **4c** = *sn*-2-O-TBDMS-1,3-di-O-(+)-TBMB-glycerol. HPLC conditions: silica gel column (Deverosil 60-3, 5 cm × 4.6 mm I.D.); $\lambda_{\text{ex}} = 310$ nm, $\lambda_{\text{em}} = 370$ nm; eluent, *n*-hexane-*n*-butanol (750:1, w/w); flow-rate 0.6 ml/min; temperature, 22–24°C.

ly available 1,2-di-O-palmitoyl-*sn*-glycerol (99% purity, Sigma) gave no peak of 2,3-di-O-(+)-TBMB-1-O-TBDMS-*sn*-glycerol (**4b**) or the 1,3-isomer (**4c**). This means that the 1,2-di-O-palmitoyl-*sn*-glycerol (**1a**) used is optically pure (*ca.* 100% e.e.). This, together with the other results in Fig. 3 and Table 1, indicates that during the derivatization procedures (silylation, Grignard

deacylation and TBMB derivatization) no migration of acyl and silyl groups occurs, which might affect the quantification in the present method. The use of di-O-palmitoyl-*rac*-glycerol (**1**) gave two peaks corresponding to **4a** and **4b** with identical intensities. This also reveals that there is no chiral discrimination by (+)-TBMB-COOH in the derivatization.

Therefore, the peak areas of **4a** and **4b** under the present HPLC conditions could be used directly to determine the optical purity of the mixture of di-O-acyl glycerols without a calibration process. The detection limit of 1,2-di-O-palmitoyl-*sn*-glycerol (**1a**) was about 0.3 pmol on-column (signal-to-noise ratio = 3).

We applied this method to determine the stereoselectivities both in lipase-catalysed hydrolysis and esterification using triolein and 2-O-benzoylglycerol, respectively (Table 2). The lipase hydrolysate and the esterificate were both derivatized to the key compound di-O-(+)-TBMB-glycerol, which was subjected to the HPLC analysis to determine the optical purity. HPLC showed that the optical purity was 42.0% e.e. (S.D. = 0.84, *n* = 5) with *sn*-1 preference in the hydrolysis and 7.9% e.e. (S.D. = 0.40, *n* = 4) with *sn*-3 preference in the esterification. Although the di-O-acylglycerols obtained by these lipase reactions were extremely small amounts

Table 1
Comparison of optical purities before and after the derivatization of standard di-O-acylglycerols

Standard di-O-acylglycerol mixture before derivatization ^a			After derivatization to di-O-(+)-TBMB-glycerol derivatives ^b	
D,L-1,2-Dipalmitin (1 , racemate) (mg)	1,2-Di-O-palmitoyl- <i>sn</i> -glycerol (1a) (mg)	Calculated optical purity (% e.e.)	Average observed optical purity (% e.e.)	S.D.
27	Free	0	0.3 (<i>sn</i> -1,2-) (<i>n</i> = 4)	0.91
18.22	9.04	33.2	32.9 (<i>n</i> = 2)	–
7.25	14.75	67.1	68.3 (<i>n</i> = 2)	–
Free	18	100	99.6 (<i>n</i> = 5)	0.83

^a Each standard solution was prepared by mixing **1** (racemate) and **1a** (*ca.* 100% e.e.) in the required and their optical purity was calculated from the ratio of the **1** and **1a** contents [% e.e. before the derivatization = $\frac{\mathbf{1a}}{\mathbf{1a} + \mathbf{1}} \cdot 100$].

^b The HPLC peak areas of di-O-(+)-TBMB glycerol derivatives (**4a** and **4b**) derived from each standard di-O-acylglycerol mixture were used directly to determine the optical purity of the mixture of di-O-acylglycerols without correction [% e.e. after the derivatization = $\frac{\text{peak area of } \mathbf{4a} - \text{peak area of } \mathbf{4b}}{\text{peak area of } \mathbf{4a} + \text{peak area of } \mathbf{4b}} \cdot 100$].

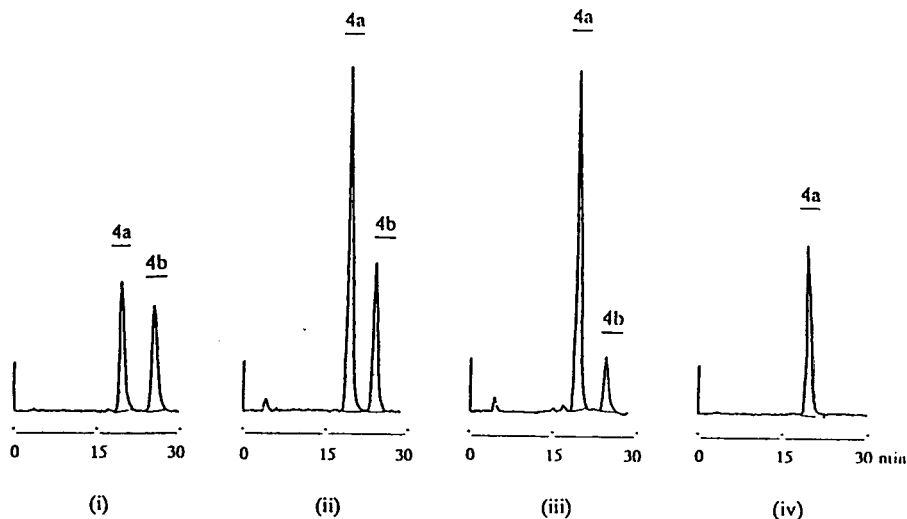


Fig. 3. Chromatograms of di-O-(+)-TBMB-glycerol derivatives derived from each standard mixture of di-O-acylglycerols (**1** and **1a**) with a known ratio (see Table 1). (i) Racemate, (ii) 33.2%, (iii) 67.1% and (iv) 100% optical purity of di-O-acylglycerols. HPLC conditions as in Fig. 2.

(ca. 5 mg, <10% yield), their corresponding di-O-TBMB derivatives were analysed with good reproducibility.

For comparison of these results, the same lots

of the lipase hydrolysate and the esterificate were also subjected to our previous method based on chiral column HPLC [8]. The two methods indicated the well matched optical

Table 2

Optical purities of di-O-(+)-TBMB-glycerols derived from di-O-acylglycerols obtained by lipase-catalysed hydrolysis and esterification

Substrate	lipase → diisopropyl ether	di-O-acylglycerol → 4	Optical purity (% e.e.)		Preference of lipase reaction
			Average	S.D.	
Hydrolysis:					
$\text{RCOO} \left[\begin{array}{c} \text{OCOR} \\ \text{OCOR} \end{array} \right] \rightarrow \text{RCOO} \left[\begin{array}{c} \text{OH} \\ \text{OCOR} \end{array} \right] \rightarrow \mathbf{4}$			42.0 ($n = 5$) ^a	0.84	<i>sn</i> -1
R = $-(\text{CH}_2)_7\text{CH} = \text{CH}(\text{CH}_2)_7\text{CH}_3$					
Esterification:					
$\text{BzO} \left[\begin{array}{c} \text{OH} \\ \text{OH} \end{array} \right] \rightarrow \text{BzO} \left[\begin{array}{c} \text{OH} \\ \text{OCOR}' \end{array} \right] \rightarrow \mathbf{4}$			7.9 ($n = 4$) ^a	0.40	<i>sn</i> -3
R' = $-(\text{CH}_2)_{14}\text{CH}_3$					

^a For the comparison of the results for the present di-O-(+)-TBMB derivative method with those for our previous method [8], the same lots of the lipase hydrolysate and the esterificate were also subjected to our previous method based on chiral column HPLC. The optical purities of the former and the latter were 43.5% e.e. with *sn*-1 preference and 5.6% e.e. with *sn*-3 preference, respectively.

purities and absolute configurations of the di-O-acylglycerols. However, it should be noted that the previous method was less sensitive and needed an expensive chiral HPLC column and GC equipment to separate the 1,3-di-O-benzoylated isomer from the *sn*-1,2-di-O-benzoylated glycerol overlapping in the HPLC separation.

Using the present method, *sn*-1,2-, *sn*-2,3- and 1,3-di-O-(+)-TBMB isomers obtained from their corresponding di-O-acylglycerols could be completely separated within 30 min by silica gel column HPLC and detected with higher sensitivity (>100-fold) using fluorescence detection than using our previous dibenzoate method with UV detection.

In conclusion, a new approach was developed to determine the optical purity of 1,2-(or 2,3)-di-O-acylglycerol, which has been one of the most difficult targets in enantiomeric separations. This method needs no special analytical equipment and allows the optical purity to be determined at the picomole level taking advantage of the strong fluorescence of (+)-TBMB-COOH.

Acknowledgements

We are grateful to Dr. K. Akasaka of Tohoku University for useful suggestions. This work was

partially supported by a Grant-in-Aid for Scientific Research from the Ministry of Education, Science and Culture of Japan, and also by Fellowships to H.U. from the Japan Society for the Promotion of Science for Japanese Junior Scientists.

References

- [1] W. Schlenk, *J. Am. Oil Chem. Soc.*, 42 (1965) 945.
- [2] H. Brockerhoff, *J. Lipid Res.*, 8 (1967) 167.
- [3] Y. Itabashi and T. Takagi, *J. Chromatogr.*, 402 (1987) 257.
- [4] T. Takagi and T. Suzuki, *J. Chromatogr.*, 519 (1990) 237.
- [5] B.G. Sempore and J.A. Bezar, *J. Chromatogr.*, 557 (1991) 227.
- [6] E. Rogalska, S. Ransac and R. Verger, *J. Biol. Chem.*, 265 (1990) 20271.
- [7] H. Uzawa, T. Noguchi, Y. Nishida, H. Ohruai and H. Meguro, *Biochim. Biophys. Acta*, 1168 (1993) 253.
- [8] H. Uzawa, H. Ohruai, H. Meguro, T. Mase and A. Ichida, *Biochim. Biophys. Acta*, 1169 (1993) 165.
- [9] Y. Nishida, H. Ohruai and H. Meguro, *Tetrahedron Lett.*, 30 (1989) 5277.
- [10] Y. Nishida, H. Ohruai, H. Meguro and C. Kabuto, *Anal. Sci.*, 7 (1991) 349.
- [11] Y. Nishida, M. Abe, H. Ohruai and H. Meguro, *Tetrahedron: Asymmetry*, 4 (1993) 1431.
- [12] H. Hori, Y. Nishida, H. Ohruai and H. Meguro, *J. Org. Chem.*, 54 (1989) 1346.



ELSEVIER

Journal of Chromatography A, 677 (1994) 45–52

JOURNAL OF
CHROMATOGRAPHY A

Novel DNA-Sepharose purification of the FadR transcription factor

Concetta DiRusso, R. Preston Rogers, Harry W. Jarrett*

Department of Biochemistry, University of Tennessee, 800 Madison Avenue, Memphis, TN 38163, USA

First received 14 February 1994

Abstract

A DNA sequence bound by the FadR transcription factor of *Escherichia coli* was covalently attached to Sepharose by two different approaches: by chemical coupling or by template-directed enzymatic synthesis using a DNA polymerase. The two kinds of DNA-Sepharose were packed into small columns and used for the purification of the FadR protein; chromatography was without using competitor DNA and the supports contained single-copy, non-repetitive DNA sequences. Comparison showed that the enzymatically prepared support, while having less bound DNA, bound more FadR protein than did the chemically prepared support. This probably results from the lack of detrimental DNA modification by the gentle enzymatic procedure. The chemically prepared support was of lower capacity but yielded purer FadR protein when compared under the same elution conditions. This may be explained by the simpler DNA sequence which could be coupled chemically; less contaminating proteins were bound by the simpler DNA sequence. However, the enzymatically prepared support could also yield comparable purity if the protocol was modified to include additional washes with salt containing buffers. In all cases, FadR was eluted from the DNA using high-salt (0.8 M) mobile phase; ligand-specific elution of FadR using a fatty acyl-coenzyme A thiol ester was ineffective. Affinity chromatography on DNA-Sepharose provided a more rapid, simple purification of FadR than conventional purification techniques and yielded biologically active protein.

1. Introduction

DNA-binding proteins serve roles as transcription factors, restriction endonucleases, DNA and RNA polymerases, and in DNA recombination and repair processes. Since many of these proteins are present in only relatively low amounts in cells, their purification can be challenging. However, due to the role of these proteins in cellular regulation, their purification and characterization is often of fundamental importance.

Affinity chromatography is a powerful protein

purification technique. For DNA-binding proteins, the technique requires that DNA be stably linked to a solid support. Different strategies which have been used to produce DNA supports and their uses in purifying DNA-binding proteins have been reviewed [1,2]. DNA affinity chromatography has several advantages in the purification of DNA-binding proteins. Because affinity chromatography techniques usually give high purity and yield, they often result in simple purification schemes. In the case of DNA-binding proteins, the DNA sequence bound by the protein is also its most distinguishing feature; because of the lack of other unique characteris-

* Corresponding author.

tics, classical purification techniques can only be applied empirically, while affinity chromatography using the DNA consensus binding sequence provides a rational approach.

One problem which has slowed the use of DNA affinity chromatography has involved the procedures used to couple DNA to supports. Either non-covalent attachment has been used with accompanying concerns about stability of the media to prolonged or harsh use or covalent attachment techniques which are known or suspected of modifying the DNA nucleotide bases must be used. Since these nucleotide bases provide the basis of the specific separation, their modification is a matter of concern. Recently, a new technique for producing DNA supports for affinity chromatography has been described [3]. The method involves chemically linking (dT)₁₈ by way of its 5' end to a solid support using chemistry which does not modify thymidine bases. A template sequence containing a 3' end poly(A) tail is then hybridized to the support. The template specified sequence is then copied enzymatically (using DNA polymerase) and covalently onto the 3' end of the (dT)₁₈ support to make a new DNA support. Furthermore, the same recent study has shown that nucleotide bases in double helical DNA are less susceptible to at least one kind of coupling chemistry. Thus, chemical coupling of double-stranded DNA may minimize nucleotide modification over that which would occur with coupling of single strands.

Here, we extend these enzymatic methods to the synthesis of a DNA-Sepharose support which specifically binds the FadR transcription factor of *Escherichia coli*. FadR regulates many genes and operons required for fatty acid metabolism [4]. At least seven promoters whose protein products are required for growth on fatty acids as a sole carbon and energy source are negatively controlled by FadR while the *fabA* gene which is required for unsaturated fatty acid biosynthesis is activated by FadR [4,5]. FadR mediates repression and activation by binding to specific target sequences within the promoter of each of the FadR-responsive genes. DNA binding by FadR is specifically inhibited by long-chain acyl

coenzyme A thiol esters. Of the FadR binding sites characterized to date that which occurs within the *fadB* promoter has the highest FadR binding affinity. This site, termed O_B, is 5'-ATCTGGTACGACCAGAT-3' [6]. In this report, we demonstrate that FadR binds specifically and with high affinity to O_B DNA-Sepharose support prepared by either chemical or enzymatic methods. However, the DNA-Sepharoses had different properties depending upon the synthesis method used. Elution of FadR from the O_B DNA-Sepharose column resulted in a homogeneous protein fraction which retained DNA-binding activity.

2. Methods

2.1. DNA-Sepharose preparation

For FadR purification two different approaches were used. One uses (dT)₁₈-Sepharose and a poly(dA) tailed template with DNA polymerase to copy the template specified sequence onto the 3' end of (dT)₁₈ enzymatically using procedures described by Solomon *et al.* [3] for DNA-silica. The other uses a double-stranded DNA in which one strand contains a 5' amino group. This double-stranded DNA is then coupled to CNBr-activated Sepharose.

2.2. Enzymatic synthesis

(dT)₁₈-Sepharose was prepared by a modification of the method of Arnt-Jovin *et al.* [7]. A 10-g amount (wet mass) of Sepharose 4B was washed thoroughly with water; 2 g cyanogen bromide were added while stirring, and the mixture was maintained at pH 11 by the addition of 5 M NaOH until reaction slowed (*ca.* 15 min). The activated Sepharose was then rapidly washed under vacuum on a coarse-sintered glass funnel with 100 ml of ice-cold water and then with 100 ml of cold 0.1 M boric acid-NaOH, pH 8. After reconstitution to 20 ml with this last buffer, 200 nmol of 5'-amino-(dT)₁₈, prepared with the Amino Link reagent as previously described [8] was added and the mixture was stirred overnight. The next day 0.5 M glycine in

the borate buffer was added and stirring was continued for 24 h. The resulting (dT)₁₈-Seph-
arose was thoroughly washed and stored at 4°C in
TE (10 mM Tris, 1 mM EDTA, pH 7.5) con-
taining 10 mM NaN₃. The (dT)₁₈ content, mea-
sured by spectroscopy from the difference of the
(dT)₁₈ added and that which did not couple, was
11.5 nmol/g Sepharose.

A 2-g amount of the (dT)₁₈-Seph-
arose was washed three times with 2 ml of buffer E [50 mM
Tris, 150 mM NaCl, 10 mM MgSO₄, 0.1 mM
dithiothreitol (DTT), 5 μg/ml bovine serum
albumin (BSA), pH 7.4]. Then, 31 nmol of O_B-
(dA)₁₈ oligonucleotide (5'-CGACTCATCTGG-
TACGACCAGATCACCTAA-(dA)₁₈) in 2 ml
of buffer E was added to the resin and incubated
at 65°C for 5 min. After cooling for 15 min, the
resin was centrifuged and unbound oligonucleo-
tide was removed. The resin was washed 3 times
with 1 ml of buffer E containing 1 mM of each
deoxyribose nucleotide triphosphates (dNTP)
and then 50 units of *E. coli* DNA polymerase I,
Klenow large fragment was added, and the
mixture was incubated at 37°C for 2 h. Control
experiments in which 5'-³²P end-labeled oligo-
nucleotide O_B-(dA)₁₈ was used demonstrated
that under these conditions, 1.6 nmol of double-
stranded DNA were produced per g. of Sepha-
rose. The DNA-Seph-
arose was then washed
thoroughly in buffer C (10 mM Tris, 1 mM
EDTA, 100 mM NaCl, 0.1 mM DTT, 10 mM
NaN₃) and stored at 4°C until needed.

2.3. Chemical synthesis

Two complementary oligonucleotides, 5'-NH₂-
et-O_B (5'-NH₂-et-CGACTCATCTGGTACGA-
CCAGATCACCTAA) and αO_B (5'-TTAGGTG-
ATCTGGTCGTACCAGATGAGTCG) were
used where NH₂-et denotes the aminoethyl
added at the 5' end using the Amino Link
reagent. A double-stranded DNA was made by
mixing 30 nmol of each in 0.3 ml of TE con-
taining 0.3 M sodium acetate, heating to 65°C,
and cooling slowly to room temperature. Three
volumes of ethanol were added and the precipi-
tated double-stranded oligonucleotide was col-
lected by centrifugation and dried. The DNA

was then dissolved in 2.5 ml of the borate buffer
and added to 2.5 g (wet mass) CNBr-activated
Seph-
arose, prepared as described above. The
mixture was stirred overnight. The next day, the
DNA-Seph-
arose was washed with the borate
buffer and with 0.5 M glycine in the same buffer.
The amount of DNA coupled, 10 nmol per g of
Seph-
arose, was determined by spectroscopy of
the uncoupled DNA. Stirring was continued in
15 ml of the glycine-borate buffer for 24 h. The
DNA-Seph-
arose was then washed thoroughly in
buffer C and stored at 4°C until needed.

2.4. Production of FadR protein

High-level expression of FadR was induced
from BL21(λDE3) carrying plasmids pCD129
and pLysS as previously described [6]. Approxi-
mately 2.5 g of cell paste were suspended in 50
ml buffer containing 20 mM Tris pH 7.5, 100
mM NaCl, 1 mM EDTA and 1 mM DTT. The
cells were lysed by sonication. Unlysed cells and
cellular debris were removed by centrifugation at
23 000 rpm in a Beckman SW28 rotor. Am-
monium sulfate was added to the supernatant to
a final concentration of 60% of saturation. The
sample was incubated at 4°C overnight. Precipi-
tated proteins were sedimented by centrifugation
at 10 000 rpm in a Beckman JA21 rotor and then
resuspended in buffer D (10 mM Tris, 1 mM
EDTA, 0.1 mM DTT, pH 7.5), dialyzed against
the same, and finally glycerol was added to a
final concentration of 50%. This crude prepara-
tion of FadR was stored at -85°C until needed.

For comparison, FadR was also purified by
using DEAE-cellulose and CM- Bio-Gel A res-
ins as previously detailed [6].

2.5. Electrophoretic mobility shift assays

Activity of FadR in the final preparations was
measured using the gel shift assay as previously
detailed [6]. The DNA fragment used for these
experiments was the 377 base pair HindIII-
EcoRI fragment isolated from pCD154 [6]. This
fragment carries a portion of the *fadB* gene
containing the promoter for the *fadBA* operon

and O_B . The DNA was labeled with [32 P]dATP and the Klenow fragment of *E. coli* DNA polymerase I.

3. Results

The chemistries used to couple DNA to chromatography supports can modify nucleotide bases. Naturally occurring and synthetic DNAs all couple to CNBr-activated Sepharose, presumably via reaction with the amino moiety of the adenine, cytosine and guanine bases [1,2,7]. Since the affinity chromatography of DNA-binding proteins relies upon interactions with these nucleotide bases for its specificity, techniques which avoid base modification are preferable.

Previously, we have shown two feasible ways of avoiding this modification. These approaches are diagrammed in Fig. 1. One way is to enzymatically copy DNA sequences onto a support using a template DNA and DNA polymerase. Using this procedure, no modification of the DNA attached to the support is anticipated. The other approach provides an alkylamino moiety on the DNA chain as a preferred site for coupling and utilizes the observation that nucleotide bases are most resistant to modification in double-stranded DNA [3]. While the nucleotide bases

are less reactive under these conditions and reaction with the aminoethyl group should predominate, some reaction (coupling) with nucleotide bases would also be expected. Here, we have compared these two basic strategies to prepare columns for purification of the transcription factor FadR.

DNA-Sepharose was prepared enzymatically using the Klenow large fragment of *E. coli* DNA polymerase I. In this procedure, a (dT) $_{18}$ -Sepharose is prepared using 5'-aminoethyl-(dT) $_{18}$ and CNBr-activated Sepharose. Since thymidine bases contain no chemical groups which should be capable of coupling, coupling is expected to occur via the 5'-aminoethyl moiety. The resulting (dT) $_{18}$ -Sepharose has a 3'-hydroxyl and can be used to prime template-directed DNA synthesis by DNA polymerases. To prepare the Sepharose needed for FadR protein purification, a template containing the desired complementary sequence and also containing a 3'-(dA) $_{18}$ tail is hybridized to (dT) $_{18}$ -Sepharose and Klenow large fragment added. The result is that the complement of the template sequence is copied covalently onto the 3'-OH end of the (dT) $_{18}$ and the template remains on the column by hybridization with the newly produced sequence. Control experiments have demonstrated that when Klenow large fragment is added, the template-

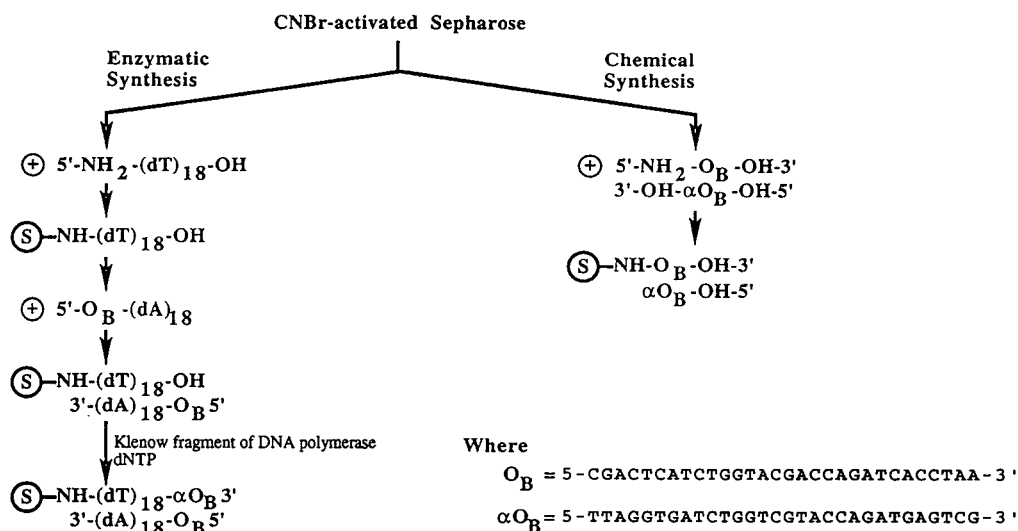


Fig. 1. Schematic presentation of the chemical and enzymatic procedures used to prepare DNA-Sepharose.

directed sequence is indeed copied onto the Sepharose and can be detected by the increase in melting temperature found for the longer DNA hybrid present after synthesis. This high-melting hybrid is not observed when the Klenow large fragment is omitted (data not shown). These procedures were originally described for DNA-silica [3] and have been adapted here to Sepharose.

To prepare a similar DNA-Sepharose chemically, two complementary oligonucleotide strands were prepared, one of which contained an aminoethyl group at its 5' end to provide a site for coupling to CNBr-activated Sepharose. The two strands were then hybridized and coupled to the support. The enzymatically and chemically prepared supports were then compared in the binding of FadR. To make comparison easier, a 15-nmol amount of DNA was used per gram of Sepharose for both procedures and all chromatographic comparisons were made between two columns of equivalent size, to which were applied equal quantities of the same extract of FadR eluted using the same conditions.

The amount of FadR specifically eluted from DNA-Sepharose prepared by the two approaches was not equivalent as shown in Fig. 2. In this figure is shown the elution profile obtained for equivalent amounts (9 mg) of a crude FadR protein preparation from the two kinds of columns of the same size (1 ml) prepared from equal amounts of DNA and run in parallel. Both columns were then washed thoroughly with buffer D and then washed with 0.2 and 0.8 M NaCl to elute the FadR protein. At 0.2 M NaCl, most of the contaminating proteins elute from the column along with a small amount of FadR protein. Most of the FadR protein however elutes in a highly purified state with 0.8 M NaCl. Fig. 2 shows that the column prepared by enzymatic synthesis bound and eluted about four-fold more of the FadR protein based upon the peak in absorption which elutes at higher salt. Additional experiments confirmed that higher yields of FadR were obtained from O_B -Sepharose prepared enzymatically. When the eluted protein obtained from the two columns was

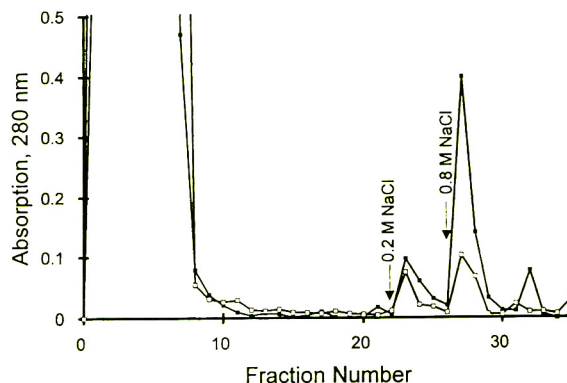


Fig. 2. The enzymatically prepared DNA-Sepharose column has higher capacity for FadR. Two 1-ml bed volume columns were prepared from DNA-Sepharose prepared by either the enzymatic procedure (■) or the chemical procedure (□). These columns contained 1.6 and 11.5 nmol of the O_B -DNA sequence, respectively. A 5-ml volume of crude, frozen FadR protein in buffer C containing 9 mg protein was applied to each column. The columns were then washed with 20 ml of buffer C (pH 7.5) and then eluted with 5-ml portions of TE containing either 0.2 or 0.8 M NaCl as shown in the figure. Fractions were 1.2 ml. Acrylamide gel electrophoresis demonstrates that the bulk of the FadR protein elutes with 0.8 M NaCl from either column (see Fig. 3).

analyzed by acrylamide gel electrophoresis, the amount of FadR protein observed on the gels was estimated to be at least three-fold higher for the enzymatic column eluted protein (data not shown). These results cannot be due to the amounts of DNA coupled to the columns. Even though the same amounts of DNA were used in column preparation, enzymatic synthesis was less efficient and resulted in about one-sixth as much attached DNA as the chemically prepared column (1.6 versus 11.5 nmol per gram, respectively). These results suggest that enzymatic synthesis results in columns in which more of the DNA is suitable for binding by the FadR protein, presumably because chemical coupling has rendered some of the DNA unsuitable for affinity binding by the protein.

Fig. 3 shows acrylamide gels of the various fractions obtained from the chromatography on the 1 ml O_B -DNA-Sepharose columns. In Fig. 3A, the fractions from the enzymatically prepared column are shown while in Fig. 3B results with the chemically prepared column are presented. In either case, the same amount of crude

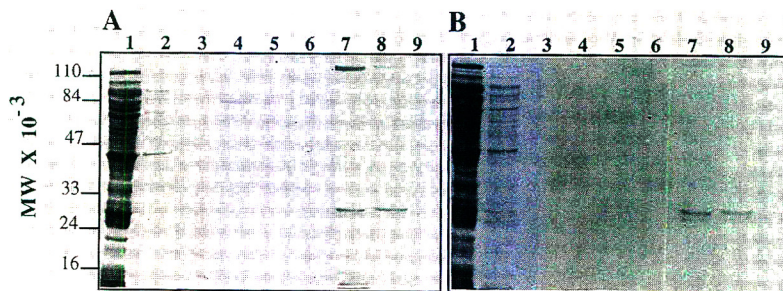


Fig. 3. Chemically synthesized DNA-Sepharose yielded higher-purity FadR. Volumes of $12.5 \mu\text{l}$ of the column fractions from Fig. 3 were diluted with sodium dodecyl sulfate (SDS) sample buffer and applied to 12% acrylamide gels [9]. Wells: 1 = crude FadR protein before chromatography; 2–9 = fraction numbers 5, 22, 23 (peak at 0.2 M NaCl), 25, 26, 27 (peak at 0.8 M NaCl), 28 and 29, respectively, from the elution profiles shown in Fig. 2. (A) Fractions from the enzymatically synthesized support; (B) for the chemical support.

FadR protein was loaded onto the column. In this figure, a volume representing about 1% of the total fraction volume was loaded onto the acrylamide gel; since this amount contained less protein in Fig. 3B, the contrast of the photograph was adjusted so that the FadR protein band is clearly visible. The results show that while the chemically prepared column binds less FadR protein (*i.e.*, about four-fold less in the experiment in Fig. 2), the protein eluted was of higher purity. This may be because of the simpler sequence of the column DNA since the chemical coupling procedure does not have or require the $(\text{dT})_{18}:(\text{dA})_{18}$ hybrid sequences. The enzymatically prepared column binds more FadR protein and also binds some other proteins as well. The higher capacity probably results from the lack of chemical modification of the DNA nucleotide bases.

Fig. 4 shows that greater purity can be obtained from the enzymatically prepared column by washing the column with intermediate salt concentrations. When the column is washed at 0.2 , 0.4 and 0.6 M NaCl , contaminating proteins are eluted from the column along with some of the bound FadR. After washing, elution at 0.8 M NaCl results in highly purified FadR protein. No further protein elutes at 1.0 M NaCl . However, elution with this more complex NaCl step gradient, while increasing the purity of the protein obtained at 0.8 M NaCl , results in lower recovery of the purified protein.

The results presented in Fig. 4 suggested that

FadR could be purified on the enzymatically prepared column by applying the crude protein, washing at 0.2 and 0.4 M NaCl , and collecting the purified protein which elutes with 0.8 M NaCl . This is the procedure we currently use and it yields FadR protein of sufficient purity for most purposes. The capacity of the enzymatically prepared O_B -DNA-Sepharose for FadR under these conditions averaged $113 \mu\text{g}$ FadR protein per ml of DNA-Sepharose (standard deviation $21 \mu\text{g/ml}$, $n = 2$). Thus, relatively small columns in

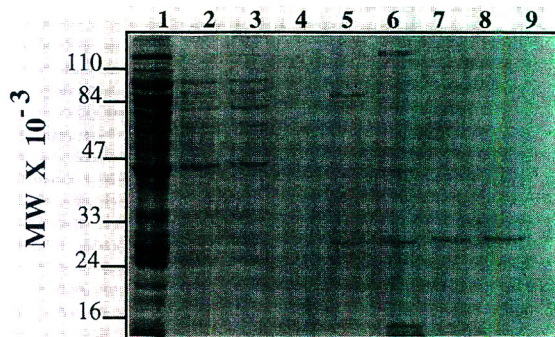


Fig. 4. The effect of different concentrations of NaCl on the elution of FadR. Crude FadR protein was loaded onto the enzymatically prepared DNA-Sepharose column, the column was washed with different buffers, and the fractions obtained examined on 12% SDS-polyacrylamide gel electrophoresis. Wells: 1 = crude FadR before chromatography; 2 = an early flow through fraction; 3 = a late flow through fraction; 4 = a late wash fraction after the column had been washed to baseline with buffer C; 5–9 = the column was washed with 0.2 , 0.4 , 0.6 , 0.8 and 1.0 M NaCl made up in TE buffer. MW = Molecular mass.

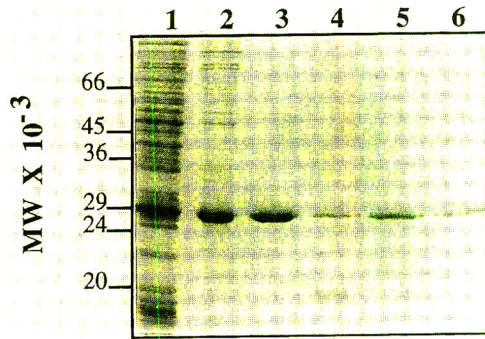


Fig. 5. Comparison of FadR purified by ion-exchange and O_B -DNA-Sepharose chromatography. A 15% SDS-polyacrylamide gel was used to monitor FadR during purification. Lanes: 1 = ammonium sulfate precipitate after dialysis (*i.e.*, crude FadR); 2 = partially purified FadR after DEAE-cellulose chromatography; 3 = FadR after CM-Bio-Gel A chromatography; 4 = FadR after O_B -DNA-Sepharose chromatography and elution with 0.4 M NaCl; 5 = 0.6 M NaCl; 6 = 0.8 M NaCl.

the range of 10 ml can purify mg amounts of FadR in a single chromatographic step.

The purity and activity of FadR purified using the O_B -DNA-Sepharose was compared to FadR purified by chromatography on sequential DEAE-cellulose and CM-Bio-Gel A columns. Fig. 5, presents a representative polyacrylamide gel on which FadR purified by each method is displayed. It was noted that a high-molecular-mass protein generally observed after purification by ion-exchange chromatography was not visible in protein samples purified using O_B -

DNA-Sepharose. FadR purified by each method showed comparable DNA binding affinity when tested using the standard protein-DNA gel mobility shift assay (Fig. 6). Therefore, we conclude that FadR obtained by either purification procedure is of comparable activity. Since the DNA-Sepharose method is simpler and more rapidly performed, it is to be preferred.

4. Discussion

DNA affinity chromatography is usually performed while including a "competitor" DNA (*e.g.*, pIpC oligomers) in the mobile phase during chromatography to diminish "non-specific" binding of proteins other than the one of interest to the column (for reviews, see refs. 1 and 2). No competitor DNA was used in the present studies since this could obscure differences between the columns. It was also found to be unnecessary; specific binding and elution of FadR could be obtained in its absence. Other affinity chromatography protocols have involved columns made from DNA concatemers containing multiple copies of the DNA target sequence [2]. This was also not done in the present study because such complex sequences may also bind other proteins as some of our results suggest (see below). By using simple sequences, sequence complexity effects can be minimized, the DNA is easier to synthesize, and the shorter sequences

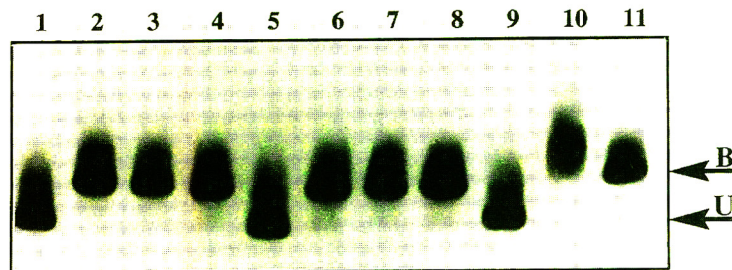


Fig. 6. Comparison of FadR-specific DNA binding activity after purification by ion-exchange and O_B -DNA-Sepharose chromatography. Electrophoretic mobility shift assays were performed as previously described [6]. U denotes migration of DNA which is unbound and B denotes migration of the labeled DNA bound by protein. Reaction mixtures contained $1 \cdot 10^{-12}$ M [32 P]fadB DNA alone for lanes 1, 5 and 9; for lanes 2-4, 10^{-7} , 10^{-8} and 10^{-9} M FadR protein, respectively, prepared using O_B -DNA-Sepharose synthesized by the enzymatic method; for lanes 6-8, 10^{-7} , 10^{-8} and 10^{-9} M FadR prepared using O_B -DNA-Sepharose synthesized by the chemical method; and for lanes 10 and 11, 10^{-8} and 10^{-9} M FadR respectively, prepared using ion-exchange chromatography.

can be used in higher molar amounts. Concatemeric sequences were also not found to be necessary for the efficient binding and chromatography of FadR.

Comparison of an enzymatic and a chemical procedure for preparing a DNA-Sepharose for the affinity chromatographic purification of FadR revealed certain advantages for each approach. The chemical procedure is simpler, yields purer FadR when used in a single-step purification, but in lower yield. The enzymatically prepared column has a higher capacity for FadR, yields larger amounts of FadR under comparable conditions but the protein obtained is of lower purity. These results cannot be explained by differences in the amount of O_B-DNA sequence on the column. The enzymatically prepared column contains less coupled DNA but binds greater amounts of FadR presumably because all of the DNA is in a native, unmodified form. However, the enzymatic procedure also requires the use of more complex DNA sequences because of the requirements that a template be hybridized prior to enzymatic copying. This more complex sequence probably accounts for the lower purity of FadR obtained since the contaminants may bind by association to these extra DNA sequences. The use of selective washing with intermediate salt concentrations removes these impurities (Fig. 4) but reduces yield.

However, these considerations about the best way to synthesize DNA-Sepharose should not detract from the clear advantages this affinity chromatography has over more conventional purification procedures. DNA-Sepharose chro-

matography was shown to be capable of producing apparently homogeneous protein in a single purification step and gave results of purity and biological activity comparable to that obtained by much more laborious conventional purification procedures. FadR purified using the enzymatically prepared column and 0.4 M washes with 0.8 M NaCl elution has yielded sufficiently pure protein for most uses and is the procedure we currently use.

Acknowledgements

This work was supported by the National Institutes of Health, grants GM 43609 and GM 38104. We thank Tamara Heimert for excellent technical assistance.

References

- [1] H.W. Jarrett, *J. Chromatogr.*, 618 (1993) 315–339.
- [2] J.T. Kadonaga, *Methods Enzymol.*, 208 (1991) 10–23.
- [3] L.R. Solomon, L.R. Massom and H.W. Jarrett, *Anal. Biochem.*, 203 (1992) 58–69.
- [4] P.N. Black and C.C. DiRusso, *Biochim. Biophys. Acta*, 1210 (1994) 123–145.
- [5] C.C. DiRusso, A.K. Metzger and T.L. Heimert, *Molec. Microbiol.*, 7 (1993) 311–322.
- [6] C.C. DiRusso, T.L. Heimert and A.K. Metzger, *J. Biol. Chem.*, 267 (1992) 8685–8691.
- [7] D.J. Arndt-Jovin, T.M. Jovin, W. Bahr, A.-M. Frischauf and M. Marquardt, *Eur. J. Biochem.*, 54 (1975) 441–418.
- [8] T.A. Goss, M. Bard and H.W. Jarrett, *J. Chromatogr.*, 508 (1990) 279–287.
- [9] U.K. Laemmli, *Nature*, 227 (1970) 680–685.

High-performance liquid chromatography in stability studies of an organophosphorus insecticide in free form and after formulation as emulsifiable concentrate

Response surface design correlation of kinetic data and parameters

Yannis L. Loukas, Ekaterini Antoniadou-Vyza*, Aspasia Papadaki-Valiraki

Department of Pharmacy, Division of Pharmaceutical Chemistry, University of Athens, Panepistimioupoli Zografou 15710, Athens, Greece

First received 9 November 1993; revised manuscript received 15 February 1994

Abstract

DCPE [α -(diethoxyphosphinoximino)dicyclopropylmethane] is an organophosphorus compound with good insecticidal activity. It is a yellow oily liquid, poorly soluble and unstable in aqueous media. The development of a useful, safe formulation, miscible with water, easy to use and retaining its activity was examined. First, the kinetics of the hydrolysis of DCPE were studied in various buffer solutions over the pH range 3–11 at 20–80°C by a reversed-phase HPLC method. Then the response surface methodology was used to investigate how the hydrolysis rate constant (response) was affected by temperature and pH (variables) over some specified region, and was described step by step. The degradation product of DCPE was isolated by extraction and identified by IR and ^1H NMR spectrometry. Also, the activation energy of DCPE hydrolysis was calculated from the dependence of the observed hydrolysis rates (k_{obs}) on temperature at constant pH. Finally, 30 emulsifiable concentrate formulations of DCPE were prepared by choosing different combinations of oil phases and emulsifiers. Five of the resulting emulsions retained their physical stability and were examined further for chemical stability of the active compound (DCPE) at different temperatures.

1. Introduction

α -(Diethoxyphosphinoximino)dicyclopropylmethane (DCPE) (**I**, Fig. 1), is a powerful insecticide that was synthesized in our laboratory [1]. It is a promising compound showing significant activity and structural originality owing to the presence and position of the two cyclo-

propane rings. It is a cholinesterase inhibitor and has high mammalian toxicity orally.

Organophosphorus compounds are widely used as insecticides and often acaricides [2]. Although they all have the basic property of inhibiting the action of cholinesterase at the ganglia, they enter the insect's body by different routes depending on the properties of the particular compound. Thus the group contains contact, stomach and systemic insecticides. After application, the organophosphorus compounds

* Corresponding author.

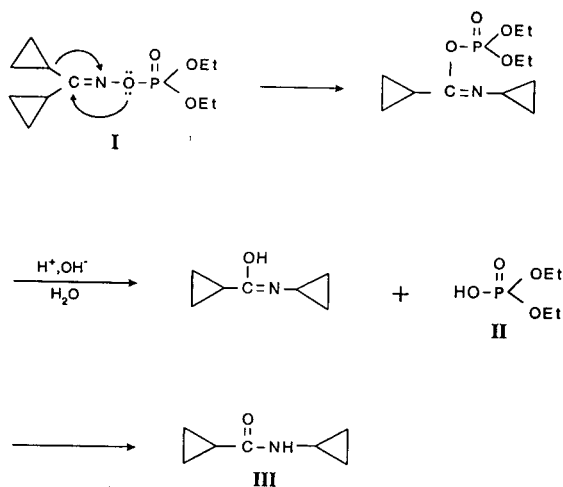


Fig. 1. Structure of I and its reactions.

are converted into their degradation products by the effect of the environment. Hydrolysis is the most common reaction that leads to detoxification. The products formed are usually less toxic than the initial pesticides. Between application of the active compounds and permitting access to the area (harvesting of the crop or other appropriate procedures), sufficient time must elapse for the active compound to be eliminated to a level considered to be safe. The shorter the time of detoxification, the safer the product is. DCPE in various emulsions has a detoxification period of 10–40 h, as shown by stability studies.

The decrease in the efficacy of pesticides depends on the environmental humidity and temperature, and therefore the degradation pathway and the decomposition kinetics are of major interest. In this study, a high-performance liquid-chromatographic (HPLC) method was developed for monitoring the degradation reactions. Further, the separation of DCPE from its degradation products and stability studies under different conditions were performed by the same method. The main degradation product was obtained following an experiment under stressed conditions and was isolated by extraction.

After the kinetic studies had been performed in buffer solutions under different conditions, in an attempt to stabilize DCPE, different emulsifiable concentrate (EC) formulations were pre-

pared. Most pesticides are formulated as ECs [3] and must retain their efficiency for at least 2 years under normal storage conditions. In all prepared EC formulations, DCPE remained unchanged for more than 1.5 years. By mixing the EC formulation with water an emulsion is prepared [oil in water (O/W) emulsion] and is applied in the form of a spray. An emulsion consists of two immiscible liquid phases, one of which is finely subdivided and uniformly dispersed in the other. Emulsions are thermodynamically unstable as a result of the excess free energy associated with the surface of the droplet. To minimize this effect a third component, the emulsifier, is added to the system to improve its stability. In this study, the effect of nine emulsifiers in 30 different EC formulations was tested.

Finally, the relationships between the degradation rate k of DCPE and the factors pH and T temperature were examined by using response surface methodology (RSM) techniques [4] on a personal computer (PC). According to this method we can build empirical models that use sequential experimentation techniques to survey a domain of interest and to focus on the most important variables and their effects. In other words, RSM is a collection of mathematical and statistical techniques that are useful for the modelling and analysis of problems in which a response of interest (here the rate constant k) is influenced by several variables (here temperature and pH). The objective is to find how the particular response is affected by the set of variables over a specified range.

2. Experimental

2.1. Materials

DCPE was synthesized and purified in our laboratory. Berol emulsifiers [5] were obtained from Berol Kemi (Stenungsund, Sweden). All other chemicals, including buffer components, were of analytical-reagent grade except methanol and acetonitrile, which were of HPLC grade.

Water was deionized and doubly distilled using a Millipore Milli-Q Plus water-purification system.

2.2. High-performance liquid chromatography

The HPLC assays for DCPE were performed on a Waters (Milford MA, USA) chromatographic system consisting of a pump (Model 590) and a multi-wavelength UV detector (Lamda-Max, Model 481). The separation of DCPE from its degradation product was performed on a 10- μm reversed-phase, $\mu\text{Bondapak C}_{18}$ column (300×3.9 mm I.D.) (Waters). A flow-rate of 1.5 ml min^{-1} was maintained and the effluent was monitored at 215 nm with a detector sensitivity of 0.05 AUFS. The sample volume was 20 μl (Rheodyne Model 717S injector fitted with a 20 - μl loop). In assay 1 the mobile phase was acetonitrile–water–methanol (40:50:10) and acetanilide ($\text{CH}_3\text{CONHC}_6\text{H}_5$) was used as an internal standard at a concentration of 4 mg ml^{-1} . In assay 2 the mobile phase was acetonitrile–water (55:45) and benzophenone (C_6H_5) $_2\text{CO}$ was used as an internal standard at a concentration of 0.33 mg ml^{-1} (because acetanilide is insoluble in EC formulations and therefore changing the mobile phase composition produces better separation). In both assays the mobile phases were vacuum filtered through a 0.45 - μm pore-size nylon membrane filter (Sartolon, Germany) prior to use. Quantification was performed by peak-height integration (Waters, Baseline-810 integration system for PC).

2.3. Kinetics

Citrate, phosphate and carbonate buffer solutions of various pH were used in all experiments. These buffer solutions were 0.1 M with respect to citrate, phosphate and carbonate, respectively, and were adjusted to a total ionic strength of 0.5 M with potassium chloride. The reaction was initiated by adding 13.1 mg of DCPE to 50 -ml volumetric flasks and diluting to volume with buffer solution to give an initial DCPE concentration of 1 mM (DCPE $M_r = 262$). A stock standard solution of acetanilide (4 mg ml^{-1}) was

prepared and stored in a refrigerator until further use as an internal standard. The reaction flasks were immediately placed in a water-bath at constant temperature (Tempette Thermo-regulator TE8D, Techne).

At appropriate time intervals, 450 - μl aliquots of the reaction mixture were removed from the flask and immediately added to a test-tube containing 50 μl of the internal standard stock standard solution. The samples were analysed for remaining DCPE by HPLC assay 1. The first-order rate constant for the disappearance of DCPE (k_{obs}) was determined from the slopes of linear plots. The logarithm of the percentage of remaining DCPE was plotted against time.

For the isolation of the degradation product of DCPE, 2 g (7.6 mM) of DCPE were dissolved in 20 ml of phosphate buffer solution (pH 7), the mixture was heated for 48 h on a water-bath at 80°C , then allowed to cool at room temperature and extracted repeatedly with diethyl ether. The combined ethereal extracts were washed with water and after drying over anhydrous Na_2SO_4 were filtered to leave an oil. The degradation product was obtained from this residue by crystallization with pentane. Recrystallization from diethyl ether–pentane gave the pure product in crystalline form. The structure of this product was investigated by ^1H NMR and IR spectrometry and is shown in Fig. 1 (amide III).

2.4. Preparation of emulsions

The typical process for the formulation of DCPE as an EC was as follows. First the oil phases (either an anhydrous non-polar solvent, such as xylene, or an oil, such as paraffin oil, soya oil, isopropyl myristate or isopropyl palmitate) were selected in which the active ingredient (DCPE) was dissolved. Then the emulsifiers were selected (Table 1). These emulsifiers are surfactants with high HLB (hydrophilic–lipophilic balance) values (>10), since O/W emulsions, such as DCPE emulsions, are favoured. The HLB value of the oil phase must be the same as that value of the emulsifiers. Also fundamental to the utility of the HLB concept is that the HLB values are algebraically additive. The emulsifier

Table 1
Emulsifiers used for DCPE EC formulations and their HLB values

Emulsifier	HLB	Application
Berol 910	13.3	Non-ionic, can be used in formulations of insecticides
Berol 948	16.0	Non-ionic, can be used especially in formulations of organophosphates
Berol 930	14.7	Blend of anionic and non-ionic, can be used as "universal combination emulsifier" for many types of insecticides
Berol 938	13.4	As Berol 930
Berol 977	16.0	Non-ionic, can be recommended for use in formulations containing organophosphates
Berol 987	16.7	As Berol 977
Tween 20	16.7	Non-ionic, promotes O/W emulsions
Tween 80	15.0	As Tween 20
Span 80	4.3	Non-ionic, used only in combination with Tweens, for appropriate HLB values

were therefore used in combinations as better emulsions were usually obtained. Thirty EC formulations were prepared which consisted of the oil phase, the blend of emulsifiers and DCPE. The usual proportions before the emulsification were approximately 50% of DCPE, 45% of oil solvent and 5% of emulsifiers. Finally, the emulsification occurred on adding the continuous phase (water) gradually to the disperse phase. Generally, depending on the intended use, the water is added to the EC at rates varying from 1 part of concentrate to 4 or as much as 100 parts of water [6]. In this study the DCPE concentration in the final emulsions was approximately 5%. The emulsions first were examined for physical stability. The stable emulsions were further examined for the chemical stability of the active ingredient (DCPE) at various temperatures by RP-HPLC.

2.5. Response surface design

In the case of DCPE, the simple design in the 3^k system was used, which is the 3^2 design, with two factors, each of them at three levels. The polarity of the media was kept constant as we were interested only in the behaviour of DCPE in aqueous solutions. We refer to the three levels of the factors as low, intermediate and high. These levels will be designated by the digits 0 (low), 1 (intermediate) and 2 (high). For example, in a 3^2 design, 00 denotes the treatment

combination corresponding to factors A and B both at the low level. The treatment combination for this design is shown in Fig. 2. It is obvious that the system has $3^2 = 9$ treatment combinations and therefore there are eight degrees of freedom between these treatment combinations.

We used a statistical program [7] with strong design of experiments (DOE) capabilities to perform the calculations and to illustrate all the interactive graphics. The nine runs listed in Table 2 define a three-level response surface design in a two-factor design matrix. These nine runs were conducted in random order so as to nullify the effects of extraneous or nuisance variables. After the responses (k_{obs}) had been collected the system was ready for analysis.

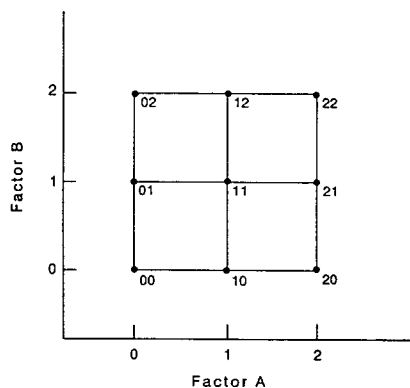


Fig. 2. Treatment combinations in a 3^2 design.

Table 2
Randomized combinations of two factors and the calculated responses

Run No.	pH	T	k
1	7	80	0.489
2	3	20	0.0075
3	11	20	0.009
4	11	80	0.451
5	7	20	0.008
6	11	50	0.131
7	7	50	0.121
8	3	80	0.511
9	3	50	0.101

2. Results and discussion

To clarify the degradation mechanism of DCPE in aqueous solutions, the degradation product was isolated by extraction. Then the degradation pathway was studied by monitoring the reaction buffer solutions using RP-HPLC.

3.1. Degradation analysis by RP-HPLC

DCPE was dissolved in various aqueous buffer solutions at various temperatures. The solutions were analysed by HPLC assay 1. Fig. 3 shows plots of the residual percentage amount of DCPE *versus* time in buffer solution of pH 7 at different temperatures. All the experimental

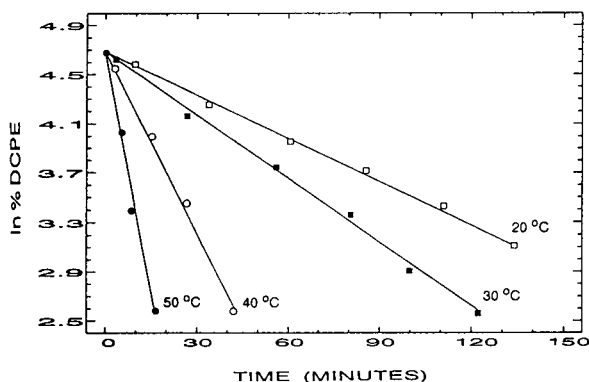


Fig. 3. Apparent first-order plots for the degradation of DCPE in buffer solution (pH = 7, $\mu = 0.5 M$) at various temperatures.

conditions and the rate constants for the degradation of DCPE are given in Table 2. In all instances the amide **III** was the only degradation product. This observation leads to the conclusion that the degradation pathway was due to a Beckman rearrangement [8] as shown in Fig. 1.

To calculate the activation energy for the degradation of DCPE in buffer solutions, the temperature dependence of the rate constants was obtained graphically according to the Arrhenius equation (Eq. 1). From the slope of the linear Arrhenius plot the activation energy was calculated to be $17.75 \text{ kcal mol}^{-1}$ ($r = 0.99$).

$$\ln k = -\frac{E_a}{R} \cdot \frac{1}{T} + \ln A \quad (1)$$

3.2. Formulation of DCPE as EC

Anhydrous xylene (one of the commonest organic solvents in EC formulations) was used in this study. The emulsifiers used are specific for pesticides and have the trade-name Berol.

As there is no general rule for preparing a stable emulsion other than through experimentation, 30 different formulations were examined for physical and chemical stability. These formulations were all the possible combinations between the oil phases and the emulsifiers used in this study. Some of them were stored in an oven at 40°C and the chemical stability of DCPE was determined by HPLC assay 2. A sample of known concentration of each formulation was injected into the HPLC system and the DCPE content was calculated from a calibration graph. These experiments were repeated many times for all formulations in an oven and for a period of 18 months. The DCPE content of the formulations was found to be unchanged.

After the confirmation that DCPE remained unchanged in EC formulations, emulsification took place on adding the appropriate amount of water. In some instances spontaneous emulsions were formed. After shaking, the emulsions were left for 24 h. In some, sedimentation (the phenomenon of downward movement of dispersed droplets) appeared. The droplets were redispersed by shaking, as they retained their in-

dividuality. In others coalescence (the phenomenon of the ultimate separation of the two immiscible phases) occurred. Coalescence is irreversible and the emulsion could not be redispersed.

Finally, five emulsions retained their physical stability and these were selected to be examined further for the chemical stability of DCPE by HPLC assay 1 at 25 and 40°C. The compositions of these stable emulsions are given in Table 3. Fig. 4 shows the apparent first-order plots for the degradation of DCPE in stable emulsions at 25 and 40°C. It is evident from the plots that DCPE appeared to have the highest stability in emulsion No. 1. Rate constants and half-lives for the degradation of DCPE in stable emulsions are given in Table 4.

It is concluded from the study of physical and chemical stability that the best results were achieved by the use of non-ionic emulsifiers [9]. This may be due to the fact that non-ionics lack strong electrical charges and have high resistance to pH changes, electrolytes and polyvalent inorganic cations. Perhaps these emulsifiers readily form a film around each droplet of dispersed material. The main purpose of this film, which is usually a monolayer, is to form a barrier which prevents the coalescence of droplets that come into contact with one another. The film possesses some degree of surface elasticity and preserves its integrity, as results from previous physical stability studies.

In addition, the film and the helical conformation of the hydrophilic chains probably function by hindering the close approach of DCPE drop-

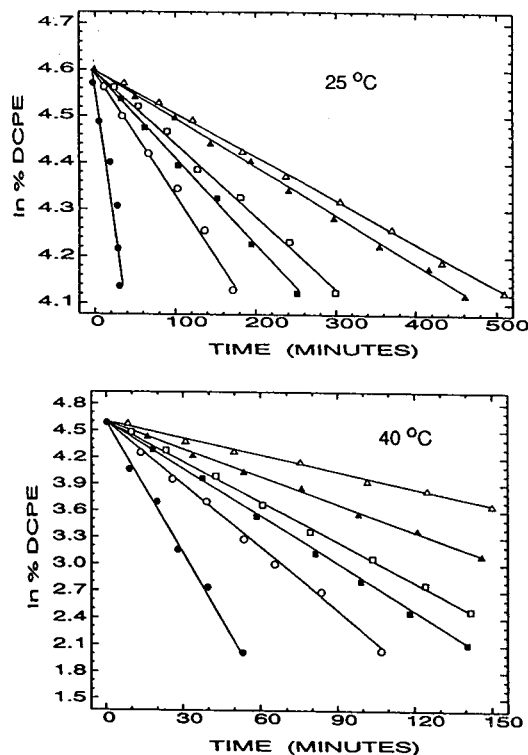


Fig. 4. Apparent first-order plots for the degradation of DCPE in stable emulsions at 25 and 40°C. ● = Aqueous solution; △ = formulation No. 1; ▲ = No. 2; □ = No. 3; ■ = No. 4; ○ = No. 5.

lets to water, thus decelerating degradation. Commonly, non-ionic emulsifiers, such as Berols and Tweens, consist of polyoxyethylene chains that extend outwards into the aqueous medium

Table 3

Compositions of the DCPE formulations that retain their physical and chemical stability

Formulation No.	Composition (g)
1	DCPE (2.1) + xylene (2.6) + Berol 977 (0.12) + Berol 987 (0.13)
2	DCPE (2.1) + xylene (2.5) + Berol 910 (0.13) + Berol 948 (0.13)
3	DCPE (2) + xylene (2.7) + Berol 930 (0.12) + Berol 938 (0.12)
4	DCPE (2) + soya oil (2.7) + Berol 930 (0.12) + Berol 938 (0.12)
5	DCPE (2) + isopropylmyristate (2.5) + Tween 80 (0.18) + Span 80 (0.07)

Table 4
Kinetic data for the chemical stability studies of DCPE in stable emulsions at 25 and 40°C

Formulation No.	<i>k</i>		<i>t</i> _{1/2}		<i>r</i>	
	25°C	40°C	25°C	40°C	25°C	40°C
Aqueous solution	13 · 10 ⁻³	54 · 10 ⁻³	51 min	12.85 min	0.993	0.995
1	9.9 · 10 ⁻⁴	6.1 · 10 ⁻³	11.7 h	113.6 min	0.983	0.991
2	1.6 · 10 ⁻³	12.7 · 10 ⁻³	7 h	54.6 min	0.993	0.988
3	2 · 10 ⁻³	13.9 · 10 ⁻³	5.8 h	49.9 min	0.988	0.985
4	2.6 · 10 ⁻³	22 · 10 ⁻³	4.45 h	31.5 min	0.985	0.986
5	3.9 · 10 ⁻³	25.2 · 10 ⁻³	2.96 h	27.5 min	0.994	0.991

and hydrocarbon chains that orientate in the non-polar environment.

3.3. Determination of temperature and pH effects on the degradation rate constant

Check of main effects and interactions

After completing the runs in the order listed in Table 2, the rate constants were calculated by HPLC assay 1. To determine which effects (linear or quadratic) of each factor or their interaction are significant, a two-way analysis of variance (ANOVA) was performed (Table 5). As $F_{0.05,1,3} = 10.13$ and $F_{AB} = MS_{AB} / MS_{\text{total error}} = 2.38$, we conclude that there is not a significant interaction between temperature and pH and the

only significant effect is temperature at a probability of $P = 0.05$ (5%).

Performance of a Pareto analysis

To assist in interpreting the results of this experiment, it is helpful to construct a standardized Pareto chart [10], which is similar to a Pareto chart, except that it shows the effect divided by its standard error. The chart includes a vertical line at the critical *t*-value for $\alpha = 0.05$ (Fig. 5). An effect that exceeds the vertical line may be considered significant. Table 6 shows the main effects of the factors temperature and pH (factors A and B), the quadratic effects of the factors (AA and BB) and the interaction between the two factors (AB). The last column in

Table 5
Analysis of variance for the examined design

Effect	Sum of squares	DF ^a	Mean square	<i>F</i> -ratio	<i>P</i> value
A (pH)	0.00013538	1	0.0001354	0.34	0.6064
B (<i>T</i>)	0.33915037	1	0.3391504	852.54	0.0001
AB	0.00094556	1	0.0009456	2.38	0.2208
AA	0.00003612	1	0.0000361	0.09	0.7858
BB	0.03289613	1	0.0328961	82.69	0.0028
Total error	0.00119344	3	0.0003978		
Total (corr.)	0.37435700	8			
<i>R</i> ² 0.996812					<i>R</i> ² (adjusted for DF) 0.991499

^a Degrees of freedom.

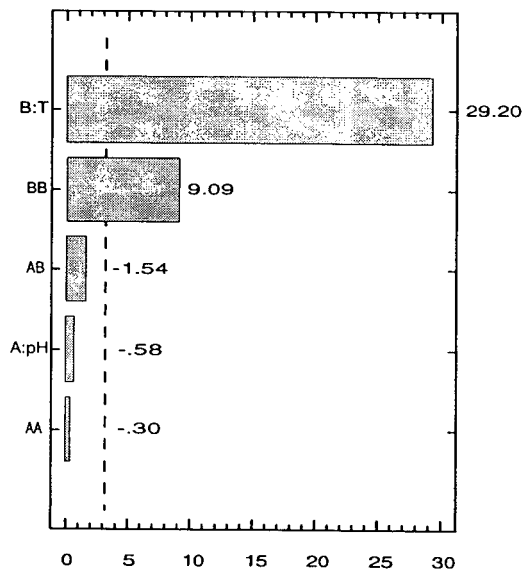


Fig. 5. Pareto chart for the factors effect on k_{obs} .

Table 6 displays the standard error estimated from the total error with three degrees of freedom. These results show that the linear effect of B is considerably larger than both the linear effect of A and the second-order effects (AB, AA, BB).

Generation of a predictive model

Using the significant main and interaction effects, a model that expresses rate constant as a function of temperature and pH was developed. This model can predict rate constants in the given region of the operating conditions. According to Table 6 and the Pareto chart (Fig. 5), we consider as significant the main and quadratic effects of temperature. The model was developed into PC software [7] that performs

Table 6
Estimated effects of the factors on k_{obs}

Average	0.1205 ± 0.0148663
A (pH)	$-9.5 \cdot 10^{-3} \pm 0.0162852$
B (T)	0.4755 ± 0.0162852
AB	-0.03075 ± 0.0199452
AA	$-8.5 \cdot 10^{-3} \pm 0.0282068$
BB	0.2565 ± 0.0282068

multiple regression analysis based on the following equation:

$$Y = C + B_1 \cdot \text{temperature} + B_2 \cdot \text{temperature}^2$$

where Y = predicted value of rate constant; C = intercept in regression equation; B_1 = coefficient for temperature; B_2 = coefficient for the quadratic effect of temperature.

This model does not include the other interaction terms because their effects are negligible and would not add to the model's predictive ability. Using the estimated constant and coefficient, the multiple regression analysis generates the prediction model:

$$Y = 0.078 - 0.006T + 0.000143T^2 (r = 0.998).$$

4. Conclusions

DCPE is a pesticide unstable in aqueous solutions. Its stability in aqueous solutions can be expressed with a predictive model by the use of a simple experimental design. Fortunately, its stability is increased and retains its activity after its formulation as an EC. The LD_{50} for DCPE has been determined in a previous study [11] and was found to be 10.86 mg kg^{-1} for male and 7.86 mg kg^{-1} for female Wistar rats after oral administration. Insecticidal studies [1] for contact toxicity have also been performed with four different insects: *Ceratitis capitata*, *Ectomyeloid ceratonia*, *Musca domestica* and *Plodia interpunctella*. These studies support the conclusions that DCPE can probably be used either as a stomach poison or as a contact insecticide. The variation in the half-life of DCPE in emulsions gives the opportunity for the applicator to select the preferred formulation.

References

- [1] E. Kostakis and A. Rouman, *Ph.D. Thesis*, University of Athens, Athens, 1984.
- [2] *The Pharmaceutical Codex*, The Pharmaceutical Press, Cambridge, 11th ed., 1979, p. 659.
- [3] D. Seaman, *Pestic. Sci.*, 29 (1990) 437.

- [4] D. Montgomery, *Design and Analysis of Experiments*, Wiley, Chichester, 1991.
- [5] *Emulsifiers for Pesticides*, Berol Kemi, Stenungsund, Sweden, 1985.
- [6] A. Marderosian, *Pesticides*, Remington's Pharmaceutical Sciences, Mack Publishing Co., Easton, PA, 18th ed., 1990, p. 1249.
- [7] *Statgraphics plus Version 6*, Manugistics, Rockville, MD, 1993.
- [8] G. Donamura and W. Heldt, *The Beckmann Rearrangement (Organic Reactions, Vol. 11)*, Wiley, New York, 1960.
- [9] A. Florence and J. Rogers, *J. Pharm. Pharmacol.*, 23 (1971) 153.
- [10] G. Box, W. Hunder and J. Hunter, *Statistics for Experimenters*, Wiley, New York, 1978.
- [11] K. Machera and E. Kostakis, *Bull. Environ. Contam. Toxicol.*, 48 (1992) 108.

Determination of phenoxyalkanoic acids and other acidic herbicides at the low ppt level in water applying solid-phase extraction with RP-C₁₈ material

S. Butz, Th. Heberer, H.-J. Stan*

Institute of Food Chemistry, Technical University of Berlin, Gustav-Meyer-Allee 25, D-13355 Berlin, Germany

First received 22 September 1993; revised manuscript received 1 March 1994

Abstract

A method for the determination of 34 phenoxyalkanoic acids and other acidic compounds in water samples was developed. Recoveries were made from 1 l of drinking water samples using solid-phase extraction (SPE). Different SPE materials and blends of octadecyl (RP-C₁₈) and phenyl (RP-Phe) were tested. After method optimization, 26 out of the 34 compounds could be extracted with recoveries better than 70% on the most suitable RP-C₁₈ material. The acidic compounds in the extract were derivatized with pentafluorobenzyl bromide and the resulting esters determined by capillary gas chromatography with mass selective detection employing selected-ion monitoring with time window programming. Detection limits between 1 and 10 ng/l were obtained with spiked drinking water samples. This method has been used successfully for the analysis of drinking and groundwater samples in field studies.

1. Introduction

The determination of acidic compounds by GC-MS after derivatization with pentafluorobenzyl bromide (PFBBBr) was the subject of a previous paper [1]. The derivatization procedure has been demonstrated to permit the sensitive determination of the target compounds at levels down to 1–100 pg injected when measured with selected-ion monitoring (SIM) and electron impact ionization (EI-MS). The low detection limits that can be achieved with test substances make this method promising for application to drinking water samples. The identification and determination of these compounds at a concen-

tration level of 100 ng/l in water for a single compound is necessary to meet the maximum tolerances set by the European Community's drinking water regulation [2]. To determine phenoxyalkanoic acids and related acidic herbicides at such low tolerance levels, the target compounds have first to be extracted from the water sample with high recovery rates. A number of publications have described liquid-liquid extraction (LLE) using diethyl ether [3–5], dichloromethane [6–9], ethyl acetate [10–12] and benzene [13]. Solid-phase extraction (SPE) has gained in popularity in recent years. A variety of materials are available that have been used successfully for the extraction of phenoxyalkanoic acids. Most publications describe the use of modified silica gels, especially RP-C₁₈ [14–23]

* Corresponding author.

or RP-C₈ [24]. The use of the polymeric materials Amberlite XAD-4 [25], PLRP-S, PRP-1 [26,27] or Wofatit Y 77 [28–30] has also been reported. An ion exchanger [31] and a combination of Carbopack B and SAX [32] have also been used.

Methods for the determination of polar contaminants are mostly performed for a few well known compounds such as the acidic herbicides 2,4-D and 2,4,5-T. The determination of a larger number of acidic compounds has been described in only a few publications [9,14,22,27]. Our aim was to develop a method that would include a wide range of acidic contaminants that need to be determined at the low ng/l level in drinking water.

In this paper, a method for the SPE of 34 phenoxyalkanoic acids and other acidic herbicides from drinking water and groundwater is described.

2. Experimental

2.1. Materials

All solvents were Pestanal products from Riedel-de Haën (Seelze, Germany). Pentafluorobenzyl bromide was obtained from Aldrich (Steinheim, Germany) and triethylamine from Merck (Darmstadt, Germany). Sample vials, screw-caps and septa were purchased from Zinsser (Frankfurt, Germany) and 200- μ l inserts for the sample vials from CS-Chromatographie Service (Langerwehe, Germany). All pesticide standards were of analytical purity from Promochem (Wesel, Germany) or of Pestanal quality from Riedel-de Haën. Stock solutions of all compounds were prepared in toluene or methanol.

Solid-phase extraction was carried out with cartridges of polypropylene with a volume of 6 ml from Baker (Frankfurt, Germany). The RP-C₁₈ material labelled C was obtained from Eurochrom (Berlin, Germany) (Europrep 60–30 C₁₈; 60 Å, 20–45 μ m, irregular) and the other two RP-C₁₈ materials, labelled A and B, were from Baker and ICT (Frankfurt, Germany),

respectively. RP-phenyl (RP-Phe) material was purchased from Baker. Adjustable transferpettors (1–10 and 10–100 μ l) were supplied by Brand (Wertheim, Germany). A Beta I freeze-drier from Christ (Osterode, Germany) was used in several experiments.

2.2. Sample preparation

A tap water sample of 1 l was spiked by adding a mixture of pesticides dissolved in methanol to obtain a concentration of 100 ng/l of each active compound. The internal standard 2,4-dichlorobenzoic acid, was added at a concentration of 200 ng/l. The sample was then acidified to pH < 2 with HCl. Each SPE cartridge was filled with 1 g of RP-C₁₈ adsorbent. Conditioning was performed successively with 10 ml of acetone, 10 ml of methanol and finally 10 ml of distilled, deionized water (pH < 2). The solvents were drawn through the cartridges by means of a gentle vacuum and the cartridge was not permitted to run dry during the whole conditioning procedure. The water sample spiked with the herbicides was then percolated through the cartridge at a flow-rate of *ca.* 8 ml/min applying a low vacuum. After drying the cartridge for 2–3 h under a gentle stream of nitrogen, the herbicides were eluted with 2.5 ml of methanol. The eluate was dried under a gentle stream of nitrogen.

2.3. Derivatization

Derivatization was performed at 90°C using 200 μ l of pentafluorobenzyl bromide (PFBr) (2% in toluene) and 2 μ l of triethylamine as catalyst as described previously [1]. The derivatized sample was then dried under nitrogen and finally dissolved in 100 μ l of toluene.

2.4. GC-MS parameters

All mass spectrometric measurements were performed with a Hewlett-Packard HP 5970 mass-selective detector combined with an HP 5890 gas chromatograph fitted with a 25 m \times 0.2 mm I.D. \times 0.33 μ m HP-5 capillary column and a

1.5 m × 0.32 mm I.D. × 0.17 μm HP-5 precolumn. The carrier gas was helium (purity 99.999%) set to a head column pressure of 100 kPa. The oven temperature was held at 100°C for 1 min following injection, then programmed at 30°C/min to 150°C, which was held for 1 min, then at 3°C/min to 205°C followed by 10°C/min to 260°C and finally held for 23 min. The injection port and transfer line temperatures were 210 and 250°C, respectively. Amounts of 2 μl of sample were injected by means of an HP 7673 autosampler using hot splitless injection with the split closed for 0.9 min. For SIM three characteristic ions were selected for each compound and scanned using corresponding time windows with dwell times between 100 and 200 ms per ion. Mass spectrometer tuning was performed weekly using the autotuning macro. The precolumn and insert liner were exchanged after not more than 50 injections.

3. Results and discussion

3.1. Target compounds

To meet the objectives for the surveillance and monitoring of acidic herbicides in water samples, a routine method with low detection limits for all active compounds had to be developed and evaluated. After having demonstrated in a previous study [1] that phenoxyalkanoic acids and other acidic herbicides can be easily detected by GC-MS as their PFBBr esters at picogram levels, the aim of this study was to find the extraction procedure best suited for sample preparation and trace enrichment. In recent years in our laboratory, LLE with dichloromethane and SPE using RP-C₁₈ material were frequently applied in parallel to the same water samples to check the reliability of SPE results. We have come to the conclusion that before using SPE as a routine method, the RP-C₁₈ material and the extraction conditions must be carefully evaluated, otherwise the results vary dramatically.

The target compounds include phenoxyalkanoic acids and their esters, other acidic pesticides and related compounds of environmental

interest, and are representative of a variety of chemical structures containing acidic protons. The structural formulae of all the compounds studied are presented in Fig. 1.

All experiments were carried out under conditions that match the requirements of water monitoring analysis with respect to the maximum tolerances for pesticides in drinking water. Therefore, all drinking water samples were spiked with a mixture of all 34 target compounds to obtain a concentration level of 100 ng/l or lower. The whole procedure of sample extraction and derivatization is presented in Fig. 2.

3.2. Influence of adsorbent drying on the recovery

Our first recovery experiments were carried out with RP-C₁₈ material from supplier A. According to earlier observations, the influence of the drying process of the adsorbent has been found to be a critical step in SPE. Independent of the type of pesticides or environmental contaminants determined in water, sometimes irreproducible results were obtained and these results correlated in many instances with incomplete drying of the RP-C₁₈ material before eluting the adsorbed compounds. Two drying procedures are executed in addition to the first drying of the column by vacuum. Some users of SPE prefer freeze-drying and, others flushing the extraction column with a gently stream of nitrogen. Both drying procedures were investigated in parallel in this study.

On comparing the recovery values for drying with nitrogen and for freeze-drying, no significant differences in the average recoveries could be observed. Therefore, nitrogen flushing was used as the standard procedure in all further experiments because of its simplicity.

3.3. Selection of RP adsorbent material

As a few of the active compounds, such as clopyralid, 4-chlorophenoxyacetic acid, flurenol and 2,4-DB in particular, were found to give inadequate recoveries, adsorbents with other chemical structures were tested. RP-Phe and a

mixture of RP-Phe and RP-C₁₈ (1:1) were used for the extraction of the target compounds from water. Using a mixed material, improved recoveries were expected because of the operation of a mixed interaction process in adsorption, taking advantage of the favourable properties of the individual phases.

RP-C₁₈ material from supplier A on average showed better recoveries than those with the RP-Phe material and the blends. The same holds true if the number of compounds with an aimed recovery of better than 70% is compared. Surprisingly, only two herbicides were found to be extracted significantly better from water with RP-Phe than with RP-C₁₈ from supplier A, namely fluroxypyr and picloram.

The influence of the solvation effect was then studied with the addition of methanol to the water sample. The recoveries with RP-C₁₈ from

supplier A and a mixture of RP-C₁₈ and RP-Phe (1:1) after the addition of methanol to the sample were found to be only slightly changed. Whereas with the mixed phase no better recoveries could be achieved, the recoveries with RP-C₁₈ were found to be slightly better. Adding methanol to the water sample prior to extraction, however, generally led to better reproducibility.

It is well known by users that the material from a supplier can vary in its quality from batch to batch. Therefore, it is common practice to check batches with the compounds under investigation before buying a greater stock. Since we undertook our first experiments with an adsorbent selected for less polar pesticides such as polycyclic aromatic hydrocarbons and polychlorinated biphenyls, a check of RP-C₁₈ materials from other suppliers was carried out. The

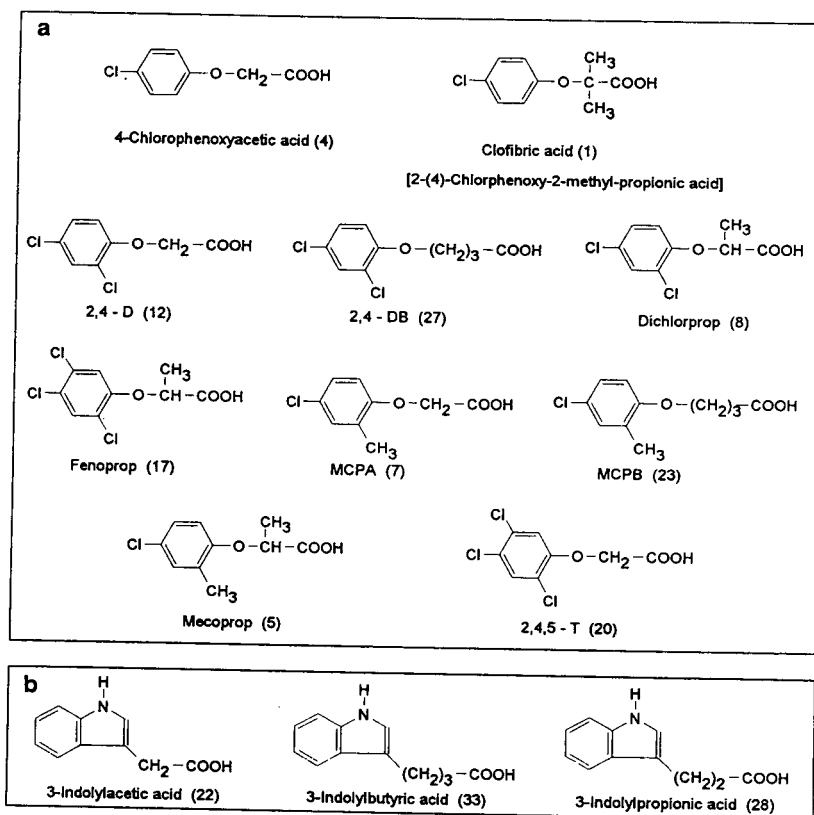


Fig. 1.

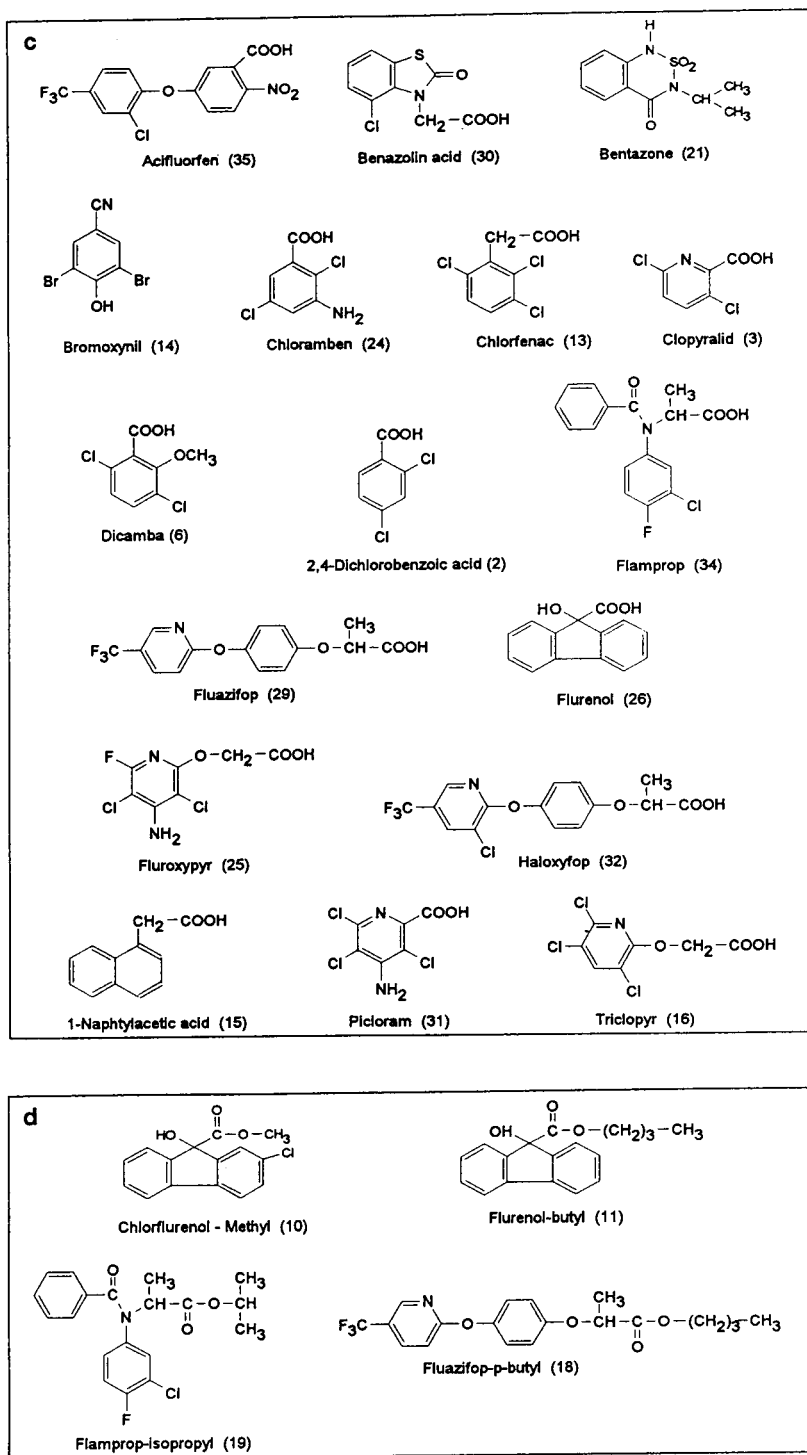


Fig. 1. (a) Phenoxyalkanoic acid herbicides and the drug clofibric acid; (b) indolycarboxylic acids; (c) other acidic herbicides and the internal standard (2); (d) herbicidal esters of considerable stability against hydrolysis.

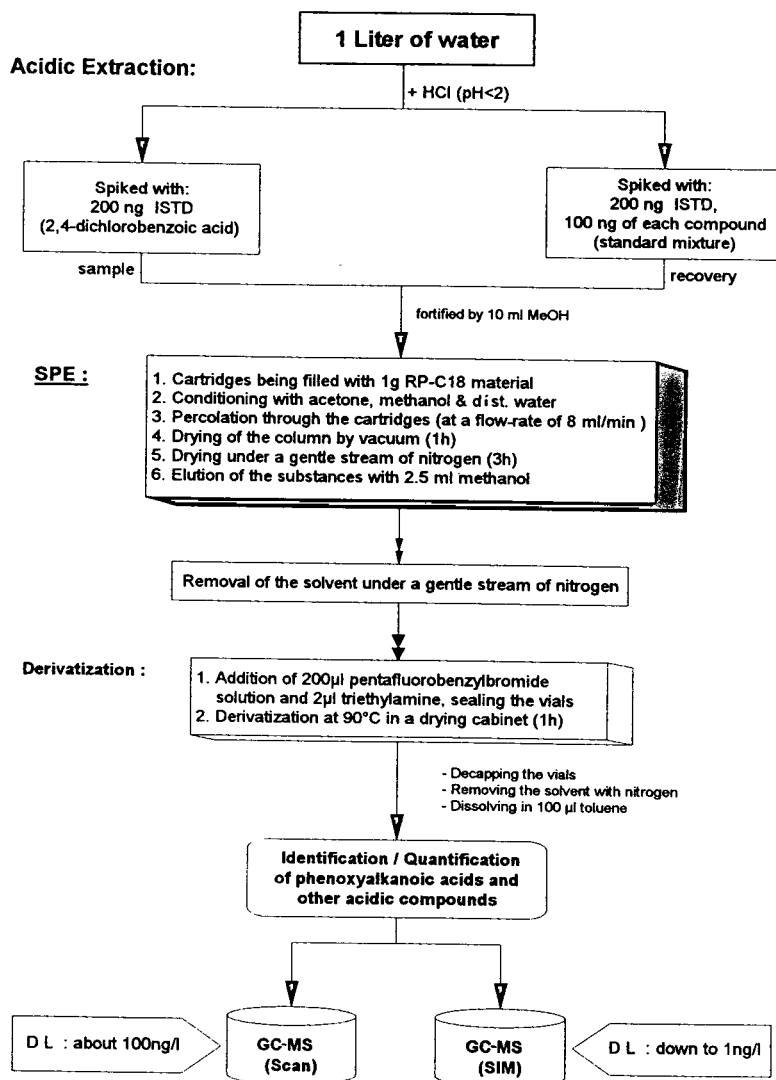


Fig. 2. Solid-phase extraction of acidic contaminants followed by pentaffluorobenzoylation and GC-MS determination. ISTD = Internal standard.

same recovery experiments were performed using RP-C₁₈ material A, B and C and a mixture of RP-C₁₈ A and RP-Phe. All experiments were carried out with the addition of methanol. The results of a series of sixfold experiments are compiled in Table 1.

A comparison of the recoveries of the adsorbents from the three suppliers reveals considerable differences between their trapping properties. Whereas with material A only 9 out of the

34 target compounds give recoveries greater than 70%, with material B 17 and with material C 26 compounds show recoveries greater than 70%. A comparison of the average recoveries of all the target compounds in Table 1 demonstrates the excellent properties of adsorbent C, with an average recovery of 87% compared with 71% for adsorbent B and only 59% for adsorbent A. Four of the investigated compounds were excluded from the evaluation of average recoveries

Table 1
Recoveries (%) with standard deviations ($n = 6$) of acidic herbicides with SPE using various adsorbent materials with water samples containing 1% of methanol

No.	Compound	C ₁₈ ^a - Phe	S.D. (%)	C ₁₈ A	S.D. (%)	C ₁₈ B	S.D. (%)	C ₁₈ C	S.D. (%)
1	Acifluorfen	43	8	68	5	58	19	77	13
2	Benazolin	38	6	37	5	75	7	89	11
3	Bentazone	67	8	76	7	56	11	71	24
4	Bromoxynil	52	24	72	24	59	15	75	27
5	Chloramben	20	4	17	3	40	5	58	6
6	Chlorfenac	54	8	72	3	109	12	92	9
7	Chlorflurenol-methyl	76	7	88	4	92	8	109	2
8	4-Chlorophenoxyacetic acid	18	3	28	3	19	2	72	11
9	Clofibric acid	78	10	96	5	81	6	106	7
10	Clopyralid	22	10	33	4	55	11	79	5
11	2,4-D	36	7	51	5	106	8	79	16
12	2,4-DB	24	13	36	6	53	6	53	5
13	Dicamba	51	9	63	3	95	9	101	10
14	2,4-Dichlorobenzoic acid	56	8	76	5	60	3	90	9
15	Dichlorprop	43	7	67	6	77	9	94	10
16	Fenoprop	54	6	65	5	70	14	100	7
17	Flamprop	53	7	60	4	75	10	88	8
18	Flamprop-isopropyl	89	7	98	7	100	8	109	14
19	Fluazifop	48	8	64	5	60	9	91	11
20	Fluazifop- <i>p</i> -butyl	55	8	65	3	79	4	101	6
21	Flurenol	26	4	25	13	20	10	33	1
22	Flurenol-butyl	75	7	81	2	95	8	109	2
23	Fluroxypyr	21	4	23	3	63	6	87	10
24	Haloxyfop	48	6	58	2	59	9	88	10
25	3-Indolylacetic acid ^b	13		12		40		42	
26	3-Indolylbutyric acid ^b	8		6		12		10	
27	3-Indolylpropionic acid ^b	40		9		40		56	
28	1-Naphthylacetic acid	49	8	56	8	75	15	104	6
29	MCPA	41	8	55	5	76	10	85	10
30	MCPB	42	4	41	8	74	6	69	6
31	Mecoprop	51	7	64	4	68	10	89	8
32	Picloram ^b	27		6		—		9	
33	2,4,5-T	75	17	82	8	88	5	102	14
34	Triclopyr	57	6	67	4	79	8	107	5
Average		49		59		71		87	
No. of compounds with recovery $\geq 70\%$		5		9		17		26	
No. of compounds with recovery $\geq 50\%$		15		22		26		29	

^a With RP-C₁₈ material A.

^b Not taken into account for averaging owing to unsatisfactory recovery.

because their recoveries were low with all the materials tested. These compounds are the three indolealkanoic acids and picloram. Whereas the indole-3-alkanoic acids are certainly of only

limited interest in general environmental monitoring, picloram may be the target of environmental monitoring. In the course of this study RP-Phe was found to be best suited for picloram

whereas RP-C₁₈ seems not to be suitable for the extraction of this compound.

The recoveries using material C demonstrate that compounds containing more than one functional group show lower recoveries. Note that with increasing aliphatic chain length the recoveries of the phenoxyalkanoic acids unexpectedly decrease from 2,4-D to 2,4-DB and from MCPA to MCPB, whereas aliphatic chain branchings increase the recoveries such that dichlorprop is better extracted than 2,4-D and mecoprop better than MCPA.

The results of our investigations showed clearly that material C is in this case superior to all the other materials tested. Therefore, it was chosen for the screening of acidic compounds in water samples. It should be emphasized that the RP-C₁₈ adsorbents A and B work satisfactorily in other applications such as with chlorinated pesticides, triazine herbicides and polycyclic aromatic hydrocarbons.

3.4. Recovery experiments at low concentration levels

To check the potential of the described extraction method, recovery experiments were carried out by spiking of a series of drinking water samples with all the target compounds at concentrations below the 100 ng/l level. In recovery experiments, the practical detection limits for each compound were determined by analysing 1 l of drinking water spiked with 50, 25, 10, 5 and 1 ng of the standard mixture. At each concentration, a threefold determination was carried out. In Fig. 3 the multiple ion detection (MID) chromatogram obtained during the analysis of the spiked drinking water is presented, which in this instance was spiked at a concentration level of 10 ng/l. The chromatogram shows that the detection limit achievable with this method for most of the target compounds is clearly below 10 ng/l.

Note that although the extraction of 3-indolybutyric acid is not satisfactory with this method, a drinking water sample containing 10 ng/l of this compound gives a positive result, as can be observed from peak 32 in Fig. 3. The only

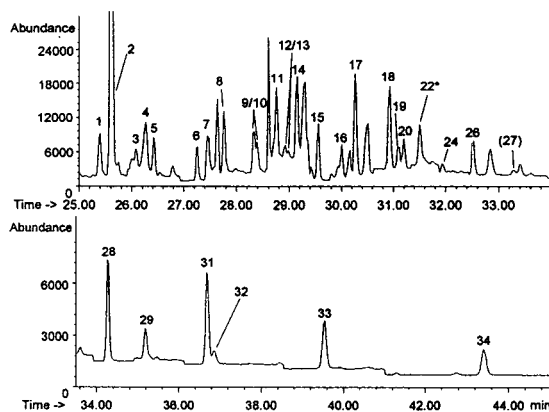


Fig. 3. MID chromatogram of an extract of a water sample spiked at 10 ng/l. Internal standard (2) added at a concentration of 200 ng/l. The asterisk indicates 3-indolyacetic acid PFB ester (21) coeluting.

compounds under investigation that could not be spotted using this procedure at the 10 ng/l concentration level were fluorenone, chloramben and, of course, picloram. As can be seen from Fig. 4, a positive confirmation of the identity of any target compound is possible by means of the three indicative ion traces that are the source of the peak seen in the MID chromatogram.

In this particular instance the demonstration was done for the small peak of 3-indolybutyric acid seen in Fig. 3 as peak 32. All peaks that can be seen in the MID chromatograms represent the equivalent of 200 pg injected, presupposing a total recovery of the spiked target compounds.

The evaluation of all spike experiments down to a concentration of 1 ng/l was carried out to obtain an estimate of the detection limit of every target compound with real drinking water sam-

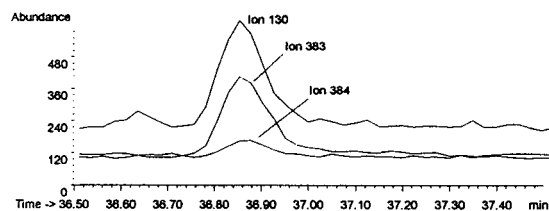


Fig. 4. Ion traces of m/z 384, 383 and 130 for 3-indolybutyric acid reconstructed from the MID chromatogram shown in Fig. 3.

ples. For every individual compound three indicative masses were recorded, as described in a previous paper [1] and demonstrated in Fig. 4 with one of them. Detection levels were determined by extracting the ion traces for each individual compound. This means a time-consuming procedure especially for quantification, because proper integration parameter setting is important and has to be checked individually. Therefore, we do not report detection limits

calculated from the calibration graphs obtained in the series of spike experiments rather than the lowest concentration level at which in three parallel analyses the target compound could definitively be seen with a signal-to-noise ratio of 3:1 or better. In Table 2 the detection limits for each compound are reported for the pure standard and in addition after extraction from drinking water samples. The detection limits for the individual compounds were found to be between

Table 2
Detection limits (DL) of the target compounds as their PFB derivatives in standard mixtures and in spiked tap water samples

No.	Compound	t_R (min)	DL (standard) (pg)	DL (SPE) (ng/l) ^a
1	Clofibric acid	25.42	2	≤ 1
2	2,4-Dichlorbenzoic acid	25.65	4	≤ 1
3	Clopyralid	26.18	20	≤ 10
4	4-Chlorophenoxyacetic acid	26.28	10	≤ 10
5	Mecoprop	26.43	10	≤ 1
6	Dicamba	27.28	2	≤ 1
7	MCPA	27.48	2	≤ 1
8	Dichlorprop	27.79	1	≤ 1
9	Chlorflurenol-methyl ^b	28.31	10	≤ 10
10	Flurenol-butyl ^b	28.40	10	≤ 10
11	2,4-D	28.72	20	≤ 5
12	Chlorfenac	28.93	20	≤ 10
13	Bromoxynil	29.07	20	≤ 10
14	1-Naphthylacetic acid	29.17	2	≤ 5
15	Triclopyr	29.56	2	≤ 1
16	Fenoprop	30.03	2	≤ 5
17	Fluazifop- <i>p</i> -butyl ^b	30.28	1	≤ 1
18	Flamprop-isopropyl ^b	30.92	3	≤ 1
19	2,4,5-T	31.12	20	≤ 10
20	Bentazone	31.17	20	≤ 10
21	3-Indolylacetic acid	31.45	10	–
22	MCPB	31.54	20	≤ 10
23	Chloramben	31.75	20	≤ 25
24	Fluroxypyr	31.94	30	≤ 10
25	Flurenol	32.15	30	≤ 25
26	2,4-DB	32.87	30	≤ 10
27	3-Indolylpropionic acid	33.28	10	–
28	Fluazifop	34.34	5	≤ 1
29	Benazolin	35.22	10	≤ 10
30	Picloram	35.48	30	–
31	Haloxypyr	36.85	10	≤ 1
32	3-Indolylbutyric acid	36.91	10	–
33	Flamprop	39.64	2	≤ 1
34	Acifluorfen	42.96	100	≤ 10

^a Detection limits are not listed for compounds with unsatisfactory recoveries.

^b Other esters.

1 and 10 ng/l, with the exception of two compounds.

The detection limits of the four active compounds that give inadequate recoveries with the SPE procedure were omitted, but the detection limits of the GC–MS method with test compounds (standards) are reported in Table 2.

It should be emphasized that the detection limits given had been estimated conservatively. This becomes evident on looking at Fig. 3, with peaks 29 and 34 of benazolin or acifluorfen having signal-to-noise ratios better than 10:1 but an estimated detection limit of 10 ng/l as given in Table 2.

3.5. Application to ground water samples

Finally, the potential of the procedure for residue analysis of drinking water is demonstrated with an example from a survey of ground and tap waters in Berlin carried out in 1992 and 1993. The recovery experiments with spiked tap water showed that nearly all of the 34 target compounds could be detected in tap water with detection limits between 1 and 25 ng/l, as compiled in Table 2. None of the real tap water samples gave positive results for any of the herbicides. The investigation of ground water samples, especially those from sites that were used for the production of drinking water, resulted in only a few positives at concentration levels clearly below the maximum tolerance of 100 ng/l. In one ground water sample mecoprop was found at 11 ng/l, as demonstrated in Fig. 5.

All three indicative ions arise simultaneously to form a peak at the retention time expected,

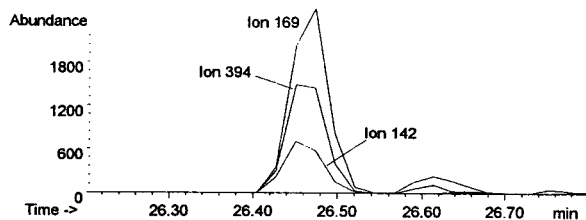


Fig. 5. Analysis of a ground water sample containing 11 ng/l of mecoprop. Ion traces of m/z 394, 169 and 142 for mecoprop PFB ester.

exhibiting the intensity ratios as calibrated within an acceptable limit of variation, an essential result for positive identification. Other positive findings in raw water samples included mecoprop and dichlorprop.

In further investigations, this method was extended to the analysis of surface and sewage water samples. The performance of this method and the results of these investigations will be presented elsewhere [33].

3.6. Derivatization and mass spectrometric detection

The derivatization procedure and the mass spectrometric detection method are described and discussed in detail elsewhere [1]. Of course, the recoveries reported are not dependent on the final determination step. The eluates can equally be applied to the analysis with TLC using automated multiple development (AMD-TLC) [18] or HPLC.

Recently, the application of phase-transfer alkylation with PFBBr was reported as an alternative derivatization procedure [34]. In the same paper, a 100-fold increase in sensitivity by using electron-capture negative-ion chemical ionization MS (ECNCI-MS) was reported but could not be reproduced in our laboratory. Only a twofold increase compared with EI-MS with SIM was observed with derivatized standards applying ECNCI-MS with two different quadrupole MS systems (Finnigan 4000 and Hewlett-Packard 5989 A MS Engine). In preliminary studies, ECNCI-MS proved to be more prone to interferences from the matrix in real water samples with out quadrupole instruments. Thus, detection limits from environmental water samples were found to be surprisingly better with EI-MS-SIM. This results from target ions with much higher m/z values in EI-MS than those in ECNCI-MS caused by easy fragmentation of the PFB esters under ECNCI conditions. These matrix problems with ECNCI-MS detection might be overcome when using a high-resolution mass spectrometer as reported by Meiring *et al.* [34], but this type of instrument is not in widespread use in environmental analysis. In a normal environ-

mental laboratory, routinely achieving a resolution of 4000 with acceptable transmission would, in our opinion, involve too large a proportion of “down-time” when analysing “dirty” samples.

Using GC–EIMS with SIM, detection limits in the low-picogram range region can be achieved [1] for many phenoxy-carboxylic acid PFB esters and related compounds (see Table 2). When performing the extraction procedure described with RP-C₁₈ material A, detection limits down to 1 ng/l can be achieved for environmental water samples with a high load of matrix [33].

4. Conclusions

Our investigations indicate that a careful selection and check of the adsorbent is a prerequisite in SPE. Adsorbents of the same type may vary so much in their ability to retain the analytes that an adsorbent from one supplier may be well suited whereas that from another supplier may give unsatisfactory results. Taking this into account, the method described has proved to be suitable for the sensitive screening of about 30 phenoxyalkanoic acids and other acidic compounds clearly below the concentration of 100 ng/l fixed by the EC as the maximum tolerance for drinking water. At a concentration level of 100 ng/l, 29 of the 34 compounds studied can be extracted with recoveries better than 50% and 26 compounds with recoveries better than 70%.

5. References

- [1] Th. Heberer, S. Butz and H.-J. Stan, *J. Assoc. Off. Anal. Chem.*, in press.
- [2] *EEC Drinking Water Guideline, 80/779/EEC, EEC No. L229/11-29*, Commission of the European Communities, Brussels, August 30th, 1980.
- [3] N.C. Jimenez, Y.H. Atallah and T.R. Bade, *J. Assoc. Off. Anal. Chem.*, 72 (1989) 840–844.
- [4] T. Tsukioka, R. Takeshita and T. Murakami, *Analyst*, 111 (1986) 145–149.
- [5] M.A.H. Franson, *Standard Methods for the Examination of Water and Wastewater*, 17th ed., Part 6000, Automated Laboratory Analyses, American Public Health Association, Washington, DC, p. 6-182–6-187.
- [6] H. Agemian and A.S.Y. Chau, *Analyst*, 101 (1976) 732–737.
- [7] W. Fresenius, K.E. Quentin and W. Schneider, *Water Analysis*, Springer, Berlin, 1988, pp. 587–588.
- [8] W. Schüssler, *Chromatographia*, 29 (1990) 24–30.
- [9] H.-B. Lee, T.E. Peart, J.M. Carron and H. Tse, *J. Assoc. Off. Anal. Chem.*, 74 (1991) 835–842.
- [10] A. Brown, R.D. Stephens and I.S. Kim, *Trends Anal. Chem.*, 10 (1991) 330–335.
- [11] I.S. Kim, F.I. Sasinis, R.D. Stephens, J. Wang and M.A. Brown, *Anal. Chem.*, 63 (1991) 819–823.
- [12] W. Weber, *Ergebnisse und Tendenzen der Analytik von Pflanzenbehandlungsmitteln und ähnlichen Stoffen sowie deren Metaboliten in Grund- und Trinkwässern, Schr.-Reihe Verein WaBoLu 68*, Gustav Fischer, Stuttgart, 1987, pp. 109ff.
- [13] J. De Beer, C.H. Van Peteghem and A.M. Heyndrickx, *J. Assoc. Off. Anal. Chem.*, 61 (1978) 1140–1154.
- [14] C. Schlett, *Z. Wasser-Abwasser-Forsch.*, 23 (1990) 32–35.
- [15] M.J.I. Mattina, *J. Chromatogr.*, 542 (1991) 385–395.
- [16] S.H. Hoke, E.E. Brueggemann, L.J. Baxter and T. Trybus, *J. Chromatogr.*, 357 (1986) 429–432.
- [17] A. Gratzfeld-Hüsgen, R. Schuster and R. Weber, *LaborPraxis*, 8 (1992) 800–803.
- [18] *DIN 38 407, Teil 11, Deutsche Einheitsverfahren zur Wasser-, Abwasser- und Schlammuntersuchung, Gemeinsam erfaßbare Stoffgruppen (Gruppe F), Bestimmung ausgewählter organischer Pflanzenbehandlungsmittel mittels Automated Multiple Development (AMD)-Technik (F11)*, Beuth Verlag Berlin, December 1990.
- [19] *DIN 38 407, Teil 14, Deutsche Einheitsverfahren zur Wasser-, Abwasser- und Schlammuntersuchung, Gemeinsam erfaßbare Stoffgruppen (Gruppe F), Bestimmung von Phenoxyalkancarbonsäuren mittels Gaschromatographie und massenspektrometrischer Detektion nach Fest-Flüssig-Extraktion und Derivatisierung (F14)*, Beuth Verlag Berlin, December 1990.
- [20] W.H. Weber, *Probenvorbereitung für die Bestimmung von Pflanzenbehandlungsmitteln und ähnlichen Stoffen aus Grund- und Trinkwässern mittels Festphasen-Extraktion*, Baker Lit. 223, Baker, Groß-Gerau, Germany.
- [21] H.J. Brauch and S. Schullerer, *Buch der Umweltanalytik*, Band 4, GIT, Darmstadt, 1992, pp. 83–88.
- [22] H.-J. Stan and Th. Heberer, *J. Chromatogr.*, 653 (1993) 55–63.
- [23] S. Butz and H.-J. Stan, *J. Chromatogr.*, 643 (1993) 227–239.
- [24] C. Sternbergh, *Chlorophenoxy Acid Herbicides Qualitative Screening (Liquid Chromatography, Ultraviolet Detection)*, ICT Lit. m 639, ICT, Frankfurt am Main, 1986.
- [25] S. Mierzwa and S. Witek, *J. Chromatogr.*, 136 (1977) 105–111.
- [26] R.B. Geerdink, A.A. Van Balkom and H.J. Brouwer, *J. Chromatogr.*, 481 (1989) 275–285.

- [27] I. Liska, E.R. Brouwer, A.G.L. Ostheimer, H. Lingeman and U.A.Th. Brinkman, *Int. J. Environ. Anal. Chem.*, 47 (1992) 267–291.
- [28] W. Dedek, K.D. Wenzel, F. Luft, H. Oberländer and B. Mothes, *Fresenius' Z. Anal. Chem.*, 328 (1987) 484–486.
- [29] W. Dedek, K.D. Wenzel, H. Oberländer, B. Mothes and J. Männig, *Fresenius' Z. Anal. Chem.*, 339 (1991) 201–206.
- [30] W. Dedek, L. Weil and L. Feistel, *Wasser*, 78 (1992) 155–164.
- [31] L. Renberg, *Anal. Chem.*, 46 (1974) 459–461.
- [32] A. Di Corcia, M. Marchetti and R. Samperi, *Anal. Chem.*, 61 (1989) 1363–1367.
- [33] Th. Heberer, S. Butz and H.-J. Stan, *J. Environ. Anal. Chem.*, in press.
- [34] H.D. Meiring, G. den Engelsman and A.P.J.M. de Jong, *J. Chromatogr.*, 644 (1993) 357–365.

Reversed-phase high-performance liquid chromatographic method using a pentafluorophenyl bonded phase for analysis of tocopherols

Steven L. Richheimer*, Michael C. Kent, Matthew W. Bernart

Hauser Chemical Research, Inc., 5555 Airport Boulevard, Boulder, CO 80301, USA

First received 18 January 1994; revised manuscript received 19 April 1994

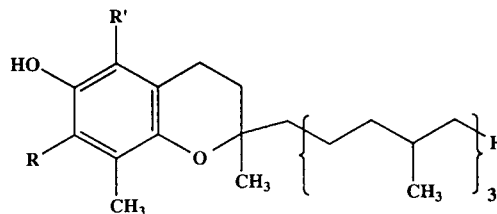
Abstract

A high-performance liquid chromatographic (HPLC) method to determine four tocopherols (α -, β -, γ -, and δ -) simultaneously was developed using a pentafluorophenyl reversed-phase column. A mobile phase of 92% aqueous methanol was used. Tocopherols were measured in vegetable oil, soybean oil deodorizer distillate, mixed tocopherol concentrate, and vitamin E pharmaceutical preparations.

1. Introduction

Several reports have appeared on the simultaneous measurement of tocopherols by high-performance liquid chromatography (HPLC) using normal-phase columns [1-4]. These methods appear to adequately separate the four major tocopherols (Fig. 1) but utilize silica columns and normal-phase solvents such as chloroform, tetrahydrofuran (THF), isopropanol (IPA), and hexane. On the other hand, to our knowledge there have been no methods reported that give satisfactory separation of α -, β -, γ -, and δ -tocopherols by reversed-phase HPLC. The difficulty appears to be in the separation of the isomeric β - and γ -tocopherols. Several groups have reported the separation of α -, β - and γ -, and δ -tocopherols [5-9], using reversed-phase columns. Satomura et al. [10] succeeded in

partially separating these tocopherol isomers on a 120-Å C_{18} column, but the β - and γ -tocopherols were not baseline separated. Moreover, the analysis required elevated temperature and a 50-min run time. Because there are definite advantages in using reversed-phase columns and solvents, we investigated this separation



	R	R'	
1	H	H	δ -tocopherol
2	H	CH ₃	β -tocopherol
3	CH ₃	H	γ -tocopherol
4	CH ₃	CH ₃	α -tocopherol

Fig. 1. Chemical structures of the tocopherols.

* Corresponding author.

problem on a variety of reversed-phase chemistries and report in this paper on the separation of all four tocopherols in less than 20 min using a commercially available pentafluorophenyl (PFP) column.

2. Experimental

2.1. Apparatus

The HPLC system consisted of a Model L-6200 pump, a Model AS-4000 autosampler equipped with a 100- μ l loop, and a Model L-4500A diode array detector (Hitachi Instruments, Fremont, CA, USA). The system was equipped with a Dynova 486 computer with a 320-megabyte hard drive (Foxborough, MA, USA) and DAD System Manager HPLC software (Hitachi Instruments). Chromatographic reports were printed on a Hewlett-Packard LaserJet 4 printer.

The preferred column was a 25 cm \times 4.6 mm Taxsil, PFP reversed-phase column with 5- μ m spherical particles (MetaChem Technologies, Torrance, CA, USA). Other PFP columns evaluated were a 25 cm \times 4.6 mm Chromegabond PFP column (ES Industries, Marlton, NJ, USA), and a 25 cm \times 4.6 mm TAC1 PFP column (Whatman, Clifton, NJ, USA).

2.2. Reagents

The tocopherols *d*- α , *d*- γ , and *d*- δ were obtained from Sigma (St. Louis, MO, USA). Rac- β -tocopherol was purchased from Matreya (Pleasant Gap, PA, USA). Methanol (S/P grade) was purchased from Baxter Diagnostics (Deerfield, IL, USA) and water was from the output of a Barnsted Model D4754 NANOpure water system (Dubuque, IA, USA). IPA, reagent alcohol, acetonitrile, and THF (UV grade) were Burdick and Jackson brand from Baxter Scientific Products (Bedford, MA, USA).

2.3. Chromatographic conditions

All columns were used without a guard column. The mobile phase was a 92:8 mixture of

methanol and water made by placing 80 ml of water in a 1-l mixing cylinder and adding methanol to volume and mixing. The flow-rate was 1.0 ml/min and the temperature was ambient. An aliquot of 10 μ l of sample was injected in isopropanol or tetrahydrofuran and detection was at 290 nm.

2.4. Procedure

A standard solution of the four tocopherols was prepared in IPA. Approximately 1 g of vegetable oil, accurately weighed, was placed in a 10-ml volumetric flask and diluted to volume with IPA. Similarly, 0.5 g of soybean oil deodorizer distillate and 10–20 mg of vitamin E preparations or mixed tocopherol concentrates were each diluted to 10.0 ml with IPA. In the event the sample did not give a clear solution in IPA, UV-grade THF was used instead. The sample and standard solutions (10 μ l) were injected directly into the column without any prior filtration. Under these conditions, triglycerides present in vegetable oils did not elute from the column but the accumulated triglycerides could be washed from the column using IPA.

3. Results

3.1. Investigation of different columns and mobile phases

Satomura et al. [10] reported poor separation of β - and γ -tocopherols on a C_{18} column using mobile phases containing methanol–water and ethanol–water. They achieved partial separation on this column using a 65:35 mixture of IPA and water at elevated temperature. A mixture of β - and γ -tocopherols in methanol was prepared and injected into a variety of different reversed-phase columns using a mobile phase of methanol–water (95:5). We observed poor to no separation of β - and γ -tocopherols on a variety of different C_{18} , proprietary media, phenyl, diphenyl, and cyano columns. However, there was nearly baseline separation of these two isomers using a PFP column. Two other commercially available 25 cm \times 4.6 mm PFP columns

Table 1
Peak resolution (R_s) of β - and γ -tocopherols utilizing the MetaChem PFP column under different HPLC conditions

Mobile phase	Flow-rate (ml/min)	Retention time of γ -tocopherol (min)	R_s
Methanol–water			
95:5	1.0	6.9	0.83
92:8	1.0	16.5	1.53
92:8	1.5	10.5	1.36
92:8 ^a	1.5	9.2	1.26
92:8 ^b	1.5	6.6	1.31
90:10	1.0	26.4	1.80
90:10	1.5	16.3	1.61
85:15	1.0	74.7	2.78
85:15	1.5	51.3	2.28

^aES Industries Chromegabond PFP column (25 cm \times 4.6 mm).

^bWhatman TAC1 PFP column (25 cm \times 4.6 mm).

were also investigated. Both the ES Industries PFP and the Whatman TAC1 PFP showed good separation of β - and γ -tocopherols, but the separation was best with the MetaChem PFP column (see also Table 1). Aqueous mobile phase mixtures employing ethanol, IPA, and acetonitrile were also investigated, but these did not improve the separation of β - and γ -tocopherols.

3.2. Selectivity of the PFP column

The chromatogram illustrated in Fig. 2 shows the results obtained with isocratic elution on a PFP column at ambient temperature using a 92:8

mixture of methanol and water on a standard mixture of α -, β -, γ -, and δ -tocopherols. Because of the unique selectivity of the PFP reversed-phase chemistry, baseline separation of these four tocopherol isomers could be easily obtained using a variety of methanol, water, flow-rate, and temperature conditions. Improved separation of β - and γ -tocopherols was obtained by increasing the water content of the mobile phase. This caused a corresponding increase in retention time of the tocopherols that could be offset partially by increasing either the flow rate or the temperature (see Table 1). However, our goal was to develop a rapid, isocratic method for the separation of tocopherols, and a mobile

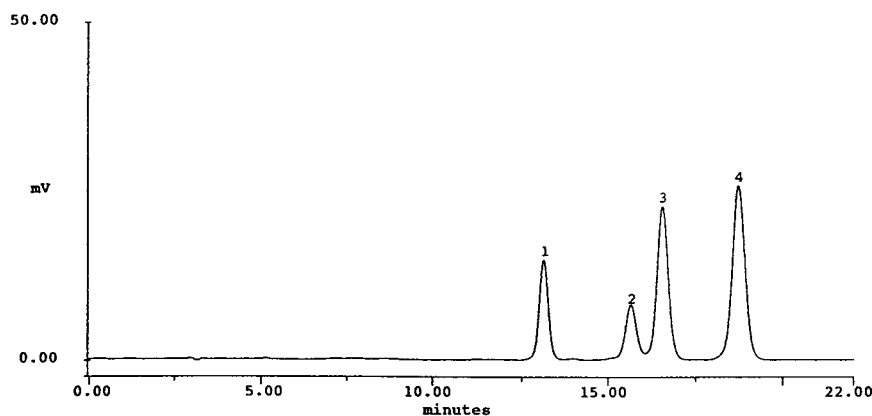


Fig. 2. Chromatogram of a standard mixture of tocopherols. Column: MetaChem PFP, 5 μ m; eluent: methanol–water (92:8, v/v); flow-rate: 1 ml/min; UV detection: 290 nm. Peaks: 1 = δ -tocopherol; 2 = β -tocopherol; 3 = γ -tocopherol; 4 = α -tocopherol.

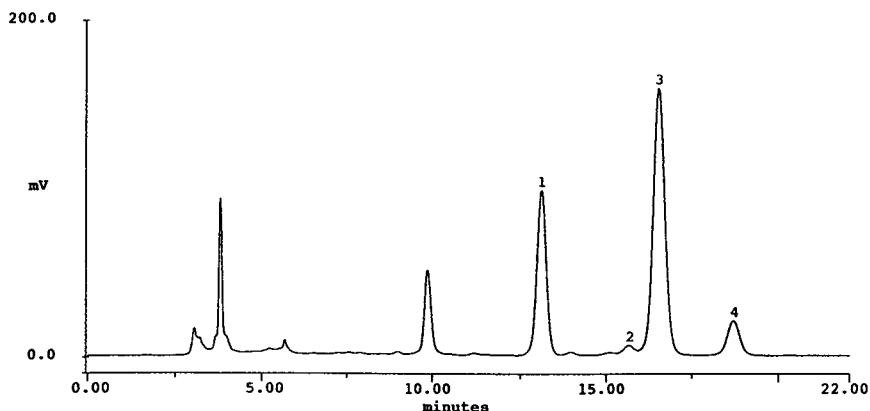


Fig. 3. Chromatogram of soybean oil deodorizer distillate, 0.5 g diluted to 10.0 ml with IPA. Chromatographic conditions and peaks are the same as in Fig. 2.

phase mixture of 92% aqueous methanol flowing at 1.0 ml/min gave baseline resolution of β - and γ -tocopherols in minimum time.

3.3. Analysis of samples

Fig. 3 shows the chromatogram obtained on soybean oil deodorizer distillate. This distillate is the starting material for most commercial production of naturally derived mixed tocopherols and vitamin E [11]. There are numerous mixed tocopherol antioxidant and vitamin E preparations on the market that could be analyzed by this method. Fig. 4 illustrates a typical chromato-

gram obtained on a liquid-filled capsule of naturally derived vitamin E.

Fig. 5 shows the chromatogram obtained on soybean oil. The method permits the identification and estimation of the four individual tocopherols in vegetable oils where they are present in low concentration. One advantage of the method when analyzing such samples is that the small β -tocopherol peak elutes before the much larger γ -tocopherol peak.

Using this method, *d*- α -tocopherol acetate eluted at a retention time of 1.3 relative to α -tocopherol, and hence, this semisynthetic tocopherol could serve as an internal standard

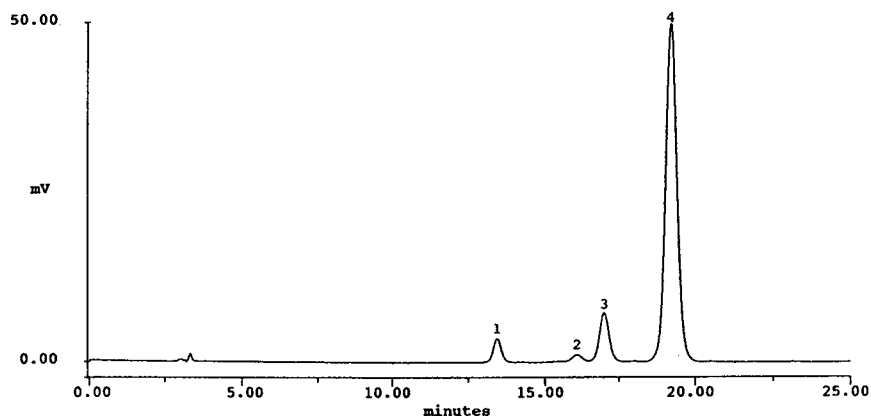


Fig. 4. Chromatogram of a sample of a 400-mg, natural-source, soft-gelatin, vitamin E capsule, 10 mg fill-diluted to 10.0 ml with IPA. Chromatographic conditions and peaks are the same as in Fig. 2.

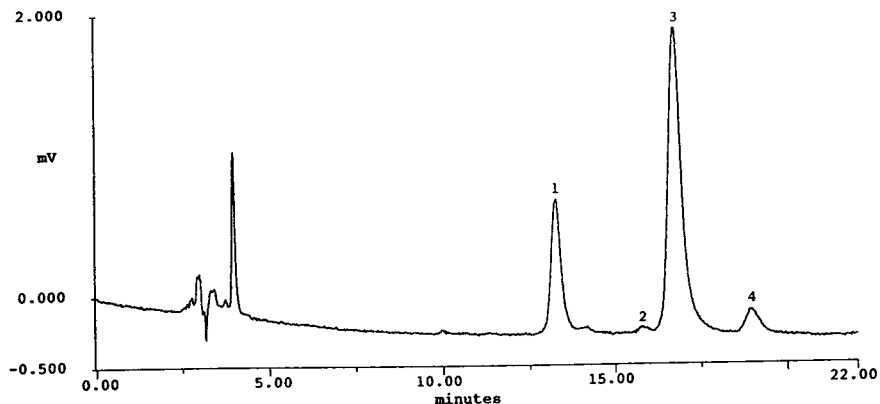


Fig. 5. Chromatogram of refined soybean oil, 1.0 g diluted to 10.0 ml with IPA. Chromatographic conditions and peaks the same as in Fig. 2.

for the analysis of naturally occurring tocopherols. In addition *trans*-retinol (vitamin A) and *trans*- β -carotene eluted at relative retention times of 0.4 and 4.7, respectively, using this method.

4. Discussion

The pentafluorophenyl bonded phase appears to provide unique selectivity for the separation of a variety of aromatic compounds [12,13]. A recent example of this unique selectivity is the report from our laboratories on the use of the PFP column for the difficult separation of taxol from other related taxanes [14]. Unlike more traditional reversed-phase media (C_{18} , C_8 , phenyl), the order of elution of β - and γ -tocopherols was reversed using the PFP column, and β -tocopherol eluted before γ -tocopherol (in the same order as normal-phase chromatography). However, the elution of the δ - and α -tocopherol was the same as with all other reversed-phase columns tested. This reversal of elution of β - and γ -tocopherols is an advantage because the natural abundance of γ -tocopherol is normally many times greater than β -tocopherol, and it is easier to separate and quantify a small fronting peak than a small tailing peak.

It is important to be able to individually quantify β - and γ -tocopherol because β -

tocopherol has five times the vitamin E activity of γ -tocopherol [15]. However, many of the published methods (including the official methods of the USP/NF [16], FCC [17], and AOAC [18], which use GC separation of the propionate esters of tocopherols) do not separate β - and γ -tocopherols. Reversed-phase HPLC has become a common method for assaying vitamins and other pharmaceutical components because of its high sensitivity, selectivity, accuracy, ease of use, and ruggedness. The method described here is much simpler to perform and more rapid than the GC methods of the official compendia and the normal-phase methods of various authors. In addition, the method determines the content of the four major tocopherols simultaneously in samples of vegetable oil, pharmaceutical vitamin E preparations, antioxidant preparations, mixed tocopherol concentrates, and crude vegetable oil distillates.

References

- [1] H.E. Woziwodski, *US Pat.*, 4 122 094 (1978).
- [2] C.G. Rammel and J.J.L. Hoogenboom, *J. Liq. Chromatogr.*, 8 (1985) 707.
- [3] W.D. Pocklington and A. Dieffenbacher, *Pure Appl. Chem.*, 60 (1988) 877.
- [4] *Technical Data Publication*, No. 886, Amicon Division, W.R. Grace and Co., Beverly, MA, 1989.
- [5] R.S. Parker, *Am. J. Clin. Nutr.*, 47 (1988) 33.

- [6] E.J. Rogers, S.M. Rice, R.J. Nicolosi, D.R. Carpenter, C.A. McClelland and L.J. Romanczyk, Jr., *J. Am. Oil Chem. Soc.*, 70 (1993) 301.
- [7] F. Khachik, G.R. Beecher, M.B. Goli, W.R. Lusby and J.C. Smith, Jr., *Anal. Chem.*, 64 (1992) 2111.
- [8] A.B. Barua, H.C. Furr, D. Janick-Buckner and J.A. Olson, *Food Chem.*, 46 (1993) 419.
- [9] K. Schwarz and W. Ternes, *Z. Lebensm. Unters. Forsch.*, 195 (1992) 95.
- [10] Y. Satomura, M. Kimura, and Y. Itokawa, *J. Chromatogr.*, 625 (1992) 372 and references cited therein.
- [11] N.O.V. Sonntag, personal communication.
- [12] A. Haas, J. Kohler and H. Hemetsberger, *Chromatographia*, 6 (1981) 341.
- [13] E. Csato, N. Fulop and G. Szabo, *J. Chromatogr.*, 511 (1990) 79.
- [14] S.L. Richheimer, D.M. Tinnermeier and D.W. Timmons, *Anal. Chem.*, 64 (1992) 2323.
- [15] A.J. Sheppard, J.A.T. Pennington and J.L. Weihrauch, in L. Packer (Editor), *Vitamin E in Health and Disease*, Dekker, New York, 1993, Ch. 2.
- [16] *United States Pharmacopeia XXII and National Formulary XVII*, United States Pharmacopeial Convention, Rockville, 1990, pp. 1451 and 1991.
- [17] Food and Nutrition Board, National Research Council, *Food Chemicals Codex*, National Academy Press, Washington, DC, 3rd ed., 1981, pp. 330–331.
- [18] W. Horwitz (Editor), *Official Methods of Analysis of the Association of Official Analytical Chemists*, AOAC, Washington, DC, 12th ed., 1975, p. 836.



ELSEVIER

Journal of Chromatography A, 677 (1994) 81-85

JOURNAL OF
CHROMATOGRAPHY A

Simultaneous high-performance liquid chromatographic determination of residual sulphamonomethoxine, sulphadimethoxine and their N⁴-acetyl metabolites in foods of animal origin

Naoto Furusawa, Takao Mukai*

School of Veterinary Medicine and Animal Sciences, Kitasato University, Towada 034, Japan

First received 18 January 1994; revised manuscript received 27 April 1994

Abstract

A rapid and sensitive method for the determination of residual sulphamonomethoxine, sulphadimethoxine and their N⁴-acetyl metabolites in beef, pork, chicken and eggs by high-performance liquid chromatography (HPLC) was developed. The extraction of these compounds was performed using a mixture of 90% (v/v) acetonitrile solution and hexane (5:4, v/v) to minimize the fat content followed by purification by alumina column chromatography. These extracts contained sulphonamide analytes which were free from interfering compounds when examined by HPLC using a LiChrosorb RP-18 column. The average recoveries from spiked meat and egg were in excess of 80% with relative standard deviations between 0.4 and 5.0%. The practical limits of detection were 0.01 ppm for all samples.

1. Introduction

In recent years, the application of veterinary drugs and feed supplements to livestock has increased to prevent diseases of animals and poultry. As a result, there is concern that residues of these compounds may be retained in foods derived from treated animals. In Japanese Food Sanitation Law, no food should contain any antibiotics or synthetic antibacterial substances. To produce animal products such as meat and eggs free from drug residues, it is necessary to set an adequate withdrawal period

after administration of the drug, based on data on the residue depletion obtained from pharmacokinetic studies, and to monitor drug residues in animal products.

Sulphamonomethoxine [SMM; 4-amino-N-(2-methoxypyrimidinyl)benzenesulphonamide] and sulphadimethoxine [SDM; 4-amino-N-(2,6-methoxy-4-pyrimidinyl)benzenesulphonamide] are widely used in Japanese farming. Pharmacokinetic studies of SMM and SDM have been performed in cows, hens and pigs, and one of their major metabolites is elucidated to be the N⁴-acetyl metabolite, which is acetylated at the N⁴-position by N-acetyltransferase [1-5]. According to Japanese Food Sanitation Law, the

* Corresponding author.

parent compounds such as SDM, and major metabolites such as N⁴-acetyl-SDM (N⁴-AcSDM), must be measured in food of animal origin. Although rapid clean-up procedures have been developed for the determination of SMM and SDM using high-performance liquid chromatography (HPLC) [6–10], simultaneous methods for these compounds and their major metabolites in various samples such as beef, pork, chicken and eggs have not been published. In this study, we developed a rapid and reliable method for the simultaneous determination of SMM, SDM and their N⁴-acetyl metabolites by HPLC in various foods of animal origin.

2. Experimental

2.1. Materials and reagents

Edible muscle tissues of swine, cattle and chicken and eggs served as samples, and were stored in a refrigerator until analysis. SMM and SDM were obtained from Wako (Osaka, Japan) and Sigma (St. Louis, MO, USA), respectively. N⁴-AcSMM and N⁴-AcSDM were generous gifts from Daiichi Seiyaku (Tokyo, Japan). Each stock standard solution (100 µg/ml) was prepared by accurately weighing 10 mg, dissolving it in 100 ml of HPLC-grade acetonitrile and diluting to the desired volume with the HPLC mobile phase. A 6-g portion of aluminium oxide 90 active basic (activity I, 60–200 µm) (Merck, Darmstadt, Germany) was placed in a column (300 × 15 mm I.D.) and sequentially washed with 30 ml of 90% (v/v) acetonitrile solution and acetonitrile. Other chemicals were obtained from Merck and were of the highest purity available.

2.2. Extraction and clean-up procedure

An accurately weighed 5-g amount of sample was homogenized in 25 ml of 90% (v/v) acetonitrile solution and 20 ml of hexane with a homogenizer (AM-1; Nippon Seiki, Tokyo). After centrifugation at 2100 g for 10 min, the supernatant was poured into a separating funnel through a No. 2 filter-paper (Toyo Roshi,

Tokyo, Japan). The extraction was repeated twice and the combined supernatant was left until completely separated into two layers. The acetonitrile layer was collected and then dried by adding anhydrous sodium sulphate followed by filtration. The filtrate was applied to an alumina column. After the column had been washed with 30 ml of acetonitrile, sulphonamides and their N⁴-acetyl metabolites were eluted with 20 ml of 90% (v/v) acetonitrile solution. The eluate was evaporated to dryness and the residue was dissolved in 1 ml of HPLC mobile phase. A 20-µl volume of the solution was injected into the HPLC system.

2.3. HPLC conditions

Analyses of standard and extracted sulphonamides were conducted using an LC-9A pump (Shimadzu, Kyoto, Japan) equipped with a 20-µl Rheodyne Model 2791 injector and an SPD-6A UV-Vis spectrophotometric detector (Shimadzu) operator at 270 nm. The separation was performed on a LiChrosorb RP-18 (7 µm) column (250 × 4 mm I.D.) (Merck) with a guard column (4 × 4 mm I.D.) (Merck) using acetonitrile–0.05 M phosphate buffer (pH 5.0) (25:75, v/v) as the mobile phase at a flow-rate of 1.0 ml/min at ambient temperature.

2.4. Calibration

Working standard solutions of concentrations 0.01, 0.02, 0.05, 0.10, 0.20 and 0.40 µg/ml of SMM, SDM, N⁴-AcSMM and N⁴-AcSDM were prepared from the stock standard solutions. Volumes of 20 µl of these solutions were injected into the column. Calibration graphs were obtained by measurement of peak heights.

3. Results and discussion

3.1. HPLC conditions

In order to determine sulphonamides, the use of HPLC appears to be much more advantageous than TLC and GC because of the high

sensitivity and speed without the complicated treatment of samples such as is needed in GC analyses [11,12]. We reported previously that six sulphonamides could be determined by HPLC using an ODS column and a mixture of acetonitrile, acetic acid and water as the mobile phase [10]. In preliminary experiments, when the same or similar HPLC conditions were used, SDM and N^4 -AcSDM could be separated but not SMM and N^4 -AcSMM. We therefore tried to separate these compounds using a combination of acetonitrile and phosphate buffer as the mobile phase. Based on several parameters such as pH and concentration of phosphate buffer, flow-rate and detection wavelength, the optimum HPLC conditions were determined.

The retention of all sulphonamides decreased on raising the pH of the buffer and with increasing concentration of acetonitrile in the mobile phase. The pH of phosphate buffer, rather than its molar concentration, affected the separation of target compounds. The flow-rate was 1.0 ml/min and the monitoring wavelength was adjusted to 270 nm because the maximum adsorption of all sulphonamides occurred at 270 nm [6,7,13]. The best separation of the compounds was obtained using acetonitrile–0.05 M phosphate buffer (pH 5.0) (25:75, v/v) as the mobile phase. Fig. 1 shows the chromatogram of N^4 -AcSMM, SMM, N^4 -AcSDM and SDM obtained under the established conditions. The target compounds were successfully separated within 12.4 min.

3.2. Calibration

The calibration graphs for SMM, SDM, N^4 -AcSMM and N^4 -AcSDM were linear between 0.02 and 0.4 $\mu\text{g/ml}$ and fitted the following equations, where y is peak height (mm) and x is concentration ($\mu\text{g/ml}$):

$$\text{SMM: } y = 376.09x \quad (r = 0.9999) \quad (1)$$

$$\text{SDM: } y = 197.75x \quad (r = 0.9996) \quad (2)$$

$$N^4\text{-AcSMM: } y = 562.08x \quad (r = 0.9999) \quad (3)$$

$$N^4\text{-AcSDM: } y = 247.77x \quad (r = 0.9994) \quad (4)$$

All of the correlation coefficients (r) were highly

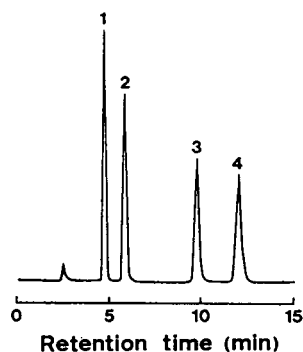


Fig. 1. Typical chromatogram of standard mixture. Peaks: 1 = N^4 -acetylsulphamonomethoxide ($t_R = 4.6$ min); 2 = sulphamonomethoxine ($t_R = 5.9$ min); 3 = N^4 -acetylsulphadimethoxine ($t_R = 9.9$ min); 4 = sulphadimethoxine ($t_R = 12.4$ min) (5 ng each). Column, LiChrosorb RP-18 (250 \times 4 mm I.D.); mobile phase, acetonitrile–0.05 M phosphate buffer (pH 5.0) (25:75, v/v); flow-rate, 1.0 ml/min; detection, 270 nm; absorbance range setting, 0.01 AUFS.

significant ($p < 0.01$) and all the calibration graphs were linear and passed through the origin. The detection limits of all the compounds were determined according to Ref. [9], and were 0.4 ng in each instance.

3.3. Extraction and clean-up

The difficulties in drug residue analyses in complex biological matrices such as animal tissues are generally caused by interfering co-extractants when target compounds are isolated [6–8,14,15]. The advantage of the present method is that SMM, SDM and their metabolites in various foods of animal origin can be determined using the same procedure without interferences. The extraction of the target compounds from meat and eggs was performed by homogenizing with 45 ml of 90% (v/v) acetonitrile–hexane (5:4, v/v) to minimize the fat content. Also, with the egg samples, this extract did not form an emulsion that would hinder the recovery of the target compounds. After centrifugation, they were completely recovered into the acetonitrile solution layer without leading to residue losses on the cellular pellet or transfer into the hexane layer (data not shown).

The extract is further purified to remove

interfering materials. Our previous work showed that basic alumina column chromatography was suitable for the clean-up of residual SMM, SDM and sulphaquinoxaline in various chicken tissues [10]. Therefore, basic alumina was used as the packing material for the column chromatography in this study. Fig. 2 shows the elution volumes of the target compounds from the alumina column using 90% (v/v) acetonitrile solution as the mobile phase. The target compounds in 5 ml of each collected fraction were determined by HPLC. All compounds were eluted with 20 ml of the mobile phase. The average recoveries ($n = 3$) of SMM, SDM, N^4 -AcSMM and N^4 -AcSDM were 98.3, 98.8, 100.1 and 99.9%, respectively, when the elution volume was 20 ml.

The resulting extracts were free from interferences, as can be seen in HPLC traces of blank pork (Fig. 3A), blank eggs (Fig. 3B), spiked pork (Fig. 3C) and spiked eggs (Fig. 3D). Similar chromatograms were obtained from beef and chicken samples (data not shown).

The use of commercial cartridge columns in order to extract and purify residual drugs in various foods of animal origin has been reported [8,9]. However, our preliminary experiments showed that sulphonamide-related compounds

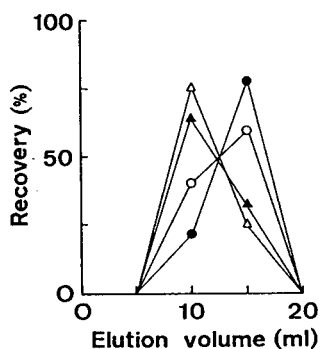


Fig. 2. Elution pattern of sulphamonomethoxine, sulphadimethoxine and their N^4 -acetyl metabolites from an alumina B column using 90% (v/v) acetonitrile solution as the mobile phase. A mixture of standard solutions of four compounds was prepared ($2.5 \mu\text{g}$ per 20 ml) and the solution was applied to the column. Results of three replicates. \bullet = Sulphamonomethoxine; \circ = N^4 -acetylsulphamonomethoxine; \blacktriangle = sulphadimethoxine; \triangle = N^4 -aceylsulphadimethoxine.

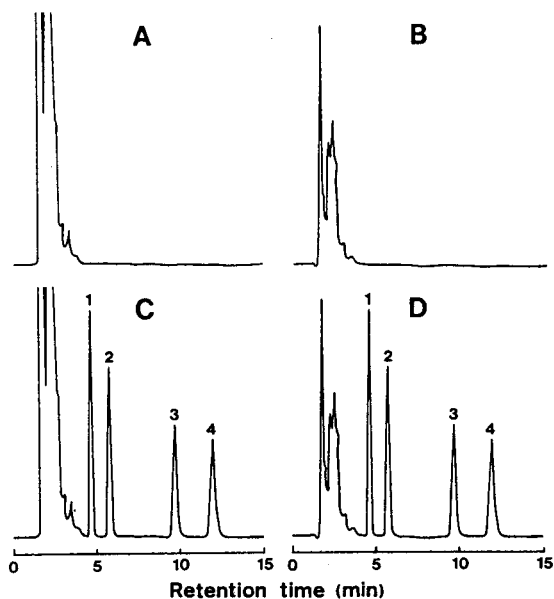


Fig. 3. Typical chromatograms of blank and spiked (0.05 ppm) pork and egg samples. (A) blank pork; (B) blank egg; (C) spiked pork; (D) spiked egg. Peaks and HPLC conditions as in Fig. 1.

including their metabolites from 5-g samples could not be determined simultaneously using the cartridges because of interfering co-extractants. Although the sequence of extraction and clean-up steps described here may be considered more or less classical, they can be evaluated in terms of the minimal steps and amounts of organic solvents which are required without interference. Moreover, packing materials such as alumina are much more economical than commercial cartridges.

3.4. Recovery studies

Using the present method, studies of the recovery of SMM, SDM, N^4 -AcSMM and N^4 -AcSDM from 5 g of beef, pork, chicken and eggs were carried out at spiking levels of 0.1, 0.5 and 1.0 ppm. As shown in Table 1, satisfactory results were obtained and the average recovery of these compounds from all samples were greater than 80% with relative standard deviations (R.S.D.) between 0.4 and 5.0%. In a practical analysis, the limits of detection from 5 g of

Table 1
Recoveries of sulphamonomethoxine, sulphadimethoxine and their N⁴-acetyl metabolites from meat and eggs

Sample	Spiked level (ppm)	Recovery (%)			
		SMM	N ⁴ -AcSMM	SDM	N ⁴ -AcSDM
Beef	0.1	98.0 (3.6)	87.5 (1.1)	96.2 (3.7)	96.0 (0.6)
	0.5	88.7 (4.4)	90.5 (2.9)	86.9 (4.4)	91.7 (0.9)
	1.0	91.3 (3.4)	85.7 (2.4)	94.3 (1.3)	90.0 (3.4)
Pork	0.1	97.6 (0.5)	89.3 (2.6)	95.7 (4.2)	95.0 (3.0)
	0.5	95.9 (1.4)	91.3 (0.6)	94.5 (0.9)	90.9 (4.6)
	1.0	95.1 (0.4)	93.4 (1.8)	95.8 (2.2)	89.3 (1.4)
Chicken	0.1	91.9 (2.9)	82.1 (1.7)	92.3 (2.5)	89.3 (2.8)
	0.5	90.4 (1.6)	88.8 (3.4)	91.3 (2.6)	91.0 (0.5)
	1.0	94.9 (2.6)	86.7 (4.7)	86.2 (2.1)	92.1 (3.3)
Eggs	0.1	90.5 (2.0)	85.7 (2.6)	93.8 (2.5)	90.9 (3.3)
	0.5	88.3 (0.7)	88.0 (5.0)	91.7 (2.6)	94.8 (2.8)
	1.0	93.8 (1.2)	90.3 (2.0)	87.0 (2.1)	89.5 (0.5)

Recoveries of four compounds from 5 g of beef, pork, chicken and eggs at the indicated levels according to the proposed method. Results are averages of five replicates. Figures in parentheses are relative standard deviations (%).

samples were 0.01 ppm for all compounds. The high recovery and low R.S.D. together with the low limits of detection indicate that this method has a good precision and may be accurate.

The method presented here has several minor technical improvements over previously published procedures. The purpose of this study was to develop a method for the simultaneous assay of SMM, SDM and their N⁴-acetyl metabolites in various foods of animal origin. Characteristics of this procedure are that it is rapid, sensitive, precise and economical. Therefore, this procedure may be useful for monitoring residual drugs in various foods of animal origin and studying pharmacokinetics.

Acknowledgements

We express our appreciation to Daiichi Seiyaku for supplying N⁴-AcSMM and N⁴-AcSDM.

References

[1] M. Shimoda, T. Shimizu, E. Kokue and T. Hayama, *Jpn. J. Vet. Sci.*, 46 (1984) 331.

[2] M. Shimoda, E. Kokue, R. Suzuki and T. Hayama, *Vet. Q.*, 12 (1990) 7.
 [3] A. Onodera, S. Inoue, A. Kasahara and Y. Ohshima, *Jpn. J. Vet. Sci.*, 32 (1970) 275.
 [4] R.S. Bajwa and J. Singh, *Indian J. Anim. Sci.*, 47 (1977) 549.
 [5] T.B. Vree, Y.A. Hekster and M.W. Tjihuis, *Antibiot. Chemother.*, 34 (1985) 130.
 [6] Y. Hori, *J. Food Hyg. Soc. Jpn.*, 24 (1983) 447.
 [7] T. Nagata and M. Saeki, *J. Food Hyg. Soc. Jpn.*, 29 (1988) 13.
 [8] S. Horii, C. Momma, K. Miyahara, T. Maruyama and M. Matsumoto, *J. Assoc. Off. Anal. Chem.*, 73 (1990) 990.
 [9] Y. Ikai, H. Oka, N. Kawamura, J. Hayakawa and M. Yamada, *J. Chromatogr.*, 541 (1991) 393.
 [10] N. Furusawa, T. Mukai and H. Itoh, *Jpn. Poult. Sci.*, 30 (1993) 359.
 [11] N. Nose, S. Kobayashi, A. Hirose and A. Watanabe, *J. Chromatogr.*, 123 (1976) 167.
 [12] N. Nose, Y. Kikuchi, F. Yamada and A. Watanabe, *J. Food Hyg. Soc. Jpn.*, 20 (1979) 115.
 [13] T.B. Vree, E.W.J. Beneken Kolmer, M. Martea, R. Bosch and M. Shimoda, *J. Chromatogr.*, 526 (1990) 119.
 [14] A.L. Long, L.C. Hsieh, M.S. Malbrough, C.R. Short and S.A. Barker, *J. Agric. Food Chem.*, 38 (1990) 423.
 [15] N. Haagsma and C.V.D. Water, *J. Chromatogr.*, 333 (1985) 256.

High-performance liquid chromatographic stability-indicating determination of zopiclone in tablets

J.P. Bounine*, B. Tardif, P. Beltran, D.J. Mazzo

Department of Biological and Chemical Analysis, Institute of Biopharmacy, Rhône-Poulenc Rorer Research and Development, 92165 Antony Cedex, France

First received 17 June 1993; revised manuscript received 7 March 1994

Abstract

A high-performance liquid chromatographic method was developed for the determination of zopiclone in pharmaceutical tablets. The ion-pair reversed-phase method utilizes UV absorbance detection and requires about 15 min per analysis. The known potential degradation products of zopiclone are separated, allowing simultaneous determination. The method was validated for reproducibility, linearity, accuracy and limits of detection.

1. Introduction

Zopiclone, 6-(5-chloro-2-pyridyl)-5-(4-methyl-1-piperazinyl)carbonyloxy-7-oxo-6,7-dihydro-5H-pyrrolo[3,4-*b*]pyrazine (RP 27267), is a rapid-acting hypnotic drug of the family of cyclopyrrolones [1]. Administered as 7.5-mg tablets under the name Imovane, it improves the length and quality of sleep.

Techniques for the determination of zopiclone include UV and TLC methods [2]. For the development of new formulations and dosage forms, it was necessary to improve the specificity of the assay for the active ingredient and the precision of the determination of small amounts of potential impurities. HPLC methods have been reported [3-8] but are mainly applicable to the determination of zopiclone and metabolites in biological fluids. The difficulty in the develop-

ment of a quantitative HPLC method is that zopiclone is virtually insoluble in water and ethanol and that potential impurities have great differences in polarity.

This paper describes results obtained with normal- and reversed-phase chromatography and with computer-aided optimization of the ion-pair chromatography of zopiclone and its principal potential impurities. Sample preparation and validation of the method are also included. This method has been successfully employed in product release and stability study testing of zopiclone.

2. Experimental

2.1. Materials, equipment and liquid chromatographic conditions

The chromatographic hardware consisted of a

* Corresponding author.

Kontron (Saint-Quentin-en-Yvelines, France) Model 420 pump, a Kontron Model 465 autoinjector with variable-volume injection, a Milton-Roy LDC (TSP, Les Ulis, France) Model 3100 UV detector and a Prolabo (Paris, France) Stabitherm column oven regulated at 25°C. Samples in the autoinjector were refrigerated at about 10°C by a Lauda RM6 circulating cryostat (Prolabo). Integration and data storage were carried out on a VG Multichrom system (Fisons Instruments, Chesline, UK). Optimix software (Varian, Les Ulis, France) was used for the simultaneous optimization of chromatographic parameters.

The final choice for the column was a LiChrospher-60 RP Select B cartridge (125 mm × 4.0 mm I.D.) (Merck, Darmstadt, Germany) with a particle diameter of 5 µm. The mobile phase consisted of a buffer with an ion-pair agent–acetonitrile–tetrahydrofuran (81:18:1, v/v/v) flowing at 1.5 ml/min. The injection volume was 20 µl and the wavelength of the UV absorbance detector was 303 nm.

2.2. Reagents and solutions

Monosodium hexane sulphonic acid (Kodak, Rochester, NY, USA), monosodium dehydrogenphosphate (Prolabo), acetonitrile (Distrilab, Caen, France), tetrahydrofuran (THF) (Merck) and water were all of HPLC grade. The buffer was made by adding 3.4 g of monosodium hexane sulphonate ($1.806 \cdot 10^{-2} M$) and 7.0 g of dihydrated monosodium dihydrogenphosphate (0.018 M) to 1 l of water. The solution was filtered before use with a 0.45-µm Millipore filter (or equivalent). The mobile phase was made by adding 180 ml of acetonitrile and 10 ml of THF to 810 ml of buffer, mixing thoroughly and degassing with helium. The final pH of the buffer was 4.55, giving an apparent pH of 5.1 for the mobile phase.

2.3. Standard and sample solution preparation

All operations were performed with protection from direct light. For 5.0-mg doses of zopiclone, ca. 50.0 mg of zopiclone standard were accurately weighed into a 50-ml volumetric flask,

dissolved in 0.1 M HCl and diluted to volume. This solution was accurately diluted 1:10 with 0.1 M HCl.

For composite sample assay, 20 tablets were accurately weighed and the average tablet mass was calculated. The tablets were triturated to a fine powder. An amount of this powder equivalent to 5 mg of zopiclone was accurately weighed into a 50-ml volumetric flask. About 40 ml of 0.1 M HCl were added and treated for 15 min in an ultrasonic bath. The solution was cooled to room temperature and diluted to volume with 0.1 M HCl. The resulting solution was filtered through a 1.6-µm glass-fibre filter (Whatman GF/A or equivalent). The standard and test solutions were stable for 24 h when kept in brown glass flasks between 4 and 10°C. For other dosages, i.e., 2.5, 3.75 and 7.5 mg, the dilutions were modified in order to obtain similar final concentrations.

2.4. Procedures

For the uniformity of content test, a 5.0-mg tablet was placed in a 50-ml volumetric flask, about 40 ml of 0.1 M HCl were added and the mixture was sonicated until the tablet had completely dissolved. The solution was cooled to room temperature and diluted to volume with 0.1 M HCl. The resulting solution was filtered through a 1.6-µm glass-fibre filter (Whatman GF/A or equivalent). A minimum of 10 units were individually analysed.

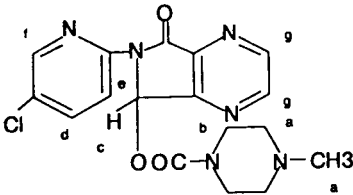
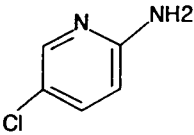
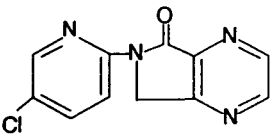
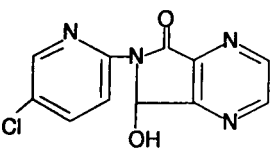
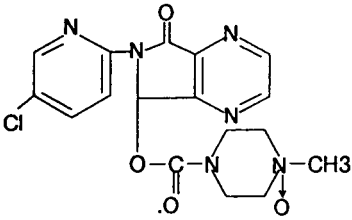
The system suitability was evaluated with a standard solution spiked with 2% of each impurity (see Table 1). The system suitability was determined by injecting 20 µl of spiked standard solution. The resolution between zopiclone and the impurity RP 29753 must be at least 2.0.

The retention time of zopiclone must be between 6.0 and 10.0 min and the column efficiency (N) for zopiclone, measured at the peak half-height, must be >4000 plates/m.

The precision of the system was determined using the relative standard deviation [R.S.D. (%)] of the peak areas for six injections of the standard solution. The R.S.D. must be lower than 2.0%.

Table 1 lists the potential chemical synthesis

Table 1
Capacity factors (k'), plate numbers and relative response factors (RRF) for zopiclone and potential degradation products

Name	Structure	Product	Capacity factor (k')	Column efficiency, N (plates/m)	RRF
Zopiclone (RP 27267)		Active pharmaceutical	12.6	5700	1.00
RP 26695		Potential degradation product	5.5	5100	0.75
RP 48497		Potential degradation product due to bright light	21.4	7900	1.53
RP 29307		Potential chemical synthesis impurity and degradation product	7.9	6500	1.45
RP 29753		Potential degradation product by oxidation	10.1	3700	0.76

impurities and degradation products along with their relative response factors.

Calculations of zopiclone content were made by the external standard method. Impurities can

be assayed by the same method. For routine operations relative response factors (RRF, Table 1) are used, because under normal storage conditions no impurity is detected. This allows the

consumption of reference impurities to be minimized. The use of a spiked standard solution with impurities, kept in a cool place, is thus limited for checking the resolution of the chromatographic system.

3. Results and discussion

As zopiclone and its potential impurities are virtually insoluble in aqueous solvents, the choice of the appropriate method was between aqueous and organic dissolution of tablets and between normal and reversed-phase chromatographic modes. In normal-phase chromatography on silica gel, mobile phases of hexane–2-propanol–diethylamine–water (85:15:1.2:0.2) or diisopropyl ether–isooctane–methanol–water–triethylamine (50:35.5:17.5:0.01:0.2) were tried. The presence of a small amount of water allows the control of the activation state of silica [9], and the addition of triethylamine is to maintain zopiclone ($pK_a = 6.7$) and basic impurities in their non-dissociated form. Although the mobile phases used were polar, the potential impurity RP 29753 was not eluted in a reasonable time. Reversed-phase separation on octadecylsilica was tried with an alkaline mobile phase of acetonitrile–water–triethylamine (50:50:0.2), using methanolic solutions of zopiclone and potential impurities. The potential impurities RP 29307 and RP 29753 were not soluble in the mobile phase after injection of 20 μ l of 0.1 mg/ml solutions. As the extraction of zopiclone tablets for UV assay was performed satisfactorily with 0.1 M HCl, a reversed-phase separation was tried with an acidic mobile phase on a LiChrospher-60 RP Select B column. With ace-

tonitrile–monosodium phosphate buffer (80:20) all peaks were separated on this column. On a classical octadecylsilica column, the peaks were not symmetrical.

The only remaining problem was that the potential impurity RP 26695 was not retained, as was expected for a very polar hydrochloride salt of an amine. However, it was possible to increase its retention by using a hydrophobic counter ion. Monosodium hexanesulphonate was chosen. The influence of the nature of organic solvents was also determined. Acetonitrile or methanol can be used to modify the retention but had little effect on resolution. THF was adopted owing to its positive influence on the peak shape of RP 29307.

With the selected parameters, a multiparametric optimization was performed with Optimix software. This is a PC-compatible version of the CAMPO system [10,11]. The possibility of using non-linear regression permits the prediction of retention times *versus* parameters such as counter-ion concentration, pH and percentage of THF as modifying solvent. After modelling various parameters, the system simulates results for all combinations of conditions. The best operating conditions can be selected according to the requirements for resolution, analysis time and pressure. The concentration of monosodium hexanesulphonate was studied in the range 0.005–0.02 M, apparent pH in the range 2.0–6.0 and THF concentration from 0 to 4.0 vol.-%. Table 2 gives the results obtained with various THF concentrations.

Other components were 0.02 M monosodium hexanesulphonate (pH 4.5)–organic phase (acetonitrile–THF) (80:20, v/v). The influence of THF content is very variable. It has no effect on

Table 2
Retention times (min) of compounds versus the percentage of THF in 0.02 M hexane sulphonic acid (pH 4.5)–acetonitrile (80:20, v/v)

THF (%)	Zopiclone (RP 27267)	RP 29307	RP 26695	RP 29753	RP 48497
0	9.88	6.94	5.22	9.26	18.2
2	12.47	6.95	5.22	9.43	16.7
4	8.79	6.52	5.23	5.06	14.6

the retention of the basic RP 26695. It decreases the retention of RP 48497 as expected. For the other compounds, the retention reaches a maximum with 2% of THF. These behaviours were not predictable and THF concentration of 1% was adopted in order to improve the shape of the peaks.

As expected, the retention of the basic compound RP 26695 is dramatically governed by the formation of an ion pair. However, surprisingly, the retention increased when the pH increased. The same behaviour was observed for zopiclone ($pK_a = 6.7$).

Fig. 1 shows the influence of pH with mixing of two mobile phases at apparent pH 2.0 and 6.0 at various acetonitrile concentrations. After modeling the system with Optimix, an optimum volume composition was simulated. The apparent pH of each mixture was measured. The final composition was chosen because it was obtained naturally with the solution of monosodium phosphate (0.018 M), without the need to adjust the pH. After addition of 1% of THF, the final apparent pH was 5.1.

The final composition of the mobile phase

giving the best resolution, mainly governed by the pH, was adjusted by varying the organic solvent content. It allows a good baseline separation without the risk of interference from RP 26695, which is eluted with a specific retention. This separation was reproducible with two other batches of analytical column in the same laboratory and two other batches in another laboratory.

The proposed procedure represents a precise, accurate and linear stability-indicating method for the determination of zopiclone and its potential degradation products in pharmaceutical tablets. A typical chromatogram of a spiked standard solution containing each of the components listed in Table 1 is shown in Fig. 2, along with a comparison with a test solution and a placebo. Excipients, (dibasic calcium phosphate, lactose, corn or wheat starch, sodium starch glycolate, magnesium stearate, hydroxypropylcellulose, polyethylene glycol, titanium dioxide) exhibited no interferences with the determination of any of the compounds investigated.

Evaluations of the precision of the method

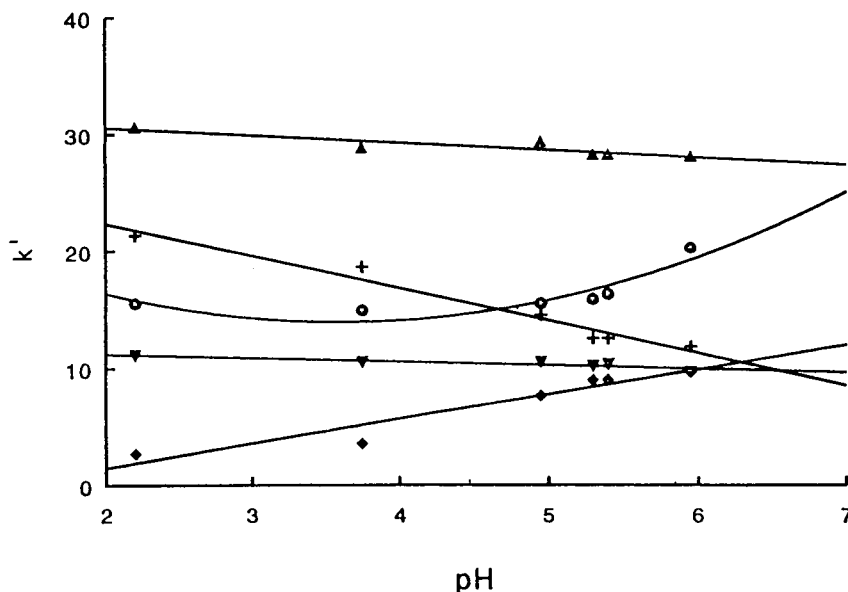


Fig. 1. Influence of pH on capacity factors (k'). Mobile phase, 0.02 M monosodium hexanesulphonate in 0.02 M monosodium phosphate-acetonitrile (80:20, v/v). ○ = zopiclone (RP 27267); ▼ = RP 29307; ◆ = RP 26695; + = RP 29753; ▲ = RP 48497.

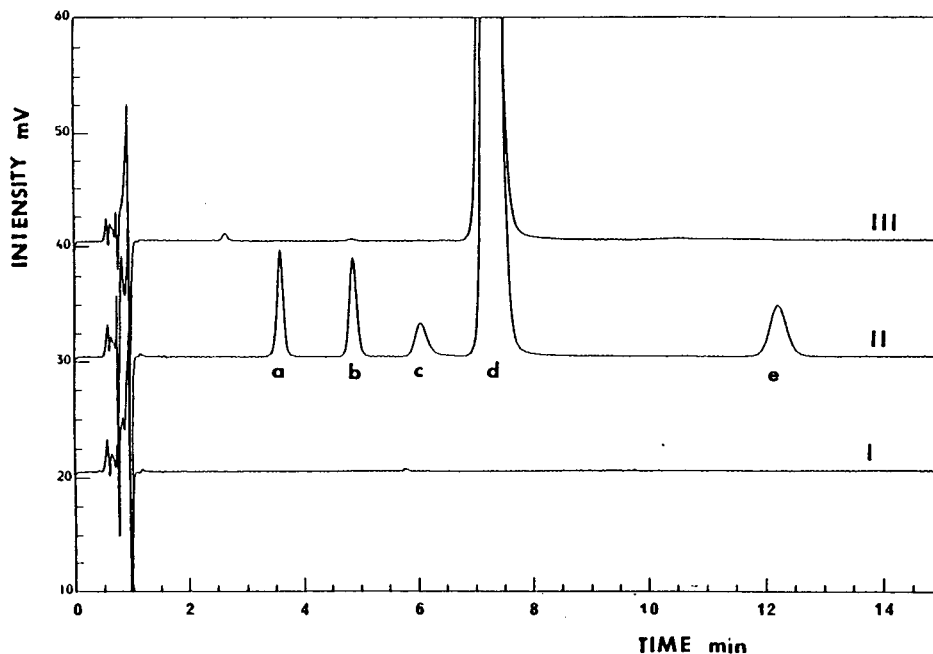


Fig. 2. Typical chromatograms for (I), placebo, (II) spiked standard and (III) test solution. (a) RP 26695; (b) RP 29307; (c) RP 29753; (d) zopiclone (RP 27267); (e) RP 48497.

were made by measuring the standard deviation of ten replicate injections of the same solution and by ten replicate assays of zopiclone. Relative standard deviations of 0.23% and 0.48%, respectively, were found. All these data demonstrate

that the method is sufficiently precise to determine the active ingredient and its potential impurities and degradation products.

The recovery of zopiclone was evaluated from 80 to 120% of the labelled tablet amount. The

Table 3
Linearity of response for zopiclone and impurities

Nominal zopiclone content (%)	Concentration (mg/50 ml)	Peak area ($\mu\text{V s}$)	Peak-area ratio, impurity/zopiclone			
			RP 26695	RP 29307	RP 29753	RP 48497
50	2.555	1 316 117				
75	3.833	1 988 241				
100	5.110	2 649 235				
125	6.388	3 296 203				
150	7.665	3 967 193				
0.5			0.0040	0.0082	0.0044	0.0078
1.0			0.0077	0.0158	0.0080	0.0153
1.5			0.0116	0.0227	0.0120	0.0232
Linear regression ^a ($y = ax + b$)		$y_a = 517446x_a - 803$	$y_b = 0.75x_b + 0.002$	$y_b = 1.45x_b + 0.001$	$y_b = 0.76x_b + 0.004$	$y_b = 1.53x_b + 0.0005$
Correlation coefficient		1.000	0.998	0.989	0.991	0.960

^a y_a = peak area (μVs); x_a = concentration of zopiclone (mg/50 ml).
 y_b = ratio area impurity/area zopiclone; x_b = % impurity.

Table 4
Repeatability of peak areas of potential degradation products for spiked solutions

Impurity (%)	Experimental peak area ($\mu\text{V s}$) ^a			
	RP 26695	RP 29307	RP 29753	RP 48497
0.2	4410 (7.6%)	8285 (2.2%)	4585 (8.5%)	8878 (5.7%)
0.1	2586 (9.9%)	4365 (9.6%)	2786 (13.8%)	5430 (16%)

^a Values in parentheses are R.S.D.s ($n = 6$).

recoveries were in the range $100 \pm 2\%$ of the expected amount.

For the potential degradation products, placebo spiked with 0.1 mg (1% of the labelled amount of tablet for 5.0-mg zopiclone tablets) of RP 26695, RP 29307, RP 29753 and RP 48497 gave recoveries of 102.2, 102.9, 99.6 and 99.9%, respectively.

The linearity of the detector response to zopiclone was determined by spiking a placebo mixture of excipients with 50, 75, 100, 125 and 150% of the theoretical tablet amount. Three replicate analyses were performed for each concentration (Table 3).

The linearity of the detector response to each impurity was determined for low concentrations by spiking a standard solution of zopiclone with 0.5, 1 and 1.5% of each individual component. The ratio of the peak area of the impurity to that of zopiclone was measured with six replicate analyses (Table 3). The slope of the regression line gave the relative response factor (RRF) of each impurity (Table 1).

The limit of detection (signal-to-noise ratio = 3) of each impurity is about 0.05% relative to the active ingredient, or 1 ng in 20 μl . The results in Table 4 indicate that 0.1%, relative to the active ingredient, or 2 ng injected in 20 μl , can be determined with an acceptable precision (R.S.D. < 10%) for RP 26695 and RP 29307. For RP 29753 and RP 48497 the limit of determination is about 0.2%.

4. Conclusions

The proposed method provides a rugged, specific procedure for the determination of zopiclone and related compounds in tablets. The sample preparation is simple and allows the accurate determination of all the compounds despite their different chemical structures and solubilities.

References

- [1] M.C. Bardone, R. Ducrot, C. Garret and C.L. Julou, presented at the 7th International Congress of Pharmacology, Paris, July 16–21, 1978, Abstract No. 2319, p. 743.
- [2] Theraplix, Paris, personal communication.
- [3] J. Gaillot, D. Heusse, G.W. Houghton, J. Marc Aurele and J.F. Dreyfus, *Pharmacology*, 27 (1983) 76.
- [4] P.J. Howard, E. McClean and J.W. Dundee, *Br. J. Clin. Pharmacol.*, 21 (1986) 614P.
- [5] A. Verstraete, M. Devos and A.M. Buisse, *Clin. Chem.*, 36 (1990) 1042.
- [6] A. Åsberg, A.R. Alertsen and O.E. Skang, *Norv. Pharm. Acta*, 48 (1986) 41–44.
- [7] L.G. Miller, B.W. Leduc and D.J. Greenblatt, *J. Chromatogr.*, 380 (1986) 211–215.
- [8] A. Le Liboux, A. Frydman and J. Caillot, *J. Chromatogr.*, 417 (1987) 151–158.
- [9] J.P. Thomas, A. Brun and J.P. Bounine, *J. Chromatogr.*, 139 (1977) 21–43.
- [10] J.P. Bounine, G. Guiochon and H. Colin, *J. Chromatogr.*, 298 (1984) 1–20.
- [11] A. Tchaplá, *Analisis*, 20 (1992) M71–M81.

Theoretical calculation of gas hold-up time in capillary gas chromatography

Influence of column, instrument parameters and analysis conditions and comparison of different methods of dead time determination

G. Castello*, S. Vezzani, P. Moretti

Istituto di Chimica Industriale, Università di Genova, Corso Europa 30, 16132 Genova, Italy

First received 17 December 1993; revised manuscript received 15 March 1994

Abstract

The gas hold-up time or dead time, t_m , of some capillary columns with different bonded liquid or carbon layer stationary phases was calculated by using equations derived by the classical theory of gas behaviour in narrow tubing, *e.g.*, Poiseuille's law. The parameters of the equations (pressure, temperature, gas viscosity, diameter and length of the column) were measured experimentally and the effect of the approximation of the measure on the final value of t_m was evaluated over a wide temperature range. The calculated t_m values were compared with those obtained by using the retention time of methane, the extrapolation of homologous series, the elution of the front of the solvent peak, flow-rate measurement with a bubble flow meter and the automatic systems of commercially available instruments.

1. Introduction

The measurement of the dead time or gas hold-up time, t_m , of a column is of great importance in gas chromatography. This parameter is a measure of the time spent in the column by the molecules of the carrier gas or of a substance that does not interact with the stationary phase and can be measured without problem when using detectors sensitive to organic and inorganic compounds, such as in thermal conductivity detection (TCD). In fact, the retention of some

gases such as hydrogen, argon, neon and air corresponds well enough with that of the commonly used carrier gas helium, except on some specific adsorption phases such as molecular sieves or porous polymers at low temperature.

The use of specific detectors not sensitive to inorganic gases, such as the widely used flame ionization detection (FID), introduced some new problems in this field, mainly because the t_m on capillary columns is high with respect to the retention of fast-eluting compounds, and any uncertainty in its determination introduces a large error in the calculation of important parameters, such as the capacity factor, k' , the

* Corresponding author.

Kováts' retention index [1] and the Rohrschneider and McReynolds polarity systems [2,3]. Further, the exact knowledge of t_m at various temperatures is necessary in order to predict the retention times during temperature-programmed analyses by means of computer calculation by starting from the adjusted retention times measured in isothermal runs [4–8].

Two main directions were followed by many workers for the determination of t_m when using TSD, one based on the use of the retention time of methane [9–12] and the order on a series of regression calculations used in order to deduce the elution time of a non-retained substance by extrapolating the behaviour of homologous series of compounds (*n*-alkanes, *n*-alkanols, ketones, esters, etc.) [9,13–28]. Both approaches have been subjected to some criticism and reviews on the advantages and drawbacks of the different methods have been published [12,23,27,29–31]. An empirical method employed for the determination of the adjusted or relative retention values of high-boiling compounds (pesticides, polychlorobiphenyls, polycyclic aromatic hydrocarbons, steroids, etc.) in high-temperature analyses takes as the zero time the front of the solvent peak. This is justified by the consideration that at high temperature the retention of a low-boiling compound is small and that the diffusion of the solvent molecules into the carrier gas stream can anticipate the output of the first-eluting portion of the solvent peak approaching the residence time of a non-retained substance.

The determination of the gas hold-up time based on measurements independent of the injection of a reference sample theoretically unretained by the stationary phase was carried out for packed columns by Kaiser [16], who measured the true gas volume of the system. When capillary columns are involved, the measurement of the true volume and of the actual flow-rate is often difficult, owing to their small values and to the use of various ionization detectors where auxiliary gas flows are added: hydrogen for FID, flame photometric (FPD) and thermionic detection (TSD), make-up carrier gas for FID, electron-capture detection (ECD) and

TSD, contributing to the total gas output from the detector. The actual carrier gas flow-rate can be measured, of course, by connecting a micro flow meter directly to the column exit, but this procedure cannot be applied during routine work and does not take into account the back-pressure due to the detector. On the other hand, the behaviour of the carrier gas in the capillary tubing can be deduced by using classical equations such as Poiseuille's law, if some parameters are known exactly: the length and diameter of the column, viscosity of the gas, temperature, etc. The essential value that permits the calculation of the flow-rate and of the velocity of the carrier gas is the pressure at the column inlet, which can be measured continuously before and during the analyses, without disconnecting the column. This approach has recently been followed by some producers of gas chromatographic equipment, by offering as an option to advanced instruments the possibility of measuring the inlet pressure and, sometimes, of calculating the flow-rate directly by using the built-in electronic system of the apparatus. Some useful measurements, however, can be made with simple laboratory manifolds and the results used to calculate the true flow-rate and the gas hold-up time.

The equation used for the calculation is the classical equation that permits the prediction of the permanent isothermal motion of a gas with constant mass flow [32]:

$$P_i^2 - P_o^2 = \frac{P_a Q_M^2}{\rho_a \pi^2 r^4} \left[\frac{\lambda L}{2r} + 2 \ln \left(\frac{P_i}{P_o} \right) \right] \quad (1)$$

where

P_i = column inlet pressure absolute
(dyn cm⁻²);

P_o = column outlet pressure absolute
(dyn cm⁻²);

P_a = atmospheric pressure, absolute
(dyn cm⁻²);

Q_M = mass flow-rate (g s⁻¹);

ρ_a = density of the carrier gas (g cm⁻³) at P_a
and at the column temperature, T_c ;

r = column radius (cm);

L = column length (cm);

λ = resistance coefficient.

The resistance coefficient, λ , depends on the type of gas motion in the column. For laminar flow (Reynold's number $Re < 2300$) the following equations can be used:

$$\lambda = 64/Re \quad (2)$$

$$Re = \rho u 2r / \mu \quad (3)$$

where u is the gas velocity (cm s^{-1}), μ the dynamic viscosity (P) and ρ the density of the carrier gas (g cm^{-3}), both at the temperature of the column, T_c . By applying Eq. 3 with the conditions yielding the greatest value of Re for a capillary column of I.D. 0.32 mm, a Reynold's number < 10 was always obtained, thus confirming the hypothesis of laminar flow, which is generally accepted (for example, the classical expression of the pressure gradient correction factor can be deduced by the differential form of the Poiseuille law by postulating laminar flow). As a consequence, the first term in brackets in Eq. 1 is of the order of magnitude of 10^5 , and the second term can be neglected, being < 2 . With flow-rate $F = Q_M/\rho$, the ratio P/ρ being constant along the column and taking into account another expression of the Reynold's numbers:

$$Re = 2Q_M/\mu\pi r \quad (4)$$

the equation that allows the determination of the calculated flow-rate, F_c ($\text{cm}^3 \text{min}^{-1}$), is

$$F_c = \frac{(P_i^2 - P_o^2)}{P_o} \frac{60\pi r^4}{16L\mu} \quad (5)$$

and can be applied to the determination of the gas hold-up time if the parameters of the column, the nature of the carrier gas and the inlet and outlet pressure are known. The linear gas velocity at the column outlet (cm s^{-1}) is

$$u_o = F_c / 60\pi r^2 \quad (6)$$

The average linear carrier gas velocity, u , in the column must be calculated by taking into account the gas compressibility by means of the pressure gradient correction factor of James and Martin [33], j :

$$u = j u_o = \frac{3}{2} \cdot \frac{(P_i/P_o)^2 - 1}{(P_i/P_o)^3 - 1} \cdot u_o \quad (7)$$

The gas hold-up time, t_m (min), is therefore

$$t_m = \frac{L}{60u} = \frac{L\pi r^2}{jF_c} \quad (8)$$

During routine work, only the knowledge of the P_i may be necessary, if all other terms are known and remain constant. Some characteristics of the equipment used or a change in the conditions of analysis can influence the final result; an investigation was therefore carried out in order to establish which corrections and additions should be made to Eq. 5 in order to obtain valid results.

2. Experimental

The measurements of the retention times were carried out by using two gas chromatographs, Models 3400 and 3600 (Varian, Palo Alto, CA, USA), each equipped with a split-splitless capillary injector and a flame ionization detector. Several capillary columns of different polarity were used: bonded-phase non-polar DB-1 (polydimethylsiloxane) ($28 \text{ m} \times 0.32 \text{ mm}$ I.D.) and polar DB-WAX (polyglycol) ($30 \text{ m} \times 0.32 \text{ mm}$) (J & W Scientific, Folsom, CA, USA); bonded-phase non-polar SPB-1 and polar Supelcowax-10 (both $30 \text{ m} \times 0.32 \text{ mm}$ I.D.); and carbon layer open-tubular (CLOT) ($30 \text{ m} \times 0.32 \text{ mm}$ I.D.), partially deactivated with a polyglycol-terephthalic acid liquid phase layer (Supelco, Bellefonte, PA, USA) [24-36]. Helium was used as the carrier gas. The results were integrated and the retention times measured with an accuracy of ± 0.001 min by using a Varian DS 650 data system.

Temperatures were monitored by the built-in systems of the gas chromatograph (with a precision of $\pm 1^\circ\text{C}$ for the injector and detector and of $\pm 0.2^\circ\text{C}$ for the column oven) and independently by auxiliary external thermocouples or precision thermometers (precision $\pm 0.1^\circ\text{C}$). Pressures were measured with mercury manometers or piezoelectric transducers, flow-rates at atmos-

pheric pressure and room temperature with a micro soap-bubble flow meter. Details of the procedures are discussed below.

3. Results and discussion

The influence of the various terms of Eq. 5 and of other parameters, such as the temperature and atmospheric pressure, was investigated experimentally and the variations of the calculated flow-rate and dead time as a function of the approximations of the measurement of the various parameters were evaluated.

3.1. Column diameter and length

These parameters are given by the producers of the capillary columns, and the accuracy of the values listed on the certification of the column is of paramount importance for the calculation. Column length can easily be checked by the number and diameter of coils, while the measure of the inner diameter requires the use of an optical microscope with a suitable reference scale to measure a section of the column, cut near the end to avoid influencing the total length. Of course, the manufacturing process should ensure constancy of the column diameter over the entire length. As the r value to the fourth power is involved in the equation, small errors in the knowledge of the diameter have a great effect on the calculation. On the other hand, if the flow-rate is measured directly and independently, e.g., with a bubble flow meter, differences between the calculated and measured values permit the r values to be corrected. As an example, a difference of -4.2% in the t_m of one of the columns tested was found when using for the calculation the certified diameter of 0.327 mm. The value of r calculated from the actual flow-rate measurement was 0.16 ± 0.0025 mm; by microscope observation the true diameter was found to be 0.320 mm. Fig. 1 shows the deviations from the best values of calculated t_m (first line) due to different approximations of the parameter of Eq. 5. The second and third lines show the maximum errors with an approximation

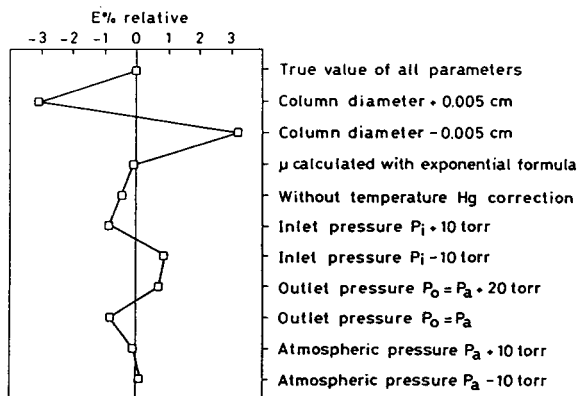


Fig. 1. Relative percentage error in the value of calculated gas hold-up time when the various terms of Eq. 5 are known with a positive or negative difference with respect of the true value. See also Table 1 for the effect of temperature.

of the column diameter of ± 0.005 cm. The uncertainty in the knowledge of this parameter is the main source of errors in the final results. The influence of the column temperature on this uncertainty is shown in Table 1.

3.2. Viscosity of carrier gas

The dynamic viscosity of the carrier gas, μ , changes with temperature [12,37–39]. Its value can be predicted by using two different expressions, a quadratic:

$$\mu = a + bT - cT^2 \quad (9)$$

or an exponential relationship [40]:

$$\mu = \alpha T^\beta \quad (10)$$

where T is the temperature in K and a , b , c , α and β are constant that depend on the gas used (see Table 2). Both expressions yield the μ values in micropoise (μP).

The difference in t_m values obtained by using the above two expressions is small: the average relative error for helium is smaller than -0.07% , as shown in the fourth line of Fig. 1 and the fourth column of Table 1, and therefore the use of the two expressions is almost indifferent with respect of the influence of other parameters. Owing to the different slopes of the two plots, the deviation assumes opposite signs at tempera-

Table 1
Relative percentage errors at different column temperature in the values of calculated gas hold-up time when the terms of Eq. 5 are known with a positive or negative deviation with respect of the true value (see also Fig. 1)

T (°C)	(1) t_{m_0} (s)	Deviation from true value										
		(2) $d + 0.005$ (cm)	(3) $d - 0.005$ (cm)	(4) $\mu_{\text{exp.}}$ (P)	(5) Hg density correction	(6) $P_i + 10$ (Torr)	(7) $P_i - 10$ (Torr)	(8) $P_o = P_s + 20$ (Torr)	(9) $P_o = P_s$ (Torr)	(10) $P_s + 10$ (Torr)	(11) $P_s - 10$ (Torr)	
23	40.2	-1.23	1.29	0.25	-0.17	-0.33	0.34	0.28	-0.33	-0.033	0.034	
33	41.1	-1.26	1.32	0.23	-0.17	-0.34	0.35	0.28	-0.34	-0.034	0.035	
45	42.2	-1.29	1.35	0.03	-0.18	-0.35	0.36	0.29	-0.35	-0.035	0.036	
60	43.5	-1.33	1.39	-0.01	-0.20	-0.36	0.37	0.30	-0.36	-0.036	0.037	
80	45.3	-1.38	1.45	-0.06	-0.20	-0.38	0.38	0.31	-0.37	-0.038	0.039	
100	47.0	-1.43	1.50	-0.11	-0.21	-0.39	0.40	0.32	-0.38	-0.039	0.040	
120	48.6	-1.48	1.56	-0.15	-0.22	-0.40	0.41	0.33	-0.40	-0.040	0.041	
140	50.2	-1.53	1.61	-0.19	-0.23	-0.42	0.42	0.34	-0.41	-0.042	0.043	
160	51.8	-1.58	1.66	-0.22	-0.23	-0.43	0.44	0.35	-0.42	-0.043	0.044	
180	53.4	-1.63	1.71	-0.24	-0.24	-0.44	0.45	0.37	-0.44	-0.044	0.045	
E(rel.) (%)		-3.05	3.20	-0.07	-0.44	-0.83	0.84	0.68	-0.82	-0.08	0.09	

Column 5 shows the error when the Hg density is not corrected for room temperature in the evaluation of pressure with an Hg manometer.

Table 2

Values of the constants used to calculate the viscosity, μ , of hydrogen, helium and nitrogen carrier gas as a function of temperature with a quadratic (Eq. 9) or exponential (Eq. 10) relationship

Carrier gas	a	$b \cdot 10^3$	$c \cdot 10^8$	α	β
He	48.36	5.77	2.15	5.024	0.648
H ₂	18.69	2.56	0.79	1.624	0.701
N ₂	10.00	6.39	2.81	2.791	0.727

tures lower and higher than the crossing point of the plots.

3.3. Pressure and flow-rate measurements

In order to apply the calculation method in its simplest version, given in Eq. 5, the values of P_o at the column outlet were taken as equal to the atmospheric pressure, P_a . The column end was therefore disconnected from the detector base, protruded from the column oven through a small hole in the insulating wall and connected to the soap-bubble flow meter by means of a short PTFE 1/8-in. tube. P_o was therefore equal to P_a , which was measured with a precision Fortin-type mercury barometer and corrected for the room temperature, T_m . If this correction, which takes into account the thermal expansion of the mercury, is not applied, the error in the final value of the calculated t_m is about $\pm 0.5\%$ (see the fifth column of Table 1 and Fig. 1). The pressure at the column inlet, P_i , was measured with a precision of ± 0.5 Torr (± 66.66 Pa), by connecting to the injector a U-type mercury manometer, and also corrected at T_m . Bourdon-type precision manometers or electronic piezoelectric pressure transducers can also be used during routine work. The accuracy of the final results depends strongly on the accuracy and precision of this equipment. Standard pressure transducers can measure the column head pressure in 0.25 p.s.i. (12.9 Torr) or 0.1 p.s.i. increments, with an uncertainty much greater than that offered by the simpler mercury manometer.

The values of the flow-rate calculated with Eq. 5, F_c , were compared with those measured at the

column outlet by using a micro soap-bubble flow meter. The values measured with this manifold, F_s , were corrected by taking into account the vapour pressure of water and the gradient of pressure between the column outlet and the flow meter, with the equation

$$F_m = \frac{F_s(P_a - P_w)}{P_a} \cdot \frac{P_a}{P_o} \quad (11)$$

where P_o is the pressure at the column outlet, P_a is the atmospheric pressure at which the flow was measured and P_w is the vapour pressure of water at the temperature of the flow meter (room temperature, T_m , as checked by inserting two thermocouples at the bottom and top of the calibrated glass tubing). F_m is therefore the gas flow-rate from the column ($\text{cm}^3 \text{min}^{-1}$) at T_m and P_a and corresponds exactly to F_c when the temperature of the column, T_c , is equal to that of the flow meter, T_m . If $T_c \neq T_m$, the values of F_m and F_c differ and a correction factor must be applied. Fig. 2 shows the change with temperature of the flow-rate and the increasing difference between F_m and F_c . The flow-rate determined by means of the bubble flow meter corresponds exactly to the true value at the column outlet when the two temperatures are equal. As the column temperature increases, the cooling of the carrier gas to room temperature at which the flow meter is operated causes a decrease in

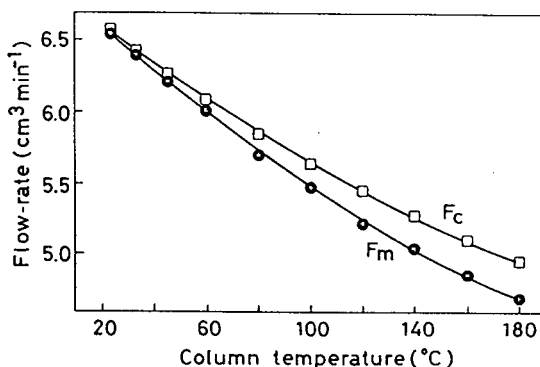


Fig. 2. (●) Carrier gas flow-rate, F_m , measured by bubble flow meter at room temperature $T_m = 23^\circ\text{C}$ and (□) effective flow-rate at the temperature of the column outlet, F_c , as a function of column temperature.

volume and therefore the value of F_m is underestimated with respect of the true flow-rate at the column outlet. A correction factor depending on temperature, γ , should therefore be applied to the results of flow meter measurements in order to obtain the true flow-rate at the column outlet, F_c :

$$F_c = F_m \left(\frac{T_c}{T_m} \right)^\gamma \quad (12)$$

This expression agrees with the application of Poisson's equation for an adiabatic transformation [41] because the carrier gas temperature quickly decreases from T_c to T_m in an insulating tube. The heat exchange between the cooling carrier gas and the external ambient is negligible and the temperature change is related only to the internal energy of the gas and the adiabatic transformation can be applied. In order to calculate γ for a given experimental apparatus, a least-squares regression starting from F_c and F_m measured over a wide temperature range is applied, yielding the final expression for γ :

$$\gamma = \frac{\sum \ln(T_c/T_m) \ln F_c - \sum \ln(T_c/T_m) \ln F_m}{\sum [\ln(T_c/T_m)]^2} \quad (13)$$

In the present instance, $\gamma = 1.134$ and its application to the measured F_m exactly compensates for the effect of the temperature difference between the column and the flow meter. Fig. 3 shows the correspondence between the F_c and the flow meter values corrected by using the γ term, F_m . The two values of the dead time agree with a relative error of -0.03% , mainly due to the stop-watch operation in the measurement of the transit time of the bubble in the flow meter and therefore fully stochastic, as shown by the lower graph in Fig. 3. The error due to the difference between T_m and T_c is much greater than that made by neglecting the correction for the vapour pressure of water, P_w (Eq. 10) and therefore any determination of the flow-rate by means of an external flow meter should be corrected by using the γ value calculated for that equipment.

The flow-rate measured directly at the column outlet does not correspond exactly to that exist-

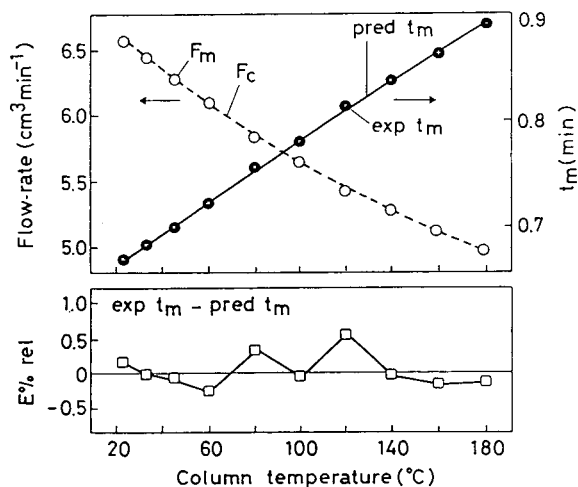


Fig. 3. Effect of the column temperature on the difference between the calculated flow-rate and that measured by the flow meter at room temperature and corrected with the adiabatic term γ . In the upper graph the open circles and the dashed line (both referred to the left-hand scale) show the experimental values corrected with $\gamma(F_m)$ and the flow-rate trend calculated by Eq. 5 (F_c), respectively. The t_m values obtained from the experimental flow meter values (upper graph, closed circles) are compared with the behaviour predicted with Eq. 5 (full line, right-hand scale). The relative percentage error between the experimental and predicted t_m (i.e., the distance between the closed circles and the full line) is shown in the lower graph.

ing in the column when it is connected to the detector, because of the back-pressure due to the restriction of the flame jet (in FID and TSD) or of the outlet tubings in ECD. This effect might be neglected if the flow of gas through the detector was only that coming from the capillary column (a few $\text{cm}^3 \text{min}^{-1}$), but in practice the correct detector operation requires the addition of hydrogen and/or make-up gas, depending on type and model. This means that the flow-rate through the flame jet may be as high as $60 \text{ cm}^3 \text{min}^{-1}$ (hydrogen plus carrier plus make-up gas) and through a pulsed-type ^{63}Ni electron-capture detector of about $30 \text{ cm}^3 \text{min}^{-1}$ (carrier plus N_2 or Ar-CH_4 ionizable counting gas). The difference between P_o and P_a , P_d , is therefore not negligible. Its value for FID with a flame jet having an inner diameter of 0.020 in. (0.13 mm), suitable for capillary operation, was measured by connecting the manometer to the tubing normal-

ly used for the hydrogen inlet, the flow meter to the flame tip, and increasing the flow-rate through the make-up line. The difference in pressure, P_d , between the column outlet (P_o) and the top of the flame jet (P_a) ranged from 2 Torr (about $8 \text{ cm}^3 \text{ min}^{-1}$ of carrier gas only) to 11 Torr (no make-up, carrier plus $20 \text{ cm}^3 \text{ min}^{-1}$ of hydrogen) to 20 Torr ($60 \text{ cm}^3 \text{ min}^{-1}$ of carrier plus hydrogen plus make-up gas). Table 1 (8th and 9th columns) and Fig. 1 show the positive and negative variations for the extreme hypotheses of $P_d = 0$ and $P_d = 20$ Torr.

The uncertainty or the approximation of the P_a , P_o and P_i values influences the values of the flow-rate and t_m . The approximations may have synergistic effect or be partially compensated for, depending on their values and signs. Table 1 (columns 6–11) and Fig. 1 show the percentage errors due to a difference of ± 10 Torr in the determination of the true values of the pressure. The application of all the necessary correction factors leads to the final expression for F_c :

$$F_c = \frac{P_i^2 - (P_a + P_d)^2}{P_a + P_d} \cdot \frac{60\pi r^4}{16L\mu} \quad (14)$$

where the various terms have the same meanings as in Eqs. 1 and 5 and P_d is a constant measured as described for a given detector. When all the constant values are known, the calculation of F_c requires only the exact measure of the inlet pressure, P_i , and of the atmospheric pressure, P_a , and the correction of the μ value for its dependence on column temperature by means of Eq. 9 and 10.

3.4. Comparison of different methods for t_m calculation

The results obtained by applying the method described above and by corrected flow meter measurements were compared with those given by various methods in the literature, using all the capillary columns listed under Experimental.

Retention time of methane

The t_m (CH_4) values obtained by injecting very small amounts of CH_4 over a wide tempera-

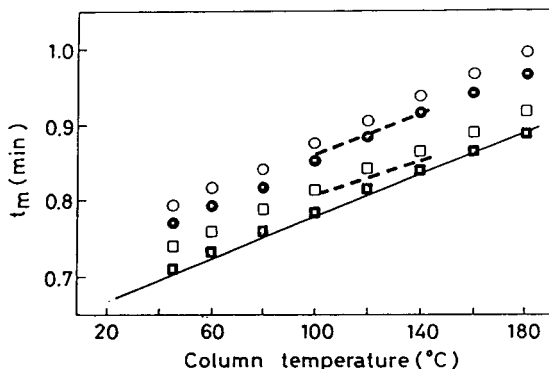


Fig. 4. Comparison between the calculated gas hold-up times, t_m , and the values measured experimentally with various methods. The full line shows the trend calculated with Eq. 14 at various temperatures on GC and CLOT columns; the symbols show the values measured at the apex of the methane peak on (○) GC and (□) CLOT columns, measured at the front of the methane peak on (●) GC and (■) CLOT columns and calculated with extrapolation from n -alkanes on GC (upper dashed line) and CLOT columns (lower dashed line).

ture range are shown in Fig. 4 and compared with t_m calculated with Eq. 14 (lowest straight line in the graph). The temperature dependence, due to the change in the gas viscosity, is the same for all the plots, but t_m (CH_4) values obtained on all the bonded-phase columns (polar, non-polar, Supelco, J & W Scientific) by measuring the time at the methane peak apex (open circles) are coincident and much greater than the t_m values obtained by calculation or measurement of the flow-rate. This is due to the non-negligible solubility of methane in the liquid phase [42]. When the CLOT column is used, the highly graphitized non-porous carbon layer, further deactivated by the addition of the polar modifier, reduces to a minimum the interaction with the methane molecules and a t_m (CH_4) closer to t_m is obtained (open squares). If the time of the methane peak front edge is measured (by elaboration of the chromatogram by means of the Varian DS 650 data system) and taken as the residence time in the column of that fraction of methane molecules less absorbed in the liquid phase, values corresponding to t_m are obtained for CLOT columns (closed squares) and smaller than that measured at the peak apex for GLC

columns (closed circles) but still greater than t_m . The hold-up time measured by using the methane peak is therefore correct only if a negligible interaction with the stationary phase can be postulated, as with CLOT columns.

Extrapolation methods

Many methods for the calculation of t_m not depending on the retention time of methane have been suggested (see Introduction and references) and have been reviewed by Haken and co-workers in several papers [27,29–31]. By using the retention times of linear alkanes, we applied to our columns at 100, 120 and 140°C the methods of Hafferkamp [14], Grobler and Balisz [17] and Al-Thamir *et al.* [22]. The final results of the three methods are coincident, which is not surprising as they used equations that follow the same mathematical approach. Fig. 4 shows the values obtained on all the polar and non-polar (upper dashed line) and on CLOT (lower dashed line) columns. The values obtained lie between those measured at the top and at the beginning of the methane peak.

Retention time of solvents

In order to check if the use of the front of the solvent peak as a measure of the gas-hold-up time is acceptable, small amounts of some widely used solvents (*n*-hexane, dichloromethane, methanol) were injected at various temperatures on to the tested columns. Fig. 5 shows that at low temperature the retention of the solvents used (measured at the apex of the peak) is greater than the true t_m and than the retention time of methane, depending on the interaction of the injected substance with the stationary phase used (*e.g.*, the most retained substance on CLOT and on polyglycol GL columns is dichloromethane, whereas on non-polar polydimethylsiloxane the greatest retention time is shown by hexane). With increase in temperature, the retention of the solvents quickly decreases and at high temperature the difference from the retention of methane becomes negligible. The front of the solvent peak, often used as the reference time for the calculation of adjusted or relative retention in the analysis of high-boiling

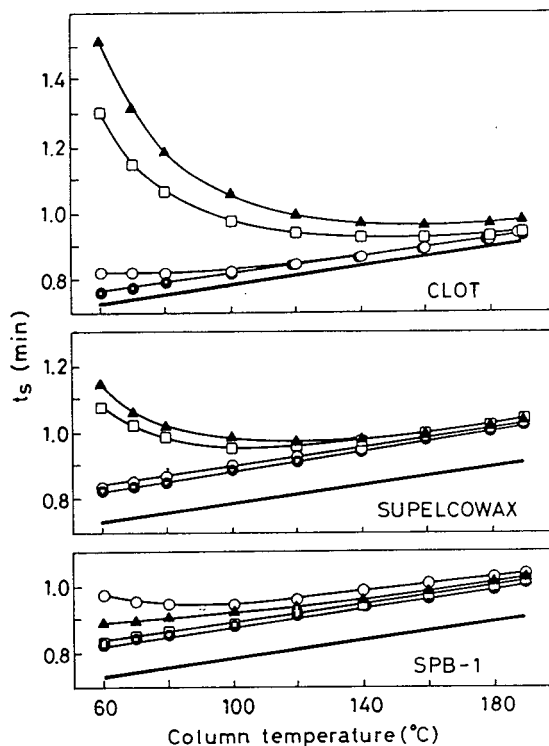


Fig. 5. Retention time of the apex of the peak of some common solvents as a function of temperature on three columns (CLOT, Supelcowax, and SPB-1, 30 m \times 0.32 mm I.D.). \circ = Hexane; \square = methanol; \blacktriangle = dichloromethane. The retention time of methane (\bullet) and the calculated t_m (lowest straight line) are also shown

compounds, is generally eluted, with the column length used, 0.02–0.03 min before the peak apex (nearly independently of temperature) with the exception of methanol (peak front about 0.1 min before the peak apex) and *n*-hexane (peak front 0.01 min before the peak apex), both on the CLOT column. The use of the solvent peak is therefore acceptable at high temperature suitably approximating the true t_m and being equivalent to the values obtained by using the methane retention or the extrapolation of homologous series.

3.5. Automatic calculation of t_m

Some modern gas chromatographs are equipped with automatic pressure-sensing units

(e.g., Model 8700, Perkin-Elmer, Norwalk, CT, USA), and some of them can calculate directly the carrier gas flow-rate or linear velocity by means of a built-in microcomputer (e.g., Model 5890, Hewlett-Packard, Boise, ID, USA [43]; Model CP-9001, Chrompack, Middelburg, Netherlands; Model 3600, Varian).

As we used a Varian Model 3600 instrument, equipped with pressure- and temperature-sensing units and with a computing unit that automatically calculates the splitting ratio, the carrier gas velocity and the column flow-rate, the results obtained with this system were compared with those given by the application of Eq. 14 when all its parameters are exactly known. The equation used by the automatic system to give the automatic flow-rate F_a (adjusted to the volume as measured by the flow meter at room temperature) is as follows using the same symbols as used in Eqs. 1, 5 and 14:

$$F_a = \frac{60\pi r^4}{16L\mu} \cdot \frac{P_i^2 - P_o^2}{P_a} \cdot \frac{T_{ref}}{T_c} \quad (15)$$

P_i is measured by the pressure transducer connected near to the back-pressure regulator of the splitter (in 0.25 p.s.i. increments; 1 p.s.i. = 6894.76 Pa), the column outlet pressure, P_o , is taken as equal to atmospheric pressure, P_a , and P_a is defined to be constant at 760 Torr (1 Torr = 133.322 Pa), T_c is monitored by the temperature-sensing probe of the column oven (± 0.1 K) and T_{ref} is taken as constant (293 K). The operator enters the column length and diameter and the type of carrier gas; the value of μ for the selected gas (H_2 , He or N_2) is calculated by using the actual T_c value and the quadratic Eq. 9. As seen above, this value differs from the actual flow-rate at the column outlet, F_c , because $P_o \neq P_a$, owing to the detector back-pressure, P_d , and to the effect of the correction factor, γ , in Eqs. 12 and 13.

The accuracy of the system depends on the exact inputs of column length and diameter, on the pressure transducer sensing increments, on the difference between the actual room temperature and the fixed 293 K value and on the deviation of atmospheric pressure from the set

value of 1 atm. The difference between P_o and P_a due to the detector restriction cannot be corrected for and, by using a split-splitless injector, the pressure transducer connected near to the back-pressure regulator will read a lower pressure than that actually at the column top when a significant gas flow is diverted through the split line. By placing the transducer connection as close to the injector as feasible, this difference can be reduced. On the other hand, the difference between the P_i value measured by the transducer connected in its standard position and that measured at the injector by using the mercury manometer was small (6 Torr) and therefore both this sources of error in the P_i value and the difference between P_o and P_a due to the detector are of the same order of magnitude as the precision of the sensing element (0.25 p.s.i. \approx 13 Torr). Also, the atmospheric pressure changes due to altitude (about 13 Torr for a 500 m rise above sea level) and to weather are comparable to the transducer error. By operating the instrument at constant atmospheric pressure (757 Torr) and room temperature (23.5°C), fairly corresponding values of gas hold-up times were therefore found (Table 3). It should be taken into account, however, that all the deviations due to the splitter effect, to the detector back-pressure, to the altitude and to meteorological events may have the same sign

Table 3

Relative percentage errors at different column temperatures between values of gas hold-up time calculated with Eq. 14 (t_c) and those displayed by the automatic system of the gas chromatograph (t_a)

T (°C)	t_a (s)	t_c (s)	$E(\text{rel.})$ (%)
23	40.7	40.2	1.00
33	41.6	41.1	0.98
45	42.5	42.2	0.66
60	43.7	43.5	0.28
80	45.5	45.3	0.56
100	47.2	47.0	0.60
120	48.9	48.6	0.66
140	50.4	50.2	0.36
160	52.0	51.8	0.32
180	53.7	53.4	0.54

and, summed together, yield automatic velocity carrier gas values which, at the level concerned, may differ from those calculated with the actual values of all the parameters.

Other instruments that use the same equation applied to the P_i values measured at the pressure-flow control unit of the gas chromatographs and that take as constant room temperature and atmospheric pressure may give the same approximation as the tested model. Therefore, the ideal automatic system should have, in addition to the pressure sensor connected as near as possible to the injector septum, a transducer of the atmospheric pressure and a probe for the room temperature and employ for calculation the extended Eq. 14, with the possibility of inputting the value of the detector back-pressure.

4. Conclusions

The method of calculation of t_m by using the actual values of temperature and pressure at the inlet and outlet of the column was found to give values corresponding to those obtained by effective measurement of the volumetric flow-rate, mainly if the flow meter reading is corrected by taking into account the difference between the temperature of the column and that at which the flow was measured.

The t_m values based on the retention time of methane, on extrapolation of homologous series or on solvent retention are greater than the actual values, depending on the interaction of the probe used with the stationary phase of the column. When the interaction is strongly reduced by using deactivated graphitized carbon layer columns, the calculated and experimental values correspond reasonably well.

By using the inlet and the atmospheric pressure and the column and room temperature measured with simple instruments and applying the corrections for the gas viscosity as a function of temperature, the calculation of t_m is easily achieved. The values obtained by using automatic systems may differ from the actual values more or less, depending on the difference between the true values of the various parameters

and the standard conditions taken as constant in the simplified equations.

Acknowledgements

The authors thank all the producers of GC instruments mentioned in the text who supplied documentation on the equipment and options used for pressure and flow measurements. Useful information about the calculation method used by Varian instruments was given by Dr. Craig Hodges. This work was supported by the Italian Ministry of University and Scientific Research (MURST).

References

- [1] E. Kováts, *Helv. Chim. Acta*, 41 (1958) 1915.
- [2] L. Rohrschneider, *J. Chromatogr.*, 22 (1966) 6.
- [3] W.O. McReynolds, *J. Chromatogr. Sci.*, 8 (1970) 685.
- [4] E.E. Akporhonor, S. Le Vent and D.R. Taylor, *J. Chromatogr.*, 405 (1987) 67.
- [5] E.E. Akporhonor, S. Le Vent and D.R. Taylor, *J. Chromatogr.*, 463 (1989) 271.
- [6] L.H. Wright and J.F. Walling, *J. Chromatogr.*, 540 (1991) 311.
- [7] N.H. Snow and H.M. McNair, *J. Chromatogr. Sci.*, 30 (1992) 271.
- [8] G. Castello, P. Moretti and S. Vezzani, *J. Chromatogr.*, 635 (1993) 103.
- [9] R.J. Smith, J.K. Haken and M.S. Wainwright, *J. Chromatogr.*, 147 (1978) 65.
- [10] J.F. Parcher and D.M. Johnson, *J. Chromatogr. Sci.*, 18 (1980) 267.
- [11] H. Becker and R. Gnauck, *J. Chromatogr.*, 366 (1986) 378.
- [12] B. Koppenhoefer, G. Laupp and M. Humel, *J. Chromatogr.*, 547 (1991) 239.
- [13] H.J. Gold, *Anal. Chem.*, 34 (1962) 1.
- [14] M. Hafferkamp, in R. Kaiser (Editor), *Chromatographie in der Gasphase*, Vol. II, Bibliographisches Institut, Mannheim, 1966, p. 93.
- [15] H.L. Hansen and K. Andresen, *J. Chromatogr.*, 34 (1968) 246.
- [16] R. Kaiser, *Chromatographia*, 2 (1969) 215.
- [17] A. Grobler and G. Balisz, *J. Chromatogr. Sci.*, 12 (1974) 57.
- [18] X. Guardino, J. Albaigés, G. Firpo, R. Rodríguez-Viñals and M. Gassiot, *J. Chromatogr.*, 118 (1976) 13.
- [19] J. Sevcik, *J. Chromatogr.*, 135 (1977) 183.

- [20] J.R. Ashes, S.C. Mills and J.K. Haken, *J. Chromatogr.*, 166 (1978) 391.
- [21] J. Sevcik and M.S.H. Lowentap, *J. Chromatogr.*, 147 (1978) 75.
- [22] W.K. Al-Thamir, J.H. Purnell, C.A. Wellington and R.J. Laub, *J. Chromatogr.*, 173 (1979) 388.
- [23] L.S. Ettre, *Chromatographia*, 13 (1980) 73.
- [24] M.S. Wainwright and J.K. Haken, *J. Chromatogr.*, 256 (1983) 193.
- [25] A. Toth and E. Zala, *J. Chromatogr.*, 284 (1984) 53.
- [26] A. Toth and E. Zala, *J. Chromatogr.*, 298 (1984) 381.
- [27] M.S. Wainwright, C.S. Nieass, J.K. Haken and R.P. Chaplin, *J. Chromatogr.*, 321 (1985) 287.
- [28] M.S. Vigdergauz and E.I. Petrova, *Chromatographia*, 25 (1988) 7.
- [29] M.S. Wainwright and J.K. Haken, *J. Chromatogr.*, 184 (1980) 1.
- [30] R.J. Smith, J.K. Haken, M.S. Wainwright and B.G. Madden, *J. Chromatogr.*, 328 (1985) 11.
- [31] R.J. Smith, J.K. Haken and M.S. Wainwright, *J. Chromatogr.*, 334 (1985) 95.
- [32] E. Marchi and A. Rubatta, *Meccanica dei Fluidi*, UTET, Milan, 1976, Ch. 13 and 14.
- [33] A.T. James and A.J.P. Martin, *Biochem. J.*, 50 (1952) 679.
- [34] L.M. Sidiski and M.V. Robillard, in P. Sandra and M.L. Lee (Editors), *Proceedings of the 14th International Symposium on Capillary Chromatography, Baltimore, 1992*, Foundation for the International Symposium on Capillary Chromatography, Miami, FL, 1992, p. 110.
- [35] G. Castello and S. Vezzani, in P. Sandra (Editor), *Proceedings of the 15th International Symposium on Capillary Chromatography, Riva del Garda, 1993*, Huethig, Heidelberg, 1993, p. 68.
- [36] G. Castello, S. Vezzani and P. Moretti, *J. High Resolut. Chromatogr.*, 17 (1994) 31.
- [37] L.S. Ettre, *Chromatographia*, 12 (1979) 509.
- [38] L.S. Ettre, *Chromatographia*, 18 (1984) 243.
- [39] W.C. Reynolds and H.C. Perkins, *Engineering Thermodynamics*, McGraw-Hill, New York, 2nd ed., 1977.
- [40] J.O. Hirschfelder, C.F. Curtiss and R. Byron-Bird, *Molecular Theory of Gases and Liquids*, Wiley, New York, 1964.
- [41] R.H. Cole and J.S. Coles, *Physical Principles of Chemistry*, Freeman, San Francisco, 1964.
- [42] V.A. Ezrets and M.S. Vigdergauz, *Chromatographia*, 9 (1976) 205.
- [43] S.S. Stafford (Editor), *Electronic Pressure Control in Gas Chromatography*, Hewlett-Packard, Wilmington, DE, 1993.



ELSEVIER

Journal of Chromatography A, 677 (1994) 107–121

JOURNAL OF
CHROMATOGRAPHY A

Gas chromatographic–mass spectrometric determination of nitro polycyclic aromatic hydrocarbons in airborne particulate matter from workplace atmospheres contaminated with diesel exhaust

P.T.J. Scheepers*, D.D. Velders, M.H.J. Martens, J. Noordhoek, R.P. Bos

Department of Toxicology, University of Nijmegen, P.O. Box 9101, NL-6500 HB Nijmegen, Netherlands

First received 24 February 1994; revised manuscript received 14 April 1994

Abstract

A method is described for the determination of 1-nitropyrene and 2-nitrofluorene in low volume ambient air samples (1–150 m³). This method is based on acetone extraction by sonication followed by solid-phase fractionation on silica gel, nitroreduction, derivatization with heptafluorobutyric anhydride and analysis with gas chromatography–mass spectrometry. On-line zinc reduction of nitroarenes was compared with a newly developed reduction by sodium hydrosulfide hydrate. This method was validated by the analysis of air samples collected from the atmosphere of workplaces associated with the use of diesel engines, samples from chassis dynamometer studies, and standard reference materials (1587 and 1650).

1. Introduction

Exposure to diesel exhaust may represent a health hazard. More specifically, chronic exposure to relatively low levels of diesel exhaust may be a risk factor in the development of lung cancer [1–3]. Because of the presumed health hazards methods for accurate exposure assessment are urgently needed [2]. Nitro polycyclic aromatic hydrocarbons (nitro-PAHs) could be useful as tracers of airborne diesel exhaust particulate matter and markers of toxicity because of their characteristic appearance in diesel exhaust [4]. 1-Nitropyrene (1-NP) is one of the most abundant nitro-PAHs that have been iden-

tified in diesel exhaust [5–22]. Apart from its presence in diesel exhaust, 1-NP was also reported to occur in other combustion processes such as coal and wood combustion, in photocopier toner and during aluminium manufacturing [6,23–27]. However, the levels in these combustion emissions (expressed as μg 1-NP/g particles) are usually much lower than diesel engine emissions [6]. Lower levels of nitro-PAHs have also been observed in the exhaust of gasoline fueled engines [6,28]. In addition, 1-NP has been reported to be non-detectable in cigarette smoke, bitumen fumes and coke oven emissions [29,30]. Relatively high levels of 1-NP were observed in grilled chicken [31]. However, in grilled and smoked sausage and fish that contained considerable amounts of PAHs, 1-NP

* Corresponding author.

was not detected [32]. Its isomers 2- and 4- but not 1-NP were reported as products of atmospheric transformations [33]. 1-NP appearing in the ambient atmosphere is believed to be primarily originating from combustion (e.g. diesel exhaust emission) sources [33,34].

2-Nitrofluorene (2-NF) is present in the particulate phase of diesel exhaust emissions as well as in the gas phase [4,12]. Besides in diesel exhaust [12,13,17,20,22,28,35–38], 2-NF has been reported to be present in ambient air samples [39,40] and in river sediments [41] and it was tentatively identified in grilled sausage and chicken [31,32].

From a toxicological perspective there are arguments that would support the use of 1-NP as a marker for the genotoxic properties of diesel exhaust: 1-NP is the most abundant representative of a group of strong direct acting mutagens in these emissions. It has been suggested to use 1-NP as an indicator of the overall direct acting mutagenicity of diesel exhaust derived particulate extracts [42,73]. 1-NP is associated with the particulate phase of diesel exhaust and would therefore also be associated with constituents that could play a role in its carcinogenic potential since these constituents are known to be located in the particulate phase of diesel exhaust [3].

The availability of reliable and sensitive techniques of determination of 1-NP in low volume air samples is a basic requirement for the use of this compound as a tracer of diesel exhaust exposure and/or marker constituent for its genotoxicity. We have developed a method consisting of a simple sample work-up and reliable gas chromatographic–mass spectrometric (GC–MS) determination that can be applied for routine analysis. This method was developed and validated for workplace air samples. Analysis of nitro-PAHs has been reported using reductive electrochemical detection [8,17,43,44], flame-ionization detection [16,20,22,38,45], electron capture detection [10,38,46,47], nitrogen selective detection [13,38,48], thermal energy analysis [10,15,20], electron ionization mass spectrometry [5,16,21,22,26,32,45], positive and negative ion chemical ionization mass spectrometry [16,19,21], negative ion atmospheric pressure

ionization mass spectrometry [49–52], methane enhanced negative ion mass spectrometry [53], high resolution mass spectrometry [35], MS–MS [12,36,54], and Fourier transform infrared spectrometry [55]. High-performance liquid chromatography (HPLC) has been used with UV [5,56,57], chemiluminescence [15,16,57], and fluorescence detection [5,13,28,40,42–44,55,57].

1-NP was detected with most of these techniques, while 2-NF was detected only with fluorescence detection [5,13,39,40,43,58], flame ionization detection [20,31,35,38], electron capture detection [17,41], chemiluminescence detection [15], and mass spectrometry [12,22,32,35,36].

The analysis of nitro-PAHs using gas chromatography may be troublesome because 1-NP may decompose during the GC analysis [59]. Nitroreduction and derivatization have been introduced to improve chromatographic qualities of the analyte. This pretreatment provides excellent chromatographic behaviour, higher detection sensitivity [19,38,60] and selectivity, such as demonstrated in the sensitive detection of arylamines in biological samples [61–63]. Nitroreduction is usually conducted after fractionation of the sample [42–44]. Metals used for on-line reduction of 1-NP include zinc, cadmium and tin [28,43,44,64]. For batchwise reduction, NaBH_4 and KBH_4 catalyzed with copper(II)chloride have been reported [38,40].

The objective of this study was to develop an analytical method for simple routine analysis of nitro-PAHs in low-volume ambient air samples. We have focused on the determination of 1-NP and 2-NF in samples that were collected in work environments contaminated with diesel exhaust.

2. Materials and methods

2.1. Chemicals

2-Aminofluorene (2-AF, 98%), 1-aminopyrene (1-AP, 99%) and 1-NP (97%) were supplied by Aldrich Europe (Bornem, Belgium). 2-Nitropyrene ($\geq 98\%$), 4-nitropyrene ($\geq 99\%$), 2-aminofluoranthene (99%), and 3-aminofluoranthene (98%) were obtained from

Chemsyn (Lenexa, MO, USA). 1-Nitro-[$^2\text{H}_9$]pyrene (1-N[$^2\text{H}_9$]P, >99%) and 2-fluoro-7-nitrofluorene (2-F-7-NF, >99.8%), used as internal standards throughout the analysis, were obtained from Sigma (St. Louis, MO, USA) and Chemsyn, respectively. Heptafluorobutyric anhydride (HFBA), 2-nitrofluorene (2-NF, 98%) and granular zinc (mesh size ca. 590 μm) were supplied by Janssen Chimica (Geel, Belgium). Glass beads (160–250 μm) were obtained from Tamson (Zoetermeer, Netherlands). Sodium hydrosulfide hydrate (NaSH, 27% water) was obtained from Aldrich (Steinheim, Germany). Sep-Pak Si cartridges were supplied by Millipore (Bedford, MA, USA). Sodium hydroxide pellets and ethanol (abs) were obtained from Merck (Darmstadt, Germany). 2-Amino-7-fluoro-fluorene (2-A-7-FF) was obtained by reduction of 2-F-7-NF with Raney Nickel according to Litvinenko and Grekov [65]. All organic solvents used were HPLC-grade (Lab-Scan, Dublin, Ireland). Demineralized (demi) water (tap water treated in a Milli RO system, Millipore) and aqua pure (demi water treated in a Nanopure system, Barnstead, Boston, MA, USA) were used. Other chemicals used were of the highest purity available.

2.2. Air and diesel exhaust samples

Total suspended particulate matter (TSPM) was sampled using a high-volume sampler (type Gromoz, Agricultural University, Wageningen, Netherlands) equipped with an open face sampler head with an entrance opening diameter of 140 mm. Air was sampled at a flow rate of ca. 1.0 m^3/min . Respirable suspended particulate matter (RSPM) was collected using a cyclone with a 50% cut-off diameter of ca. 5 μm at 0.050 m^3/min [66]. This fraction slightly overestimates the respirable fraction such as defined in the European Standard EN481. For RSPM sample collection a medium-volume sampler (consisting of an oil-free vacuum pump, a gas meter and a restriction valve) was used. The operation of high- and medium-volume samplers was kept under surveillance continuously. The flow rate was checked every 15 min and adjusted if neces-

sary. Sampling times varied from 2–10 h per filter.

The inhalable suspended particulate matter (ISPM) was sampled in the breathing zone of railroad workers using small-size air sampling pumps equipped with IOM sampler heads (Institute of Occupational Medicine, Edinburgh, Scotland). Air was sampled at a flow of ca. 0.0020 m^3/min using an electronically flow-controlled personal air sampling pump. The air volumes of these samples ranged from 0.5 to 1 m^3 .

Particulate matter was collected on PTFE coated polystyrene membrane filters (TE 38, Schleicher and Schüll, Dassel, Germany). The filters were placed in an exsiccator prior to weighing. This procedure was repeated after collecting the air samples. Gravimetric determinations were conducted using a Mettler AE 163 analytical balance (Mettler-Toledo, Zürich, Switzerland).

Diesel exhaust particulate samples were obtained from the TNO Road Vehicle Research Institute (Delft, Netherlands). Briefly, samples from heavy duty and light duty vehicles (HDV and LDV) were collected on two Pallflex TA60A20 filters (Pallflex, Putnam, CO, USA), placed in series, under constant pressure sampling conditions. In the case of LDV samples, the filters were combined with a back-up Amberlite XAD₂ adsorbent cartridge for collection of volatile PAHs. The filter and adsorbent extracts were combined prior to analysis.

2.3. Apparatus

For automated reduction of nitro-PAHs an HPLC system consisting of a Spectra Physics SP 8800 ternary HPLC pump and a Spectra-Physics SP 8875 autosampler equipped with a 50- μl loop were used. Final analysis of derivatized amino-PAHs was performed on a Varian 4300 GC equipped with a Varian 8100 autosampler and a Varian Saturn 1 IonTrap MS detector. In the interlaboratory comparison at the Agricultural Research Department of the State Institute of Quality Control of Agricultural Products (RIKILT-DLO, Wageningen, Netherlands), a VG Autospec EQ high-resolution (HR) mass

spectrometer (VG Instruments, Altrincham, England) equipped with an HP5890 gas chromatograph and an HP7673A autosampler (Hewlett-Packard, Palo Alto, CA, USA) were used.

2.4. Reference materials

Standard Reference Material (SRM) 1587 consisting of a methanolic solution of seven nitro-PAHs with certified concentrations for 1-NP and 2-NF (Table 1) produced by the National Institute of Standards and Technology (NIST, Gaithersburg, MD, USA), was kindly supplied by the TNO Institute of Environmental Sciences (Delft, Netherlands). The NIST SRM 1650, a diesel exhaust particulate matter with a certified 1-NP content, was supplied by CN Schmidt (Amsterdam, Netherlands). This particulate sample was collected from several diesel engines with direct fuel injection and would be representative for heavy duty engines. The extract of a particulate sample from a Yanmar diesel engine (single cylinder; 4 kW full load) fueled with CEC-RF03-A-84 reference fuel was used for reproducibility testing. The soot was collected on a Gelman glass fibre filter type A/E (Gelman, Ann Arbor, MI, USA) at 100 to 130°C at the beginning of collection (for more details see [67]).

2.5. Filter extraction

The filters loaded with TSPM were cut into pieces. The filter pieces were extracted in 25 ml of acetone by sonication for 15 min. The extract

Table 1
Certified concentrations of 1-NP and 2-NF in the standard reference materials used

Material	Concentration ($\mu\text{g/g}$)	
	1-NP	2-NF
SRM 1587	8.95 ± 0.28	9.67 ± 0.39
SRM 1650	19 ± 2	0.27^a

^a Not certified.

was pipetted into a large glass tube and reduced in volume under N_2 at 50°C. The filter was extracted twice more with 10 ml of acetone by sonication for 5 min. The three resulting extracts were combined, reduced in volume to about 5 ml under N_2 at 50°C and centrifuged for 5 min at 600 g. The solvent was collected by pipetting into a pre-weighed glass tube and reduced in volume under N_2 at 50°C. The remaining residue was washed with 5 ml of acetone and centrifuged for 5 min at 600 g. The acetone washing was added to the concentrated acetone extract and the solvent was subsequently removed under N_2 at 50°C. The amount of dry extract was determined gravimetrically. The dry extract was dissolved in acetone, sonicated and divided in four pre-weighed glass tubes. Each of the portions corresponded to a sampled air volume of ca. 25–150 m^3 . The four portions were evaporated to dryness under N_2 and weighed. Two portions were used for nitro-PAH analysis. The third and fourth portions were stored at -20°C for future analysis. All the dry extracts were stored at -20°C in the dark, until further analysis. When analyzing RSPM, ISPM, and diesel exhaust samples derived from HDV, the whole filters were extracted thrice with 10 ml of acetone. The RSPM samples were divided into two equal portions in the same way as described above. One of these was analyzed. The other portion was kept at -20°C in the dark for future analysis.

2.6. Fractionation

Extracts of air and diesel exhaust samples, as well as standard solutions in dichloromethane, were fractionated into non-polar, intermediately polar and polar fractions through solid-phase extraction with Sep-Pak Si cartridges on a vacuum manifold [8]. After activation of the cartridge with 5 ml of dichloromethane, 200 μl of sample or standard solution was loaded onto the cartridge. It was flushed with air until all of the solvent had passed through the cartridge. Non-polar compounds were washed from the cartridge with 3 ml of *n*-hexane and discarded. The intermediately polar fraction containing the com-

pounds of interest was eluted from the cartridge with 5 ml of dichloromethane. The solvent was removed under N₂ at 30°C until dryness.

2.7. On-line reduction (method A)

The fractions containing the nitro-PAHs were dissolved in 200 µl methanol and pipetted into glass inserts in crimp-cap vials. Nitro-compounds were reduced (overnight) to their amino analogues on a stainless steel 40 mm × 3 mm I.D. reduction column, filled with granular zinc and glass beads (1:1, w/w). The column was placed at 40°C in the column oven of an HPLC system. The mobile phase consisted of 90% methanol, 10% aqua pure with 15 mM glacial acetic acid and 5 mM sodium chloride at a flow of 1 ml/min. Aliquots of 50 µl of fractionated sample solutions in methanol were injected into the HPLC system. Fractions of 5 ml of mobile phase effluent containing the amino-PAH were collected using a fraction collector (Pharmacia, Uppsala, Sweden). The fraction collector was kept in the dark in a N₂ atmosphere to prevent light induced oxidation of amino-PAHs. To prevent the formation of H₂, after the reduction column a back pressure was created by installing a stainless steel 150 mm × 4.6 mm I.D. column containing a C₁₈ stationary phase. This resulted in a considerable extension of the time needed to process each sample, but was preferred over a loss in reduction efficiency because of gas formation in the reduction column. Between the pump and the autosampler an oxygen scrubber, consisting of a stainless steel 150 mm × 4.6 mm I.D. column filled with zinc, was placed to prevent oxidation of the zinc and thus extending the lifetime of the reduction column. Amino-PAHs were extracted from the mobile phase effluent after reduction of the volume to ca. 0.5 ml under N₂ at 50°C by adding 2 ml of toluene and 0.5 ml of a 0.3 M sodium hydroxide solution to neutralize the acetic acid. After 5 min of centrifugation at 600 g the toluene layer was collected and dried under N₂ at 50°C.

The amino-PAHs were derivatized with HFBA to HFB-amino-PAHs by redissolving the residue of the aforementioned toluene layer in 100 µl of

n-hexane. Next, 20 µl of HFBA were added, mixed and kept at 40°C for 30 min. The samples were cooled in cold tap water and 1 ml of *n*-hexane and 0.5 ml of aqua pure were added to remove the excess of HFBA. After centrifugation for 5 min at 600 g, the water layer was carefully removed. The remaining *n*-hexane was removed under N₂ at 40°C until dryness. The residue was redissolved in 50 µl of isoctane and placed in tapered inserts in screw-cap vials for analysis by GC-MS.

2.8. Reduction using NaSH (method B)

The nitro-PAHs were reduced by a simple one-tube reduction step adopted from Hisamatsu and co-workers [55]. Briefly, an aliquot of 0.5 ml of ethanol and 0.5 ml of a 10% aqueous NaSH solution were added to the dried fractionated samples and mixed. After 0.5 h incubation at 100°C, 250 µl of 1.2 M aqueous sodium hydroxide solution and 3 ml of *n*-hexane were added. After 3 min centrifugation at 1250 g, the *n*-hexane layer was collected and dried under N₂ at 40°C. The dried residue of the *n*-hexane layer was dissolved in 100 µl of *n*-hexane. An aliquot of 20 µl of HFBA was added and the sample was kept at 60°C for 30 min. After cooling in cold tap water, 3 ml of *n*-hexane were added to dilute the sample and 100 µl of aqua pure were added to neutralize the excess of HFBA. After 3 min centrifugation (1250 g) the water layer was carefully removed and the remaining *n*-hexane layer was dried under N₂ at 40°C. The residue was dissolved in 40 µl of isoctane and placed in a tapered insert in a screw cap vial for analysis by GC-MS.

2.9. Analysis by GC-MS

Aliquots of 1 µl of sample followed by 0.5 µl of solvent wash (separated by an air gap) were injected on-column in a septum equipped programmable injector (SPI) at 5 µl/s with a 0.1 min post-injection "hot needle" time. The column system consisted of a 2.5 m × 0.53 mm I.D. deactivated fused-silica retention gap (different brands) and a 30 m × 0.25 mm I.D. DB-5MS

coated ($d_f = 0.25 \mu\text{m}$) fused-silica capillary column (J and W Scientific, Folsom, CA, USA). The carrier gas used was helium at a column head pressure of 96 kPa. The SPI was programmed from a 1-min hold at 95°C to a final temperature of 280°C at 90°C/min, with a 10-min hold at 280°C. Separation was achieved programming the GC oven temperature from a 1-min hold at 95°C to a final temperature of 200°C at 20°C/min, followed by 5°C/min to a final temperature of 280°C with a 5-min hold at 280°C. The transfer line and ion source were kept at temperatures of 290°C and 235°C, respectively. The mass spectrometer was operated in the EI mode at an electron ionization energy of 70 eV. A mass range of m/z 150–450 was scanned at a rate of 1 scan/s between 10 and 11 min and between 15.5 and 17 min after injection when the compounds of interest and their internal standards eluted from the column. HFB derivatives of 2- and 4-aminopyrene and 2- and 3-aminofluoranthene have an identical mass spectrum as the HFB derivative of 1-AP. These compounds were analyzed in order to verify the identity of the peak with the same retention time as the derivatized 1-AP standard. The counter-expertise analysis parameters were essentially the same, except that the injection was splitless at 280°C and the oven temperature was kept at 95°C for 3 instead of 1 min. The column length was 60 instead of 30 m. The HRMS was operated in the EI+ mode at an electron ionization energy of 35 eV. A mass range of m/z 377.1–396.1 was scanned between 22 and 27 min after injection and a mass range of m/z 413.1–423.1 was scanned between 29 and 36 min after injection at a rate of ca. 3 scans/s and a resolution of 6000.

2.10. Preparation of standards and calibration

Stock solutions and dilutions of the nitro compounds and internal standards were made in ethanol. In the case of the analysis of RSPM (method B) *n*-hexane was used for further dilution of the stock. The final concentrations were 0 to 100 pg/ μl on column (method A) and 0 to 900 pg/ μl on column (method B). Just before frac-

tionation, to each dilution internal standard was added with a final concentration of 50 pg/ μl on column (method A) and 120 and 350 pg/ μl (method B) for RSPM and TSPM samples, respectively. Standards used for calibration and the SRM 1650 and 1587 were analyzed in duplicate. Ca. 3 mg of SRM 1650 was used. Of SRM 1587 a dilution was prepared corresponding to a concentration of 100 pg/ μl on-column.

2.11. Determination of reduction recovery

The recovery of the on-line zinc reduction was evaluated by comparison of the plots of peak areas vs. concentration after injection of several dilutions of the nitro or amino analogues of the compounds of interest. Dilutions were prepared in such a way that final concentrations of 100 to 1000 pg on column were tested. The ratio of the slopes, acquired through linear regression analysis, of the nitro and amino analogues provided accurate determinations of the reduction recovery.

For method B ethanol solutions of the nitro and amino analogues and of 1-N[²H₉]P and 7-F-2-NF of similar concentrations were prepared. Nitro or amino analogues were mixed with internal standard solutions for each one of final dilutions ranging from 60 to 540 pg on column. These samples were treated with NaSH as if they were samples.

2.12. Estimation of the limit of determination

The limit of determination was estimated by testing the intra-day repeatability of the analysis of a diesel exhaust particulate sample extract spiked with 1-NP and 2-NF in the range 1.25–25.0 ng/g particulate matter. This sample was collected from the inside of a front wheel cover of a diesel fueled LDV using a soft brush. It was used as a surrogate diesel exhaust sample, containing a mixture of soot particles from various mobile sources. In the sample 1-NP and 2-NF were not detected. Spiked extracts were fractionated, and reduced, in triplicate, prior to GC–MS analysis, in duplicate. The reduction was conducted using method B.

2.13. Calculations

The dry acetone extract weights were adjusted for the contribution of solvent and filter residues. The correction factor was determined by extraction of blank filters, evaporating the solvent under N_2 and calculating the dry extract weight per mg filter and per ml acetone. A calibration curve was constructed by plotting the ratio of the peak areas of 1-NP and the internal standard vs. the 1-NP amount in the solution. The 1-NP levels that were calculated from the calibration curve were corrected for the 97% purity of the 1-NP reference. The same was done for 2-NF. Results of duplicate analysis were calculated as arithmetic means. Differences between the results of the analysis of the series of TSPM

samples were evaluated in a two-tailed paired Students' t-test.

3. Results

In Fig. 1 the mass spectra of reduced and derivatized 1-NP, 2-NF and the respective internal standards 1-N[2H_9]P and 7-F-2-NF are presented. The quantitations in the samples were based on the molecular ions.

During the fractionation on Sep-Pak Si recoveries of 1-NP and 2-NF were excellent ($100.4 \pm 3.6\%$ and $95.2 \pm 1.0\%$, respectively). The recovery of the on-line zinc reduction (method A) amounted to ca. 102% for 1-NP and ca. 93% for 2-NF. In Table 2 the results of recovery

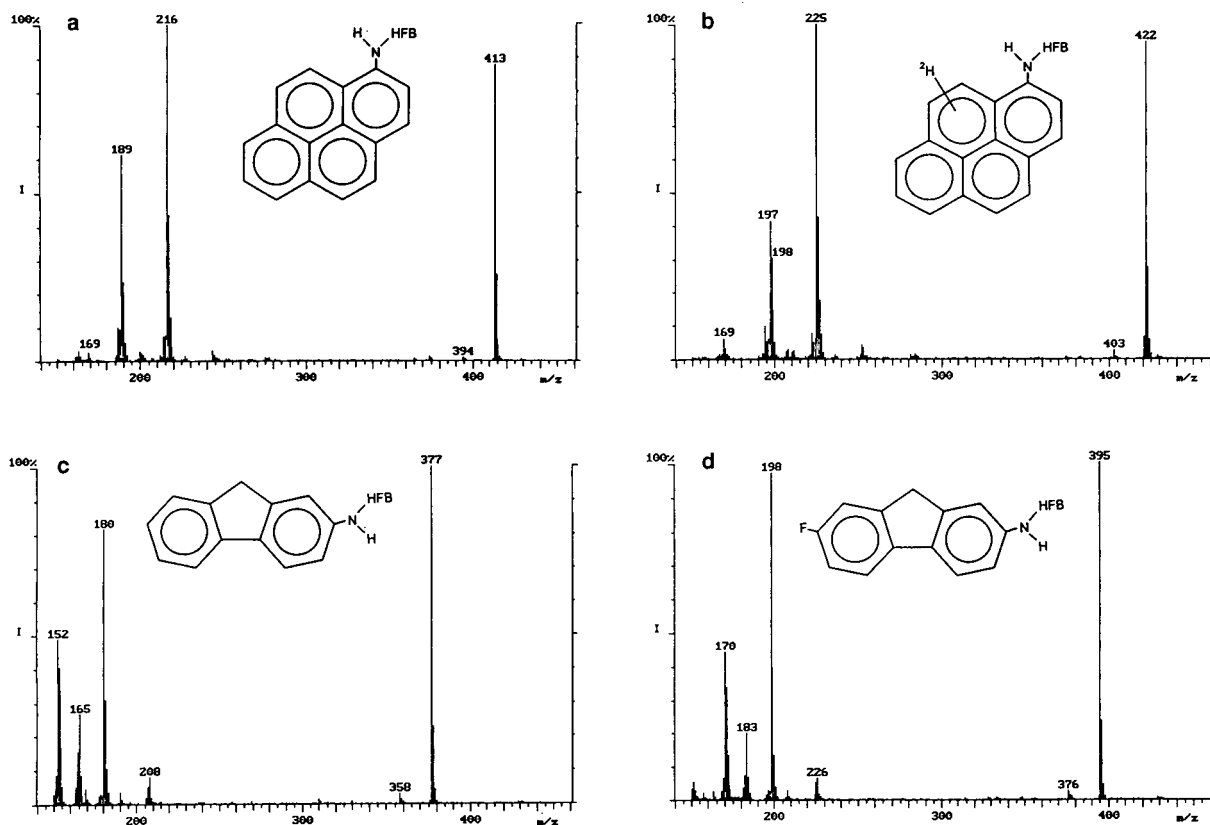


Fig. 1. Electron ionization mass spectrum of reduced and derivatized 1-NP (a), 1-N[2H_9]P (b), 2-NF (c), and 7-F-2-NF (d). The molecular ions are m/z 413, 422, 377, and 395, respectively. The fragments $[M - 197]^+$ (m/z 216, 225, 180 and 198, respectively) were formed through loss of COC_3F_7 . The fragments $[M - 224]^+$ (m/z 189, 198, 153, and 171, respectively) were formed through loss of $CNHCO_3F_7$.

Table 2
Recovery of 1-NP and 2-NF after reduction with NaSH

Concentration of 1-NP and 2-NF (pg/ μ l on column)	Recovery (%)	
	1-NP	2-NF
60	108.3 \pm 15.0	97.3 \pm 3.9
120	114.8 \pm 12.4	87.8 \pm 8.5
270	104.0 \pm 2.7	90.5 \pm 4.2
540	106.5 \pm 3.3	93.1 \pm 1.0

Determinations in triplicate (mean \pm S.D.).

tests of reductions using NaSH (method B) are presented. The mean recoveries for 1-NP and 2-NF were 108.4 \pm 4.6 and 92.2 \pm 4.0%, respectively. In Table 3 the extraction efficiencies from the aqueous solution, directly after the NaSH reduction, are presented for four different or-

Table 3
Extraction efficiencies directly after the NaSH reduction

Solvent	Extraction efficiency (%)	
	2-NF	1-NP ^a
Dichloromethane	70.6 \pm 2.6	71.3 \pm 11.8
Toluene	57.7 \pm 5.0	67.0 \pm 21.0
Hexane	64.4 \pm 7.2	96.8 \pm 8.4
Ethyl acetate	66.5 \pm 4.3	81.0 \pm 6.9

Determinations in triplicate (mean \pm S.D.).

^a 7F-2-NF was used as internal standard.

Table 4
Repeatability of the analyses of SRM 1587

Day	Concentration (μ g/g)		Deviation from certified values (%)	
	1-NP	2-NF	1-NP	2-NF
1	8.98	9.13	0.3	-5.6
2	10.96	8.57	22.5	-11.4
3	7.58	9.58	-15.3	-0.9
4	8.23	8.68	-8.0	-10.2
Mean	8.94 \pm 1.46	8.99 \pm 0.46	-0.1	-7.0

Determinations in duplicate.

Table 5
Dilutions of 2-NF and 1-NP spiked into a diesel exhaust extract and analyzed in triplicate

Concentration on column (pg/ μ l)	R.S.D. (%)	
	2-NF	1-NP
10	11.1	9.7
20	6.9	4.7
40	1.1	3.8
80	1.9	4.1
120 ^a	0.3	3.0
160	1.8	2.8
200	2.2	1.7

^a Analyzed in duplicate.

ganic solvents. Hexane was selected to be used because of the excellent recovery of 1-NP. The recoveries for 2-NF were moderate and not much dependent on the choice of solvent.

The SRM 1587 was analyzed on four different occasions (see Table 4) showing good reproducibility and accuracy for both 1-NP and 2-NF when compared to the certified values. Two portions of SRM 1650 were analyzed in duplicate resulting in a 1-NP concentration of 18.0 \pm 0.4 μ g/g (mean \pm S.D.). This was within 5.5% of the certified value.

Table 5 presents the results of repeatability tests for the analysis from diesel exhaust derived particulate extracts spiked with 1-NP and 2-NF. The relative standard deviations of determinations in triplicate remained well below 10%,

down to amounts of 20 pg 1-NP and 2-NF injected on column.

Fig. 2 shows the GC–MS total ion chromatogram and single-ion chromatograms of 1-NP and 1-N[²H₉]P. The results of the analysis of ca. 3 mg SRM 1650 and of a workplace sample are presented.

The results of the duplicate analysis (methods A and B) and of the counter-expertise (B') of 36 samples of TSPM derived from 12 different workplace atmospheres and a reference sample are presented in Table 6. In more than half of the samples analyzed, 1-NP was detected. Most of the samples with non-detectable 1-NP were outdoor samples. Only in three out of 22 indoor samples 1-NP could not be detected using method A. Using method B this number was 2. In a supplementary single analysis on the GC–HRMS

system 1-NP was detected in all of the indoor samples and all of the outdoor samples, except for the sample collected at the farm. The outdoor samples containing detectable 1-NP levels were collected on a river vessel close to exhaust pipes of the main ship's engine and power supply. In addition to these samples, 1-NP was detected using method B in outdoor atmospheres at a level of 36 pg/m³ on a busy street crossing in a city centre. On the airport platform a relatively high level of 1-NP was detected using method A. The high level of 1-NP that was determined using method A was not reconfirmed in the analysis of this particular sample using methods B and B'. It may have been caused by contamination of the sample. Therefore, this observation was excluded from further (statistical) analysis. The two series of results obtained from the analysis of the TSPM samples were evaluated in a paired two-sided t-test. We did not observe a difference in 19 analyzed 1-NP levels using either method A or B. These results correlated significantly ($r = 0.85$, $p < 0.0001$). The interlaboratory comparison of the analysis of a series of 21 samples (B–B') resulted in a correlation coefficient of 0.92 ($p < 0.0001$).

In Table 7 the results of the GC–HRMS analyses are expressed as the 1-NP content of the dust (in $\mu\text{g/g}$ dust) and of the soluble organic fraction (SOF) (in $\mu\text{g/g}$ SOF). The lowest levels of 1-NP were observed in outdoor samples. The SOF and TSPM of the samples collected in the city centre contained more than tenfold higher amounts of 1-NP than the sample collected in a forest area.

Extracts of RSPM derived from different workplace atmospheres were analyzed using method B. In Table 8 the results of these analysis are presented. In ten of the samples 1-NP was detected. Nine of these samples originated from indoor workplaces associated with the use of fork lift trucks. One of the samples was collected outdoors on a river vessel. We did not detect 2-NF in any of the RSPM samples.

We have identified 1-NP in two samples out of a series of ten low-volume ISPM samples (0.7–0.9 m³) collected in the breathing zones of railroad workers during an 8 h working period.

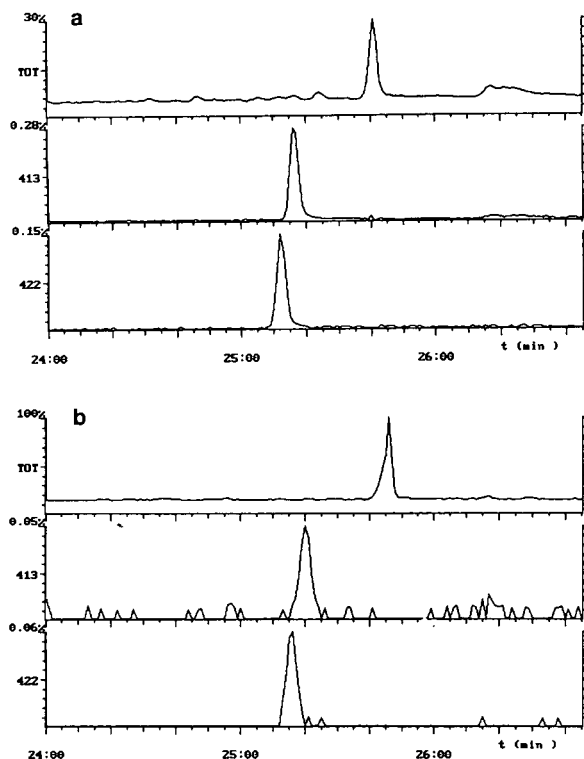


Fig. 2. GC–MS total ion chromatogram and single-ion chromatograms at m/z 413 and m/z 422 of 1-nitropyrene and 1-nitro[²H₉]pyrene, respectively. Analysis of SRM 1650 (a) and a TSPM sample collected in a concrete manufacturing facility in the vicinity of an operating fork lift truck (b).

Table 6

Air concentrations of 1-NP as determined from extracts of TSPM collected at workplaces associated with the use of diesel engines

Facility	Sources of diesel exhaust	Sample volume (m ³)	1-NP		
			A (ng/m ³)	B (ng/m ³)	B' (ng/m ³)
River vessel	Ship's engine	385	0.093	ND ^a	0.031
		325	ND	0.11	0.10
		365	ND	ND	0.021
Repair shop for trains	Train engines	345	0.39	0.16	0.28
		155	0.44	0.42	0.34
		275	ND	0.24	0.26
		465	0.24	0.29	0.39
Army driving lessons	Armoured cars	345	ND	ND	0.012
		150	ND	ND	0.015
Flower auction	Trucks	340	0.11	0.086	0.080
		395	0.16	ND	0.082
Farming	Tractor	127	ND	ND	ND
Gardening	Passing traffic	420	ND	0.034	0.036
Airport platform	Platform vehicles ^b	225	0.45	ND	0.042
		260	ND	ND	0.045
		275	ND	ND	0.037
		135	0.45	0.64	0.61
Concrete manufacturing	Fork lift trucks	150	0.70	0.85	0.71
		425	0.17	0.11	0.12
Chemical plant	Fork lift trucks	400	0.38	0.25	0.56
		450	0.11	0.095	0.11
		405	0.25	0.39	0.29
		200	0.78	1.6	1.2
Aluminium rolling	Fork lift trucks	210	1.6	0.93	1.2
		265	1.2	0.77	0.98
		205	0.59	0.62	0.87
		465	0.15	0.088	0.071
Galvanization workshop	Fork lift trucks	360	0.19	0.14	0.15
		135	ND	0.12	0.14
		230	ND	ND	0.044
		215	ND	ND	0.0066
Grass verge maintenance	Lawn mowers	215	ND	ND	0.0066
River vessel	Ship's aggregate	605	0.33	0.45	0.79
Reference	Unknown	427	ND	ND	0.0017

(A) On-line zinc reduction based method; (B) SHH reduction based method with EI/ITD detection and (B') HRGC-MS detection. Determinations A and B in duplicate.

^a ND = Not detected.

^b Lift platforms, power supplies, trucks, pull-offs.

The 1-NP levels were 1.84 and 2.90 ng/m³. The 1-NP content of the dust was 2.74 and 0.87 μg/g ISPM, respectively. In the other eight samples 1-NP was not detected.

Results of the analysis of particulate matter sampled directly from the tail pipe of vehicles

tested on a chassis dynamometer are presented in Table 9. A modern technology heavy duty engine emitted the highest levels of 1-NP per km in an urban driving pattern. The light duty vehicle equipped with an oxydation catalyst emitted much lower levels of 1-NP per km in

Table 7

1-NP content in extracts of TSPM collected at workplaces associated with the use of diesel engines as determined after reduction with NaSH (mean \pm S.D.)

Source	1-NP		N
	SOF ($\mu\text{g/g}$)	TSPM ($\mu\text{g/g}$)	
Ship's aggregate	11.9	7.6	1
Fork lift trucks (light duty)	6.8 \pm 5.6	3.2 \pm 2.8	12
Fork lift trucks (heavy duty)	6.1 \pm 2.3	1.2 \pm 1.4	2
Train engines	6.0 \pm 2.6	1.3 \pm 0.8	4
Trucks	2.2 \pm 0.13	0.36 \pm 0.035	2
Ship's engine	2.0 \pm 0.94	0.97 \pm 0.57	3
Platform vehicles	1.4 \pm 0.45	0.60 \pm 0.23	3
Passing traffic	1.2	0.49	1
Armoured cars	0.40 \pm 0.025	0.11 \pm 0.0014	2
Lawn mowers	0.33	0.099	1
Unknown (reference)	0.076	0.034	1

three different driving patterns. We did not investigate the influence of the catalyst on these emission levels.

4. Discussion

We have presented an accurate and simple method for the detection and quantification of 1-NP and 2-NF associated to airborne particu-

lates derived from various sources, mainly diesel fuel combustion. We have demonstrated that the 1-NP content of fresh and aged diesel exhaust particulates can be determined from low-volume air samples.

The sonication technique that we have used yields quantitative extractions from SRM 1650. Supercritical fluid extraction did not provide significantly higher yields of 1-NP than extraction by sonication [22]. Acetone was selected as an

Table 8

1-NP content in extracts of RSPM collected at workplaces associated with the use of diesel engines as determined after reduction with NaSH

Facility	Sources of diesel exhaust	Sample volume (m^3)	1-NP	
			RSPM ($\mu\text{g/g}$)	(ng/m^3)
Repair shop for trains	Train engines	23.3	4.7	0.48
		1.4	10.6	3.9
		4.5	4.5	0.79
Concrete manufacturing	Fork lift trucks	21.8	1.9	0.63
		18.3	4.2	0.82
Chemical plant	Fork lift trucks	20.3	5.6	0.39
		20.0	7.0	0.31
Aluminium rolling	Fork lift trucks	21.3	7.7	1.0
		23.8	5.4	0.71
River vessel	Ship's aggregate	30.3	9.1	0.72

Table 9
Determinations of 1-NP in exhaust derived from trucks during simulated driving cycles

Vehicle	Driving pattern	1-NP	
		$\mu\text{g/g}$ dust	$\mu\text{g/km}$
Heavy duty	Sub urban	1.94	2.13
	Sub urban	1.94	3.28
	Urban	3.39	6.48
	Motorway	1.94	0.87
	Motorway	2.73	1.37
Light duty ^a	European Driving Cycle (cold start)	— ^b	0.32
	European Driving Cycle (hot start)	— ^b	0.22
	US '75 Driving Cycle	— ^b	0.36

^a With oxidation catalyst.

^b Amount of sampled particulate matter not determined.

extraction solvent because it very efficiently extracts nitro-PAHs from diesel exhaust particulates [68]. Because of lack of accurate methods of spiking diesel exhaust soot samples the efficiency of the extraction procedure could not be determined.

The fractionation on silica provides sufficient clean-up for samples of aged diesel exhaust particulate matter including the SRM 1650. When analyzing particles sampled directly from the tailpipe on a chassis dynamometer further fractionation may be needed.

Zinc reduction may be used in an on-line reductive treatment of nitro-PAHs from environmental samples combined with HPLC and/or GC-MS analysis [64]. In practice, on-line reduction may be troublesome and unreliable because of variations in the quality of the reductive column and the complexity of the laboratory equipment. We have also tested some other materials such as tin chloride and copper borium hydride [38,69] for catalytic reduction of nitro-PAHs. These methods did not meet the requirements regarding the reduction efficiency or caused practical problems during separation of the amino-PAHs. We have selected the batch-wise NaSH reduction because of the excellent

recoveries of 1-NP and 2-NF, its good reproducibility, simplicity, and low cost.

For determination of the repeatability of the newly developed 1-NP analysis (method B), the test sample was analyzed repeatedly. The inter-day coefficient of variation amounted to 7.7% ($n = 7$). For the series of TSPM samples the repeatability was 10.8% for method A and 8.4% for method B (based on a series of seventeen TSPM samples with detectable 1-NP levels for both methods). The reproducibility as calculated from the interlaboratory comparison of the analysis of a series of 21 TSPM samples (B-B') amounted to 16.6%.

The results of the analysis of spiked diesel exhaust particulate samples demonstrated an excellent repeatability for both compounds, indicating a limit of determination down to 10 pg on-column. This corresponds to a level of 1-NP and 2-NF as low as ca. 1 ng/g particulate matter (with a relative standard deviation of ca. 10%).

The peak designated as 1-NP signal was not attributable to known nitropyrene isomers or nitrofluoranthenes. The HFB derivatives of the corresponding amino analogues were injected as standards. The retention order was 2-NF < 2-F-7-NF \ll 3-nitrofluoranthene < 4-nitropyrene < 2-

nitrofluoranthene \leq 1-N[²H₉]P \leq 1-NP < 2-nitropyrene.

On average particulate emissions from the light duty engines such as used in power supplies and in fork lift trucks contained higher levels of 1-NP than heavy duty engines with (mostly) direct fuel injection. This is consistent with the observation that indirect injected engines (LDVs) tend to have higher 1-NP emissions than direct injected engines (HDVs) [70]. The 1-NP content of the dust and of the SOF observed in this study (cf. Table 7) was lower than the levels that were observed in freshly emitted diesel exhaust particles, reported in the 1980's [6–11,17].

We detected 2-NF in a sample collected in the vicinity of a power supply of a river vessel. The 2-NF content was ca. 25 times smaller than the 1-NP content in the same sample. The sample may have contained a considerable amount of freshly emitted diesel exhaust particles, resulting in a higher level of more volatile compounds such as 2-NF.

The occurrence of 2-NF has been reported several times in fresh (diluted) samples collected on a filter directly from the exhaust of a diesel engine running on a chassis dynamometer. These samples have shown condensation of lower molecular weight hydrocarbons from the gas phase onto the particles [71], suggesting that the occurrence of 2-NF in these samples may be associated with the specific sampling conditions in a dilution tunnel [72]. Paschke and co-workers [22] have also identified 2-NF in particulate matter scraped directly from the exhaust pipe of a bus engine (sample collection procedure not specified). This material may have contained nitro-PAHs that were adsorbed onto particles deposited in the tail pipe or formed by conversion of deposited PAHs by passing nitrogen oxides. We did not find reports of mass spectral based evidence of the recovery of 2-NF from ambient particles. So far, the only reports have been based on fluorescence detection [39].

The analysis of 1-NP from dilution tunnel samples derived from HDV and LDV showed that the method needs to be improved further. In the series of HDV samples 1-NP was detected

in five out of seven samples, whereas in the series of LDV samples only three out of sixteen samples showed detectable amounts of 1-NP. We estimate that improvements in sample work-up and/or detection may result in a higher score of samples with detectable 1-NP levels.

We have demonstrated the accurate identification and quantification of levels of 1-NP from low-volume air samples and diesel exhaust samples using a non-laborious work-up and a current GC-MS technique. The method shows good reproducibility and may be used for routine analysis of nitro-PAHs from workplace air samples containing diesel exhaust combustion products.

Acknowledgements

This study was financed by the Labour Inspectorate of the Dutch Ministry of Social Affairs and Employment. Gratitude is expressed to P. Hendriksen and D.M. Heaton of the Institute of Road Traffic of the TNO Institute (Delft, Netherlands) and to O. van Pruissen of the Chemical Reaction Engineering Section of the Faculty of Chemical Technology and Materials Science at Delft University of Technology (Netherlands) for supplying samples of diesel exhaust. We would like to thank W.A. Traag of RIKILT-DLO, Wageningen, Netherlands, for analysis of nitro-PAHs on the GC-HRMS.

References

- [1] Deutsche MAK-Kommission, *Dieselmotor-Emissionen, MAK-Werte-Liste*, VCH, Weinheim, 1987.
- [2] NIOSH, *Carcinogenic effects of exposure to diesel exhaust*, Current Intelligence Bulletin 50, NIOSH, Cincinnati, OH, 1988.
- [3] IARC, *IARC Monographs on the evaluation of carcinogenic risks to humans. Diesel and gasoline engine exhausts and some nitroarenes*, IARC, Lyon, France, 1989.
- [4] D. Schuetzle and J.A. Frazier, in N. Ishinishi, A. Koizumi, R.O. McClellan and W. Stöber (Editors), *Carcinogenic and mutagenic effects of diesel engine exhaust*, Elsevier, Amsterdam, 1986, p. 41.
- [5] D. Schuetzle and J.M. Perez, *J. Air Pollut. Control Assoc.*, 33 (1983) 751.

- [6] T.L. Gibson, *Atmos. Environ.*, 16 (1982) 2037.
- [7] I. Salmeen, A.M. Durisin, T.J. Prater, T. Riley and D. Schuetzle, *Mutat. Res.*, 104 (1982) 17.
- [8] S.M. Rappaport, Z.L. Jin and B. Xu, *J. Chromatogr.*, 240 (1982) 145.
- [9] M.G. Nishioka, B.A. Petersen and J. Lewtas, in M. Cooke, A.J. Dennis and G.L. Fisher (Editors), *Polynuclear Aromatic Hydrocarbons*, Battelle, Columbus, OH, 1982, p. 603.
- [10] R. Nakagawa, S. Kitamori, K. Horikawa, K. Nakashima and H. Tokiwa, *Mutat. Res.*, 124 (1983) 201.
- [11] R.A. Gorse, Jr., T.L. Riley, F.C. Ferris, A.M. Perso and L.M. Skewes, *Environ. Sci. Technol.*, 17 (1983) 198.
- [12] D. Schuetzle, *Environ. Health Perspect.*, 47 (1983) 65.
- [13] D. Schuetzle, F.S.-C. Lee, T.J. Prater and S.B. Tejada, *Int. J. Environ. Anal. Chem.*, 9 (1981) 93.
- [14] B.A. Tomkins, R.S. Brazell, M.E. Roth and V.H. Ostrum, *Anal. Chem.*, 56 (1984) 781.
- [15] W.C. Yu, D.H. Fine, K.S. Chiu and K. Biemann, *Anal. Chem.*, 56 (1984) 1158.
- [16] A. Robbat Jr., N.P. Corso and P.J. Doherty, *Anal. Chem.*, 58 (1986) 2078.
- [17] W.M. Draper, *Chemosphere*, 15 (1986) 437.
- [18] K. Levsen, J. Schilhabel and U. Puttins, *J. Aerosol Sci.*, 18 (1987) 845.
- [19] U. Sellström, B. Jansson, Å. Bergman and T. Alsberg, *Chemosphere*, 16 (1987) 945.
- [20] R. Niles and Y.L. Tan, *Anal. Chim. Acta*, 221 (1989) 53.
- [21] J. Schilhabel and K. Levsen, *Fresenius' J. Anal. Chem.*, 333 (1989) 800.
- [22] T. Paschke, S.B. Hawthorne and D.J. Miller, *J. Chromatogr.*, 609 (1992) 333.
- [23] H.S. Rosenkranz, E.C. McCoy, D.R. Saunders, M. Butler, D.K. Kiriazides and R. Mermelstein, *Science*, 209 (1980) 1039.
- [24] T. Nielsen, B. Seitz and T. Ramdahl, *Atmos. Environ.*, 18 (1984) 2159.
- [25] J.L. Mumford and J. Lewtas, *J. Toxicol. Environ. Health*, 10 (1982) 565.
- [26] W.R. Harris, E.K. Chess, D. Okamoto, J.F. Remsen and D.W. Later, *Environ. Mutagenesis*, 6 (1984) 131.
- [27] K.B. Olsen, D.R. Kalkwarf and C. Veverka Jr., in M. Cooke and A.J. Dennis (Editors), *Polynuclear Aromatic Hydrocarbons*, Battelle, Columbus, OH, 1985, p. 973.
- [28] T. Handa, T. Yamauchi, M. Ohnishi, Y. Hisamatsu and T. Ishii, *Environ. Int.*, 9 (1983) 335.
- [29] K. El-Bayoumy, M. O'Donnell, S.S. Hecht and D. Hoffmann, *Carcinogenesis*, 6 (1985) 505.
- [30] R. Williams, C. Sparacino, B. Petersen, J. Baumgarner, R.H. Jungers and J. Lewtas, *Intern. J. Environ. Anal. Chem.*, 26 (1986) 27.
- [31] Y. Ishinishi, T. Kinouchi, H. Tsutsui, M. Uejima, K. Nishifuji, in Y. Hayashi, M. Nagao, T. Sugimura, S. Takayama, L. Tomatis, L.W. Wattenberg and G.N. Wogan (Editors), *Diet, nutrition and cancer*, Japan Scientific Societies Press, Tokyo, 1986, p. 107.
- [32] B.K. Larsson, H. Pyysalo and M. Sauri, *Z. Lebensm. Unters. Forsch.*, 187 (1988) 546.
- [33] J. Arey, B. Zielinska, R. Atkinson, A.M. Winer, T. Ramdahl and J.N. Pitts Jr., *Atmos. Environ.*, 20 (1986) 2339–2345.
- [34] B. Zielinska, J. Arey and R. Atkinson, in P.C. Howard, S.S. Hecht and F.A. Beland (Editors), *Nitroarenes*, Plenum Press, New York, 1990, p. 73.
- [35] X.B. Xu, J.P. Nachtman, S.M. Rappaport, E.T. Wei, S. Lewis and A.L. Burlingame, *J. Appl. Toxicol.*, 3 (1982) 196.
- [36] T.R. Henderson, R.E. Royer, C.R. Clark, T.M. Harvey and D.F. Hunt, *J. Appl. Toxicol.*, 2 (1982) 231.
- [37] M.C. Paputa-Peck, R.S. Marano, D. Schuetzle, T.L. Riley, C.V. Hampton, T.J. Prater, L.M. Skewes, T.E. Jensen, P.H. Ruehle, L.C. Bosch and W.P. Duncan, *Anal. Chem.*, 55 (1983) 1946.
- [38] R.M. Campbell and M.L. Lee, *Anal. Chem.*, 56 (1984) 1026.
- [39] H.-J. Moriske, I. Block, H. Schleibinger and H. Rüden, *Zentralbl. Bakteriol. Mikrobiol. Hyg. Abt. 1 Orig. B.*, 181 (1985) 240.
- [40] H. Schleibinger C. Leberl and H. Rüden, *Zentralbl. Bakteriol. Mikrobiol. Hyg.*, 187 (1988) 44.
- [41] T. Sato, K. Kato, Y. Ose, H. Nagase and T. Ishikawa, *Mutat. Res.*, 157 (1985) 135.
- [42] N. Saitoh, Y. Wada, A. Koizumi and S. Kamiyama, *Jpn. J. Hyg.*, 45 (1990) 873.
- [43] W.A. MacCrehan and W.E. May, in M. Cooke and A.J. Dennis (Editors), *Polynuclear Aromatic Hydrocarbons*, Battelle, Columbus, OH, 1985, pp. 857.
- [44] W.A. MacCrehan, W.E. May, S.D. Yang and B.A. Benner Jr., *Anal. Chem.*, 60 (1988) 194.
- [45] M. Bolgar, J.A. Hubball, J.T. Cunningham and S.R. Smith, in M. Cooke and A. Dennis (Editors), *Polycyclic Aromatic Hydrocarbons*, Battelle Press, Columbus, OH, 1985 p. 199.
- [46] D.L. LaCourse and T.E. Jensen, *Anal. Chem.*, 58 (1986) 1894.
- [47] R.C. Garner, C.A. Stanton, C.N. Martin, F.L. Chow, D. Hubner and R. Herrmann, *Environ. Mutagenesis*, 8 (1986) 109.
- [48] D. Schuetzle, T.E. Jensen, J.C. Ball, *Environ. Int.*, 11 (1985) 169.
- [49] W.A. Korfmacher, P.P. Fu and R.K. Mitchum, in M. Cooke and A. Dennis (Editors), *Polycyclic Aromatic Hydrocarbons*, Battelle Press, Columbus, OH, 1985, p. 749.
- [50] W.A. Korfmacher, L.G. Rushing, J. Arey, B. Zielinska and J.N. Pitts Jr., *J. High Resolut. Chromatogr. Chromatogr. Comm.*, 10 (1987) 641.
- [51] W.A. Korfmacher, L.G. Rushing, R.J. Engelbach, J.P. Freeman, Z. Djuric, E.K. Fifer and F.A. Beland, *J. High Resolut. Chromatogr. Chromatogr. Comm.*, 10 (1987) 43.
- [52] R.J. Engelbach, W.A. Korfmacher and L.G. Rushing, *J. High Resolut. Chromatogr. Chromatogr. Comm.*, 11 (1988) 661.

- [53] W.A. Kormacher, Z. Djuric, E.K. Fifer and F.A. Beland, *Spectros. Int.*, 6 (1988) 1.
- [54] W.E. Bechtold, J.S. Dutcher, A.L. Brooks and T.R. Henderson, *J. Appl. Toxicol.*, 5 (1985) 295.
- [55] Y. Hisamatsu, T. Nishimura, K. Tanabe and H. Matsushita, *Mutat. Res.*, 172 (1986) 19.
- [56] A. Robbat and T.Y. Liu, *J. Chromatogr.*, 513 (1990) 117.
- [57] T.-Y. Liu and A. Robbat, *J. Chromatogr.*, 539 (1991) 1.
- [58] H.-J. Moriske, I. Block and H. Rden, *Forum Stde Hygiene*, 35 (1984) 113.
- [59] J.A. Sweetman, F.W. Karasek and D. Schuetzle, *J. Chromatogr.*, 247 (1982) 245.
- [60] D.W. Later and M.L. Lee, *Anal. Chem.*, 54 (1982) 117
- [61] M.S. Bryant, P.L. Skipper, S.R. Tannenbaum and M. Maclure, *Cancer Res.*, 47 (1987) 602.
- [62] W.G. Stillwell, M.S. Bryant and J.S. Wishnok, *Biomed. Environ. Mass Spectr.*, 14 (1987) 221.
- [63] P. Del Santo, G. Moneti, M. Salvadori, C. Saltutti, A. Delle Rose and P. Dolara, *Cancer Lett. (Shannon Irel.)*, 60 (1991) 245.
- [64] K. Hayakawa, N. Terai, K. Suzuki, P.G. Dinning, M. Yamada, M. Miyazaki, *Biomed. Chromatogr.*, 7 (1993) 262.
- [65] L.M. Litvinenko and A.P. Grekov, *Zhur Obschei Khim.*, 27 (1957) 234.
- [66] E. Vrins and P. Hofschreuder, *J. Aerosol Sci.*, 14 (1983) 318.
- [67] O.P. Van Pruissen, J.P.A. Neeft, M.M. Makkee and J.A. Moulijn, *Proc. 9th World Clean Air Congress, August 30–September 4, 1992, Montreal, Quebec*, Air and Waste Management Association, Pittsburgh, PA, 1992, IU-18F.10.
- [68] H. Lee, S.M. Law and S.T. Lin, *Toxicol. Lett.*, 58 (1991) 59.
- [69] J. Jger, *J. Chromatogr.*, 152 (1978) 575.
- [70] N. Yamaki, T. Kohnno, S. Ishiwata, in N. Ishinishi, A. Koizumi, R.O. McClellan, W. Stber (Editors), *Carcinogenic effects of diesel engine exhaust*, Elsevier, Amsterdam, 1986, p. 17.
- [71] P.T. Williams, M.K. Abbass, L.P. Tam, G.E. Andrews, K.L. Ng and K.D. Bartle, *Society of Automotive Engineers Technical Paper Series*, no. 880351 Society of Automotive Engineers, Warrendale, PA, 1988.
- [72] R.L. Bradow, in J. Lewtas (Editor), *Carcinogenic and mutagenic effects of diesel engine exhaust*, Elsevier, Amsterdam, 1982, p. 33.
- [73] P.T.J. Scheepers, D.D. Velders, P. Fijneman, M. van Kerkhoven, J. Noordhoek and R.P. Bos, in preparation.



ELSEVIER

Journal of Chromatography A, 677 (1994) 123–132

JOURNAL OF
CHROMATOGRAPHY A

Automated in situ gas chromatographic–mass spectrometric analysis of ppt level volatile organic trace gases using multistage solid-adsorbent trapping

Detlev Helmig*, James P. Greenberg

National Center for Atmospheric Research, Boulder, CO 80307-3000, USA

First received 31 January 1994; revised manuscript received 28 March 1994

Abstract

A fully automated sampling/injection system for the gas chromatographic–mass spectrometric (GC–MS) analysis of volatile organic compounds at tropospheric background levels was developed. Organic trace gases from air samples up to 100 l were trapped in temperature-controlled solid-adsorbent traps. The instrument utilized a one stage sampling/desorption inlet system designed as a closed device that did not require any replumbing steps between sampling and analysis. For analysis, the adsorbent trap was thermally desorbed and backflushed onto the chromatographic column where organic trace gases were directly cryofocused. Adsorbents tested were Carbotrap, Carbotrap C, Carbosieve S III, Tenax TA, Tenax GR and multistage combinations of these adsorbents. Interferences from blanks and adsorbent artifacts were minimized by backflushing the adsorbent trap, switching valve and transfer line between sampling sequences at temperatures above the levels used during trapping and sample transfer. The high sample volumes that could be concentrated and the low background levels allowed structural identification in GC–MS (electron impact ionization scan mode) at minimum levels of ca. 100 pg per peak (ca. 10^{-12} mol) equivalent to atmospheric concentrations at the lower parts per trillion (v/v) level. The volatility range of organic compounds that could be identified was approximately from pentane to pentadecane. The system was completely computer controlled and could be operated continuously and unattended around the clock for in situ analysis. The instrument was successfully deployed at the Mauna Loa Observatory, Hawaii, USA in July and August 1992.

1. Introduction

Volatile organic trace compounds (VOCs) in the atmosphere play an important role in the formation and transformation of atmospheric oxidants [1–3]. At remote background sites, such as the Mauna Loa Observatory (MLO), Hawaii, USA (elevation 3.4 km), air characteristic of the

free troposphere is often present [4] and the influence of recent anthropogenic emissions is low. Consequently the atmosphere at such a site may be representative of large regions of the remote marine troposphere. The identification and quantification of the VOCs present may provide valuable information about chemical transformations and atmospheric reaction pathways.

For the structural identification of individual

* Corresponding author.

atmospheric VOCs, several analytical problems have to be considered: sample collection and storage, separation of VOCs of interest, and detection and identification. Ambient air samples can be collected into evacuated stainless-steel canisters (either by opening them to atmospheric pressure or by pressurizing air to a few atmospheres using metal bellows pumps) or by sampling into bags made of PTFE materials [5]. Another approach is the use of solid-adsorbent traps [6,7] or the cryogenic freezeout of the analytes onto inert surfaces [8–11]. Cryogenic freezeout techniques allow the sampling of high volumes but have the disadvantage of concentrating water and carbon dioxide concurrent with the organic trace gases, which can cause interferences in the gas chromatographic (GC) analysis.

Solid adsorbent materials are designed to specifically trap organic vapors from atmospheric samples without enriching water and carbon dioxide. Among solid-adsorbent sampling techniques described, multi-adsorbent traps recently have received increased attention because the advantages of single adsorbents can be combined in one system and the range of compounds to be collected and desorbed is widened [12–18].

For qualitative analysis with individual compound identification, canisters, bags or adsorbent traps are usually transported to the laboratory for GC–mass spectrometric (MS) analysis. One disadvantage of most of the methods listed above is the time delay between the sampling at the site and the analysis. Adjustments in the sampling strategy during field experiments are difficult because of the delay and the physical separation which can occur between the sampling and the analytical site. Also, typical canister sizes allow the sampling of only a few liters of air which poses a limitation for achievable detection limits: For structural identification of VOCs in the electron impact ionization (EI) scan mode, typical MS instruments need compound amounts in the low nanogram range per peak. This is equivalent to a sample volume of approximately 10 to 100 l for atmospheric samples in the lower parts per trillion (ppt; throughout, ppt refers to a v/v ratio) range. Other disadvantages of all of these techniques are the possible instability of certain

analytes in canisters or in traps and possible contamination during transport, storage, handling and the plumbing steps required for capping the containers and reattaching to the analytical device.

A solid adsorption sampling method for in situ GC–MS analysis was recently described by Yokouchi et al. [19] and applied for quantitative measurements of organic trace gases at tropospheric background levels. Sample volumes of 200 ml were concentrated on Tenax TA and analyzed by thermal desorption GC–MS in the selected ion monitoring (SIM) mode. With the increased MS sensitivity in the SIM mode, selected organic compounds could be measured down to the low ppt level, but no identifications of unknown species by scan analysis were possible.

To overcome the listed drawbacks we designed a closed solid adsorbent sampling system with thermal desorption injection for automated, unattended on-site GC–MS analysis. All stages of the analysis, including sample loading and injection, as well as the temperature controlling and ramping of individual zones were controlled by a personal computer system. Organic trace gases were separated from air on temperature-controlled solid-adsorbent traps and then directly transferred by thermal desorption onto the chromatographic system. The system allows the sampling of volumes up to 100 l. This provides sufficient detection limits to achieve MS identifications of unknown VOCs in the EI scan mode at low ppt levels. The instrument was successfully employed during the second field campaign of the MLO Photochemical Experiment.

2. Experimental

A diagram of the analytical system is shown in Fig. 1. Ambient air was drawn through a sampling line (6.4 mm O.D. PTFE-lined stainless-steel tubing; Alltech, Deerfield, IL, USA) at a flow-rate of about 5 l min^{-1} from a sampling port located 9 m above ground. A PTFE-coated glass fiber filter (Pallflex T60A20, Putnam, CT, USA) was used as an inlet filter to exclude particulates from air sampled. The sampling line was wrap-

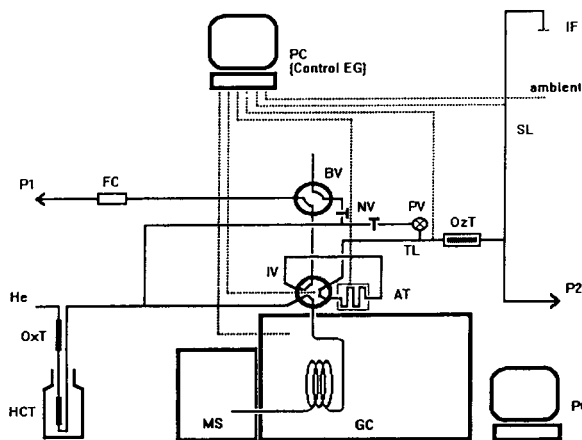


Fig. 1. Plumbing diagram of the automated GC-MS system. AT = Adsorbent trap; BV = backflush/sampling valve (4-port, 0.25 in., Valco, Houston, TX, USA); Control EG = CONTROL EG software; FC = mass flow controller; GC = Hewlett-Packard 5980 gas chromatograph; HCT = hydrocarbon trap (SGE, Austin, TX, USA); He = helium carrier gas and purge gas; IF = inlet filter; IV = injection valve (6-port, 0.125 in., Valco); MS = Hewlett-Packard mass-selective detector 5971A; NV = needle valve; OxT = oxygen trap (Baxter, McGaw Park, IL, USA); OzT = ozone trap; P1 = sampling pump; P2 = sampling line pump; PC = personal computer; PV = purge valve (0.25 in. stainless-steel bellows shut-off valve, NUPRO, Willoughby, OH, USA); SL = sampling line; TL = transfer line. Monitored temperature zones are indicated by dotted lines. Temperature controlled zones were the adsorbent trap, injection valve and transfer line.

ped with 22-gauge (i.e., cross-section 0.35 mm^2) PTFE insulated wire, ceramic fiber insulation and aluminum foil and heated to 15°C above ambient temperature by passing a low-voltage high current (approximately 10 V/5 A) through the PTFE wire. The heating of the sampling and transfer line reduced possible sample carryover for more sticky compounds.

Part of the main flow was directed through an oxidant scrubber and a 30 cm long transfer line (same material as the sampling-line). The oxidant scrubber was used to selectively remove ozone in order to reduce possible artifact formation from reactions occurring on the adsorbent bed during sampling. We used potassium iodide ($5 \text{ cm} \times 6.4 \text{ mm}$ O.D. PTFE-lined stainless-steel tubing filled with KI-coated glass wool [20]) in some of our experiments.

The sample air was then passed through the sampling trap, which was filled either with a single solid adsorbent or a combination of different solid adsorbents. Flow-rates through the adsorbent trap depended on the dimensions of the trap and the adsorbent used. Coarse adsorbent grain sizes (20–40 mesh = $420\text{--}840 \mu\text{m}$) were used to allow high sampling flow-rates. Adsorbents used in this study were Tenax TA porous polymer (20–35 mesh = $500\text{--}840 \mu\text{m}$, Alltech), Tenax GR (20–35 mesh, Alltech), Carbotrap (20–40 mesh, Supelco, Bellefonte, PA, USA), Carbotrap C (20–40 mesh, Supelco) and Carbosieve S III (60–80 mesh = $180\text{--}250 \mu\text{m}$, Supelco). The hydrophobic properties of these selected adsorbents prevent the trapping of excess water while they allow the trapping and thermal release of organic gases over a wide volatility range. The capacity of solid adsorbents increases with decreasing temperature. Therefore, cooling the traps during sampling increases the sampling efficiency, particularly for lighter compounds. The lowest possible temperature is limited by the dewpoint of the sampled air, because the trapping of water interferes with the following GC analysis. The sampling-trap temperatures selected were determined empirically and controlled at 5°C below ambient temperature for Tenax GR and Tenax TA. The charcoal-based adsorbents showed a somewhat higher affinity for water and had to be controlled at about 5°C above ambient temperature. Further characteristics of each of the individual adsorbents used in our experiments have extensively been described in the literature [12,16,21–26] and will not be further detailed here. Adsorbent traps were made from $45 \text{ cm} \times 3.4 \text{ mm}$ O.D. and $30 \text{ cm} \times 6.4 \text{ mm}$ O.D. tubing, coiled into a spiral and tightly inserted into a low-mass brass cylinder (7 cm length \times 3.5 cm diameter, 0.5 mm wall thickness). The adsorbent was held in place by small silanized glass wool plugs on either side. Typical maximum flow-rates were in the range of 200 to 400 ml min^{-1} for the 3.2 mm O.D. tubing traps and about 400 to 800 ml min^{-1} for the 6.4 mm O.D. tubing traps. A mass-flow controller downstream of the adsorbent trap insured that the flow through the trap was maintained con-

stant. The flow-rates used to sample ambient air were set to about 80% of the maximum possible flow-rate.

Heating of the adsorbent trap was provided by a 240 W heating wire (Watlow Electric, St. Louis, MO, USA) soldered onto the outside of the brass cylinder. Cryogen (liquid nitrogen) was sprayed into the cylinder through a nozzle made of 0.25 in. (1 in. = 2.54 cm) stainless-steel tubing, in which approximately 40 holes (1 mm diameter) were drilled. A throttle valve was incorporated into the cryogen line to adjust the cryogen flow. The power of the trap heater was regulated by an adjustable resistor. This system allowed the trap temperature to be controlled within a range of about $\pm 2^\circ\text{C}$ at both the cooled and heated setpoints. The controllable temperature range for the sampling trap was from -175 to 325°C .

A purge valve in front of the adsorbent trap allowed purging the trap with helium. The total helium flow was 0.5 l min^{-1} higher than the sampling flow-rate and consequently helium would flow in both directions through the transfer line with the excess flow being backflushed into the sampling line. The helium purge was initiated at the end of the sampling step to remove any oxygen remaining from air sampled prior to the thermal desorption procedure. A backflush valve downstream of the injection valve allowed the backflushing of the entire adsorption system and the transfer line between sampling periods. All tubing and fitting materials in contact with the sample were made either from PTFE, PTFE-lined or -coated stainless-steel or fused-silica-coated stainless steel (Restek, Bellefonte, PA, USA). For additional purification, the carrier, backflush and purge gases (He , 99.9995%) were passed through an oxidant trap and then through a hydrocarbon trap, which was immersed in liquid nitrogen. A Hewlett-Packard 5980 GC system and an HP 5971A mass-selective detector were used for GC separation and detection.

The enrichment system was fully automated and computer controlled by an IBM AT personal computer which was equipped with an internal analog input/digital output board (part CIO-DAS08, ComputerBoards, Mansfield, MA,

USA) and an external analog multiplexer (CIO-EXP16) and an external relay board (SSR-Rack24). It was operated by CONTROL EG software (Quinn-Curtis, Needham, MA, USA). A scheme showing the computer-controlled zones and devices is also given in Fig. 1. A total of up to 22 analog input channels are available, six of which were used for temperature measurements. Monitored temperature zones included the ambient air inlet, sample adsorbent trap, GC oven, injection valve, transfer line and the main sampling line. Ten of the possible 24 output channels were used for the control of the backflush valve, injection valve, purge valve, injection valve heater, injection valve cooling (fan), transfer line heater, main sampling line heater, trap heater, trap cryogen valve and remote GC-MS start. Temperature-programmed zones included the adsorbent trap, transfer line and injection valve. The transfer line and injection valve were kept at room temperature during sampling and heated during sample transfer and in the backflush mode to reduce sample carryover.

The sequence and operating parameters of a typical sample and analysis cycle is shown in Table 1. It consists of different stages for sampling preparation, equilibration time, sampling, injection, trap purge and GC analysis-trap backflush. During sampling, the trap temperature was adjusted with respect to ambient temperature. The trap setpoint was recalculated and reset every 1 min using ambient temperature as an input value. For thermal desorption, the gas sampling valve, which contained the sample trap instead of a sample loop, was switched into the inject position to backflush the contents of the trap onto the analytical column. Typically, the trap was heated at a controlled rate of $25^\circ\text{C min}^{-1}$ to allow elution of lower boiling compounds at lower temperatures. Concurrent with the heating of the trap, the injection valve temperature was raised from ambient to 50°C . This strategy allows early eluting compounds to pass through the injection valve while it was at lower temperature, therefore minimizing thermal cracking artifacts. The GC-MS start signal was sent about 6 min before the thermal desorption start to allow cooling of the GC oven (negative

Table 1
Analysis sequence with typical parameters used during the field study (2 h sampling time)

	Analysis step						
	Sampling preparation	Sampling	Analysis preparation	Trap purge	Sample transfer	Analysis	Conditioning
Sampling valve	Sampling/backflush	Sampling/backflush	Sampling/backflush	Sampling/backflush	Injection	Sampling/backflush	Sampling/backflush
Backflush valve	Backflush	Sampling	Sampling	Sampling	Backflush	Backflush	Backflush
Purge valve	Closed	Closed	Closed	Open	Closed	Closed	Closed
Adsorption trap temperature	↓ Ambient ± x ^a	Ambient ± x	Ambient ± x	Ambient ± x	↑ Maximum desorption temperature at 20°C min ⁻¹	Maximum desorption temperature + 25°C	Maximum desorption temperature + 25°C
Injection valve temperature	↓ Ambient	Ambient	Ambient	Ambient	↑ 50°C	50°C	50°C
Transfer line temperature	↓ 25°C	25°C	25°C	25°C	↑ 75°C	75°C	75°C
GC oven temperature	150°C	150°C	↓ -60°C	-60°C	-60°C	↑ 200°C at 6°C min ⁻¹	150°C
Typical time	10 min + 3 min equilibration	115 min	5 min	0.5 min	10 min	45 min	75 min

↓ = Down to; ↑ = up to.

^a The adsorbent trap sampling temperature was kept at a constant offset to ambient temperature (see description in text).

temperature ramping to -60°C) from its standby temperature of 150°C. During the thermal desorption the GC oven was kept at low temperature to cryofocus desorbed VOCs onto the column head. The trap was kept at the maximum desorption temperature (typically 275°C) for 5 min, after which the injection valve was switched back to the backflush position and the temperature program was started.

3. Results and discussion

The enrichment system was employed during a six-week field experiment at MLO in July and August 1992. Atmospheric measurements at the observatory site during nighttime downslope flow are usually characteristic of maritime free tropospheric air and show very low concentrations of VOCs [27]. The analysis of a 22.5-l sample

collected with the GC-MS system is shown in Fig. 2. This sample was collected with a KI ozone trap and using a multiadsorbent trap containing 0.7 ml Carbotrap C, 1.2 ml Carbotrap and 0.3 ml Carbosieve S III. These adsorbents were arranged in order of increasing sampling capacity, with the weakest adsorbent (Carbotrap C) on the trap inlet side. GC separation was performed on a 60 m × 0.32 mm DB-1 (0.25 μm film, J & W) column. The oven temperature was held at -60°C for 10 min during desorption and then raised to 200°C at a rate of 6°C min⁻¹ and then held at 200°C for 5 min. Peak identifications for the illustrated chromatogram are given in the figure caption. The retention time values given represent the time elapsed from the GC-MS start signal and include the time needed for oven cooling and thermal desorption. For comparison the chromatogram of a 22.5-l blank sample is also included in Fig. 2 (plotted at 10 × the

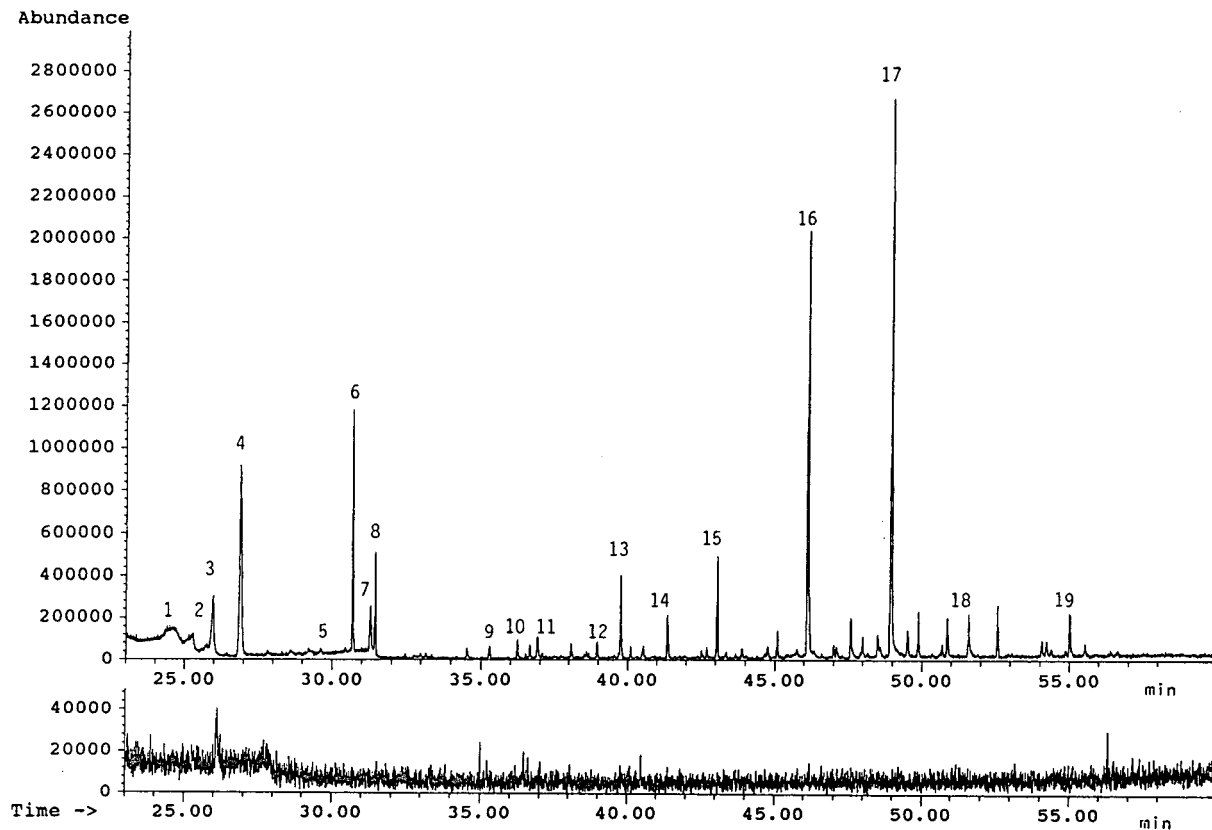


Fig. 2. GC-MS chromatogram of a 22.5-l (normalized to 20°C and 1013 mbar) ambient air sample collected at Mauna Loa Observatory from 14 h 17 min to 15 h 24 min on August 1, 1992. Major peaks: 1 = trichlorofluoromethane (F-11); 2 = acetone; 3 = dichloroethene; 4 = 1,1,2-trichloro-1,2,2-trifluoroethane (F-113); 5 = chloroform; 6 = 1,1,1-trichloroethane; 7 = benzene; 8 = tetrachloromethane; 9 = toluene; 10 = hexanal; 11 = tetrachloroethene; 12 = *m/p*-xylene; 13 = heptanal; 14 = benzaldehyde; 15 = octanal; 16 = nonanal; 17 = decanal; 18 = undecanal; 19 = 6,10-dimethyl-5,9-undecadien-2-one. The trace below the sample chromatogram shows the analysis of a 22.5-l liquid nitrogen blowoff sample (plotted at 10-fold amplification).

amplification of the sample chromatogram). The blank sample was simulated by collecting the blowoff of a liquid nitrogen cryogen dewar. The cryogen blowoff was cleaner than available zero air and was therefore also used in addition to zero air as a test gas for blank experiments. The blank sample was collected through the inlet stack and analyzed under the same conditions as the sample.

From the comparison of concurrent quantitative measurements of selected hydrocarbons by GC-flame ionization detection (FID) [28] and halogenated compounds by GC-electron-capture detection (ECD) [29,30] made at the same site, the achievable detection limit can be estimated.

Measurements made near the time of the sample collected in the chromatogram illustrated in Fig. 2 gave ambient air concentrations of approximately 274 ppt trichlorofluoromethane (F-11), 9.7 ppt chloroform, 146 ppt 1,1,1-trichloroethane, 8.3 ppt benzene, 105 ppt tetrachloromethane, 1.8 ppt toluene and 2.9 ppt tetrachloroethene. Assuming no compound loss during sampling, thermal desorption, sample transfer and chromatographic separation, these concentrations at the collected sample volume of 22.5 l for the GC-MS sample correspond to compound amounts in this sample of approximately 38 ng ($270 \cdot 10^{-12}$ mol) F-11, 1.2 ng ($9.7 \cdot 10^{-12}$ mol) chloroform, 20 ng ($150 \cdot 10^{-12}$ mol)

1,1,1-trichloroethane, 0.65 ng ($8.3 \cdot 10^{-12}$ mol) benzene, 16 ng ($110 \cdot 10^{-12}$ mol) tetrachloromethane, 0.17 ng ($1.8 \cdot 10^{-12}$ mol) toluene and 0.48 ng ($2.9 \cdot 10^{-12}$ mol) tetrachloroethene. The mass spectra of all listed compounds showed sufficient signal-to-noise ratios for peak identification in the scan mode. Fig. 3 shows as an example the mass spectrum of the toluene peak at a concentration of about 1.8 ppt from the sample chromatogram. The computerized library search for this spectrum gave toluene as the best fit with an agreement quality of 78%. From this comparison it can be concluded that this enrichment/injection GC-MS system allows MS identifications of certain VOCs down to ca. 10^{-1}

ng or ca. $1 \cdot 10^{-12}$ mol. For sample sizes of up to 100 l this is equivalent to ambient concentrations of sub-ppt levels. In practice, however, detection limits of individual compounds depend on a number of parameters including trapping efficiency, recovery during thermal desorption and sample transfer and possible compound losses through decomposition. Also, with our instrument, which did not have flow-controlled carrier gas, the MS sensitivity changed during the temperature programmed chromatographic run because of the decrease in source pressure at higher oven temperatures. Further important parameters affecting the sensitivity are the ionization yield and the fragmentation pattern.

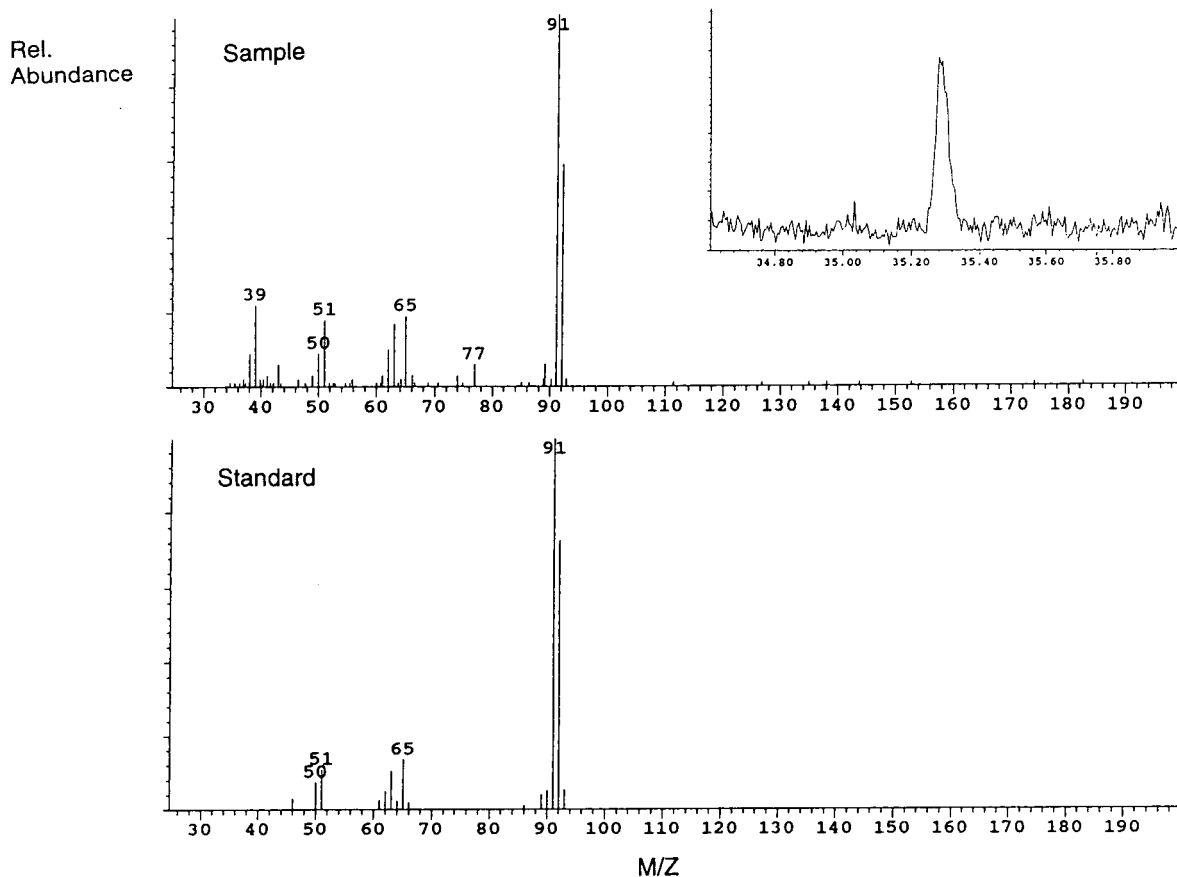


Fig. 3. Mass spectrum obtained from the toluene peak at an ambient concentration of ca. 1.8 ppt (peak number 9 in Fig. 2). The upper spectrum is the sample spectrum and the average of 3 scans around the peak maximum after background subtraction. The insert in the upper spectrum is an enlargement of the total ion current peak. For comparison the toluene standard spectrum from the National Bureau of Standards Library is plotted underneath. Signals below m/z 45 are not included in the standard spectrum.

Chlorofluorocarbons (CFCs), for example, show very distinct mass spectra and can generally be identified with higher sensitivity than hydrocarbons such as alkanes or alkenes. Depending on the scan range (usually above m/z 32 or 44 to reduce signals from air leaks) compounds with low mass fragmentation signals, such as methanol, acetaldehyde or acetone cannot be identified as sensitively because of the lack of or low intensity of molecular ions and fragmentation signals above the lower scan threshold.

The experimental design successfully avoided several common sampling and chromatographic problems. System contaminants were efficiently removed and sample carryover from previous runs was minimized by having the sample trap and transfer line backflushed between samples at higher temperatures than during sampling and desorption. The sample had to pass through only one switching valve, which reduced potential sources of contamination and kept sample loss to a minimum. Oxidant traps reduced artifacts, which can be formed during sampling by reactions with prior adsorbed compounds or with the solid adsorbent itself. KI traps used for ozone removal have been shown to be efficient O_3 scrubber. We found evidence for possible artifact formation (alkyl iodides) from the use of these traps during some of our experiments. These results and alternative ozone trap systems will be discussed elsewhere [31].

About 60 organic trace gases were identified in the course of this experiment using a variety of different solid adsorbents and sampling conditions [32]. The range of compounds that could be analyzed depended on the adsorbents used and the chromatographic conditions. The earliest eluting compounds identified from all adsorbents were F-11, acetone and isoprene, with GC retention indices near 500 (DB-1). The heaviest compounds identified were in the elution range of pentadecane (retention index 1500). The charcoal-based adsorbent traps used showed significantly higher trapping efficiency for lighter compounds than Tenax TA and Tenax GR (elution range approximately from acetone to methylchloroform). The breakthrough volumes of compounds in this elution range are too low to

allow quantitative trapping on Tenax at the temperatures and sample volumes used. The widest range of compounds could be analyzed using the multi-adsorbent trap system described above.

The lower compound range is also limited by the parameters used during thermal desorption and sample transfer: the relatively slow heating rate during the thermal desorption causes individual species to be eluted onto the column over a period of several minutes. At -60°C oven temperature compounds more volatile than F-11 are, therefore, not cryofocused as a sharp band on the GC column used in this study. Peak broadening, as observed for the earliest eluting peaks in Fig. 2, reflects this effect. In order to widen the compound range for lighter compounds a stronger column phase or a second stage trap, kept at lower temperatures until flash heated, is required. The inclusion of a rapidly heated second stage, however, has the potential of introducing blanks and artifacts through compound decomposition during the fast heatup and from contamination by the additional components. We are currently developing a two-stage injection system, where the sample is transferred from the solid adsorbent trap to a cryogenically cooled, low-volume freezeout trap (deactivated 0.53 mm I.D. fused-silica tubing), which then is rapidly heated for sample injection onto the GC column. We have already found that, using the multi-adsorbent trap system, compounds down to the range of propane can be analyzed with this arrangement.

Among the tested solid adsorbents, Carbotrap, Carbotrap C and Carbosieve S III were found to be the most resistant to degradation artifacts from the adsorbent itself. Signals identified in blank runs were from hexamethyltrisiloxane (column bleed) and occasionally small amounts of F-11. The Tenax TA/GR adsorbents showed some significant artifact formation. Major artifacts identified here were benzaldehyde, acetophenone, phenol and benzonitrile. Also, small amounts of *n*-aldehydes (C_9 and C_{10}) and occasionally compounds with signals at m/z 220/205 (tentatively identified as alkylated phenols) were identified in zero air

blank runs, but it could not be determined if these compounds were residual contaminants in the zero air or if they were formed on the adsorbent. The identified Tenax artifacts are consistent with previous reports in the literature. These reports indicate that Tenax is prone to chemical degradation and aging effects [6,33–38].

The sample chromatogram shows relatively high levels of *n*-aldehydes. A series of experiments were performed to confirm the compound identity (determination of retention indices on three different column phases and analysis of *n*-aldehyde standards) and also to investigate whether or not these *n*-aldehydes were system contaminants (blank runs with liquid nitrogen blowoff and purified zero air). It has previously been shown that *n*-aldehydes can be formed artificially on Tenax, in particular during the sampling of ozone-enriched air [35,36]. However, we found *n*-aldehydes in approximately equal relative abundance and distribution from all adsorbent systems we tested. Furthermore, we did not find a substantial change in the pattern during removal of the ozone trap. The GC–MS measurements were also consistent with parallel measurements on a separate GC–FID instrument. On the GC–FID instrument sample preconcentration was performed by cryogenic trapping on glass beads and the same aldehyde species and the same pattern and relative abundances were observed [28]. From these observations we conclude that it is unlikely that the aldehydes observed were adsorbent or system contaminants. The measurements made here are also consistent with reports in the literature, where the same *n*-aldehyde species and similar relative abundances were observed [39,40]. We are planning more future research on the occurrence of the *n*-aldehydes and will detail this discussion more extensively in a following publication.

The experiments performed at MLO were solely of a qualitative nature and compound quantifications were performed with two GC–FID systems operated at the same site [28]. No quantitative GC–MS measurements were performed due to the lack of low-concentration

calibration standards for most of the identified species. Among the different trapping systems tested, the multi-adsorbent trap containing Carbotrap C, Carbotrap and Carbosieve S III gave the best results because of the wide compound range that could be trapped and analyzed and the low levels of observed blanks and artifacts.

Acknowledgement

We thank E. Atlas (NCAR) and Th. Thompson and J. Elkins (NOAA-CMDL) for providing quantitative data of the CFC analysis. We also thank P. Zimmerman for his support in the development and deployment of the instrument and, also, W. Pollock and the staff of the NOAA-CMDL Mauna Loa Observatory for valuable help during the field campaign. The National Center for Atmospheric Research is sponsored by the National Science Foundation.

References

- [1] A.M. Hough and R.G. Derwent, *Atmos. Environ.*, 21 (1987) 2015–2033.
- [2] A. Lopez, M.O. Barthomeuf and M.L. Huertas, *Atmos. Environ.*, 23 (1989) 1465–1478.
- [3] A.R. MacKenzie, R.M. Harrison, I. Colbeck and C.N. Hewitt, *Atmos. Environ.*, 25A (1991) 351–359.
- [4] B.A. Ridley and E. Robinson, *J. Geophys. Res.*, 97 (1992) 10 285–10 290.
- ✓ [5] J. Rudolph, K.P. Müller and R. Koppmann, *Anal. Chim. Acta*, 236 (1990) 197–211.
- ✓ [6] J.E. Bunch and E.D. Pellizzari, *J. Chromatogr.*, 186 (1979) 811–829.
- ✓ [7] A. Fabbri, G. Crescentini, F. Mangani, A.R. Mastrogiacomo and F. Bruner, *Chromatographia*, 23 (1987) 856–860.
- [8] R.A. Rasmussen, D.E. Harsch, P.H. Sweany, J.P. Krasnec and D.R. Cronn, *J. Air Pollut. Control Assoc.*, 27 (1977) 579–581.
- [9] S.O. Farwell, S.J. Gluck, W.L. Bamesberger, T.M. Schutte and D.F. Adams, *Anal. Chem.*, 51 (1979) 609–615.
- [10] W.A. McClenny, J.D. Pleil, M.W. Holdren and R.N. Smith, *Anal. Chem.*, 56 (1984) 2947–2951.
- [11] A. Hagman and S. Jacobsson, *J. Chromatogr.*, 448 (1988) 117–126.

- [12] L.D. Ogle, R.C. Hall, W.L. Crow, A.E. Jones and J.P. Gise, in L.H. Keith (Editor), *Identification and Analysis of Organic Pollutants in Air*, Butterworth, Boston, MA, 1984, pp. 171–182.
- [13] R.W. Bishop and R.J. Valis, *J. Chromatogr. Sci.*, 28 (1990) 589–593.
- [14] L. Löfgren, P.M. Berglung, R. Nordlinder, G. Petersson and O. Ramnäs, *Int. J. Environ. Anal. Chem.*, 45 (1991) 39–44.
- [15] A.J. Pollack, M.W. Holdren and W.A. McClenny, *J. Air Waste Manag. Assoc.*, 41 (1991) 1213–1217.
- [16] D.L. Heavner, M.W. Ogden and P.R. Nelson, *Environ. Sci. Technol.*, 26 (1992) 1737–1746.
- [17] P. Ciccio, A. Cecinato, E. Brancaleoni, M. Frattoni and A. Liberti, *J. High Resolut. Chromatogr.*, 15 (1992) 75–84.
- [18] Y.-Z. Tang, Q. Tran, Ph. Fellin, W.K. Cheng and I. Drummond, *Anal. Chem.*, 65 (1993) 1932–1935.
- [19] Y. Yokouchi, H. Bandow and H. Akimoto, *J. Chromatogr.*, 642 (1993) 401–407.
- [20] J. Greenberg, B. Lee, D. Helmig and P. Zimmerman, *J. Chromatogr.*, in press.
- [21] K. Figge, W. Rabel and A. Wieck, *Z. Anal. Chem.*, 327 (1987) 261–278.
- [22] H. Rothweiler, P.A. Wäger and C. Schlatter, *Atmos. Environ.*, 25B (1991) 231–235.
- [23] M.L. Riba, B. Clement, M. Haziza and L. Torres, *Toxicol. Environ. Chem.*, 31–32 (1991) 235–240.
- [24] J.F. Pankow, *Anal. Chem.*, 60 (1988) 950–958.
- [25] J.F. Pankow, *J. Chromatogr.*, 547 (1991) 488–493.
- [26] X.L. Cao and C.N. Hewitt, *Atmos. Environ.*, 27A (1993) 1865–1872.
- [27] J.P. Greenberg, P.R. Zimmerman, W.F. Pollock, R.A. Lueb and L.E. Heidt, *J. Geophys. Res.*, 97 (1992) 10 395–10 413.
- [28] J. Greenberg, D. Helmig and P. Zimmerman, *J. Geophys. Res.*, (1994) in preparation.
- [29] E. Atlas, personal communication, 1993.
- [30] Th. Thompson and J. Elkins, personal communication, 1994.
- [31] D. Helmig and J. Greenberg, *J. High Resolut. Chromatogr.*, (1994) in preparation.
- [32] D. Helmig, W. Pollock, J. Greenberg and P. Zimmerman, *J. Geophys. Res.*, (1994) in preparation.
- [33] E. Pellizzari, B. Demain and K. Krost, *Anal. Chem.*, 56 (1984) 793–798.
- [34] E.D. Pellizzari and K.J. Krost, *Anal. Chem.*, 56 (1984) 1813–1819.
- [35] M. Mattson and G. Petersson, *Int. J. Environ. Anal. Chem.*, 11 (1982) 211–219.
- [36] J.M. Roberts, F.C. Fehsenfeld, D.L. Albritton and R.E. Sievers, in L.H. Keith (Editor), *Identification and Analysis of Organic Pollutants in Air*, Butterworth, Boston, MA, 1984, pp. 371–387.
- [37] J.F. Walling, J.E. Bumgarner, J.J. Driscoll, C.M. Morris, A.E. Riley and L.H. Wright, *Atmos. Environ.*, 20 (1986) 51–57.
- [38] D. Helmig and J. Arey, *Sci. Tot. Environ.*, 112 (1992) 233–250.
- [39] Y. Yokouchi, H. Mukai, K. Nakajima and Y. Ambe, *Atmos. Environ.*, 24A (1990) 439–442.
- [40] P. Ciccio, E. Brancaleoni, M. Frattoni, A. Cecinato and A. Brachetti, *Atmos. Environ.* 27A (1993) 1891–1901.



ELSEVIER

Journal of Chromatography A, 677 (1994) 133–140

JOURNAL OF
CHROMATOGRAPHY A

Gas chromatographic separation of the enantiomers of volatile fluoroether anesthetics by derivatized cyclodextrins.

III. Preparative-scale separations for enflurane

Daniel U. Staerk, Aroonsiri Shitangkoon, Gyula Vigh*

Department of Chemistry, Texas A&M University, College Station, TX 77843-3255, USA

First received 18 January 1994; revised manuscript received 12 April 1994

Abstract

Preparative-scale gas chromatographic separation of the enantiomers of enflurane, a volatile anesthetic, has been achieved with a 1 m long, 10 mm I.D. column, packed with 25% (w/w) trifluoroacetyl- γ -cyclodextrin-coated 60/80 mesh Chromosorb A, installed in a custom-designed preparative gas chromatograph. An effluent-sampling interface valve, located between the exit of the preparative column and the fraction collector, takes 10- μ l samples of the effluent every 15 s and sends them onto a short, efficient analytical capillary column providing on-line enantiomeric analysis of the eluting bands. This permits the precise calculation of product purity, recovery and production rate for the preparative separation and leads to aggressive, yet safe, fraction pooling schemes.

1. Introduction

Prompted by the first successful capillary GC separation of the enantiomers of fluoroether anesthetics [1], in Part I of this series we have determined the operating parameters which lead to maximized separation selectivities and reasonable capacity factors for all the commercially available fluoroether anesthetics on all the commercially available cyclodextrin-based chiral GC stationary phases [2]. In Part II, we have demonstrated how this information can be used to develop a preparative GC separation for the enantiomers of one of the fluoroether anesthetics, isoflurane [3]. In the present paper we will detail the preparative scale GC separation of

the enantiomers of another fluoroether anesthetic, enflurane ($\text{CHFClCF}_2\text{OCHF}_2$), that became possible due to the use of an improved packing material and a custom-designed preparative GC system that affords on-line enantiomeric analysis of the effluent of the preparative column.

2. Experimental

A custom-designed preparative gas chromatographic system has been constructed according to Fig. 1 from a modified Model 439 GC apparatus (Chrompack, Middelburg, The Netherlands), equipped with a septumless split/splitless injector, a flame ionization detector, and a Model 4270 integrator (Varian, Walnut Creek, CA,

* Corresponding author.

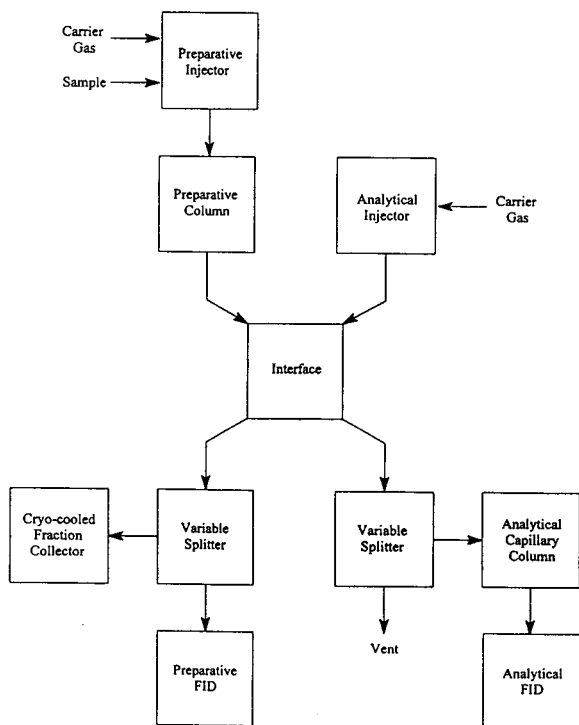


Fig. 1. Schematic of the preparative chromatographic system.

USA) for data acquisition, a modified Model FF thermostatted circulating oil-bath system (Science Electronics, Dayton, OH, USA), modified HP 5982 MS interface heated transfer lines (Hewlett-Packard, Avondale, PA, USA), a modified, heated Series 7000 (Rheodyne, Cotati, CA, USA) switching valve-based effluent sampling interface, a modified variable split injector (Tracor, Houston, TX, USA) and a custom-made analytical capillary column installed in an HP 5890 Series II gas chromatograph (Hewlett-Packard, Avondale, PA, USA), a septumless split/splitless injector, a flame ionization detector, and a CHEMSTATION data collection/analysis system.

The preparative scale GC separations were completed on 1.0 m \times 10.0 mm I.D. stainless-steel preparative columns, which were packed as described in Ref. [3] with 60/80 mesh (approximately 175–250 μ m) Chromosorb A (Supelco, Bellefonte, PA, USA), coated with 25% (w/w)

trifluoroacetyl- γ -cyclodextrin, GTA (ASTEC, Whippany, NJ, USA). The preparative column was operated isothermally at 40°C.

The effluent of the preparative column was analyzed on-line for enantiomeric purity using a 7.0 m \times 0.25 mm I.D. fused-silica capillary column, statically coated [4] with a 0.25 μ m thick film of GTA. Hydrogen was used as carrier gas at a linear velocity of 124 cm/s (methane was used as unretained compound). The capillary column was operated isothermally at 38°C.

Enflurane was obtained from Anaquest, a division of BOC Health Care (Murray Hill, NJ, USA).

3. Results and discussion

3.1. Column packing

Chromosorb A was found to yield a better packing material than Chromosorb W AW used in Part II of this work [3], both in terms of mechanical strength and column efficiency, and it could be coated with as much as 25% (w/w) of the GTA stationary phase, just as Chromosorb W AW. With hydrogen as carrier gas, the efficiency maximum of the 1 m \times 10 mm I.D. column was found at a linear velocity of 5 cm/s, yielding a height equivalent to a theoretical plate (HETP) value of 1.0 mm.

3.2. The custom-designed preparative chromatographic system

Our objective has been to create a preparative GC system which, in addition to the preparative scale separations, can be used to determine, on-line, prior to fraction collection, the enantiomeric purity of the effluent of the preparative column. The system, shown in Fig. 1, has been built using commercially available, easily modified components. The Chrompack 439 gas chromatograph is used to supply the carrier gas for the preparative column and facilitate the injection of the racemic enflurane feed via a gas-tight syringe. The preparative column is equipped with an oil jacket and is operated

isothermally using a circulating thermostatted oil bath. This arrangement allows the use of widely different column sizes and configurations, unconstrained by the GC oven.

Since fairly large selectivity values ($\alpha > 1.3$) are required for a successful preparative separation, a capillary column providing only a few thousand theoretical plates is all that is necessary for the on-line enantiomeric analysis of the effluent of the preparative column. These few thousands of plates can be generated easily with very short capillary columns (3 to 10 m) which are coated with a thin film (0.25 μm) of the same stationary phase as the preparative column, and operated at very high carrier gas linear velocities.

At the exit of the preparative column there is a heated interface, constructed from a programmable injection valve (e.g. a pneumatically operated, electronically activated Rheodyne Model 7000 valve), which samples the effluent of the preparative column and injects these samples (in our case 10 μl of the effluent gas) onto the analytical capillary column installed in the HP 5890 Series II gas chromatograph. As shown in Fig. 2, the cycling frequency of the interface valve is limited by the sum of the following time intervals: the duration of the pressure pulse that is caused by the turning of the interface valve to the inject position and back to the refill position (A), the duration of the flat baseline section before the peak of the less retained enantiomer (B), the duration of the first peak (C), the duration of the second peak (D), both determined at the highest effluent concentration expected during the preparative separation, and the duration of the flat baseline section after the peak of the more retained enantiomer necessary for reliable peak area determination (E). Additionally, the separation time on the analytical capillary column has to be an integer number multiple of the cycle time. Of the components of the cycle time, segments C and D can be adjusted most readily by changing the temperature of the capillary (to adjust separation selectivity), the film thickness (phase ratio) of the capillary to adjust the capacity factor (peak end) of the second component, and a combination of the

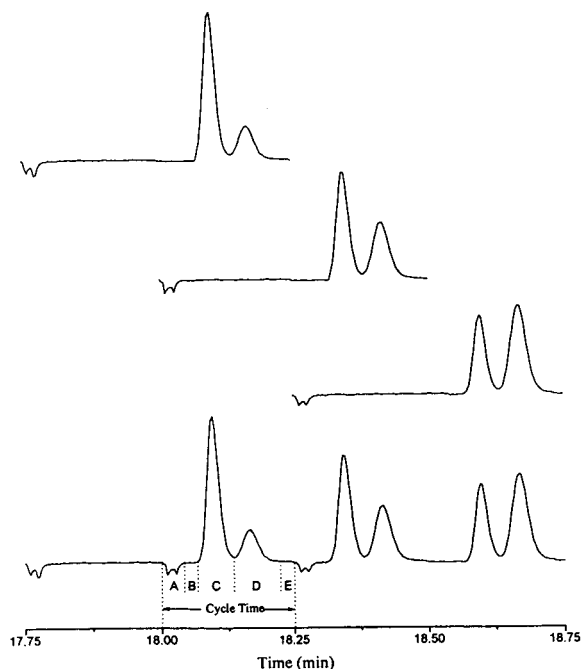


Fig. 2. Determination of the cycling time of the effluent sampling interface valve using the analytical chromatograms of three successive fractions of the preparative effluent. For details, see text. Top trace: individual analytical chromatogram of the first fraction injected onto the capillary column. Second trace: individual analytical chromatogram of the second fraction injected onto the capillary column. Third trace: individual chromatogram of the third fraction injected onto the capillary column. Bottom trace: actual detector trace that results from the three successively injected fractions. Analytical column: 7.0 m \times 0.25 mm I.D. fused-silica capillary, coated with a 0.25- μm film of GTA, operated isothermally at 38°C with a H_2 carrier gas velocity of 124 cm/s.

length of the capillary and the linear velocity of its carrier gas to provide the necessary efficiency. In our case the actual separation time on the analytical capillary column is 30 s and the cycle time is 15 s, which results in 75 to 80 enantiomeric composition data points during an average preparative separations. As an example, the signal of the flame ionization detector in the HP 5890 gas chromatograph [analytical flame ionization detection (FID)] is shown in Fig. 3 as a function of time during the preparative-scale separation of a 50-mg enflurane sample.

Due to the finite switching time of the inter-

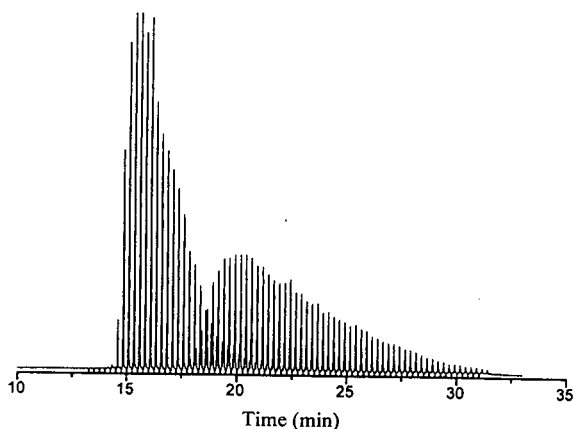


Fig. 3. Analytical detector trace during the preparative separation of a 50-mg enflurane sample. Preparative column: 25% (w/w) GTA on 60/80 mesh Chromosorb A packed into a 10 mm I.D., 1 m long stainless-steel column operated isothermally at 40°C with H₂ carrier gas at a linear velocity of 5.0 cm/s. Effluent-sampling interface valve cycle time: 15 s. Analytical column: 7.0 m × 0.25 mm I.D. fused-silica capillary, coated with a 0.25- μ m film of GTA, operated isothermally at 38°C with a H₂ carrier gas velocity of 124 cm/s.

face valve, a variable splitter (fashioned from parts of a Tracor variable split injector) is installed between the exit of the interface valve and the analytical capillary column. The split ratio can be changed over a broad range to prevent overload of the analytical capillary and hence provide the required number of plates for the analytical separation. The original injector of the HP 5890 gas chromatograph can be used for the quantitative calibration of the entire analytical system, because it is located upstream of the interface valve.

The other exit of the interface is connected to a second variable splitter. The minor stream from the splitter is taken to the detector [either thermal conductivity detection (TCD) or FID] of the preparative GC apparatus to monitor the actual effluent concentration histories (envelope chromatograms). Since in our system the fraction collection (cut-point selection) is governed by the results of the on-line enantiomeric purity analysis, there is no absolute need for an additional bulk detector on the preparative GC apparatus. Nevertheless, we decided to record these chro-

matograms as well (using FID of the Chrompack GC apparatus) to obtain information that could corroborate the results of the on-line enantiomeric analysis. The envelope chromatograms shown in Fig. 4 were obtained for the increasing enflurane loads of 1, 3, 6, 20, 32, 50, 75 and 120 mg. Regardless of sample size, the concentration of the more retained enantiomer is below the detection limit after 35 min.

The major stream from the variable splitter is connected to the fraction collector (e.g., a custom-modified cryo-cooled PSGC 10-40 fraction collector, VAREX, Burtonsville, MD, USA, used in Part II of this study [3]).

Naturally, all system components, modules, and transfer lines (fused-silica or stainless-steel capillaries) are thermostatted to prevent undesirable wall adsorption and memory effects.

The stability and reproducibility of the entire preparative system is demonstrated in Fig. 5 by a 1-h segment of a single day's production campaign (50 mg enflurane injections, 35 min preparative cycle time, 15 s interface valve cycling time), and in Fig. 6 by one separation segment from each of two successive production campaigns completed on two consecutive days (50 mg enflurane injections, 35 min preparative cycle time, 15, and 30 second interface valve cycling time).

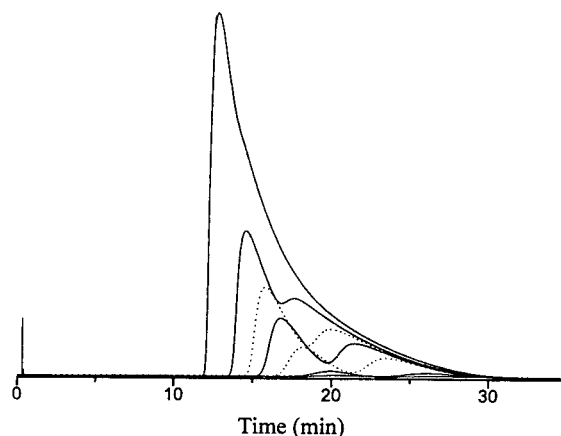


Fig. 4. Preparative FID traces (envelope chromatograms) for enflurane samples of increasing size. Preparative column: as in Fig. 3. Enflurane sample loads: 1, 3, 6, 20, 32, 50, 75, and 120 mg, respectively, increasing as peak height.

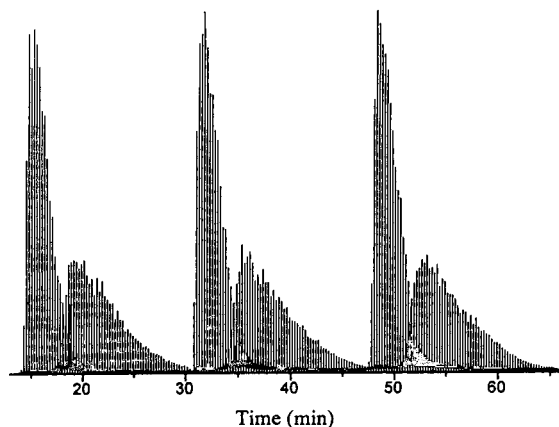


Fig. 5. Stability and reproducibility of the preparative system: a 1-h segment of the analytical FID trace during a single day's production campaign (50-mg enflurane injections, 35-min preparative cycle time, 15-s interface valve cycling time). Conditions as in Fig. 3.

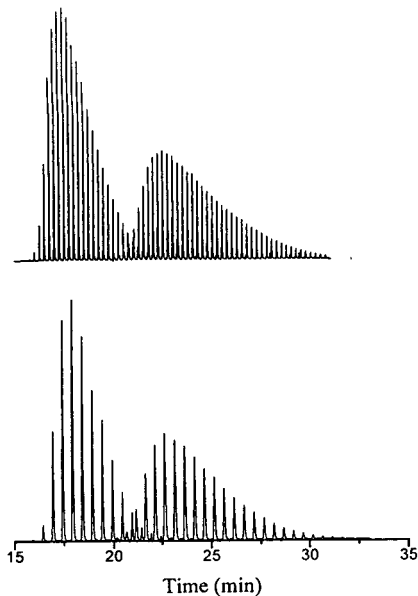


Fig. 6. Stability and reproducibility of the preparative system: one separation segment each of two successive production campaigns completed on two consecutive days (50 mg enflurane injections, 35-min preparative cycle time, 15-, and 30-s interface valve cycling time). Conditions as in Fig. 3.

3.3. Preparative results

In order to obtain an idea of the loading capacity of the 1 m × 10 mm I.D. column, a series of enflurane injections were made in the 3 to 250 mg load range. (The envelope chromatograms for some of these separations are shown in Fig. 4.) The on-line effluent enantiomer concentration data were obtained in each case (as shown, for example, for the 50 mg load in Fig. 5) and the peak areas of the enantiomers were used to calculate the enantiomeric purity vs. production and enantiomeric purity vs. % recovery curves as presented, for example, in Fig. 7 for the 120 mg injection. The inset in Fig. 7 shows the reconstructed chromatogram of the enantiomers and reveals that at the 120 mg load level there is already a significant interference between the less and the more retained enantiomers. The reconstructed chromatogram also reveals that at this load the isotherm effects, rather than the "sorption effect", dominate the peak shape [5].

Using the production vs. enantiomeric purity curves (such as in Fig. 7), the production vs. feed relationships can be calculated for various product purities as shown in Fig. 8 for the less

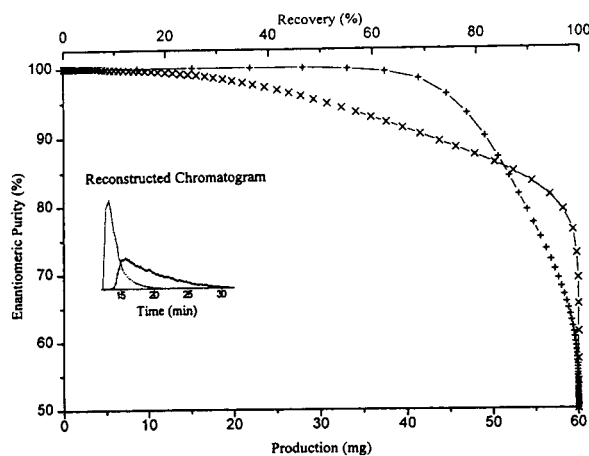


Fig. 7. Enantiomeric purity as a function of production and % recovery for a 120-mg injection calculated from the reconstructed chromatogram shown in the inset. Conditions as in Fig. 3. + = less retained enantiomer; × = more retained enantiomer.

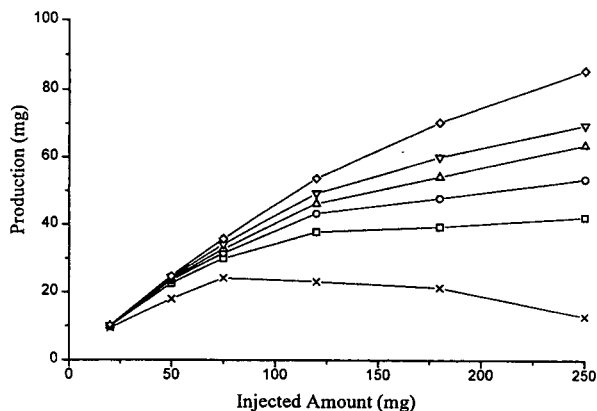


Fig. 8. Production for the less retained enflurane enantiomer as a function of the injected sample amount at various levels of product purity. Conditions as in Fig. 3. \diamond = 80%; ∇ = 90%; \triangle = 95%; \circ = 97%; \square = 99%; \times = 100% purity, respectively.

retained enantiomer and Fig. 9 for the more retained enantiomer. These graphs allow us to determine the maximum injection sizes that should be used in the production campaigns for a particular product purity level.

If the less retained enantiomer is to be produced at 100% purity, the maximum injection size should be 75 mg, leading to 24 mg of the pure product; at higher loads the production decreases. If the purity requirement is relaxed to

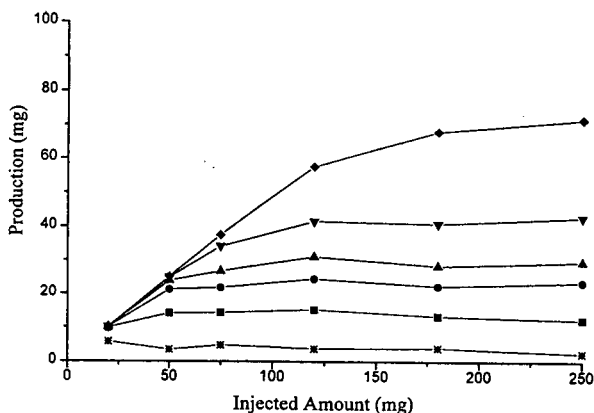


Fig. 9. Production for the more retained enflurane enantiomer as a function of the injected sample amount at various levels of product purity. Conditions as in Fig. 3. \diamond = 80%; ∇ = 90%; \triangle = 95%; \circ = 97%; \square = 99%; \times = 100% purity, respectively.

99%, the production increases significantly (to 35 mg) as the injection size is increased to 120 mg, but then levels off. At 97% or lower purity levels the production of the less retained enantiomer increases continuously as the injected amount is increased in the range tested (up to 250 mg feed).

The picture is quite different for the more retained enantiomer. As shown in Fig. 9, only about 6 mg can be produced at 100% purity, and it requires an injection size of 20 mg. Above this load, production drops slowly. At 99% enantiomeric purity the production plateau of 13 mg is reached with an injection size of 50 mg. In the load range tested, the production plateau does not disappear until the purity requirement is relaxed to 80%.

3.4. Production results

Figs. 8 and 9, which are based on single-injection separations, underestimate the production levels that can be achieved if the separations are repeated round-the-clock. This is because in a production campaign the repetitive injections can be timed such that the end of the second peak in a separation coincides with the start of the first peak in the subsequent preparative separation. Since the front of the first peak moves forward as the load is increased while the tail end of the second peak (representing infinite dilution) remains constant, the elution width of the peak pair becomes important as more cycles of lighter load can be carried out in a 24-h production day than heavier load (e.g. 90 cycles at 16 min each for 25 mg load, 65 cycles at 22 min each for 250 mg load).

Assuming that both enantiomers are to be recovered at the same purity level, Fig. 10 shows the daily production levels (and the amount of material that has to be recycled because its enantiomeric purity is below the specified level) as a function of the specified product purity and the amount of racemate feed injected in each cycle. The daily production surface for the more retained enantiomer is shown by the thickest line, the surface for the less retained enantiomer by the moderately thick line, while the daily

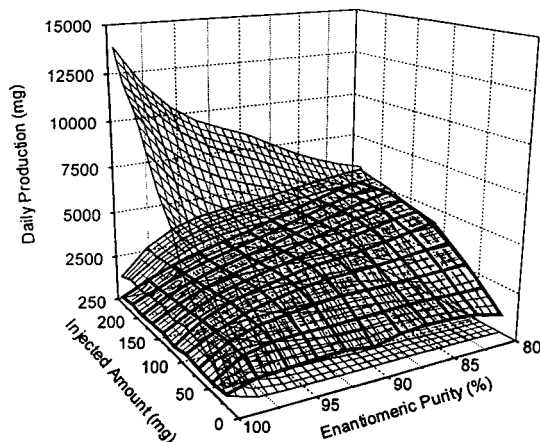


Fig. 10. Daily production as a function of sample loads and enantiomeric purity of product (symmetric purity regime). Conditions as in Fig. 3. Thickest line: more retained enantiomer; medium line: less retained enantiomer; thinnest line: daily recycle.

recycle surface is shown by the thinnest line. For 100% enantiomeric purity in both products, 75 mg injections should be used resulting in about 1900 mg of the less retained and 375 mg of the more retained enantiomers, and the recycle burden is about 3700 mg. Larger injections greatly increase the recycled amount and lead to slightly lower productions for both enantiomers. At 99% purity levels the trends are the same. However, when the purity requirement is relaxed to below 98%, the production surface for the less retained enantiomer loses its local maximum as the injected amount is increased (i.e. production continues to increase as load is increased, though at a decelerating rate), while that of the more retained enantiomer retains its local maximum. Thus, depending on the objectives of the campaign (production of larger, equal or lesser quantities of the first or second enantiomers), different operating conditions can be selected. The local maximum in the production surface of the more retained enantiomer remains, even at as low a product purity as 80%.

If the production campaign calls for the production of enantiomers of different purity, a three-dimensional daily production vs. product purities graph can be created for each injection level. As an example, the surface belonging to

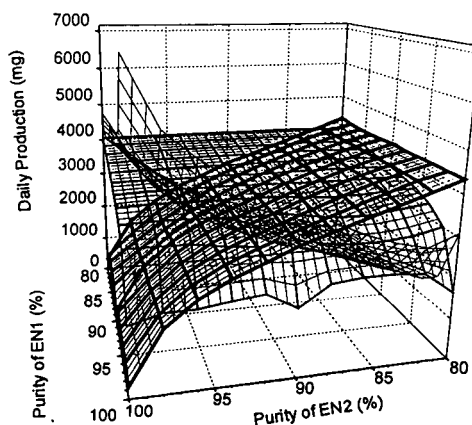


Fig. 11. Daily production as a function of the enantiomeric purity of both products for 120 mg enflurane injections. Conditions as in Fig. 3. Thickest line: more retained enantiomer; medium line: less retained enantiomer; thinnest line: daily recycle.

the 120-mg injection campaign is shown in Fig. 11. Once the required purities are set, the feed size that leads to the highest daily productions can be easily selected from the successive graphs.

4. Conclusions

A custom-designed preparative gas chromatographic system has been assembled from easily modified commercially available components. In addition to the preparative separation, the system accomplishes the on-line enantiomeric analysis of the effluent of the preparative column. On-line enantiomeric analysis is achieved by the use of a short, efficient capillary column, which is connected to a programmable effluent-sampling interface valve. For best characterization of the preparative column effluent, the analysis time on the capillary column has to be an integer number multiple of the cycle time of the sampling interface valve. This crucial condition can be met by the simultaneous adjustment of the operation temperature, length and phase ratio of the capillary column, as well as the linear velocity of its carrier gas. The on-line enantiomeric analysis permits the use of aggressive, yet safe production regimes.

Using this system and a 1 m long, 10 mm I.D. column packed with a chiral stationary phase, a successful preparative separation scheme has been developed for the production of gram/day quantities of the pure enantiomers of the volatile fluoroether anesthetic, enflurane. Further work is underway in our laboratory to use the system and extend this method development scheme for the production of other enantiomers of value or interest.

Acknowledgements

Partial financial support by the National Science Foundation (CH-8919151), the US Department of Education (Grant No. 415004), Anaquest Inc., the Dow Chemical Company and

the College of Science, Texas A&M University is gratefully acknowledged. ASTEC is acknowledged for providing us with the GTA phase used in this study.

References

- [1] J. Meinwald, W.R. Thompson, D.L. Pearson, W.A. König, T. Runge and W. Francke, *Science*, 251 (1991) 560.
- [2] A. Shitangkoon, D.U. Staerk and Gy. Vigh, *J. Chromatogr. A*, 657 (1993) 387.
- [3] D.U. Staerk, A. Shitangkoon and Gy. Vigh, *J. Chromatogr. A*, 663 (1994) 79.
- [4] K. Grob, *Making and Manipulating Capillary Columns for Gas Chromatography*, Huethig Verlag, Heidelberg, 1986, p. 156.
- [5] J. Roles and G. Guiochon, *J. Chromatogr.*, 589 (1992) 223.

Large-volume injection in packed-capillary supercritical fluid chromatography

Bart N. Zegers*, Henk-Jan de Geus, Sylvia H.J. Wildenburg, Henk Lingeman, Udo A.Th. Brinkman

Department of Analytical Chemistry, Free University, De Boelelaan 1083, 1081 HV Amsterdam, Netherlands

Received 11 January 1994

Abstract

Injection of large sample volumes in packed-capillary supercritical fluid chromatography (SFC) with thermionic detection (TID) was performed using a packed precolumn set-up. The precolumn (2.0×1.0 mm I.D.) was loaded with an aqueous sample and dried with nitrogen at room temperature. After drying, desorption with a supercritical fluid to the analytical column was performed by switching restrictors mounted on valves. During desorption the analytes were focused on the top of the analytical column and next the analysis was started by again switching the restrictors. Parameters influencing the system, *e.g.*, desorption strength of the supercritical fluid, desorption volume and desorption flow-rate, were studied. By injecting large, *i.e.*, $75 \mu\text{l}$, volumes of an aqueous sample, the analyte detectability was improved *ca.* 1000-fold compared with conventional 100-nl injections in hexane. This resulted in limits of detection of about $1 \mu\text{g l}^{-1}$ for three organophosphorus pesticides. The repeatability at the $5\text{--}15 \mu\text{g l}^{-1}$ level was better than 7% ($n = 8$), and good linearity over two orders of magnitude was found with spiked river water samples. To emphasize the potential of the system, a larger precolumn (10×2.0 mm I.D.) was tested, which was loaded with 47 ml of a river water sample. A further 1000-fold gain in sensitivity was obtained, and detection limits for the on-line trace enrichment-SFC-TID set-up now were in the 0.1 ng l^{-1} range.

1. Introduction

Packed-capillary supercritical fluid chromatography (SFC) can be used in combination with a wide variety of stationary phases and both liquid chromatographic (LC), *e.g.*, fluorescence or UV-Vis, and more sensitive and selective gas chromatographic (GC), *e.g.*, flame ionization or thermionic (TID) detection without the need to split the column effluent [1–3]. From economic and environmental points of view, other advan-

tages of the technique are the small amounts of mobile phase needed and its low toxicity.

As regards injection, there are, however, still two important limitations. Sample introduction cannot be performed directly in the mobile phase and another medium has to be chosen for this purpose, usually an organic solvent such as hexane or acetone. The problem with the use of organic solvents for injection is that they are not always compatible with the selected detector. The second and more important limitation is that only relatively small injection volumes are possible, which results in unfavourable limits of

* Corresponding author.

detection in units of concentration. In the last 5 years, several techniques have been described that allow the injection of large volumes. Most of these techniques are based on time vent [4–6] and solvent backflush [7] or combinations of both [7] and have in common that they use apolar solvents (*e.g.*, hexane, chloroform) and were especially developed for capillary SFC. Recent reviews covering these developments have been given by Greibrokk and Berg [8], Koski and Lee [9] and Cortes [10]. Recently a new device has been described that is based on complete solvent elimination inside an inlet column followed by refocusing of the analytes on the top of a capillary column [11,12]. This system effects a 1000-fold increase in sensitivity; the repeatability is good and aqueous samples can be injected. Drawbacks of this system are that injection is performed at 100°C and that it is not possible to flush the capillary inlet column after injection in order to perform a clean-up, which may result in memory effects.

Both of the above problems can be overcome by coupling a packed LC precolumn on-line with a packed-capillary SFC system. The precolumn is used for both trace enrichment and sample clean-up. A relatively large volume of liquid sample is pumped through the precolumn, at room temperature, and the analytes are trapped. After clean-up, the precolumn is dried with nitrogen. Modified carbon dioxide can then be used for the desorption of the precolumn. Advantages of this set-up are the possibility of analysing aqueous samples on-line with SFC and of introducing large volumes, which will improve the limits of detection. Two approaches for the on-line coupling are possible. After loading and drying with nitrogen, the precolumn can either be simply switched between the SFC mobile phase delivery system and the analytical column with subsequent direct desorption and analysis, as was shown by Niessen *et al.* [13]. Alternatively, the precolumn can be desorbed with refocusing of the analytes on the top of the analytical column prior to analysis. This can be done by regulating the pressure of the mobile phase, which will strongly influence the solubility of the analytes. A high pressure in the precolumn

results in a high desorption power whereas a low pressure in the analytical column will cause strong retention of the analytes. The different pressures can be obtained by properly switching restrictors on and off. The second approach allows one to reconcentrate the analytes on top of the analytical column and to regenerate and reload the precolumn for the next run while the previous sample is analysed.

In this paper, the second approach is discussed. Three organophosphorus pesticides (OPPs) of mutually different polarity were chosen to evaluate the performance of the LC–SFC–TID or, rather, the solid-phase extraction (SPE)–SFC–TID system. Parameters that are likely to affect the desorption efficiency, *viz.*, the strength of the desorption fluid, the desorption volume and the desorption flow, were studied. The first parameter is influenced by pressure, temperature and percentage of methanol. As it is experimentally complicated to vary the desorption temperature, the whole study was performed at room temperature. In other words, sorption and desorption of the analytes occurred at the same temperature. The effect of the desorption flow-rate on the desorption efficiency was studied by varying the dimensions of the restrictors. Variation of the desorption volume for several modifier percentages was studied in order to obtain maximum recovery. After optimization the technique was applied to the analysis of spiked river water samples.

2. Experimental

2.1. Direct injections

The system configuration is shown in Fig. 1A. A Phoenix-20 syringe pump (SFC pump in Fig. 1A) (Carlo Erba, Milan, Italy) was used for mobile phase delivery and pressure control. For direct SFC–TID analysis, valve 3 (Type EC10U; Valco, Schenkon, Switzerland) was switched to allow the mobile phase from the SFC pump to flow through the capillary between ports a and b and via valve 4 to the analytical column. Direct SFC injections were performed with valve 4, a

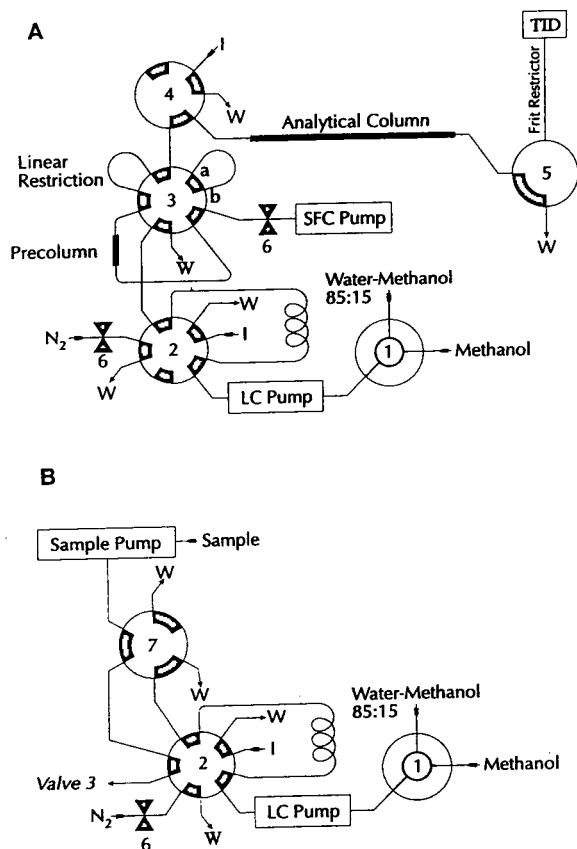


Fig. 1. (A) SPE-SFC-TID set-up. 1 = Solvent selection valve; 2 and 3 = ten-port switching valves; 4 = injection valve with internal 100-nl injection loop; 5 = three-port switching valve; 6 = on-off valve. The analysis and desorption can be performed with different methanol percentages in the mobile phase by connecting a second (analytical) pump and an on-off valve at port a of valve 3 and blocking port b with a stopper; the SFC pump then becomes the desorption pump. (B) Set-up for the introduction of large volumes with a sample pump. Valve 7 is a six-port switching valve. The set-up is connected to the SPE-SFC-TID set-up in (A) via valve 3.

100-nl Valco Type CI4W injection valve. The fused-silica column (135 × 0.32 mm I.D.) was slurry packed with LiChrosorb RP-18 (7 μm) bonded silica (Merck, Darmstadt, Germany). The column temperature was maintained at 50°C by a thermostated water-bath. Valve 5 (Valco Type EC3W) directed the column effluent through a 100-μm frit restrictor (Dionex/Lee Scientific, Salt Lake City, UT, USA) to the detector. The frit restrictor was used for pressure

control and was shortened to give a flow-rate of 10 μl min⁻¹ at 150 bar. The restrictor was situated in the detector base of a Carlo Erba NPD-40 thermionic detector as discussed by Verga [14]. After optimization as described by Mol *et al.* [15], the hydrogen and air flow-rates were set at 35 and 252 ml min⁻¹, respectively; the distance between the rubidium bead and the jet tip was 1.5 mm. The detector base was maintained at 300°C by an Ether type 17-90B heat controller. The thermionic detector was connected to a Model 180 electrometer (Carlo Erba) and for data acquisition a Model 4400 integrator (Varian, Walnut Creek, CA, USA) was used.

It was necessary to cool the syringe of the Phoenix-20 pump below 10°C during the filling procedure in order to obtain maximum filling percentages. This was done by slightly releasing the nut at the front of the syringe and allowing the carbon dioxide to expand adiabatically. A known volume of modifier (methanol) was added to the syringe. The resulting percentages (expressed as mol-% mol⁻¹) were calculated using interpolated carbon dioxide densities at various temperatures, taken from the tabulated data of Angus *et al.* [16], and the known densities of methanol. The SFC pump was allowed to stabilize overnight after filling. All analyses were performed using a pressure programme in which the mobile phase density was varied during a run [17].

2.2. LC-SFC-TID

A laboratory-made precolumn (2.0 × 1.0 mm I.D.) packed with Bondesil C₁₈ (40 μm, preparative grade) material (Analytichem International, Harbor City, CA, USA) was used for trace enrichment. The sample solutions were prepared in water-methanol (85:15, v/v) and injected in a 75.1-μl injection loop on valve 2 (Valco Type EC10U). A Model 2150 LC pump (LKB, Bromma, Sweden) was used to load the sample on the precolumn with water-methanol (85:15, v/v) at a flow-rate of 0.10 ml min⁻¹. The same pump was used to condition the precolumn with water-methanol (85:15, v/v) at a flow-rate of 0.25 ml

min⁻¹ for 5 min and to regenerate the precolumn with methanol at a flow-rate of 0.50 ml min⁻¹ for 5 min. After loading of the sample, the precolumn was dried with nitrogen for 10–15 min at a flow-rate of 100 ml min⁻¹.

Desorption of the precolumn was performed by the simultaneous switching of valves 3 and 5 to the positions shown in Fig. 1A; the modified carbon dioxide was then directed through the precolumn. The linear restrictor (8.0–35.0 cm × 15 μm I.D.) (Polymicro Technologies, Phoenix, AZ, USA) between the precolumn and the analytical column was used to control the desorption flow-rate. After desorption with a certain volume, determined by the filling percentage reading of the SFC pump, valves 3 and 5 were simultaneously switched and the analysis was started using the same pressure programme as was used for direct SFC-TID.

In several series of experiments desorption was performed with a different modifier percentage to that used for the analysis. This was done by connecting a second SFC pump (Phoenix-20) and an on-off valve to port a of valve 3 and by blocking port b of that valve with a stopper (not shown in Fig. 1A). The first SFC pump and the SFC pump at port a were used for desorption and analysis, respectively.

Introduction of larger, *i.e.*, 3–50 ml, sample volumes was performed using the set-up shown in Fig. 1B. A Model 4140 LC pump (Kipp & Zonen, Delft, Netherlands) at a flow-rate of 0.3 ml min⁻¹ was used. A laboratory-made six-port valve (valve 7) was used to switch from the sample to the water-methanol (85:15, v/v) used for conditioning and flushing the precolumn. The exact sample volume introduced was determined by calibration of the sample delivery flow-rate and measurement of the loading time. When using a larger (10 × 2.0 mm I.D.) precolumn, the same set-up as in Fig. 1B was used to introduce sample volumes of up to 50 ml at a flow-rate of 2.5 ml min⁻¹. Regeneration and conditioning were both performed for 6 min with a flow-rate of 2.5 ml min⁻¹. Drying of the precolumn was done with 100 ml min⁻¹ of dry nitrogen for 30 min; 300 μl of modified carbon dioxide were used to desorb this precolumn at a pressure of 150 bar and a flow-rate of 60 μl min⁻¹.

2.3. Chemicals

Carbon dioxide (99.97%) and nitrogen (99.999%) were obtained from Hoek Loos (Schiedam, Netherlands), HPLC-grade hexane from J.T. Baker Chemicals (Deventer, Netherlands), HPLC-grade methanol from Rathburn (Walkerburn, UK) and diazinon (98%), pyrazophos (99%) and azinphos-methyl (99%) from Riedel-de Haën (Seelze, Germany). Solutions for direct SFC injections were made in hexane. River Meuse samples were taken at Keizersveer, Netherlands. To each 85 ml of sample, 15 ml of methanol were added, then the samples were filtered through a 0.2-μm Red Rim filter obtained from Schleicher & Schüll (Dassel, Germany).

3. Results and discussion

3.1. Preliminary tests

In order to be able to evaluate the performance of the SPE-SFC-TID system, first direct injections of the three OPPs used as model compounds were made in the SFC-TID system. The limits of detection for the pesticides varied from 30 to 100 pg (signal-to-noise ratio = 3) using 100-nl injections in hexane (Table 1). Hexane was used as this solvent has a less detrimental effect on the separation than acetone. Calibration plots from the limits of detection up to 4–12 ng injected were linear. The repeatability of the system for these pesticides varied from 3 to 11% ($n = 13$; injected on one day), and the reproducibility was 7–13% ($n = 8$; injected on two different days). The limits of detection expressed in units of concentration are of the order of 1 mg l⁻¹, which certainly is not sufficient for trace-level environmental studies. A second disadvantage is that the injection medium is hexane, which makes it necessary to perform a time-consuming sample treatment procedure to extract the analytes from an aqueous matrix. In addition, the more polar analytes can only be extracted by a more polar solvent, which will adversely affect the SFC separation.

Next, on-line SPE-SFC-TID was attempted

Table 1
Calibration data for direct injections of three organophosphorus pesticides in hexane

Analyte	Limit of detection ^a (mg l ⁻¹)	Largest amount injected (mg l ⁻¹)	Calibration graph ^b	
			$y = a(\sigma_x)x + b(\sigma_y)^c$	R^2
Diazinon	0.3	40.0	$y = 135 (2.7)x - 22.4 (42.7)$	0.995
Pyrazophos	0.6	80.0	$y = 44.4 (0.3)x - 42.7 (56.5)$	1.000
Azinphos-methyl	1.0	120.0	$y = 31.3 (0.5)x - 69.7 (48.6)$	0.998

Column: 135 × 0.32 mm I.D. packed with 7- μ m LiChrosorb RP-18. Mobile phase: carbon dioxide modified with 1.2 mol-% methanol at 50°C. Pressure programme: 0 min, 150 bar; 1 min, 150 bar; 6 min, 200 bar; 11 min, 210 bar; 14 min, 150 bar.

^a Signal-to-noise ratio = 3.

^b Ten data points in duplicate.

^c Taken from limit of detection to largest amount injected.

by adding a short precolumn to the system (*cf.*, Fig. 1), which should trap the OPPs from aqueous samples. It was necessary to add some methanol to the sample to diminish the adsorption of the pesticides on the glass surfaces and the inner wall of the capillaries. No breakthrough was observed for these analytes after loading volumes of up to 10 ml containing 15 vol.-% of methanol. The procedure involves conditioning of the precolumn, loading of the aqueous sample on the precolumn and drying of the precolumn with nitrogen; these steps can all be implemented by switching valve 2 (Fig. 1A). Drying of the column material is necessary to prevent blockage of the linear restriction between the precolumn and the analytical column (valve 3, Fig. 1A) by water, which has a very high viscosity compared with modified carbon dioxide. A drying time of 10–15 min was selected as it was found to be long enough to achieve complete drying of the precolumn. Next, desorption was started by simultaneously switching valves 3 and 5. As a result, the modified carbon dioxide is led through the precolumn and the linear restrictor. The linear restrictor keeps the pressure through the precolumn high, which ensures efficient desorption of the analytes from the precolumn sorbent. As there is no restrictor at the end of the analytical column, there is a considerable pressure drop over the linear restriction between the precolumn and the analytical column. This drop in density provides the required strong retention of the analytes on the analytical column and as a result they become

focused on the top of the analytical column during the desorption procedure. The analysis is then started by switching valves 3 and 5 and starting the pressure programme. By switching valve 5 the restrictor to the detector is switched in-line with the analytical column and separation and detection can take place, while the precolumn is switched to allow its simultaneous regeneration. In order to study the effects of several parameters on the desorption efficiency, a solution of the three OPPs was prepared in water–methanol (85:15, v/v). The concentrations were 5 μ g l⁻¹ for diazinon, 10 μ g l⁻¹ for pyrazophos and 15 μ g l⁻¹ for azinphos-methyl.

3.2. Optimization of SFE–SFC–TID system

The first parameter studied was the amount of methanol used to modify the carbon dioxide. Fig. 2 shows the effect of the modifier percentage on the desorption efficiency (expressed as relative TID response) of the analytes at 150 bar. The recovery of diazinon was low without methanol and rapidly increased when methanol was added, becoming maximum between 0.4 and 1.3 mol%. The other two compounds show similar plots but because they are more strongly retained by the precolumn packing material the optimum modifier percentages are 0.8 and 1.0 mol% for pyrazophos and azinphos-methyl, respectively. It is interesting to note the decreasing recovery at higher methanol percentages, which is caused by inefficient refocusing of the analytes

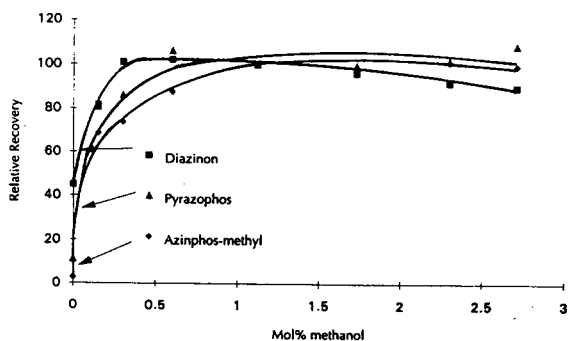


Fig. 2. Influence of the percentage of modifier on the recovery of (□) diazinon, (▲) pyrazophos and (◆) azinphos-methyl; response (peak area) for 1.1 mol% is 100%. Injected amount, 75.1 μl of 5 $\mu\text{g l}^{-1}$ diazinon, 10 $\mu\text{g l}^{-1}$ pyrazophos and 15 $\mu\text{g l}^{-1}$ azinphos-methyl. All points are the means of at least six measurements; the relative standard deviations vary from 4 to 19%. Desorption with 300 μl of carbon dioxide modified with 1.1 mol% methanol at 150 bar and 60 $\mu\text{l min}^{-1}$. Precolumn: 2.0 \times 1.0 mm I.D. packed with 40- μm Bondesil C₁₈. Analytical column: 135 \times 0.32 mm I.D. packed with 7- μm LiChrosorb RP-18. Mobile phase: carbon dioxide modified with 1.2 mol% methanol at 50°C. Pressure programme: 0 min, 150 bar; 1 min, 150 bar; 6 min, 200 bar; 11 min, 210 bar; 14 min, 150 bar.

on the top of the analytical column. Because of this LC-type effect, the peaks are broadened and their integration becomes problematic, which results in lower peak areas.

Fig. 3 shows the influence of the desorption pressure on the desorption efficiency of

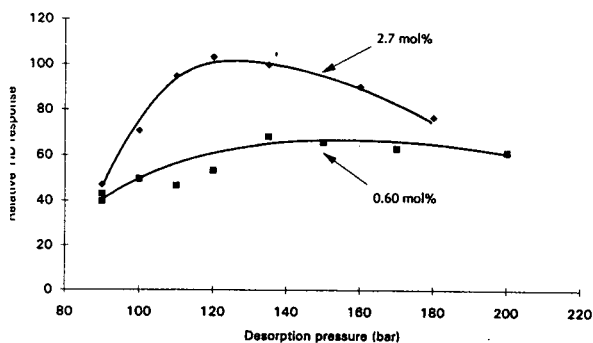


Fig. 3. Influence of the desorption pressure on the recovery of pyrazophos for (□) 0.60 and (◆) 2.7 mol% methanol-modified carbon dioxide; response (peak area) for 135 bar and 2.7 mol-% is 100%; for each point $n = 2$. Injected amount, 75.1 μl of 10 $\mu\text{g l}^{-1}$ pyrazophos; for each point $n = 2$. Desorption with 200 μl of carbon dioxide at 60 $\mu\text{l min}^{-1}$. Other conditions as in Fig. 2.

pyrazophos for two modifier percentages. A higher methanol percentage is seen to have a more pronounced effect on the desorption efficiency than variation of the desorption pressure. One also sees that the maximum recovery occurs at slightly lower desorption pressures when using higher methanol percentages. The sharp decrease in recovery with 2.7 mol% methanol-modified carbon dioxide can be explained by the LC effect described above. Fig. 4 illustrates this effect in more detail by showing the retention time of pyrazophos on the analytical column as a function of the desorption pressure for the two methanol percentages in Fig. 3. With 2.7 mol% methanol the retention time of pyrazophos on the analytical column drops immediately on increasing the desorption pressure, but with 0.6 mol% methanol it remains constant up to 140 bar. The other pesticides showed a similar dependence of the desorption efficiency and the retention time on the desorption pressure.

Fig. 5 shows the desorption efficiency of azinphos-methyl as a function of the desorption flow-rate. Because the influence of the desorption flow-rate is modest, one can conclude that mass transfer in the precolumn is rapid enough even at the maximum flow-rate used. This is interesting as it opens up the possibility of using larger precolumns. The lower desorption efficiency at low desorption flow-rates can be explained by the longer time necessary for desorption. During

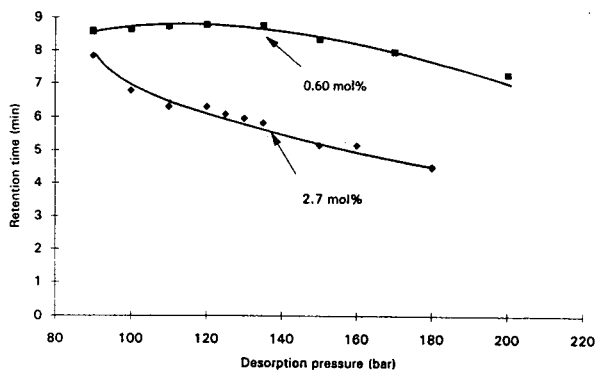


Fig. 4. Influence of the desorption pressure on the retention time of pyrazophos for (□) 0.60 and (◆) 2.7 mol-% methanol-modified carbon dioxide. Conditions as in Fig. 3.

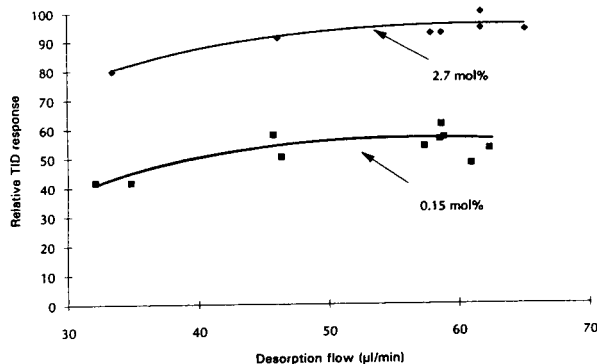


Fig. 5. Influence of the desorption flow-rate (as determined by the restrictor dimensions and calculated by dividing the desorption volume by the desorption time) on the recovery of azinphos-methyl for (■) 0.15 and (◆) 2.7 mol% methanol-modified carbon dioxide; response (peak area) for 60 $\mu\text{l min}^{-1}$ and 2.7 mol-% is 100%; for each point $n = 2$. Injected amount, 75.1 μl of 15 $\mu\text{g l}^{-1}$ azinphos-methyl. Desorption with 200 μl of carbon dioxide at 150 bar. Other conditions as in Fig. 2.

this time the analytes will diffuse axially in the analytical column, which will cause peak broadening.

Fig. 6 shows the dependence of the desorption efficiency on the desorption volume with pure carbon dioxide and carbon dioxide containing 1.1 mol% methanol as the desorption fluid, and with diazinon as test solute. In both instances a

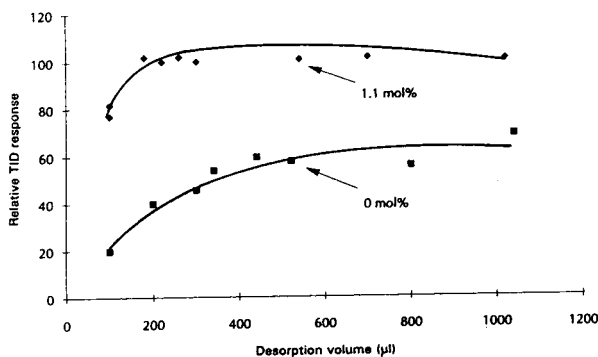


Fig. 6. Influence of the desorption volume on the recovery of diazinon for (■) 0 and (◆) 1.1 mol-% methanol-modified carbon dioxide; response (peak area) for 150 bar, 300 μl with 1.1 mol% methanol modified carbon dioxide is 100%; for each point $n = 2$. Injected amount, 75.1 μl of 5 $\mu\text{g l}^{-1}$ diazinon. Desorption at 150 bar and 60 $\mu\text{l min}^{-1}$. Other conditions as in Fig. 2.

plateau is reached, but for the modified carbon dioxide this plateau is distinctly higher than for pure carbon dioxide. The results also indicate that the actual desorption volume used is of less importance than the amount of modifier added. For the other OPPs studied the effect of methanol addition was even more dramatic: for pyrazophos the recovery with 1.1 mol% methanol was six times higher than that without methanol, and for azinphos-methyl the gain was more than one order of magnitude.

Finally, in this study two SFC pumps were normally used in order to be able to vary the modifier percentage of the fluid used for desorption without having to change the mobile phase used for the analytical separation. However, as is shown in Fig. 4, there is a difference in retention time for different amounts of modifier in the desorption fluid although the mobile phase used in the analytical column is the same. This obviously is the result of the fact that all the desorption fluid is flushed through the analytical column. Actually, apart from influencing retention times, the use of two different mobile phases will also diminish the reproducibility of the experiments. However, as was demonstrated above (*cf.*, Fig. 2), it is not necessary to use a desorption fluid having a different composition to the mobile phase if the mobile phase contains enough modifier. Therefore, it was decided to carry out the testing of the analytical performance of the system with only one SFC pump containing 1.2 mol% methanol. With this mobile phase composition desorption of the three pesticides was optimum when a desorption pressure of 150 bar, a desorption volume of 300 μl and a desorption flow-rate of 60 $\mu\text{l min}^{-1}$ were chosen. An injection volume of 75 μl of aqueous sample was used to load the precolumn.

3.3. Analytical performance

In order to calculate the absolute recovery of the compounds, the peak areas of direct injections of a 5–15 mg l^{-1} solution of the OPPs in hexane were compared with those of 15–45 $\mu\text{g l}^{-1}$ solutions of pesticide in water–methanol

(85:15, v/v) when these were analysed by means of SFE–SFC–TID, using 75- μ l sample volumes. The calculated recoveries varied from $106 \pm 5\%$ ($n = 6$) for diazinon via $112 \pm 7\%$ ($n = 6$) for azinphos-methyl to $140 \pm 11\%$ ($n = 6$) for pyrazophos. One problem is that hexane is not an ideal solvent for these pesticides and causes some peak distortion and analyte losses due to adsorption on surfaces. This probably explains the high recoveries found with the on-line trace enrichment approach. The repeatability of the procedure varied from 4 to 6% ($n = 8$, 5–15 μ g l⁻¹) and the reproducibility was 5–8% ($n = 2 \times 8$, 5–15 μ g l⁻¹). These values are significantly better than those found with direct SFC–TID (see above). This may be due to the fact that the large-volume injections cause a decrease in the relative volume error, and/or to the disturbance caused by the introduction of hexane (see above).

In Table 2 the analytical data for the determination of the pesticides in spiked river Meuse samples are given. The calibration graphs are linear over two orders of magnitude. Fig. 7 shows SPE–SFC–TID traces for a river Meuse sample spiked with the pesticides at the 3–9 μ g l⁻¹ level, a river Meuse blank and a distilled water blank. In all instances 75- μ l water samples were processed. As the breakthrough volumes of the analytes are higher than 10 ml (see above), 3 ml were loaded on to the precolumn. This improved the limits of detection for diazinon and azinphos-methyl to 8 and 50 ng l⁻¹, respectively

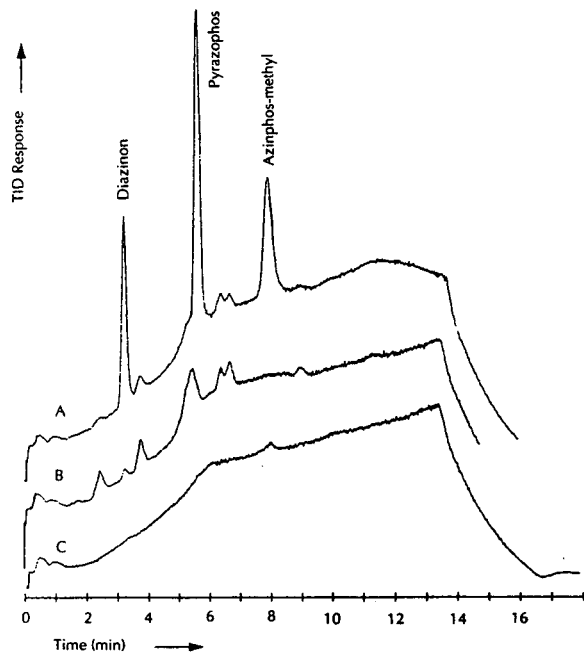


Fig. 7. SPE–SFC–TID of (A) methanol–river Meuse water (15:85, v/v) spiked with 3 μ g l⁻¹ of diazinon, 6 μ g l⁻¹ of pyrazophos and 9 μ g l⁻¹ azinphos-methyl, (B) methanol–river Meuse water (15:85, v/v) blank and (C) methanol–demineralized water (15:85, v/v). Injected amount, 75.1 μ l; precolumn, 2.0 \times 1.0 mm I.D. packed with 40- μ m Bondesil C₁₈. Desorption with 300 μ l of carbon dioxide modified with 1.2 mol% methanol at 150 bar and 60 μ l min⁻¹. SFC conditions as in Fig. 2.

(Table 3). Because a small (unidentified) peak showed up in SPE–SFC–TID of the blank surface water sample close to pyrazophos, the

Table 2
Calibration data for three organophosphorus pesticides in spiked river Meuse water

Analyte	Limit of detection ^a (μ g l ⁻¹)	Largest amount injected (μ g l ⁻¹)	Calibration graph ^b	
			$y = a(\sigma_a)x + b(\sigma_b)^c$	R^2
Diazinon	0.2	100	$y = 52.3 (1.0)x - 42.7 (40.4)$	0.997
Pyrazophos	1.8	200	$y = 40.4 (2.1)x - 46.5 (110)$	0.989
Azinphos-methyl	0.5	300	$y = 19.8 (0.9)x - 12.5 (10.6)$	0.987

Injected amount, 75 μ l; precolumn, 2.0 \times 1.0 mm I.D. packed with 40- μ m Bondesil C₁₈. Desorption with 300 μ l carbon dioxide modified with 1.2 mol-% methanol at 150 bar and 60 μ l min⁻¹. For SFC conditions, see Table 1.

^a Signal-to-noise ratio = 3.

^b Eight data points in duplicate.

^c Taken from limit of detection to largest amount injected.

Table 3
Limits of detection found with different sample introduction methods

Method of sample introduction	Sample volume	Sample solvent	Limit of detection ^a (g l ⁻¹)		
			Diazinon	Pyrazophos	Azinphos-methyl
Direct (internal) loop injection	100 nl	Hexane	$0.3 \cdot 10^{-3}$	$0.6 \cdot 10^{-3}$	$1.0 \cdot 10^{-3}$
Loop injection + precolumn (2.0 × 1.0 mm I.D.)	75 μl	Methanol-river water (15:85)	$0.2 \cdot 10^{-6}$	$1.8 \cdot 10^{-6}^b$	$0.5 \cdot 10^{-6}$
Sample pump + precolumn (2.0 × 1.0 mm I.D.)	3 ml	Methanol-river water (15:85)	$8 \cdot 10^{-9}$	$1.8 \cdot 10^{-6}^b$	$50 \cdot 10^{-9}$
Sample pump + precolumn (10.0 × 2.0 mm I.D.)	47 ml	Methanol-river water (15:85)	$50 \cdot 10^{-12}$	$1.8 \cdot 10^{-6}^b$	$400 \cdot 10^{-12}$

^a Desorption with 300 μl of carbon dioxide modified with 1.2 mol-% methanol at 150 bar and 60 μl min⁻¹. For SFC conditions, see Table 1.

^b Matrix inference.

detection limit for this OPP was higher, *viz.*, 1.8 μg l⁻¹.

As mentioned above, the amount of modifier is the critical parameter to be dealt with during preconcentration. It was decided, therefore, to try a larger precolumn, *i.e.*, 10 × 2.0 mm I.D. The sample volume was increased correspondingly and 47 ml of river Meuse water were now used for on-line SPE-SFC-TID. The chromatogram for a sample spiked with 150–450 pg l⁻¹ of the three pesticides is shown in Fig. 8. As can be seen, both diazinon and azinphos-methyl can still be detected, but pyrazophos has been lost owing to co-elution with some other peaks. In this instance, the limits of detection (see Table 3) were very good, *viz.*, 50 pg l⁻¹ for diazinon and 400 pg l⁻¹ for azinphos-methyl.

4. Conclusions

With the present on-line SPE-SFC system it is possible to enhance analyte detectability about 1000-fold compared with systems using conventional injection. The analytical data such as repeatability, reproducibility and linearity are fully satisfactory. The LC-type precolumn used

for the SPE step shows well defined behaviour during both sorption and desorption. It can be used at room temperature, which is a distinct advantage when working with thermolabile compounds. The low desorption pressures that can be used when modified carbon dioxide is selected as the mobile phase help to increase the lifetime of the precolumn. Actually, in this study the precolumns were replaced, merely as a precaution, once a week. On opening them, no holes were observed; obviously the pressure changes did not cause any damage.

With the SPE-SFC-TID set-up described, organophosphorus pesticides can easily be detected and determined at levels far below the threshold values of 0.1–1 μg l⁻¹ set by the European Community for drinking and surface waters. In other words, the system can be recommended for the determination of pesticides and related environmental contaminants that are too polar to be determined by means of capillary GC, or for which LC combined with diode-array UV detection is not appropriate because of a lack of chromophoric groups. Another interesting aspect of the system is that the on-line set-up will facilitate automation, an option which is, of course, not restricted to the use of TID. Finally,

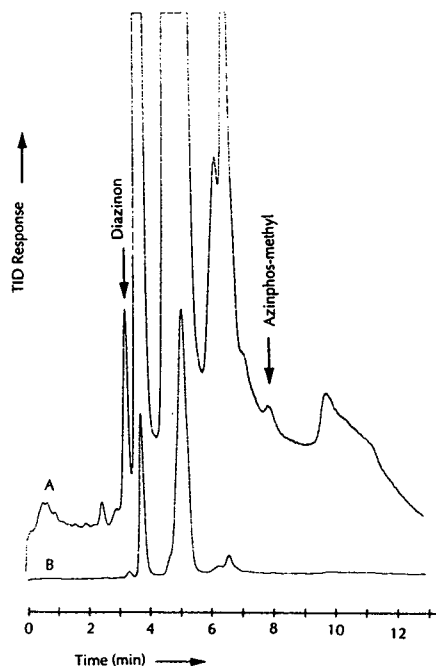


Fig. 8. Chromatogram of a large-volume injection with the SPE-SFC-TID system for methanol–river Meuse water (15:85, v/v) spiked with 150 pg l^{-1} of diazinon, (300 pg l^{-1} of pyrazophos) and 450 pg l^{-1} of azinphos-methyl at two different attenuations [(A) $\times 32$; (B) $\times 1$]. Injected amount, 46.8 ml ; precolumn, $10 \times 2.0 \text{ mm I.D.}$ packed with $40\text{-}\mu\text{m}$ Bondesil C_{18} . Desorption with $300 \text{ }\mu\text{l}$ of carbon dioxide modified with 1.2 mol\% methanol at 150 bar and $60 \text{ }\mu\text{l min}^{-1}$. SFC conditions as in Fig. 2.

it should be emphasized that the precolumn-based approach allows the direct introduction of even large aqueous samples and thus simplifies sample pretreatment. The preliminary results on the use of 10-mm long precolumns are encouraging, with limits of detection in the sub-ng l^{-1} range. Although our experience is at present limited and further work will consequently have to be carried out in the application area, it seems fair to state that the gain in analyte detectability offered by the present system opens up new perspectives for SFC as a separation technique for trace-level analysis.

Acknowledgements

The authors thank Dr. Ch.E. Kientz for supplying the analytical column. M.J.H. Vos is

thanked for her preliminary research on this project. The Foundation of Chemical Research in The Netherlands and the Foundation for Technical Sciences are gratefully acknowledged for a grant (No. 349-1561).

References

- [1] M.L. Lee and K.E. Markides, *Analytical Supercritical Fluid Chromatography and Extraction*, Chromatographic Conferences, Provo, UT, 1990.
- [2] T.L. Chester, J.D. Pinkerston and D.E. Raynie, *Anal. Chem.*, **64** (1992) 153R.
- [3] B. Wenclawiak, *Analysis with Supercritical Fluids: Extraction and Chromatography*, Springer, Berlin, 1992.
- [4] B.E. Berg and T. Greibrokk, *J. High Resolut. Chromatogr.*, **12** (1989) 322.
- [5] S. Ashraf, K.D. Bartle, A.A. Clifford, I.L. Davies and R. Moulder, *Chromatographia*, **30** (1990) 618.
- [6] I.J. Koski, K.E. Markides and M.L. Lee, *J. Microcol. Sep.*, **3** (1991) 521.
- [7] M.L. Lee, B. Xu, E.C. Huang, N.M. Djordjevic, H.C. Chang and K.E. Markides, *J. Microcol. Sep.*, **1** (1989) 7.
- [8] T. Greibrokk and B.E. Berg, *Trends Anal. Chem.*, **12** (1993) 303.
- [9] I.J. Koski and M.L. Lee, *J. Microcolumn Sep.*, **3** (1991) 481.
- [10] H.J. Cortes, in H.J. Cortes (Editor), *Multidimensional Chromatography*, Marcel Dekker, New York, 1990, p. 251.
- [11] H.J. Cortes, R.M. Campbell, R.P. Himes and C.D. Pfeiffer, *J. Microcol. Sep.*, **4** (1992) 239.
- [12] R.M. Campbell, H.J. Cortes and L. Shayne Green, *Anal. Chem.*, **64** (1992) 2852.
- [13] W.M.A. Niessen, P.J.M. Bergers, U.R. Tjaden and J. van der Greef, *J. Chromatogr.*, **454** (1988) 243.
- [14] G.R. Verga, *J. Chromatogr.*, **279** (1983) 657.
- [15] J.G.J. Mol, B.N. Zegers, H. Lingeman and U.A.Th. Brinkman, *Chromatographia*, **32** (1991) 203.
- [16] S. Angus, B. Armstrong and K.M. de Reuck, *Carbon Dioxide, International Thermodynamic Tables of the Fluid State—3*, Pergamon Press, Oxford, 1976.
- [17] H. de Geus, B.N. Zegers, H. Lingeman and U.A.Th. Brinkman, *Int. J. Environ. Anal. Chem.*, **56** (1994), in press.



ELSEVIER

Journal of Chromatography A, 677 (1994) 151–157

JOURNAL OF
CHROMATOGRAPHY A

In-line isotachophoretic focusing of very large injection volumes for capillary zone electrophoresis using a hydrodynamic counterflow

M. Mazereeuw, U.R. Tjaden*, J. van der Greef

Division of Analytical Chemistry, Leiden/Amsterdam Center for Drug Research, Leiden University, P.O. Box 9502, 2300 RA Leiden, Netherlands

First received 25 February 1994; revised manuscript received 29 March 1994

Abstract

A simple in-line isotachopheresis–capillary zone electrophoresis system for preconcentration of large sample volumes up to 25 μl is described. Model samples of $1 \cdot 10^{-4}$ – $2.5 \cdot 10^{-9}$ M solutions of antimuscarinic drugs were used and a volumetric calibration graph over the range 2.6–20.8 μl of $1 \cdot 10^{-7}$ M neostigmine and propantheline was designed. The relative standard deviations of three 500-nl injections of $1 \cdot 10^{-4}$ M neostigmine and propantheline were 1.6 and 4.1%, respectively. Applying UV–Vis absorbance detection, concentrations in the region of 10^{-9} M could be detected.

1. Introduction

Capillary zone electrophoresis (CZE) is on its way to becoming an established technique in laboratories. The main reasons for this are the high separation power and ease of operation. Major drawbacks with CZE are, however, the lack of sample loadability and the low concentration sensitivity of the commonly used UV–Vis absorbance detection. Owing to the short optical path length, typically 50–100 μm , the detection limits are in the range of 10^{-6} – 10^{-7} M [1]. Of course, the mass sensitivity is very impressive owing to the intrinsic small detection volume. Typical injection volumes in CZE are in the nanolitre range. In addition, a significant lowering of the level of interfering compounds, espe-

cially in the analysis of complex samples, is necessary. Another shortcoming of CZE is its limited selectivity. Coupling with, *e.g.*, LC pretreatment techniques seems to be essential, but places high demands on the elution volumes.

Different on-line LC and electrophoretic sample enrichment and/or clean-up techniques for CE have been described in recent years [2–18]. The electrophoretic techniques, such as ITP and field amplified injection, are based on sample stacking due to local field strength differences [7–18]. In ITP, the sample compounds are separated according to their ionic mobilities into different zones between the boundaries of a discontinuous buffer system, *i.e.*, the leading and terminating buffer. When a steady state is reached, all zones migrate with equal velocity and have distinct borders. Sharp differences in field strengths between each zone correct diffu-

* Corresponding author.

sion band broadening. The steady-state concentrations of the compound zones are proportional to the concentration of the leading buffer, as can be derived from the Kohlrausch equation [19]. For trace compounds this results in sample concentration.

In the “classical” electrophoresis set-up, a detection device is considered to be the last active part of the CE system and the capillary “downstream” of the detector is considered as an unimportant necessity. In coupled ITP systems, this part can be used to extend the volume of the separation system dramatically. In other words, the detector is moved up to the inlet of the capillary and is not necessarily at the end of the CE system.

Owing to the intrinsic stabilizing properties of a steady state, ITP can be performed with a hydrodynamic flow in capillaries, without loss of analyte or band broadening [19]. This also means that large volume differences and dead volumes, *e.g.*, in capillary connections, do not affect either the concentration process or a steady-state situation.

These interesting features form the basis of an extended-volume ITP–CZE system, the preliminary results of which are presented in this paper. A few characteristics of the coupled columns with different inner diameter will be discussed.

2. Experimental

2.1. Chemicals

Triethylamine >99% pure (TEA), glacial acetic acid and HPLC-grade methanol were obtained from Merck (Darmstadt, Germany) and β -alanine from Aldrich (Steinheim, Germany). The antimuscarinic drugs neostigmine hydrobromide (N) and propantheline hydrobromide (P) were purchased from Sigma (St. Louis, MO, USA). Crystal violet (CV) (Janssen Chimica, Beerse, Belgium) was used as a visible dye to follow the preconcentration process.

The leading buffer was 10 mM TEA solution containing 50% (v/v) methanol, adjusted to pH

5 with acetic acid. This buffer was also used as the background electrolyte in CZE. As a terminating buffer 10 mM β -alanine containing 50% (v/v) methanol adjusted to pH 5 with acetic acid, was used. All buffer solutions were prepared freshly every day.

Stock solutions of 10 mM analyte (pH 4.3) were stored at 5°C.

All solutions were prepared with water obtained from a Milli-Q system (Millipore, Bedford, MA, USA).

2.2. Apparatus

The experimental set-up is shown in Fig. 1. A programmable capillary injection system (P) (Prince, Lauerlabs, Emmen, Netherlands) suitable for siphoning and sucking was used to control the preconcentration process and the high-voltage power supply. Untreated 100 (1 and 2) and 220 μ m I.D. (3), approximately 300 μ m O.D., fused-silica capillaries (SGE, Ringwood, Victoria, Australia) with lengths of 60, 10 and

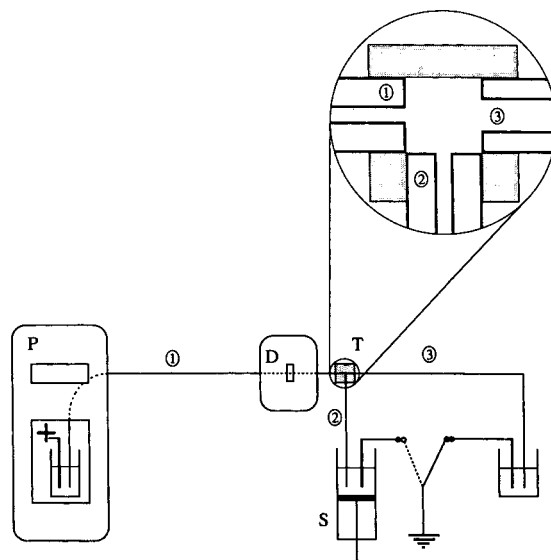


Fig. 1. Schematic representation of the ITP–CZE set-up. P = programmable capillary injection system; D = UV–Vis absorbance detector; T = laboratory-made polyethylene T-piece; S = injection syringe used as a ground electrode vessel. Untreated fused-silica capillaries of I.D. 100 μ m (1 and 2) and 220 μ m (3) are used.

50 cm, respectively, were connected with laboratory-made polyethylene T-piece with an internal volume of *ca.* 20 nl. A simple T-piece for low-pressure fittings was manufactured from transparent polyethylene. With a 300 μm O.D. drill, a T-shaped channel was created in which the three fused-silica tubes were inserted.

The outlet of capillary 2 (see Fig. 1) could be (de)blocked manually by means of a septum. The septum was positioned on the plunger of an injection syringe (S) used as an electrode vessel. Next to the outlet of the syringe a large opening was created for the ground electrode and to avoid any inducement of pressure differences. Capillary 2 was mounted on the syringe by means of a fingertight-union combination and (de)-blocked by moving the plunger.

Three leveled electrode vials with two ground electrodes and an anode were used. During the switch-over from ITP to CZE the ground electrode connections were changed.

Detection at 200 nm was performed on the 100 μm I.D. capillary (1) at 50 mm from the T-piece using a Spectra 100 UV-Vis absorbance detector (D) (Spectra-Physics, Mount View, CA, USA) at a wavelength of 200 nm. The signal was registered on a Model 40 flat-bed recorder (Kipp & Zonen, Delft, Netherlands).

2.3. ITP-CZE procedure

The ITP-CZE procedure as developed by Reinhoud *et al.* [12] was modified and is shown schematically in Fig. 2. In step A the total capillary system is filled with leading buffer, which is also used as the CZE background electrolyte. The outlet of capillary 2 (see Fig. 1) is closed and the capillary is loaded with sample, dissolved in terminating buffer. In the following step B, the sample vial is replaced with the anode vial containing terminating buffer and the ITP process is initially started at +10 kV, decreased to +7 kV after 1 h. To compensate for the electroosmotic flow (EOF) and to move back the preconcentrated sample zone to the capillary inlet during the ITP process, a hydrodynamic counterflow is applied. After focusing and moving back the sample zone simultaneously for

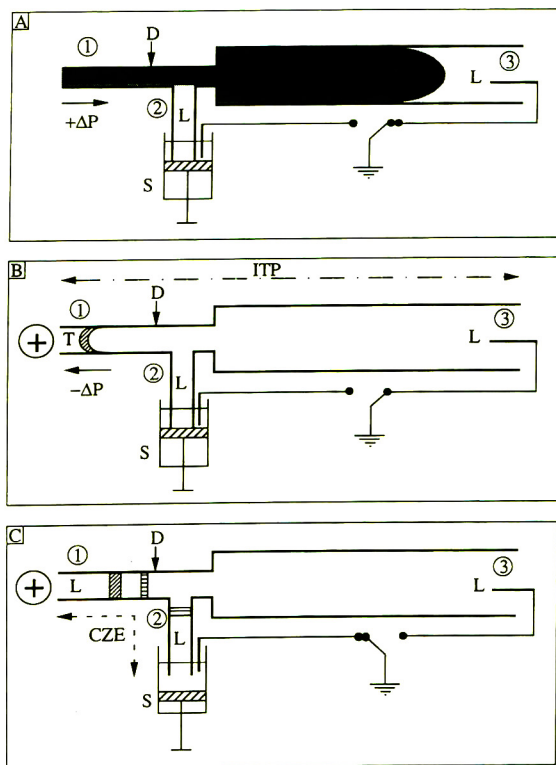


Fig. 2. Schematic representation of the ITP-CZE procedure in three steps (A, B and C). The focusing step is performed between the terminating (T) and leading (L) buffers in capillaries 1 and 3 and controlled with a pressure difference ΔP . Capillary 2 can be (de)blocked by means of the syringe vessel S. D = detection device.

5–150 min depending on the volume of analyte injected, the visible marker crystal violet, which has the lowest mobility (see Fig. 4a), reaches the inlet of the capillary. Then, in the final step C, the terminating buffer vial is replaced with a leading buffer-containing vial, the electrodes are exchanged, capillary 2 deblocked and CZE is started and performed at +30 kV.

3. Results and discussion

Concentrating a large volume takes a relatively long time, mainly depending on the applied field strength, the migration path length and the mobility of the compounds. Therefore,

increasing the diameter of the preconcentration system is preferred to increasing the capillary length. In the latter instance, the sample volume is only increased linearly by changing the length, while the diameter affects the volume according to the square root, which makes shorter capillaries, *i.e.*, migration path length, and a high electric field strength possible. Unfortunately, Joule heating plays a more prominent role in wide-bore capillaries. An optimum compromise between the focusing time and diameter has to be found. Coupling of columns with different inner diameters results in inhomogeneous electrophoretic conditions, *e.g.*, the electric field strength, which are considered in this section.

The ITP channel consisted in fact of two capillaries with different inner diameters, which can be considered as a series combination of two resistors, R_1 and R_2 . For a capillary with length L (cm), the electric resistor R (S^{-1}) can be defined as

$$R = \frac{4L}{\pi d^2 \kappa} \quad (1)$$

where d is the inner diameter of the capillary (cm) and κ the specific conductivity ($S \text{ cm}^{-1}$) of the electrolyte. If the current I is considered to be constant, the ratio of the field strengths over two coupled capillaries (E_1/E_2) can be expressed by the equation

$$\frac{E_1}{E_2} = \frac{d_2^2}{d_1^2} \cdot \frac{\kappa_2}{\kappa_1} \quad (2)$$

The EOF volume throughput, Φ_{eof} ($\mu\text{l min}^{-1}$), can be calculated from

$$\Phi_{\text{eof}} = v_{\text{eof}} \cdot \frac{\pi d^2}{4} \quad (3)$$

where v_{eof} is the EOF flow-rate (mm min^{-1}), which can be expressed as

$$v_{\text{eof}} = \mu_{\text{eof}} E \quad (4)$$

where μ_{eof} represents the electroosmotic mobility ($\text{mm}^2 \text{ min}^{-1} \text{ V}^{-1}$). Combining Eqs. 2, 3 and 4 demonstrates that the ratio of the EOF volume throughput in the two capillaries ($\Phi_{1,\text{eof}}/\Phi_{2,\text{eof}}$) is independent of the capillary diameters and

$$\frac{\Phi_{1,\text{eof}}}{\Phi_{2,\text{eof}}} = \frac{\mu_{\text{eof}}}{\mu_{\text{eof}}} \cdot \frac{d_2^2}{d_1^2} \cdot \frac{\kappa_2}{\kappa_1} \cdot \frac{4\pi d_1^2}{4\pi d_2^2} = 1 \quad (5)$$

for a continuous buffer system ($\kappa_2/\kappa_1 = 1$), neglecting the influence of Joule heating, and can therefore be equally compensated over the coupled capillaries by means of a hydrodynamic counterflow. Thus no pressure build-up is generated in the capillary connection which can disturb the preconcentration or steady state.

However, Eq. 2 shows that the EOF cannot be considered constant in a discontinuous buffer system because of the differences in conductivity. Further, the field strength differences and hence the differences in migration rate will be strongly dependent on the choices of the inner diameters. As a consequence, the preconcentration time in the wide-bore capillary, compared with the small-bore part, will increase significantly with increase in capillary diameter.

In Table 1 the set-up shown in Fig. 1 is compared with a set-up in which the volume extension is achieved by using a long small-bore capillary and a homogeneous field strength is present. A continuous background electrolyte was considered. As can be seen, the field strengths in both extension capillaries are similar. As the electrophoretic velocity is proportional to the field strength (Eq. 4), the migration time and hence the focusing time in system II will be approximately five times longer than in system I. Therefore, a short wide-bore capillary is to be preferred above a long small-bore capillary with the same inner volume.

Another consequence of coupling capillaries

Table 1
Comparison of two extended volume systems with different inner diameters

Parameter	System I	System II
Total volume (μl)	23.7	23.7
Inner diameter (1) (μm)	100	100
Inner diameter (3) (μm)	220	100
Length (1) (m)	0.6	0.6
Length (3) (m)	0.5	2.42
Electric field strength (kV m^{-1})	3.4 ^a	3.3

^a Calculated according to Eq. 2.

with different inner diameters is the difference in EOF due to the unequal heat dissipation ΔT , proportional to the square of the inner diameter [20]:

$$\Delta T = \frac{Qd^2}{16\lambda} \quad (6)$$

where Q is the heat generated ($\lambda \text{ cm}^{-3} \text{ K}^{-1}$) and λ is the thermal conductance ($\text{W cm}^{-1} \text{ K}^{-1}$). This can result in a pressure build-up which can disturb the flow profile, especially in the T-piece section. Therefore, we constructed an Ohm's law plot (Fig. 3) to calculate the maximum voltage at which the curve begins to deviate from linearity. The voltage was *ca.* +15 kV. In this study a voltage of +10 kV was applied. Although application of higher field strengths results in shorter focusing times, perturbation of the ITP process may occur.

The T-piece does not contribute significantly to the EOF, owing to the low zeta potential in comparison with fused silica and a sharp bend (90°C) being present in the CZE channel. As a consequence, a small pressure build-up, depending on the length of the non-contributing part, will exist and possibly influence the efficiency during the CZE step. However, comparison of CZE separations without and with the T-piece (Fig. 4a and b) shows no significant differences in efficiency.

Owing to the self-regulating properties of a

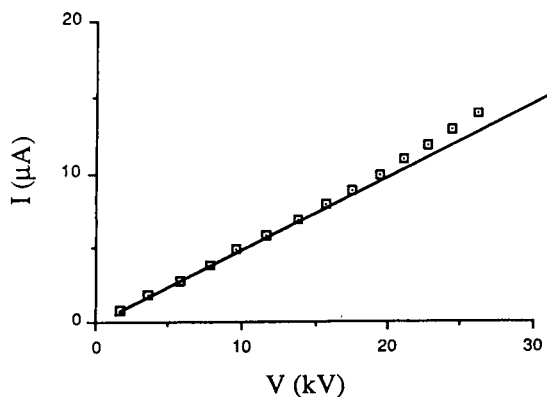


Fig. 3. Ohm's law plot for leading buffer in the coupled 100 and 220 μm I.D. capillaries. A small deviation from the ideal line, due to Joule heating, is present.

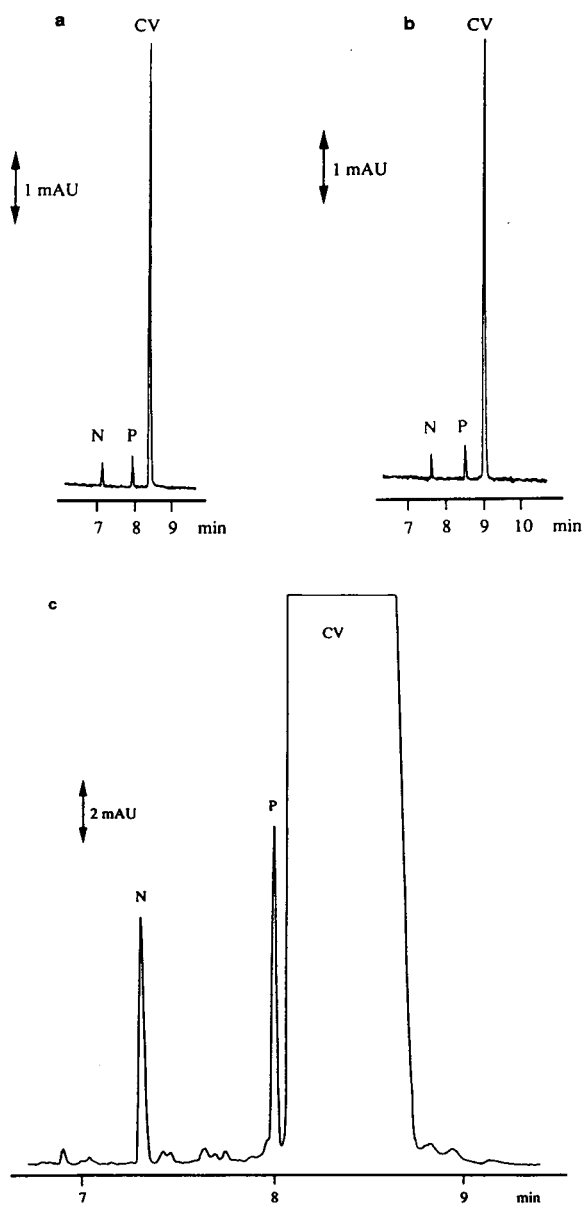


Fig. 4. Electropherograms for a 128-nl injection, (a) without and (b) with a T-piece, of $1 \cdot 10^{-6} \text{ M}$ neostigmine (N) and propantheline (P) and $1 \cdot 10^{-5} \text{ M}$ crystal violet (CV), (c) ITP-CZE of a 20.8- μl sample of $1 \cdot 10^{-7} \text{ M}$ N and P and $1 \cdot 10^{-5} \text{ M}$ CV as a visual marker. The ITP step is performed for 2.5 h using +10 kV initially, lowered to +7 kV after 1 h. The hydrodynamic counterflow is induced by a -30 mbar pressure at the capillary inlet. All samples are dissolved in terminating buffer. The CZE is performed in leading buffer using a field strength of 400 V cm^{-1} ($10.6 \mu\text{A}$). The ITP-CZE procedure is described under Experimental.

steady state in ITP, the focusing time can theoretically be infinitely long without analyte loss or band broadening and capillary connections with a relatively large dead volume, as present in our system, are applicable. Limitations to the hydrodynamic flow rate are determined by the extent in which a steady state is able to stabilize itself. Extreme conditions, *i.e.*, a strong electroosmotic flow induced by a high field strength, that is compensated by a strong counterflow, will disturb the focusing process and the steady state and, consequently, analyte loss will occur. An optimum compromise between focusing time and conditions has to be found.

3.1. Quantitative aspects

In Fig. 4b and c a comparison is made between 128 nl of $1 \cdot 10^{-6}$ M N and P without ITP preconcentration and 20.8 μ l of $1 \cdot 10^{-7}$ M N and P after ITP focusing. It can be easily seen that a dramatic increase in the detection signal was obtained. The concentration of CV in both samples was $1 \cdot 10^{-5}$ M. Although the preconcentration step took *ca.* 2.5 h, high efficiency and good resolution were still achieved.

The relative standard deviation of the peak areas with three 500-nl injections of $1 \cdot 10^{-4}$ M N, P and CV were 1.6, 4.1 and 1.7% respectively. The loading procedure was found to be satisfactorily linear over the range 2.6–20.8 μ l of sample solution. The plots of peak area and height *versus* the volumes of N and P were given by the equations $y = 0.064(\pm 0.001)x + 0.02(\pm 0.01)$ ($r^2 = 0.9997$, $n = 4$) and $y = 0.090(\pm 0.004)x - 0.01(\pm 0.05)$ ($r^2 = 0.9975$, $n = 4$), respectively, where y is in area units and x in μ l. Peak areas give better results than peak heights. This can be explained by the fact that diffusion has a relatively larger influence on short than long sample plugs during the CZE step.

As there is basically no limitation on the injection volume, detection limits are determined by the amount of background signal caused by impurities in, *e.g.*, the buffer system or solvents, and the available analysis time. Fig.

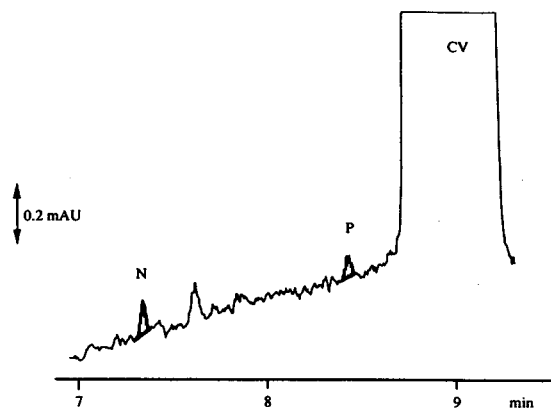


Fig. 5. ITP-CZE of a 20.8- μ l sample of $2.5 \cdot 10^{-9}$ M neostigmine (N) and propranolol (P) and $2.5 \cdot 10^{-6}$ M crystal violet (CV) as a visual marker. Experimental conditions as in Fig. 4.

5 shows the signal after focusing 20.8 μ l of $2.5 \cdot 10^{-9}$ M N, and P and $2.5 \cdot 10^{-6}$ M CV.

A larger sample volume and more selective detection will improve the detection limit.

4. Conclusions

Large sample volumes of up to 20.8 μ l of $1 \cdot 10^{-7}$ M, N and P can be preconcentrated using ITP and easily detected with UV-Vis absorbance detection. However, a long focusing time was required. The relative standard deviations of the peak areas for three 500-nl $1 \cdot 10^{-4}$ M N, P and CV injections were in the range 1.6–4.1%. Detection limits are determined by the amount of impurities that mask the analyte signal and the available analysis time, but $2.5 \cdot 10^{-9}$ M N and P could be detected. Optimization and improvement of the injection volume, determination limit, analysis time and applications are under investigation.

5. References

- [1] S.F.Y. Li, *Capillary Electrophoresis: Principles, Practice and Applications*, Elsevier, New York, 1992.
- [2] N.A. Guzman, M.A. Trebilcock and H.P. Advis, *J. Liq. Chromatogr.*, 14 (1991) 997.

- [3] A.J.J. Debets, M. Mazereeuw, W.H. Voogt, D.J. van Iperen, H. Lingeman, K.-P. Hupe and U.A.Th. Brinkman, *J. Chromatogr.*, 608 (1992) 151.
- [4] M.M. Bushey and J.W. Jorgenson, *Anal. Chem.*, 62 (1990) 978.
- [5] J. Cai and Z. El Rassi, *J. Liq. Chromatogr.*, 15 (1992) 1179.
- [6] F. Foret, V. Sustacek and P. Bocek, *J. Microcol. Sep.*, 2 (1990) 229.
- [7] D.S. Stegehuis, U.R. Tjaden and J. van der Greef, *J. Chromatogr.*, 591 (1992) 341.
- [8] D.S. Stegehuis, H. Irth, U.R. Tjaden and J. van der Greef, *J. Chromatogr.*, 538 (1992) 393.
- [9] D. Kaniansky and J. Marak, *J. Chromatogr.*, 498 (1990) 191.
- [10] V. Dolnik, K.A. Cobb and Novotny, *J. Microcol. Sep.*, 2 (1990) 127.
- [11] N.J. Reinhoud, U.R. Tjaden and J. van der Greef, *J. Chromatogr.*, 641 (1993) 155.
- [12] N.J. Reinhoud, U.R. Tjaden and J. van der Greef, *J. Chromatogr. A*, 653 (1993) 303.
- [13] R.L. Chien and D.S. Burgi, *Anal. Chem.*, 64 (1992) A489.
- [14] F. Foret, E. Szoko and B.L. Karger, *J. Chromatogr.*, 608 (1992) 3.
- [15] R.L. Chien and D.S. Burgi, *Anal. Chem.*, 64 (1992) 1046.
- [16] D.S. Burgi and R.L. Chien, *Anal. Chem.*, 63 (1991) 2042.
- [17] C. Schwer and F. Lottspeich, *J. Chromatogr.*, 623 (1992) 345.
- [18] F.E.P. Mikkers, F.M. Everaerts and T.P.E.M. Verheggen, *J. Chromatogr.*, 169 (1979) 11.
- [19] F.M. Everaerts, J.L. Beckers and T.P.E.M. Verheggen, *Isotachopheresis: Theory, Instrumentation and Practice*, Elsevier, Amsterdam, 1976.
- [20] J.H. Knox, *Chromatographia*, 26 (1988) 329.

Influence of sample injection time of ions on migration time in capillary zone electrophoresis

Hong-Wei Zhang, Xing-Guo Chen, Zhi-De Hu*

Department of Chemistry, Lanzhou University, Lanzhou, Gansu 730000, China

First received 14 December 1993; revised manuscript received 16 March 1994

Abstract

It was found that the sample injection time of ions during hydrodynamic injection affects the migration time in capillary zone electrophoresis (CZE). The relationship between sample injection time and migration time is different depending on the conditions, *i.e.*, in stacking and non-stacking runs, because the dominant factors that determine the relationship are different. In non-stacking runs, theoretically, a simple relationship is obtained, *i.e.*, the migration time decreases linearly with increasing injection time, which is identical with experimental results for different ions. For stacking runs, a new mathematical model is developed to account for the increase in migration time with increasing sample injection time. The predictions of the model agree well with experimentally determined profiles for different ions.

1. Introduction

The use of capillary electrophoresis (CE), because of its high efficiency and separation power, is growing dramatically. It was introduced by Mikkers *et al.* [1,2] and developed by Jorgenson and Lukacs [3,4]. In particular, capillary electrophoresis holds the promise of becoming the separation method of choice for bio-related compounds such as amino acids, peptides, nucleic acid and proteins.

Much work has been done to determine the influence of various factors on migration times and apparent mobilities. Issaq and co-workers [5,6] investigated the effect of the buffer type and concentration on analyte mobility and directly related the separation factor to analysis

time. Jones and Jandik [7] established an empirical correlation between ionic equivalent conductance and analyte migration time in CE. Atamna *et al.* [8] investigated the influence of the buffer cation on mobility. Mizukami *et al.* [9] investigated the relationship between migration time and pK_a in CE. Huang and Ohms [10] discussed the effect of a non-uniform electrical field on the migration behaviour of different species. Beckers and Ackermans [11] developed a model for the calculation of migration behaviour and discussed the effect of sample stacking on resolution, calibration graphs and pH shifts in capillary zone electrophoresis (CZE). Gebauer *et al.* [12] described sample self-stacking in zone electrophoresis and discussed the effect of the concentration of the major component in the sample on the elution times of the individual minor compounds. The experimental phenomenon de-

* Corresponding author.

scribed by Mikkers *et al.* [2] (Fig. 1 in ref. 2) indicated that the amount of sample injected influenced the migration behaviour. It is the aim of this paper to present a theoretical description to show how and why the sample injection length influences the migration time under stacking and non-stacking conditions.

We investigated the relationship between sample injection time of ions during hydrodynamic injection and migration time under two different conditions: stacking and non-stacking runs. Sample stacking (concentration of the analyte zone) is the process that occurs when a voltage is applied along a capillary tube containing a sample plug with a specific conductivity lower than that of the surrounding running buffer. In other words, the resistivity (ρ_1) of the sample zone is higher than that (ρ_2) of the surrounding running buffer. Moreover, because electric field strength is inversely proportional to the specific conductivity of the liquid, the field strength is higher along the sample plug compared with the running buffer. Consequently, the analyte ions in the sample plug will migrate rapidly towards the steady-state boundary between the low-concentration plug and the surrounding running buffer. Once the ions have passed the concentration boundary between the sample plug and the rest of the capillary, they immediately experience a lower electric field and slow down. As a result, the ionic analyte zone becomes narrow. This phenomenon is termed sample stacking. When the resistivity (ρ_1) of sample zone is equal to that (ρ_2) of surrounding running buffer, the field strength along the sample zone is equal to that of the running buffer. To distinguish it from the sample stacking process, we call this process non-stacking. The stacking mechanism occurs for both positive and negative ions.

The aims of this study were twofold. First, in non-stacking runs, a linear relationship between sample injection time and migration time was found. This theoretical relationship is identical with the experimental results. Second, we developed a mathematical model accounting for the changes in analyte zone length in a stacking run. From this model, the experimental relationship between sample injection length and migration time can be explained reasonably well.

2. Experimental

2.1. Instrumentation

The CE system employed was the Quanta 4000 (Waters Chromatography Division of Millipore, Milford, MA, USA) with a negative power supply. Indirect UV detection was achieved with the use of a mercury lamp and a 254-nm optical filter. Waters AccuSep fused-silica capillaries are used throughout. The capillary dimensions were 60 cm total length with a 52-cm distance from point of injection to the centre of detector cell. Both 75 and 100 μm I.D. capillaries were used. Data acquisition was carried out with a Maxima 820 Chromatography Workstation (Waters) with a System Interface module (SIM) connecting the CE system to the station. The detector time constant was set at 0.1 s and the data acquisition rate was 20 points s^{-1} . Collection of electrophoretic data was initiated by a signal cable connection between the Quanta 4000 and the SIM.

2.2. Preparation of support electrolytes

The chromate electrolytes used for CE were prepared from a concentrate containing 100 mM Na_2CrO_4 (analytical-reagent grade) and 0.68 mM H_2SO_4 . When preparing both a 5 mM chromate and a 10 mM chromate supporting electrolyte, the concentration of electroosmotic flow modifier (OFM Anion-BT; Waters) was 0.5 mM. In both instances, the dilute sulphuric acid was added to the chromate concentrate to pre-adjust the electrolyte pH to 8.0.

2.3. Standard solutions

Experiments were divided into two series, with stacking and non-stacking runs.

Stacking

The concentration of the supporting electrolyte was 5 mM (pH 8.0). The samples of NaNO_3 , Na_2SO_4 and KBr were dissolved in and diluted with distilled, deionized water to $5.0 \cdot 10^{-5}$ M. The conductivity of the supporting electrolyte was $10.5 \cdot 10^2 \mu\text{S cm}^{-1}$ and the con-

ductivities of the NaNO_3 , Na_2SO_4 and KBr sample solutions were 11.0, 12.1 and $9.7 \mu\text{S cm}^{-1}$, respectively.

Non-stacking

Sample solutions of NaNO_3 , Na_2SO_4 and KBr were prepared in a buffer identical with that used as the supporting electrolyte. The concentration of the supporting buffer was increased to 10 mM and the concentration of sample ions was chosen to be sufficiently low ($2.5 \cdot 10^{-5} M$) that the relative difference in conductivity between the buffer and the sample ions was small enough to be negligible. The conductivity of the supporting electrolyte was $18.9 \cdot 10^2 \mu\text{S cm}^{-1}$ and the conductivities of the sample solutions of NaNO_3 , Na_2SO_4 and KBr were 1950, 1930 and $1910 \mu\text{S cm}^{-1}$, respectively.

2.4. System operation

Gravity injection was used in the experiments because of its simplicity and because it does not have the bias involved in electromigration injection. A 3-min capillary purge was performed prior to all injections. The purge was accomplished with a 12–15 p.s.i. vacuum (1 p.s.i. = 6894.76 Pa) applied to the receiving electrolyte vial.

3. Results and discussion

3.1. Non-stacking

Under non-stacking conditions, with a short injection plug, the electropherogram displays a sharp peak, and with a long injection plug, the electropherogram displays a peak with characteristic flat-topped shape, which is shown in Fig. 1. In the latter instance, it is assumed that on the electropherogram the migration time is the time to which the centre of the flat top of the “trapezoid” corresponds (see Fig. 1). For non-stacking runs, there is no concentration stacking and the diffusion is towards both sides of the sample zone; this means the diffusion does not influence migration time. Hence, with the above

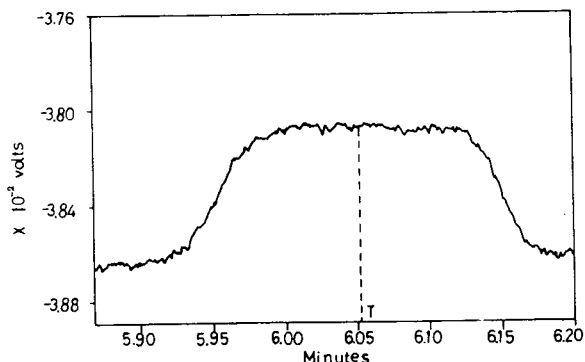


Fig. 1. Electropherogram of SO_4^{2-} in a non-stacking run with a 30-s injection length. The time to which the centre of the flat top of the “trapezoid” corresponds is the migration time of SO_4^{2-} . Experimental conditions are given in Fig. 3.

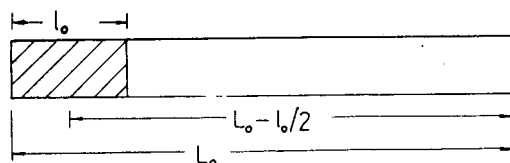


Fig. 2. Effect of injection length on the distance from the centre of the initial sample injection plug to the centre of the detector.

assumption, only one factor needs to be considered when investigating the influence of sample injection length on migration time, namely that different initial sample injection lengths cause different effective distances from the centre of the initial sample injection length to the detector. This effect is shown schematically in Fig. 2, where L_0 is the length of the capillary to the optical centre of detector, l_0 is the initial sample length and $L_0 - l_0/2$ is the distance from the centre of the initial sample injection to detector. The initial sample length l_0 is related to the migration time T by the equation

$$T = \frac{L_0 - l_0/2}{(\mu_e + \mu_{eo})E} = \frac{(L_0 - l_0/2)V}{(\mu_e + \mu_{eo})L} \quad (1)$$

where V = applied voltage, L = total length of capillary, μ_e = electrophoretic mobility and μ_{eo} = coefficient of electroosmotic flow. Moreover, l_0 is expressed by the equation

$$l_0 = t_i V_i \quad (2)$$

where t_i is the sample injection time and V_i is the average injection velocity, which is assumed to be a constant for different injection times. Eq. 2 can be substituted into Eq. 1 to yield

$$T = \frac{(L_0 - V_i t_i / 2)V}{(\mu_e + \mu_{eo})L} \quad (3)$$

For a given system, L_0 , V , μ_e , μ_{eo} , L and V_i are constants, so from Eqs. 1 and 3, it can be concluded that the migration time T decreases linearly with increasing sample injection length l_0 or sample injection time t_i .

To confirm this analysis, we carried out the following experiment. Migration times T were measured with different injection times t_i for three different anions in non-stacking runs. Fig. 3 shows T as a function of t_i for three different anions, Br^- , SO_4^{2-} and NO_3^- . At first glance there may be a false impression that the migration velocity of analyte ions in a capillary increases with increasing sample injection length. Actually, the essence of the plots is that the

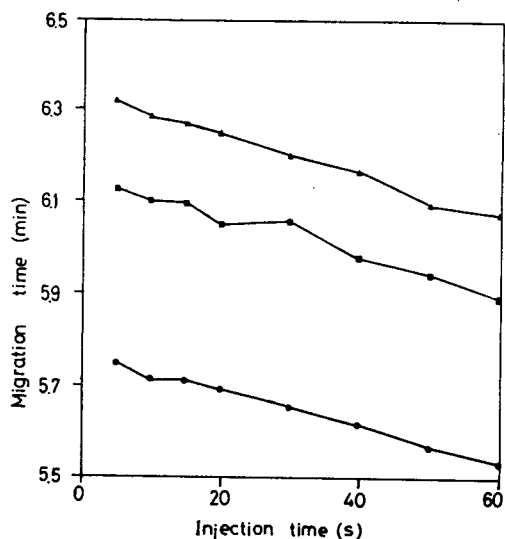


Fig. 3. Measured relationship between migration time and injection time for (▲) nitrate, (■) sulphate and (●) bromide in non-stacking runs. The samples ($2.5 \cdot 10^{-5}$ M) were prepared in the supporting electrolyte, which is 10 mM chromate–0.5 mM OFM Anion-BT (pH 8.0). Capillary: I.D. 100 μm , $L = 60$ cm and $L_0 = 52.5$ cm. Applied negative voltage, 10 kV. Detection at 254 nm.

sample injection length does not affect the migration velocity of analyte ions or, in other words, the migration velocity of an ion is the same at different injection times. The plots are not horizontal lines, but sloping, for the same reason as above, *i.e.*, that different initial sample injection lengths lead to different distances from the centre of the initial sample injection length to the detector. In our experiments, obviously larger injection times (60 s or 4.2 cm or 330 nl) were included, because our interest was in the relationship between t_i and T rather than peak spreading. The same applies to the experiments with stacking runs. We observed that the migration time decreases approximately linearly with increasing injection time t_i in all instances. These experimental results are in agreement with theoretical predictions. Regression analysis was performed for experimental data on t_i and T , and the correlation coefficients were 0.996 for Br^- , 0.995 for NO_3^- and 0.98 for SO_4^{2-} . These correlation coefficients provide a good confirmation of Eq. 3. It also holds for different electrolytes and different experimental conditions such as capillary dimensions, applied voltages and electric field strength.

3.2. Stacking

In stacking runs, how does the sample injection time influence the migration time? First, we carried out the following experiments. We measured the migration times T with different injection times t_i for different ions in stacking runs. The migration time T was plotted as a function of the sample injection time t_i for three anions, Br^- , SO_4^{2-} and NO_3^- , as shown in Figs. 4, 5 and 6, respectively. T increases non-linearly with increasing t_i . Evidently, the relationship is completely different and the trend is opposite to those for non-stacking runs. In an attempt to describe and explain these experimental results, a theoretical approach to simulate the stacking process is presented below.

Description of migration in stacking runs

In the whole process of a sample zone running from the inlet to the outlet of the capillary, the

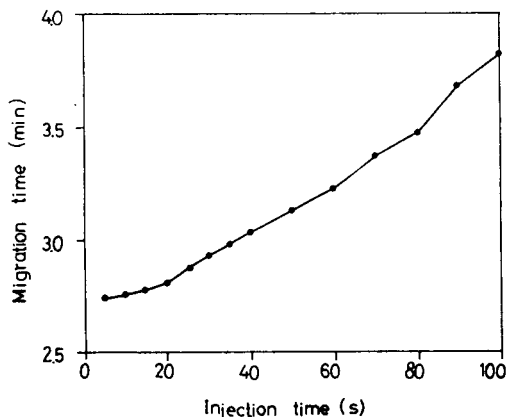


Fig. 4. Measured relationship between migration time and injection time for bromide ($5.0 \cdot 10^{-5} M$) in stacking runs. Supporting electrolyte, 5 mM chromate–0.5 mM OFM Anion-BT (pH 8.0). Capillary: I.D. 75 μm , $L = 60$ cm and $L_0 = 52.5$ cm. Applied negative voltage, 20 kV. Detection at 254 nm.

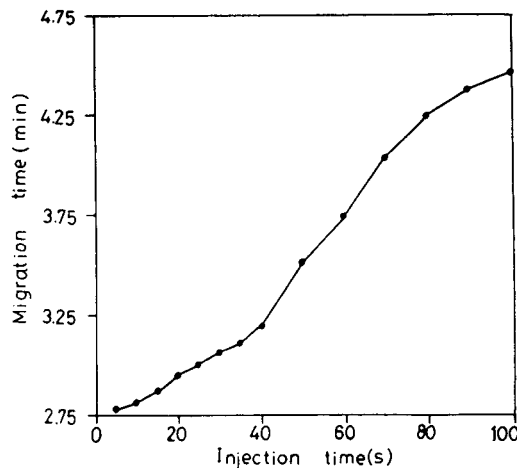


Fig. 6. Measured relationship between migration time and injection time for nitrate ($5.0 \cdot 10^{-5} M$) in stacking runs. Conditions as in Fig. 5.

sample zone length changes all the way; in other words, the sample zone length is a function of time. The concentration of the sample in the capillary also changes with time owing to the changes in the sample zone length, so the electric resistivity of the sample zone is also a function of

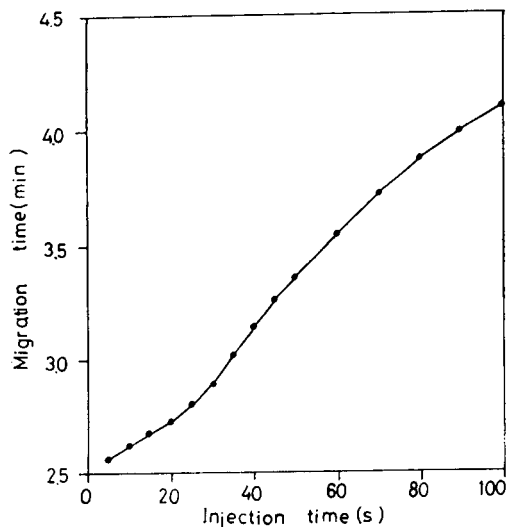


Fig. 5. Measured relationship between migration time and injection time for sulphate ($5.0 \cdot 10^{-5} M$) in stacking runs. Conditions as in Fig. 4, except for the capillary I.D. (100 μm).

time. In the same way, the changes in the sample zone length lead to corresponding changes in the electric resistance, the voltage and the electric field strength of the sample zone, so these parameters are also a function of time. For the running buffer, it is assumed that its resistivity is approximately constant, *i.e.*, not a function of time. This assumption holds because the properties and concentration of the buffer hardly change with time, whereas the electric resistance, the voltage and the electric field strength of the buffer zone are all functions of time, owing to the changes in the sample zone length.

The following symbols corresponding to the above physical parameters are used in the subsequent mathematical treatment: $l(t)$ = length of sample zone at the moment t ; $\rho_1(t)$ = electric resistivity of sample zone at moment t ; $R_1(t)$ = electric resistance of sample zone at moment t ; $V_1(t)$ = voltage of sample zone at moment t ; $E_1(t)$ = electric field strength of sample zone at moment t ; $R_2(t)$ = electric resistance of buffer zone at moment t ; $V_2(t)$ = voltage of buffer zone at moment t ; $E_2(t)$ = electric field strength of buffer zone at moment t ; $L - l(t)$ = length of buffer zone at moment t ; ρ_0 = resistivity of sample zone when $t = 0$ or $l(t) = l_0$; and ρ_2 = resistivity of buffer.

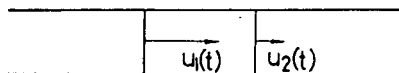


Fig. 7. Schematic representation of sample stacking in a stacking run. In the mathematical model it is assumed that the terminating edge of the analyte zone migrates faster than the leading edge, thus reducing the zone length.

In our model, it is assumed that the total amount of analyte is conserved in the sample zone during the stacking period [13]. Moreover, it is assumed that the coefficient of electroosmotic flow (μ_{eo}) in the sample is equal to that in buffer zone and both of them are constants. The electrophoretic mobility (μ_e) of the sample is also constant. Sample stacking is shown schematically in Fig. 7 [13]. The leading edge of the analyte zone migrates with a velocity $u_2(t)$ in an electric field of strength $E_2(t)$ at moment t . The terminating edge of the analyte zone migrates with a velocity $u_1(t)$ in an electric field of strength $E_1(t)$ at moment t . The velocity of the analyte between the two edges is also $u_1(t)$. These two velocity expressions are, respectively,

$$u_2(t) = (\mu_{eo} + \mu_e)E_2(t) \quad (4)$$

$$u_1(t) = (\mu_{eo} + \mu_e)E_1(t) \quad (5)$$

The resistances of the analyte and buffer zones are given by

$$R_1(t) = \rho_1(t) \cdot \frac{l(t)}{s} \quad (6)$$

$$R_2(t) = \rho_2 \cdot \frac{L - l(t)}{s} \quad (7)$$

respectively, where s is the cross-sectional area of the capillary. From Eqs. 6 and 7, the voltages of the analyte and buffer zones can be expressed by, respectively,

$$V_1 = \frac{\rho_1(t) \cdot \frac{l(t)}{s}}{\rho_1(t) \cdot \frac{l(t)}{s} + \rho_2 \cdot \frac{L - l(t)}{s}} \cdot V \quad (8)$$

$$V_2 = \frac{\rho_2 \cdot \frac{L - l(t)}{s}}{\rho_1(t) \cdot \frac{l(t)}{s} + \rho_2 \cdot \frac{L - l(t)}{s}} \cdot V \quad (9)$$

Then the expressions of the electric field strengths of analyte and buffer zones are, respectively [11],

$$E_1(t) = \frac{\rho_1(t)}{\rho_1(t)l(t) + \rho_2[L - l(t)]} \cdot V \quad (10)$$

$$E_2(t) = \frac{\rho_2}{\rho_1(t)l(t) + \rho_2[L - l(t)]} \cdot V \quad (11)$$

Obviously, before sample stacking finishes, $\rho_1(t) > \rho_2$, so $E_1(t) > E_2(t)$ and, as a result, $u_1(t) > u_2(t)$. The terminating edge migrates faster than the leading edge, so the sample zone becomes narrow.

In a stacking run, because of sample stacking, the peak shape, unlike the flat-topped shape in a non-stacking run, is sharp. The measured migration time T to which the maximum response of the detector system corresponds is the time required for the leading edge of the analyte zone to migrate in the capillary (see Fig. 7). Based on this approximation, the migration time T of analyte zone is determined by the following integral equation:

$$\int_0^T (\mu_{eo} + \mu_e)E_2(t) dt = L_0 \quad (12)$$

Eq. 11 can be substituted into Eq. 12 to yield

$$\rho_2 V (\mu_{eo} + \mu_e) \int_0^T \{[\rho_1(t) - \rho_2]l(t) + \rho_2 L\}^{-1} dt = L_0 \quad (13)$$

Further, because the resistivity of strong electrolyte solution is inversely proportional to the solution concentration, $\rho_1(t)$ can be expressed as

$$\rho_1(t) = \frac{A}{n} = \frac{Asl(t)}{nl(t)s} \quad (14)$$

where A is a constant and n is total number of moles of electrolyte in the analyte zone. For a given system, n and s are also constants, so Eq. 14 can be simplified to

$$\rho_1(t) = kl(t) \quad (15)$$

where $k = As/n$. The constant k can be determined by the following equation:

$$k = \rho_0/l_0 \quad (16)$$

The combination of Eqs. 13, 15 and 16 leads to

$$\rho_2 V (\mu_{e0} + \mu_e) \int_0^T \{[\rho_0 l(t)/l_0 - \rho_2] l(t) + \rho_2 L\}^{-1} dt = L_0 \quad (17)$$

It is difficult to determine how the sample injection length l_0 influences the migration time T from Eq. 17, because $l(t)$ is also related to l_0 , so it is necessary to establish the mathematical model for $l(t)$.

Mathematical model for $l(t)$

In investigating the influence of the sample injection length l_0 on the migration time T in stacking runs, the dominant factor that needs to be considered is that different injection times lead to different electric field strengths in the buffer zone, which affects the migration velocity of the analyte zone, whereas the diffusional effects on the migration velocity of the analyte zone are negligible. Therefore, in the following mathematical model, we consider only the effect of sample stacking on $l(t)$ in order to simplify the process. We define $\Delta u(t)$ as

$$\Delta u(t) = u_1(t) - u_2(t) \quad (18)$$

The combination of Eqs. 4, 5, 10 and 11 now provides an expression for $\Delta u(t)$:

$$\Delta u(t) = \frac{(\mu_{e0} + \mu_e)V}{\rho_1(t)l(t) + \rho_2[L - l(t)]} [\rho_1(t) - \rho_2] \quad (19)$$

Eq. 19 can be arranged and rewritten as

$$\Delta u(t) = \frac{(\mu_{e0} + \mu_e)V}{l(t) + \rho_2 L [\rho_1(t) - \rho_2]^{-1}} \quad (20)$$

where $(\mu_{e0} + \mu_e)V$ is a constant for a given system. Combining Eqs. 15 and 20 gives

$$\Delta u(t) = \frac{(\mu_{e0} + \mu_e)V}{\frac{1}{k} \cdot \rho_1(t) + \rho_2 L [\rho_1(t) - \rho_2]^{-1}} \quad (21)$$

In Eq. 21, as $\rho_1(t)$ decreases and approaches ρ_2 , the term $\rho_1(t) - \rho_2$ decreases and tends to zero, which leads to the term $\rho_2 L [\rho_1(t) - \rho_2]^{-1}$ increasing and approaching infinity as a limit, and the

term $(1/k)\rho_1(t)$ in the denominator decreases and tends to $(1/k)\rho_2$, which is a constant. Therefore, the conclusion can be drawn that $\Delta u(t)$ decreases and approaches zero as a limit with decrease in $\rho_1(t)$. Moreover, because of the relationship in Eq. 15, the same conclusion for $l(t)$ can be drawn: $\Delta u(t)$ decreases and tends to zero with shortening of $l(t)$.

Now we analyse the change in $l(t)$ in a stacking run to establish its mathematical model. At the beginning of analyte zone stacking, the analyte zone l_0 is longest, so the initial rate $\Delta u(t)$ of sample stacking is highest, which leads to the analyte zone $l(t)$ becoming shorter extremely rapidly. In turn, the shorter $l(t)$ causes a decrease in $\Delta u(t)$, which in turn generates a slower shortening of $l(t)$. Consequently, the overall effect is that $l(t)$ becomes shorter extremely rapidly at the beginning, but considerably more slowly after a few seconds. With the shortening of $l(t)$, $\Delta u(t)$ becomes smaller and smaller, and finally tends to zero, which in turn makes $l(t)$ becoming shorter more and more slowly, finally approaching a limit. The limit is represented by a horizontal asymptote: $l(t) = l_{\min}$. When $t = \infty$, then $l(t) = l_{\min}$. The sample stacking model is simulated as shown in Fig. 8. The profile tends towards the exponential decay form as l_{\min} :

$$l(t) = (l_0 - l_{\min}) e^{-at} + l_{\min} \quad (22)$$

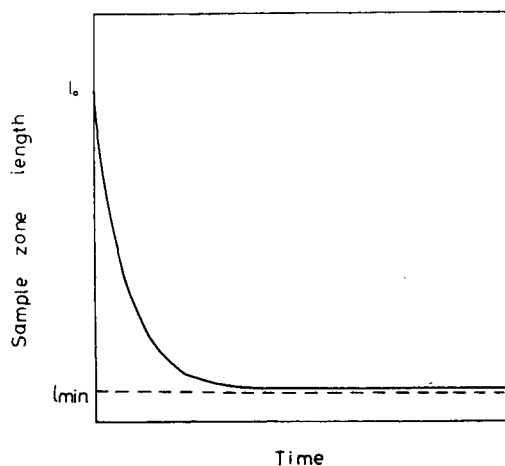


Fig. 8. Mathematical model, $l(t)$ vs. t , in a stacking run. The units are arbitrary.

where a is a positive constant. It can be noted from Eq. (22) that

$$\text{when } t = 0, l(t) = l_0$$

$$\text{when } t = \infty, l(t) = l_{\min}$$

We observe that $l(t)$ becomes short initially very rapidly, but soon slows considerably and finally approaches a limit. The simulated equation is identical with the above analysis.

Relationship between l_0 and T

From Eq. 15, the following relationship can be obtained

$$\rho_2 = kl_{\min} \quad (23)$$

The combination of Eqs. 15, 23 and 22 leads to

$$l(t) = [(1 - \rho_2/\rho_0) e^{-at} + \rho_2/\rho_0] l_0 \quad (24)$$

Now we have the relationship between $l(t)$ and l_0 . On substitution of Eq. 24 into Eq. 17, the following relationship can be obtained:

$$\begin{aligned} \rho_2 V (\mu_{e_0} + \mu_e) \int_0^T \{(\rho_0 - \rho_2 e^{-at}) \\ [(1 - \rho_2/\rho_0) e^{-at} + \rho_2/\rho_0] l_0 + \rho_2 L\}^{-1} dt \\ = L_0 \end{aligned} \quad (25)$$

Eq. 25 is the final equation describing the relationship between the length of sample injection l_0 and migration time T . The parameters ρ_2 , V , μ_{e_0} , μ_e , ρ_0 , L and a are constants. The term $\rho_0 - \rho_2 e^{-at}$ is positive at any moment t of a stacking run because $\rho_0 > \rho_2$ and $\rho_2 e^{-at}$ decreases with time t ; the term $(1 - \rho_2/\rho_0) e^{-at}$ is also positive at any moment t of a stacking run because $\rho_0 > \rho_2$, and the term $\rho_2 L$ is a constant, so the overall term in the denominator $(\rho_0 - \rho_2 e^{-at})[(1 - \rho_2/\rho_0) e^{-at} + \rho_2/\rho_0] l_0 + \rho_2 L$ increases with increasing l_0 at any moment t . That is, the integrand in Eq. 25 decreases with increasing l_0 . Therefore, it can be concluded that with increase in l_0 , the migration time T increases, which is in agreement with the experimental results. Our model is also confirmed by the experimental results of Mikkers *et al.* [2] (Fig. 1 in ref. 2) which indicated that with increasing injection amount, the migration time also increases. It should be emphasized that our theoretical model is developed for strong elec-

trolytes. Eq. 25 is complicated and its further detailed mathematical solution and confirmation are currently being investigated.

Under non-stacking conditions, from Fig. 3, if the difference in two injection times is 40 s, the migration time changes by 9 s for Br^- , 10 s for SO_4^{2-} and 11 s for NO_3^- (about 3% of the migration time). Under stacking conditions, from Figs. 4, 5 and 6, if the injection time changes from 0 to 40 s, the migration time changes by about 15 s for Br^- (about 9% of the migration time), 33 s for SO_4^{2-} (about 20% of the migration time) and 27 s for NO_3^- (about 15% of the migration time). Obviously, the influence of injection time on migration time for a stacking run is greater than that for a non-stacking run. In the present experiments, in a non-stacking run, if the injection time exceeds 40 s it significantly influences the migration time; in a stacking run, if the injection time exceeds 20 s it significantly influences the migration time.

Although large injection volumes lower the separation performance, in practical analyses by CZE for the determination of compounds present in samples at very low concentrations (*e.g.*, in the EC drinking-water directive, the concentration of any pesticide should be lower than 0.1 ppb) [14], large injection volumes have to be applied in order to introduce a detectable amount of the analytes. Moreover, in CZE, special injection methods have been developed and allow the introduction of samples as large as the entire volume of the separation capillary [14–16]. Therefore, a large injection length is sometimes necessary. From our work, however, it should be noted that a large injection length leads to changes in migration time compared with a small injection length, so qualitative evaluations of electropherograms based on migration time must be performed with great care when the injection lengths vary.

4. Conclusions

In non-stacking runs, because a different initial sample injection length causes different distance from the centre of the initial sample

injection length to the centre of the detector cell, consequently the migration time decreases with increasing sample injection time, which exactly reflects that the sample injection time does not affect the migration velocity of analyte ions. In stacking runs, the opposite experimental phenomenon was observed compared with non-stacking runs, because an increase in sample injection time decreases the migration velocity of analyte ions. In both instances, the experimental results and theoretical predictions are in agreement.

Acknowledgement

Thanks are expressed to the National Natural Science Foundation of China for financial support.

References

- [1] F.E.P. Mikkers, F.M. Everaerts and Th.P.E.M. Verheggen, *J. Chromatogr.*, 169 (1979) 1.
- [2] F.E.P. Mikkers, F.M. Everaerts and Th.P.E.M. Verheggen, *J. Chromatogr.*, 169 (1979) 11.
- [3] J.W. Jorgenson and K.D. Lukacs, *Anal. Chem.*, 53 (1981) 1298.
- [4] J.W. Jorgenson and K.D. Lukacs, *J. Chromatogr.*, 218 (1981) 209.
- [5] H.J. Issaq, I.Z. Atamna, C.J. Metral and G.M. Muschik, *J. Liq. Chromatogr.*, 13 (1990) 1247.
- [6] H.J. Issaq, I.Z. Atamna, G.M. Muschik and G.M. Janini, *Chromatographia*, 32 (1991) 155.
- [7] W.R. Jones and P. Jandik, *J. Chromatogr.*, 546 (1991) 445.
- [8] I.Z. Atamna, C.J. Metral, G.M. Muschik and H.J. Issaq, *J. Liq. Chromatogr.*, 13 (1990) 2517.
- [9] M. Mizukami, N. Nimura, T. Kinoshita, T. Hanai and H. Hatano, *J. High Resolut. Chromatogr. Chromatogr. Commun.*, 14 (1991) 561.
- [10] X. Huang and J.I. Ohms, *J. Chromatogr.*, 516 (1990) 233.
- [11] J.L. Beckers and M.T. Ackermans, *J. Chromatogr.*, 629 (1993) 371.
- [12] P. Gebauer, W. Thormann and P. Bocek, *J. Chromatogr.*, 608 (1992) 47.
- [13] A. Vinther and H. Soeberg, *J. Chromatogr.*, 559 (1991) 3.
- [14] M.W.F. Nielen, *Trends Anal. Chem.*, 12 (1993) 345.
- [15] R.L. Chien and D.S. Burgi, *Anal. Chem.*, 64 (1992) 1046.
- [16] D.S. Burgi and R.L. Chien, *Anal. Chem.*, 63 (1991) 2042.



ELSEVIER

Journal of Chromatography A, 677 (1994) 169–177

JOURNAL OF
CHROMATOGRAPHY A

Polymerase chain reaction heteroduplex polymorphism analysis by entangled solution capillary electrophoresis

Jing Cheng^a, Takao Kasuga^a, Keith R. Mitchelson^{a,*}, Eric R.T. Lightly^b,
Nigel D. Watson^c, William J. Martin^b, David Atkinson^d

^aDepartment of Molecular and Cell Biology, University of Aberdeen, Aberdeen AB9 1AS, UK

^bDepartment of Technology Development, Rowett Research Institute, Greenburn Road, Bucksburn, Aberdeen AB2 9SB, UK

^cForensic Science Unit, Department of Pure and Applied Chemistry, University of Strathclyde, 204 George Street, Glasgow G1 1XW, UK

^dLand Resources Department, Scottish Agriculture College, 581 King Street, Aberdeen AB9 1UD, UK

First received 7 March 1994; revised manuscript received 5 April 1994

Abstract

Heteroduplex DNA polymorphism analysis (HPA) makes use of conformational polymorphisms to alter electrophoretic mobility of fragments and can be used to detect non-restrictable loci. We have developed a novel application of entangled solution capillary electrophoresis (ESCE) to separate heteroduplex and homoduplex DNA molecules. The addition of ethidium bromide and glycerol to the free solution sieving buffer resulted in the improved peak resolution and good reproducibility. Reannealed polymerase chain reaction products could be used directly for mutation screening and with fully automated ESCE the entire HPA may be completed in less than 30 min including sample handling. This technology could provide a rapid and highly efficient way for screening rare mutations among large numbers of individuals.

1. Introduction

High-performance capillary electrophoresis (HPCE) has been increasingly used for discriminating DNA length polymorphism in many areas of medical science [1,2], agriculture and biological analysis [3]. It has been applied to the rapid analysis of double-stranded DNA (dsDNA) [1,4] and single-stranded DNA (ssDNA) [5,6] where reliability, speed and automated data handling are an advantage.

The great demands for identifying disease-causing genes and characterizing the mutations

that disrupt them has enabled substantial progress in the development and application of various mutation-scanning methods. Sequence polymorphisms in polymerase chain reaction (PCR)-amplified DNA fragments can be efficiently detected by techniques such as denaturing gradient gel electrophoresis [7], single-stranded conformation polymorphism analysis [8], RNase A cleavage [9], chemical cleavage of mismatch [10] and heteroduplex polymorphism assay (HPA) [11]. Among these techniques HPA has proved to be one of the most sensitive and simple methods for mutation detection and therefore has found application in many areas, especially in medical research [12–15]. However,

* Corresponding author.

conventionally HPA has used polyacrylamide gel electrophoresis (PAGE). Heteroduplex molecules with single, or low numbers of mismatches are often resolved poorly or not at all by PAGE.

We report here a method for heteroduplex DNA polymorphism analysis using entangled solution capillary electrophoresis (ESCE) and non-denaturing conditions. Using our conditions, heteroduplex DNA of 126 base pairs (bp) with a single-nucleotide mismatch can be differentiated from the homoduplex in less than 30 min. In addition, PCR products were applied directly for the analysis without any pre-treatment. The conditions for this pilot analysis have not been previously reported, although the resolution of heteroduplex with single-base substitution has very recently been achieved using constant denaturant CE [16].

2. Experimental

2.1. DNA

Φ X174 DNA Hae III digest (Sigma) was used as the molecular mass marker and diluted to a concentration of 20 ng/ μ l before injection.

Separate PCR reactions were performed in a total mixture of 25 μ l with 50 mM KCl, 10 mM Tris-HCl, pH 8.3, 1.5 mM MgCl₂, 200 μ M each of deoxyadenosine 5'-triphosphate, deoxycytidine 5'-triphosphate, deoxyguanosine 5'-triphosphate and thymidine 5'-triphosphate, 25 μ g gelatine, 225 nM primer oligonucleotides and 0.5 units of Taq DNA polymerase (Boehringer) with 5 ng template DNA from each of four European *Heterobasidion annosum* genotypes [17]. Oligonucleotides were fungal rRNA primers: HA1 (5'-TTAGCGAGACCCTTGTGGTG-3') and HA2 (5'-GATTTGAGGTCAAGTTTCGA-3') which amplify part of the intergenic transcribed spacer region flanking the 5.8S rRNA gene (S = Svedberg unit = 10⁻¹³ s).

Heteroduplex DNAs were prepared as follows: 10 μ l of each of the two PCR products were mixed in a 0.5-ml Eppendorf tube, heated to 94°C for 5 min and then allowed to cool slowly to room temperature. The DNAs were then

maintained at this temperature until electrokinetic loading onto the capillary.

2.2. Buffer

The stock buffer system for ESCE consisted of 90 mM Tris base, 90 mM boric acid, 2 mM EDTA, pH 8.5 (1 \times TBE), to which 0.5% (w/v) hydroxypropylmethylcellulose (HPMC) was added. The viscosity of a 2% aqueous solution of this cellulose derivative (H-7509, Sigma) was 4000 cP at 25°C. The HPMC was dissolved into the 1 \times TBE buffer using the method recommended by Ulfelder et al. [2]. Ethidium bromide (3 μ M) and 4.8% (v/v) of glycerol (final concentrations) were then added to the above solution. The buffer was filtered using a 0.2- μ m filter and kept at 4°C before use.

2.3. Capillary electrophoresis

ESCE was performed on the P/ACE system 2050 (Beckman) in the reversed-polarity mode (negative potential at the injection end of the capillary). The temperature was set at 22°C and UV absorbance was monitored at 260 nm. Post-run analysis of data was performed using the Gold Chromatography Data System (version 7.11). Surface-modified fused-silica capillary, DB-17 (J & W Scientific) was used for all analysis. The capillary (57 cm \times 100 μ m with effective length of 50 cm) was conditioned daily with five volumes of the above-mentioned buffer and then subjected to voltage equilibration for 15 min until a stable baseline was achieved. Samples were introduced into the capillary by electrokinetic injection at negative polarity of 175 V/cm for 13 s. Separations were performed under constant voltage at 228 V/cm for 30 min. The capillary was rinsed with two column volumes of the buffer after each run prior to the next injection.

3. Results and discussion

In a typical heteroduplex mixture four DNA fragments are present. They include two

homoduplex DNA fragments AB and A'B', and two corresponding heteroduplex DNA fragments AB' and A'B. Electrophoretic migration of mismatched heteroduplex DNAs is retarded relative to homoduplex DNA because of conformational distortion created by the mismatched region(s).

PCR-amplified products from the ITS2 region of *H. annosum* rRNA gene repeat were used in a HPA assay for mutation detection using ESCE. Three intersterility groups (S, F and P) can be distinguished by the sequence variations in the ITS regions [17]. The amplification products formed a series of molecules which differ by a range of mutations from a single-base substitution to three deletions and three-base substitutions (see Table 1). The details of these sequence variations are also shown in Fig. 1. Despite the variety of mismatches present in the heteroduplex molecules, fractionation by conventional PAGE does not clearly resolve all molecular species (data not shown). In addition, heteroduplex bands appear diffuse. This may be due to multiple and changing conformations assumed by the heteroduplex molecules, or may be due to insufficient heat dissipation in conventional PAGE.

To establish the buffer system the separation of Φ X174 DNA Hae III digest marker was examined by CE. Glycerol and ethidium bromide were introduced into the entangled polymer sieving buffer which is basically the 1 × TBE buffer with 0.5% (w/v) HPMC (Fig. 2a). Ethidium bromide has previously been reported to improve the resolution of dsDNA fragments by CE [18]. Ethidium bromide preferentially intercalates into G + C-rich sequence, increasing the chain length and altering the mobility of

S_{Fi}: HA1----T-----XX---A--G--A----C----HA2 (125 bp)
 S_{Ha37}: HA1----C-----XX---A--G--A----C----HA2 (125 bp)
 F_{It}: HA1----C-----XX---A--G--X----C----HA2 (124 bp)
 P_{GB}: HA1----C-----TG---G--A--A----T----HA2 (127 bp)

Fig. 1. Illustration of the base differences among the PCR-amplified products from samples S_{Fi} (S strain), S_{Ha37} (S strain), F_{It} (F strain) and P_{GB} (P strain) of *H. annosum*. HA1/HA2 are *H. annosum* specific oligos (17 bp). X indicates the absence of a nucleotide residue. Homoduplex DNAs are 125 bp for S_{Fi}, 125 bp for S_{Ha37}, 124 bp for F_{It} and 127 bp for P_{GB}.

some DNA fragments. Here it was found that the addition of glycerol improved the resolution and reproducibility in the separation of all DNA fragments especially for these ranging from 200 to about 1200 bp regardless of the G + C content, but also retarded the migration of the DNA (see Fig. 2b and c). The detailed study will be reported elsewhere. The best resolution was achieved by the addition of both glycerol and ethidium bromide (Fig. 2a).

Homoduplex and heteroduplex PCR mixtures from S_{Fi} (S strain) and F_{It} (F strain) were separated by ESCE and shown in Fig. 3. From the electropherograms it can be clearly seen that two PCR-amplified DNA fragments differing by one base deletion and one base substitution (1D + 1S/1B) are well resolved by ESCE in less than 20 min. Pre-treatment of PCR products such as desalting and deproteinising are not necessary. In our hands, ESCE with desalted heteroduplex molecules did not improve resolution between peaks but did increase both the detection and the mobility of all species (results not shown). The gain in run speed and sensitivity

Table 1
Pair-wise comparison of the differences among the PCR products

	S _{Ha37}	S _{Fi}	F _{It}	P _{GB}
S _{Ha37}	0	0D + 1S/0B	1D + 0S/1B	2D + 3S/2B
S _{Fi}		0	1D + 1S/1B	2D + 4S/2B
F _{It}			0	3D + 3S/3B
P _{GB}				0

D = Deletion; S = substitution; B = base pairs.

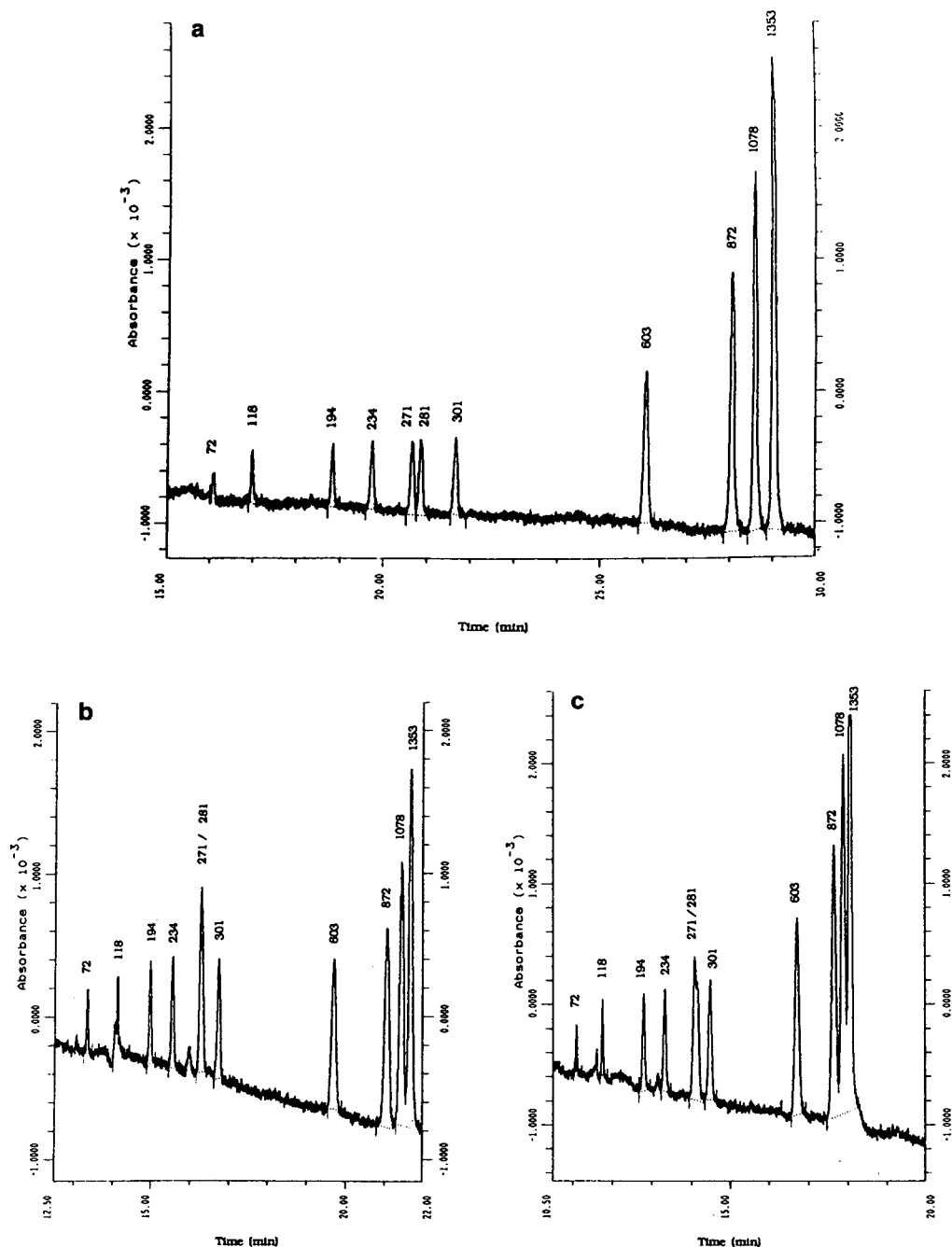


Fig. 2. Electropherograms of Φ X174 DNA Hae III digest marker (diluted to 20 ng/ml with water) obtained using the sieving buffer (a) with both glycerol (4.8%, v/v) and ethidium bromide ($3 \mu\text{M}$), (b) without ethidium bromide and (c) without glycerol and ethidium bromide. The unit of the DNA fragment length is base pairs. The sample was electrokinetically loaded into the capillary (DB-17, $57\text{cm} \times 100 \mu\text{m}$, the effective length was 50 cm) at 175 V/cm for 10 s. The separation was carried out at 228 V/cm for 30 min. The UV absorbance was monitored at 260 nm. The temperature of the external surface of the capillary was maintained between $23 \pm 0.3^\circ\text{C}$.

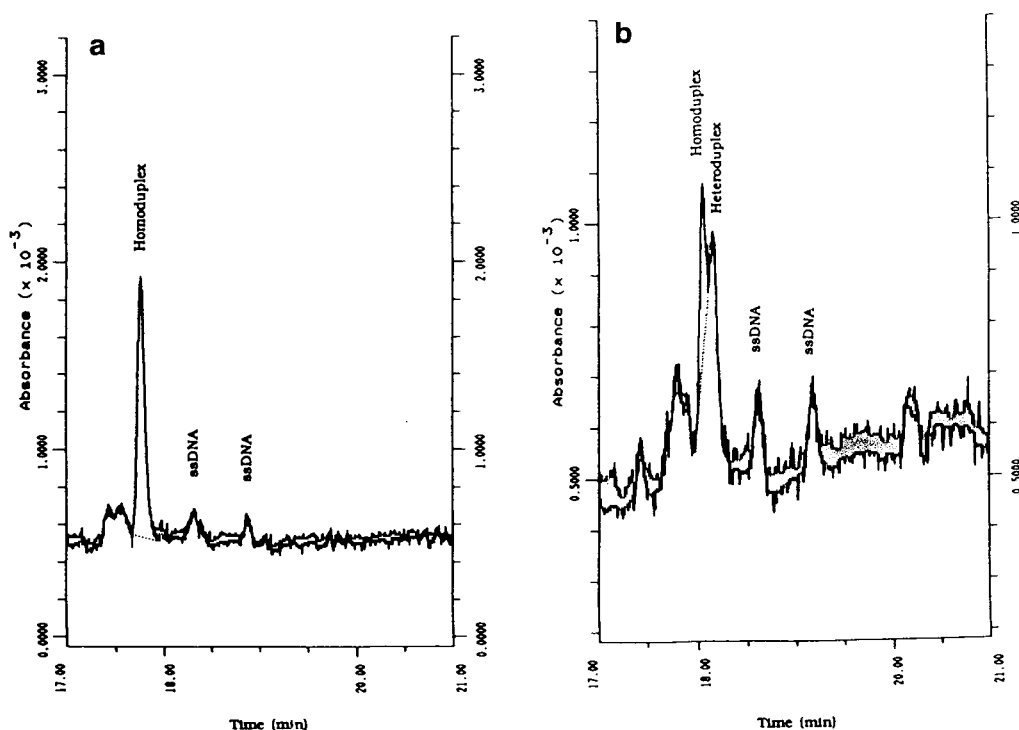


Fig. 3. Electropherograms of PCR mixtures from S_{Fi} (S strain) and F_{It} (F strain) homoduplex (a) and heteroduplex (b). ESCE conditions as in Fig. 2a except the injection lasted for 13 s.

however does not justify the additional processing and handling required to desalt the DNAs.

Homoduplex and heteroduplex PCR mixtures from S_{Fi} (S strain) and P_{GB} (P strain) were separated by ESCE and shown in Fig. 4. From the electropherograms it can be seen that baseline separation between the homoduplex DNA fragments and the heteroduplex molecules containing a two-base deletion and a four-base substitution mismatch (2D + 4S/2B) was obtained.

Homoduplex and heteroduplex PCR mixtures from F_{It} (F strain) and P_{GB} (P strain) were separated by ESCE and shown in Fig. 5. Heteroduplex molecules containing a three deletion and a three-base substitution mismatch (3D + 3S/3B) were further separated at baseline level compared to the results achieved with the (2D + 4S/2B) mismatch heteroduplex (see Fig. 4b). Additionally, partial separation of the two

homoduplex fragments differing by three base pairs can also be seen in both Fig. 5a and b.

Homoduplex and heteroduplex PCR mixtures from S_{Fi} (S strain) and S_{Ha37} (S strain) were separated by ESCE and shown in Fig. 6. The results show that the heteroduplex DNA fragments from the same strain containing one base substitution mismatch (0D + 1S/0B) could not be resolved from homoduplex molecules by ESCE.

Homoduplex and heteroduplex PCR mixtures from F_{It} (F strain) and S_{Ha37} (S strain) were separated by ESCE and shown in Fig. 7. The results show that the heteroduplex DNA fragments containing one-base deletion mismatch (1D + 0S/1B) in 124 bp can still be resolved from homoduplex molecules.

Our previous analysis of this sequence by conventional restriction polymorphism analysis [17] showed that European P strain can be

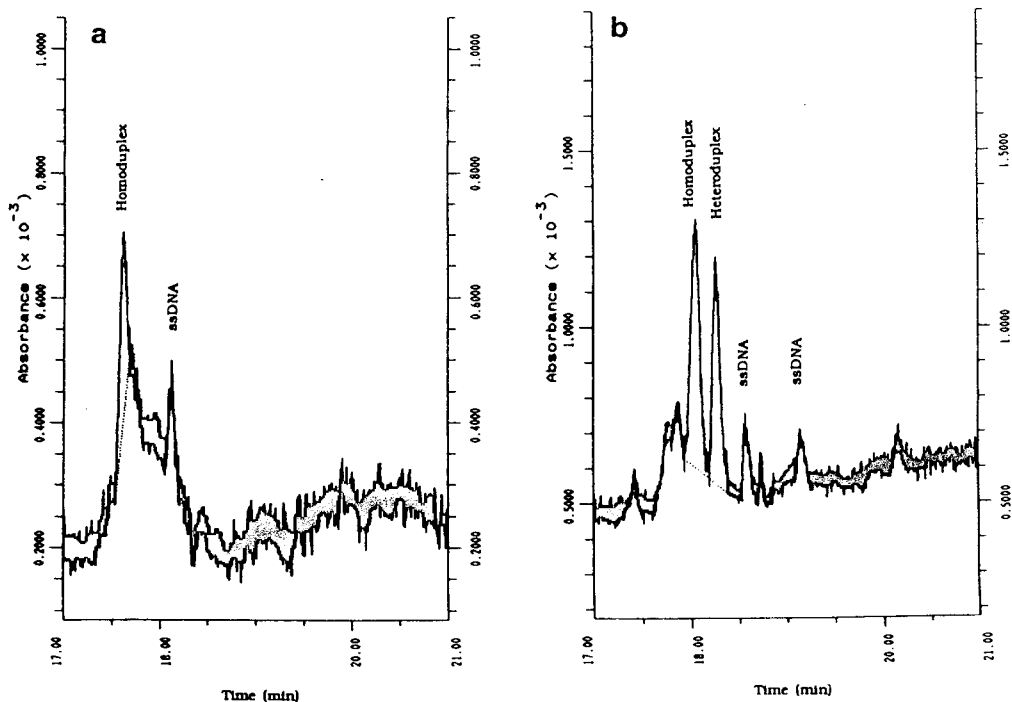


Fig. 4. Electropherograms of homoduplex (a) and heteroduplex (b) PCR mixtures from S_{Fi} (S strain) and P_{GB} (P strain). ESCE conditions as in Fig. 2a except the injection lasted for 13 s.

differentiated from European S and F strains of *H. annosum*. However, discrimination could not be achieved between S strain isolates varying by a single-base pair substitution, or between F and S strains differing by (1D + 0S/1B) or (1D + 1S/1B) (Table 1). Here we demonstrate ESCE of heteroduplex molecules greatly improves strain identification in that F and S strain isolates may now be clearly differentiated. Above all, the method is rapid, reproducible and simple as well as permitting superior resolution to the fractionation achieved by conventional PAGE.

Although a single-base substitution mismatch was not resolved by our system this study clearly demonstrates that the combination of a single-base deletion mismatch *cis*-linked with a single-base substitution mismatch can be resolved from a single-base deletion mismatch by non-denaturing ESCE. The presence of a single-base deletion mismatch amplifies the change of the mobility of heteroduplex caused by the single-base substitution mismatch (Fig. 3). This observation

has previously been reported by Van den Akker et al. [19] using a Pharmacia PhastGel electrophoresis system. In our DNA model the single-base substitution mismatch is located 78 bp from the single-base deletion, which are 22 and 27 bp from the fragment termini, respectively. This is comparable to the distance between mismatch regions with which Van den Akker et al. [19] achieved PAGE fractionation using a portion of the *Escherichia coli lac Z α* gene. While clear fractionation of *H. annosum* heteroduplex DNAs occurred, optimisation of our ESCE conditions may be required for particular DNA species as factors such as fragment length, DNA sequence, or the nature of the DNA mismatch can influence the migration of heteroduplex species. However, this present work and the results of Van den Akker et al. [19] suggest that a variety of single-base substitution mutations *cis*-linked to a single deletion mismatch can be resolved electrophoretically from molecules possessing a single deletion mismatch under non-

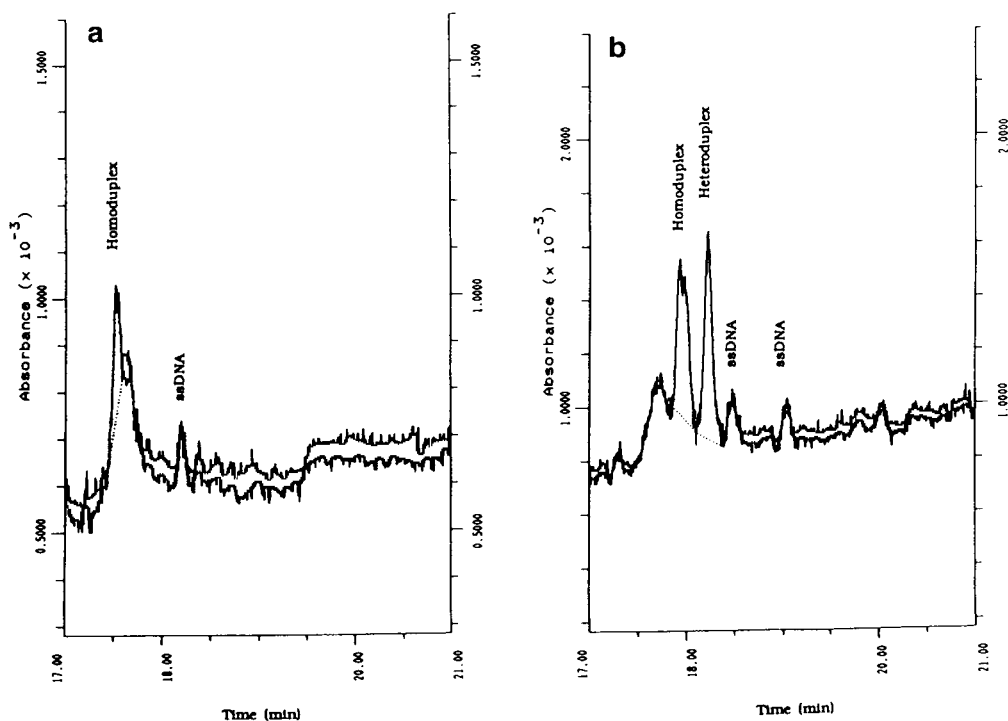


Fig. 5. Electropherograms of homoduplex (a) and heteroduplex (b) PCR mixtures from F_{It} (F strain) and P_{GB} (P strain). ESCE conditions as in Fig. 2a except the injection lasted for 13 s.

denaturing and ambient temperature conditions. Therefore, the technique should be useful for fractionation of a variety of heteroduplex DNA molecules from biological samples.

Khrapko et al. [16] describe an application of HPCE to the analysis of conformational polymorphisms in DNA molecules part-melted in a denaturing (chemical and thermal) environment, termed constant denaturant capillary electrophoresis (CDCE). While the resolution between mismatched heteroduplex and homoduplex molecules achieved by the CDCE technique are impressive, the DNA sequences employed in that study have particular features that allow application of CDCE. The DNA fragment had a CG-rich domain (a CG-clamp) that conferred duplex stability under denaturing conditions necessary for amplification of conformational differences in CG-poor domain containing the mismatch. Notably, small changes in temperature above that required to observe conformational polymorphism could melt the CG-clamp at

which discrimination between heteroduplex and homoduplex molecules was no longer detectable. While we do not wish to compare the ESCE system directly to CDCE, analysis using the latter requires the choice of either DNA molecules possessing a CG-clamp domain, or the synthesis of PCR products with CG-clamp extensions necessary to provide the duplex stability in heteroduplex molecules in denaturing conditions. The ESCE system does not require the provision of natural or artificial CG-clamp domains and hence may be used on a range of natural PCR species or other DNA fragments. The ESCE system does achieve good resolution of mismatched molecules in each case tested except for the single-base substitution mismatch (Fig. 6). In addition, the migration of homoduplex and heteroduplex molecules during ESCE was not highly sensitive to temperature in the range of 18 to 22°C although resolution between molecular species improved at the lower temperature (results not shown).

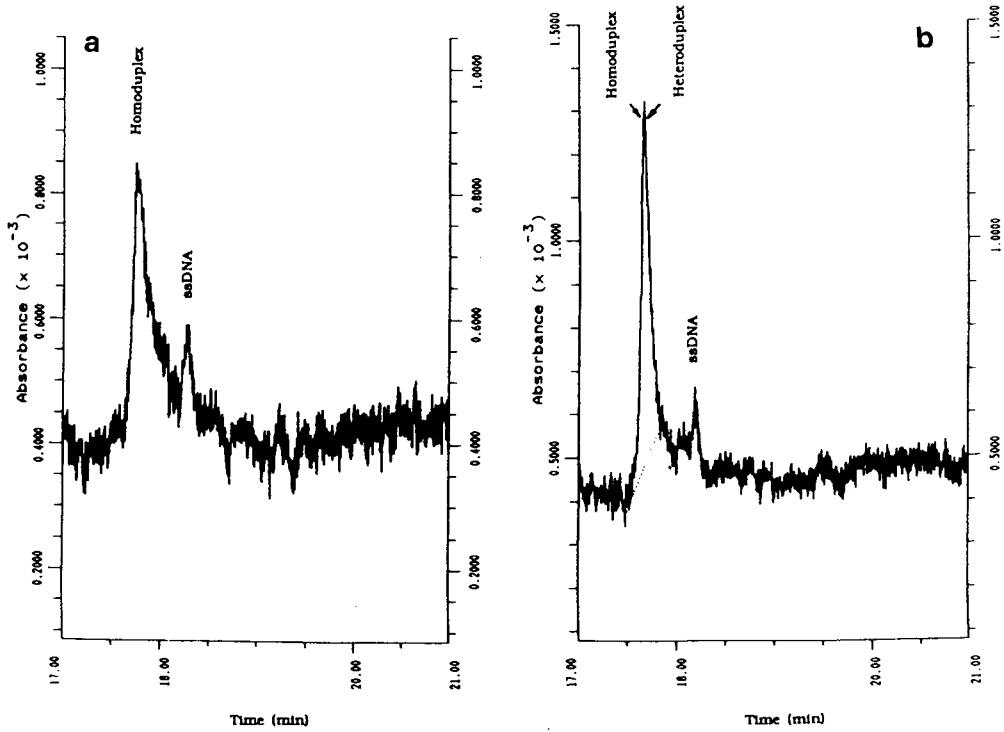


Fig. 6. Electropherograms of homoduplex (a) and heteroduplex (b) PCR mixtures from S_{Fi} (S strain) and S_{Ha37} (S strain). ESCE conditions as in Fig. 2a except the injection lasted for 13 s.

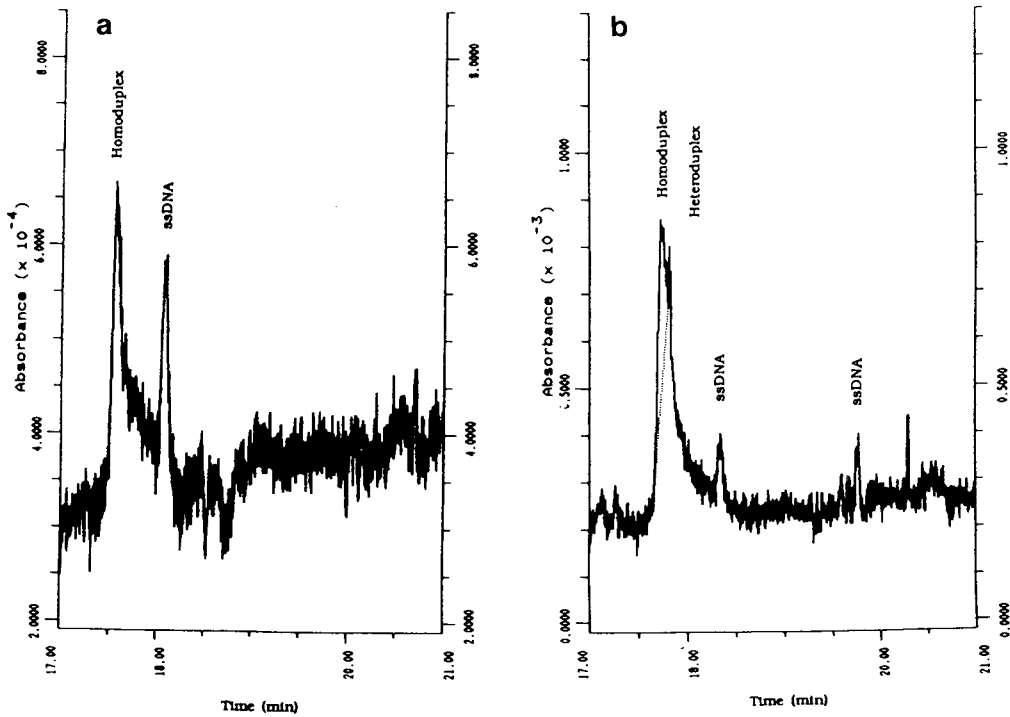


Fig. 7. Electropherograms of homoduplex (a) and heteroduplex (b) PCR mixtures from F_{I1} (F strain) and S_{Ha37} (S strain). ESCE conditions as in Fig. 2a except the injection lasted for 13 s.

The conditions we established in this work are not selective in regard to DNA sequence information and therefore generally applicable to heteroduplex polymorphism analysis using HPCE. The separation between mismatched heteroduplex and homoduplex was observed to increase with each additional substitution mismatch or deletion mismatch. Although we have not explored position effects we feel that ESCE will be able to be used to predict the nature of mismatches in defined PCR fragments. In addition, creation of a series of single-point deletions in a DNA template covering a locus would provide a set of analytical tools for detection of substitution mismatches by ESCE. The deletion series would be used to form mismatch heteroduplex with amplification products from individuals. The position of common substitution mutations could be identified by the extent to which the mutation altered migration in ESCE. Rare, novel substitution mutations would also be identifiable directly by the unusual migration of their heteroduplexes formed with the deletion series standards. It is also believed that use of laser induced fluorescence rather than UV would dramatically improve the sensitivity of detection of heteroduplex conformation isomers resolved by ESCE. More work is in progress to further develop the applications of ESCE for mutation detection.

Acknowledgements

This work was supported by the Scottish Office (SOAFD), the UFC-Biotechnology Initiative and the NERC (GR9/370). The authors wish to thank Beckman Instruments, Inc. for the loan of the P/ACE system 2050 and the capillary column.

References

- [1] H.E. Schwartz and K.J. Ulfelder, *Anal. Chem.*, 64 (1992) 1737–1740.
- [2] K.J. Ulfelder, H.E. Schwartz, J.M. Hall and F.J. Sunzeri, *Anal. Biochem.*, 200 (1992) 260–267.
- [3] F. Martin, D. Vairalles and B. Henrion, *Anal. Biochem.*, 214 (1993) 172–179.
- [4] M. Strege and A. Lagu, *Anal. Chem.*, 63 (1991) 1233–1236.
- [5] N. Bianchi, C. Mischiati, G. Feriotto and R. Gambari, *Nucleic Acids Res.*, 21 (1993) 3595–3596.
- [6] T. Satow, T. Akiyama, A. Machida, Y. Utagawa and H. Kobayashi, *J. Chromatogr. A*, 652 (1993) 23–30.
- [7] V. Sheffield, D.R. Cox, L.S. Lerman and R.M. Myers, *Proc. Natl. Acad. Sci. U.S.A.*, 86 (1989) 232–236.
- [8] M. Orita, Y. Suzuki, T. Sekiya and T. Hayashi, *Genomics*, 5 (1989) 874–879.
- [9] R.M. Myers, Z. Larin and T. Maniatis, *Science*, 230 (1985) 1242–1246.
- [10] R.G.H. Cotton, N.R. Rodrigues and D.R. Campbell, *Proc. Natl. Acad. Sci. U.S.A.*, 85 (1988) 4397–4401.
- [11] M.B. White, M. Carvalho, S. O'Brien, D. Derse and M. Dean, *Genomics*, 12 (1992) 301–306.
- [12] R. Sorrentino, I. Cascino and R. Tosi, *Hum. Immunol.*, 33 (1992) 17–23.
- [13] V. Chowdhury, R.J. Olds, D.A. Lane, J. Conard, I. Pabinger, K. Ryan, K.A. Bauer, M. Bhavani, U. Abildgaard, G. Finazzi, G. Castaman, P.M. Mannucci and S.L. Thein, *Br. J. Haematol.*, 84 (1993) 656–661.
- [14] D.J. Wilkin, K.E. Koprivnikar and D.H. Cohen, *Genomics*, 15 (1993) 372–375.
- [15] I. Dianzani, C. Camaschella, A. Ponzzone and R.G.H. Cotton, *Trends Genet.*, 9 (1993) 403–405.
- [16] K. Khrapko, J.S. Hanekamp, W.G. Thilly, A. Belenkii, F. Foret and B.L. Karger, *Nucleic Acids Res.*, 22 (1994) 364–369.
- [17] T. Kasuga, C. Woods, S. Woodward and K.R. Mitchelson, *Curr. Genet.*, 24 (1993) 433–436.
- [18] R. Singhal and J. Xian, *J. Chromatogr. A*, 652 (1993) 47–56.
- [19] E. van den Akker, J.E.F. Braun, G. Pals, M.V.M. Lafleur and J. Retel, *Nucleic Acids Res.*, 20 (1992) 6745–6746.



ELSEVIER

Journal of Chromatography A, 677 (1994) 179–185

JOURNAL OF
CHROMATOGRAPHY A

Determination of sorbic acid in food products by capillary zone electrophoresis in a hydrodynamically closed separation compartment

D. Kaniansky*, M. Masár, V. Madajová, J. Marák

*Department of Analytical Chemistry, Faculty of Natural Sciences, Comenius University, Mlynská Dolina CH-2,
842 15 Bratislava, Slovak Republic*

Received 25 February 1994

Abstract

A simple, selective and rapid capillary zone electrophoresis method for the determination of sorbic acid in food products is described. The determination was carried out in a hydrodynamically closed separation compartment at pH 5.2 and for the samples taken into this study (soft drinks, wine, fruit and juice concentrates, margarine and marmalade) only simple sample preparation procedures were needed. A very good reproducibility in the migration time of the analyte (R.S.D. = 0.61%) was achieved and as could be expected no negative effect of matrix constituents on this performance parameter was detected. The recoveries of sorbic acid in the spiked samples ranged from 98–102% and 2–3% R.S.D.s in parallel determinations of the acid were typical.

1. Introduction

Sorbic acid is a widely used preservative in food products and, therefore, numerous methods were proposed for its determination in various food matrices [1]. At present, however, high-performance liquid chromatography (HPLC) [2–4], thin-layer chromatography (TLC) [5,6], and gas chromatography (GC) [7,8] combined with suitable sample preparation procedures are dominantly used.

A considerable reduced sample preparation is typical when sorbic acid is analyzed by capillary

isotachopheresis (ITP) as demonstrated for various food matrices [2,9–12]. Although the time for an ITP analysis (15–20 min) compares favourably with the above chromatography techniques (see, e.g., ref. [2]) it is less favourable when large series of samples are to be analyzed in a routine control laboratory.

Under ITP separating conditions sorbic acid has a large light absorptivity at a 254 nm wavelength [2,9–12]. In addition, from the quoted works it is also apparent that ITP-migrating and UV-light-absorbing constituents of food matrices typically represent only smaller parts of the total signals as obtained from the UV detector for the ITP separands. These facts imply that capillary electrophoresis techniques handling smaller sam-

* Corresponding author.

ple loads than ITP with the quantitation based on the zone length measurements [13] should be considered as suitable candidates for a rapid electrophoretic determination of sorbic acid in food products. ITP in the spike mode of detection (see, e.g., ref. [14]) and capillary zone electrophoresis (CZE) [15–19] meet such requirements and the latter of these techniques was investigated in this work.

Recent reviews of the CZE instruments show [20,21] that at present CZE is almost exclusively carried out in hydrodynamically opened separation compartments as proposed by Jorgenson and Lukacs [19]. This arrangement of the separation compartment is usually employed with non-zero nett electroosmotic flow. A simultaneous analysis of both positively and negatively charged ions in one run and a negligible band broadening due to electroosmosis are apparent advantages of this approach. On the other hand, any change of ζ potential in the opened separation compartment (e.g., due to adsorption of the sample constituents) is influencing the migration velocities of the separands and, consequently, time based peak area measurements. In the analysis of complex biological fluids even very careful sample pretreatment need not eliminate this problem [22]. Although it can be diminished via appropriate normalization procedures [22,23] irreproducibilities in migration velocities due to changes of the electroosmotic flow during the run can be corrected for only with difficulties. As some food matrices can cause similar problems we preferred the use of hydrodynamically closed separation compartment [15–18]. The main reasons for this preference were in high reproducibilities of the migration times as reported for some constituents in serum [18] and highly proteinous tissue extracts [24]. However, in this context it is necessary to stress that in the closed systems the electroosmotic flow has a negative impact on the band broadening [16,25,26]. Here, appropriate measures, such as coated inner walls of the capillary tubes and/or the use of suitable additives in the carrier electrolyte [15,17,18] must be taken to achieve acceptable separation efficiencies.

2. Experimental

2.1. Instrumentation

A CS isotachophoretic analyser (Villa-Labeco, Spišská Nová Ves, Slovak Republic) was assembled in the single-column mode. The separation unit of the analyser consisted of a laboratory-developed CZE injection valve (90-nl sample loop), a column provided with a 0.30 mm I.D. capillary tube (O.D. \approx 0.65 mm) made of fluorinated ethylene-propylene (FEP) copolymer (Villa-Labeco). The length of the capillary tube was 250 mm (200 mm to the detector) and the column was provided with a UVD 2 on-column photometric detector (Villa-Labeco).

The signal from the photometric detector was registered by a TZ 4200 line recorder (Laboratorní Přístroje, Prague, Czech Republic) and in parallel by an HP 3390A reporting integrator (Hewlett-Packard, Avondale, PA, USA). The data provided by the integrator (peak area and peak area/peak height ratio) served for the evaluation of the quantitation and for the calculation of the column efficiency as described in the literature [27].

2.2. Chemicals

Chemicals used for the preparation of the electrolyte solutions were obtained from Serva (Heidelberg, Germany), Sigma (St. Louis, MO, USA) and Lachema (Brno, Czech Republic). Polyethyleneglycol 5 000 000 (PEG) obtained from Serva was used as an anticonvective additive in the carrier electrolyte solutions.

Water from an Aqualabo two-stage demineralization unit (Aqualabo, Brno, Czech Republic) was further purified by circulation through laboratory-made polytetrafluoroethylene (PTFE) cartridges packed with Amberlite MB-1 mixed-bed ion exchanger (Serva). The electrolyte solutions were prepared from freshly recirculated water and filtered through a 0.45- μ m syringe filter (Gelman, Ann Arbor, MI, USA).

2.3. Samples

Fanta and Sprite (soft drinks), Diplomat (wine) and Halvarine (margarine) were bought in a local supermarket. Athena Orange, Athena Lemon, Exotic Zeus, Lesná Zmes and Cherry Sukus (juice and fruit concentrates) and Apricot Spread (marmalade) were kindly provided by NOKO (Nové Mesto nad Váhom, Slovak Republic).

Soft drinks and wine were diluted with an aqueous solution of Na_2SO_4 in required ratios so that the final concentrations of sorbic acid were within the concentration span for which the calibration graphs were measured. The final concentrations of Na_2SO_4 were 10^{-3} M (this electrolyte in the sample solution was present to minimize adsorption of sorbic acid on the walls of sample containers made of polyethylene).

Margarine (weighed amount of 0.35–0.40 g) was dissolved in 15 ml of *n*-heptane and 10 ml of a 1 mM aqueous solution of Bis-Tris (see Table 1) was added to extract sorbic acid from the organic phase. The aqueous phase was separated in a separatory funnel and the organic phase was extracted repeatedly with a fresh portion of the aqueous extractant. The extracts were made up to 25 ml with the extractant. Also in this instance the aqueous phase contained Na_2SO_4 at a 10^{-3} M concentration.

Weighted amounts of juice and fruit concentrates and marmalade (0.2–0.5 g) were diluted in 10-ml volumes of 10^{-3} M aqueous solution of Na_2SO_4 and sonicated for 5 min. The solutions were filtered and the filtrates analyzed by CZE.

3. Results and discussion

3.1. Separating conditions and some performance characteristics of the separation system

The composition of the carrier electrolyte used in this work is given in Table 1. Sorbic acid ($\text{p}K_a = 4.77$) is ionized from 75% in this carrier

Table 1
Electrolyte system

Solvent	Water
Anion	MES ^a
Concentration (mM)	100
Counter-ion	Bis-Tris ^b
Concentration (mM)	10
pH	5.2
Additive	PEG ^c
Concentration (% w/v)	0.2

^a MES = 2-(N-Morpholino)-ethanesulfonic acid.

^b Bis-Tris = 2,2 - Bis(hydroxymethyl) - 2,2',2'' - nitrilotriethanol.

^c PEG = Polyethyleneglycol 5 000 000.

electrolyte. Such a distribution into the ionic forms is less favourable as far as the separation efficiency is concerned because a maximum efficiency requires a full ionization of the separand [28], i.e., in this particular instance a higher pH. On the other hand, reduced effective mobilities of the anionic matrix constituents (favoured by a low pH of the carrier electrolyte) were desired to achieve a high selectivity of the analysis via a reduced number of migrating sample constituents. No detailed search for an optimum electrolyte system in terms of the resolutions of the separands was carried out as various food matrices differing not only in the concentrations of the matrix constituents but also qualitatively (e.g., refs. [1,29]) make such a search cumbersome and only of a limited general validity.

Benzoic and ascorbic acids are probably the only among current food additives [1,12] which could interfere in the analysis of sorbate by CZE. We found that under our separating conditions they migrated with higher effective mobilities (lower $\text{p}K_a$ values than that of sorbic acid) and did not disturb the analysis of the preservative (see Fig. 2). Electropherograms in Fig. 1 show that for most of the samples the carrier electrolyte provided high analytical selectivities with acceptable separation efficiencies for the analyte (see Table 2). The same applies for the samples of somewhat higher complexities (Fig. 2) as the matrix constituents unresolved

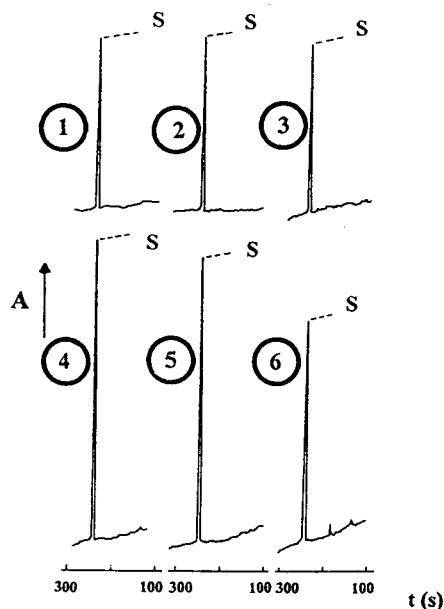


Fig. 1. Determination of sorbic acid (S) in food products. 1 = Halvarine; 2 = Apricot Spread; 3 = Diplomat wine; 4 = Fanta soft drink; 5 = Sprite soft drink; 6 = Lesná Zmes fruit lemonade concentrate. The samples were pretreated as described under Experimental. The composition of the electrolyte system is given in Table 1. The driving current was 150 μA . A = Increasing light absorption.

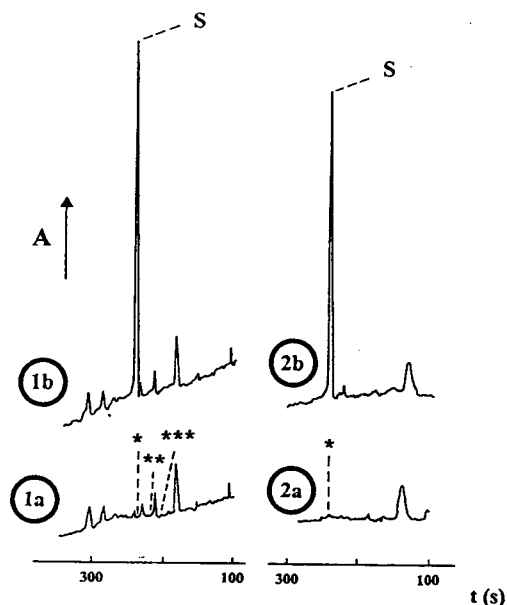


Fig. 2. CZE of sorbic acid (S) in fruit concentrates. 1 = Cherry Sukus; 2 = Athena Orange (a = fruit concentrates without the preservative; b = the same fruit concentrates as in a containing sorbic acid). The samples were pretreated in a way described under Experimental. The separations were carried out in the electrolyte system given in Table 1 with a 150 μA driving current. *, **, *** = Migration positions of sorbate, ascorbate and benzoate, respectively.

Table 2
Separation performance characteristics for sorbic acid ($n = 72$)

Parameter ^a	
Migration time (s)	246.1
R.S.D. (%)	0.61
Column efficiency (N/m) ^b	175 000
R.S.D. (%)	10
Concentration span of the analyte (μM)	5–70

R.S.D. = Relative standard deviation; N/m = number of theoretical plates per metre; n = number of data points.

^a The average values calculated from the data obtained in 72 runs within 7 days in three (separately prepared) solutions of the carrier electrolyte. The data obtained in the runs with both model and practical samples (listed in Table 5) are included.

^b Calculated from the data provided by the integrator (see Experimental).

from the analyte introduced only negligible systematic errors into its quantification.

As mentioned in the Introduction the separations in a hydrodynamically closed separation compartment were preferred to minimize uncontrolled fluctuations in the migration time of the analyte due to unpredictable changes of ζ potential. The relevant data in Table 2 show that the migration time of sorbate was very reproducible also when random errors due to the use of different solutions of the carrier electrolyte were included.

The I.D. of the capillary tube as used in this work is less suitable from the point of view of thermal dispersion [16,25,26]. However, the use of a less conductive carrier electrolyte enabled us to apply a field strength of ca. 400 V/cm (for a 150 μA driving current) to achieve rapid and high-efficiency CZE separations. In this context it is necessary to stress that an overall dispersion

included also a contribution due to electroosmosis [16,25,26]. Although fluoroplastic surfaces have lower ζ potentials than, e.g., of fused silica [30,31] the use of a high-molecular-mass polyethyleneglycol (Table 1) in the carrier electrolyte was essential in minimizing the electroosmotic dispersion. This anticonvective additive was preferred as it gave the highest separation efficiencies for a model group of ionic separands when high-molecular-mass water-soluble polymers such as hydroxyethylcellulose, methylhydroxyethylcellulose, poly(vinyl alcohol), poly(vinylpyrrolidone) and polyethyleneglycol were compared under otherwise identical working conditions [32].

In the CZE analysis of complex ionic mixtures capillary tubes of preferred dimensions are overloaded easily by sample macroconstituents (see, e.g., ref. [33]). The use of the capillary tube of a higher I.D. provides one way in solving these problems as the load capacity of the column is proportional to its cross-section. Therefore, in our instance the sample load could be increased up to 90 nl also for less diluted highly ionic fruit concentrates (see, e.g., Fig. 2) without any indication of the column overloading [18]. In addition, a 0.3 mm pathlength of the detection cell enabled us to achieve for sorbic acid the limit of detection at a $5 \cdot 10^{-7}$ M concentration (254 nm detection wavelength and a 90-nl injec-

tion volume) with a simple on-column photometric detector.

3.2. Quantitation

Parameters of the regression equations related to the calibration graphs are given in Table 3. The concentration range for which the data were measured covered the concentrations of the preservative in appropriately diluted food products and/or in their extracts.

The reproducibilities of the determinations of sorbic acid were assessed for five concentrations (the lowest concentration corresponded to the limit of determination [34]) by using the data provided by the integrator (peak areas and peak heights) and those evaluated from the electropherograms as registered by the line recorder (peak heights). The relative standard deviations presented in Table 4 show that the peak area measurements were, in general, more scattered. This problem was associated with the detector noise which prevented reproducible assignments of the start and end points of the analyte peak and, consequently, reduced reproducibilities in the peak integration. Undoubtedly, this also explains a lower correlation coefficient for the regression equation: peak area vs. sorbic acid concentration (Table 3). It was shown recently by Wanders [35] that analogous problems are

Table 3

Parameters of the regression equations ($y = a + bx$) and correlation coefficients for sorbic acid at 5–70 μ M concentrations ($n = 19$)

Parameter	Peak area ^a , integrator	Peak height ^a	
		Integrator	Recorder
a (mV min)	-274.00	–	–
b (mV min/ μ mol)	154	–	–
r	0.9964	–	–
a (mV)	–	0.471	1.12
b (mV/ μ mol)	–	2.497	2.739
r	–	0.9996	0.9995

y = Peak area (peak height); a = intercept; b = slope; x = concentration (μ M); n = number of data points; r = correlation coefficient.

^a The data were obtained in the same runs.

Table 4
Reproducibilities of the determinations of sorbic acid at different concentrations for various data evaluations

Concentration (μM)	Peak area ^a , integrator		Peak height ^a			
	R.S.D. (%)	<i>n</i>	Integrator		Recorder	
			R.S.D. (%)	<i>n</i>	R.S.D. (%)	<i>n</i>
5 ^b	2.3	3	0.9	3	2.1	3
10	6.9	4	2.4	4	1.0	4
30	2.8	4	3.6	4	3.2	4
50	5.3	4	1.0	4	1.0	4
70	5.1	4	1.0	4	0.9	4

^aThe data were obtained from the same runs.

^bOne of the four analysis was excluded by a test.

typical when current chromatography software packages are used to data analysis in CZE, especially while working with a low signal-to-noise ratio.

The concentrations of sorbic acid were determined in some food products which were claimed by the manufacturers to contain this preservative. Mean values of the parallel determinations are given in Table 5. The results of the parallels deviated by less than 5% with 2–3% R.S.D.s being dominant. Tabulated results (Table 5) also show differences due to the use of

different alternatives in the peak height measurements in the same CZE runs.

A current preparative of sorbic acid served as a reference analyte in our measurements. As in none of the samples an actual (“true”) concentration of the preservative was known, accuracies of the analyses could not be assessed directly. Nevertheless, 98–102% recoveries of sorbic acid in the studied food products (evaluated from the spiked samples) and negligible systematic errors due to matrix constituents (experiments with samples without the preserva-

Table 5
Examples of the determination of sorbic acid in various food products

Food products	Determined (mg/kg)		Maximum permitted (mg/kg)	Sample preparation ^a
	A	B		
Fanta (soft drink)	203.5	206.2	200	Dilution (1:25, v/w), filtration
Sprite (soft drink)	195.6	194.8	200	As for Fanta
Diplomat (wine)	146.2	146.1	200	Dilution (3:100, v/v), filtration
Athena Orange (juice concentrate)	137.0	136.9	300	Dilution (3.9:100, w/v), filtration
Athena Lemon (juice concentrate)	2.4	2.5	–	Filtration
Apricot (marmalade)	118.5	119.4	400	Extraction (1:25, w/v), filtration
Halvarine (margarine)	180.6	178.9	200	Extraction (3.9:150, w/v)

A, B = Peak height measurements from the integrator and the recorder, respectively.

^aFor details, see Experimental section.

tive (Fig. 2)) indicate that also this performance parameter was met.

In conclusion we can state that CZE performed in a hydrodynamically closed separation compartment offers a rapid and reproducible alternative to the determination of sorbic acid in food products. When necessary a 4-min analysis time as achieved in this work can be further reduced by relevant means (e.g., length of the column, a higher field strength combined with an appropriate carrier electrolyte solution).

Simple sample preparation procedures used for food products investigated in this work probably need not be of a general applicability. Then an extraction procedure as described by Eichler and Rubach [12] for ITP seems a convenient alternative also for CZE. On-line ITP pretreatment providing a powerful sample clean-up also for very complex ionic matrices [36] should be also considered in such situations.

References

- [1] J. Davídek, J. Hrdlička, M. Karvánek, J. Pokorný, J. Seifert and J. Velíšek, *Laboratorní Příručka Analýzy Potravin*, SNTL, Prague, 2nd ed., 1981.
- [2] S. Donhauser, K. Glas and B. Gruber, *Monatsschr. Brauwiss.*, 37 (1984) 252.
- [3] M.S. Ali, *J. Assoc. Off. Anal. Chem.*, 68 (1985) 488.
- [4] M.L. Puttermans, C. Branders, L. Dryon and D. Massart, *J. Assoc. Off. Anal. Chem.*, 68 (1985) 80.
- [5] L. Krull and R. Matissek, *Dtsch. Lebensm. Rundsch.*, 84 (1988) 144.
- [6] W. Haensel and R. Stroemmer, *Dtsch. Lebensm. Rundsch.*, 83 (1987) 315.
- [7] E. Rabe, *Veroeff. Arbeitsgem. Getreideforsch.*, 35 (1984) 114.
- [8] T. Tsuda, H. Nakamishi, T. Morita and J. Takebayashi, *J. Assoc. Off. Anal. Chem.*, 68 (1985) 902.
- [9] K.-P. Kaiser and H. Hupf, *Dtsch. Lebensm. Rundsch.*, 75 (1979) 346.
- [10] K. Rubach, C. Breyer and E. Kirchhoff, *Z. Lebensm.-Unters.-Forsch.*, 170 (1980) 99.
- [11] K. Rubach and C. Breyer, *Getreide Mehl Brot*, 35 (1981) 91.
- [12] D. Eichler and K. Rubach, in C.J. Holloway (Editor), *Analytical and Preparative Isotachophoresis*, Walter de Gruyter, Berlin, New York, 1984, p. 117.
- [13] F.M. Everaerts, J.L. Beckers and Th.P.E.M. Verheggen, *Isotachophoresis: Theory, Instrumentation and Applications*, Elsevier, Amsterdam, 1976.
- [14] D. Kaniansky, V. Madajová, J. Marák, E. Šimuničová, I. Zelenský and V. Zelenská, *J. Chromatogr.*, 390 (1987) 51.
- [15] S. Hjertén, *Free Zone Electrophoresis*, Almqvist & Wiksell, Uppsala, 1967.
- [16] R. Virtanen, *Thesis*, Helsinki University of Technology, Otaniemi, 1974.
- [17] F.E.P. Mikkers, F.M. Everaerts and Th.P.E.M. Verheggen, *J. Chromatogr.*, 169 (1979) 1.
- [18] Th.P.E.M. Verheggen, A.C. Schoots and F.M. Everaerts, *J. Chromatogr.*, 503 (1990) 245.
- [19] J.W. Jorgenson and K.D. Lukacs, *Anal. Chem.*, 53 (1981) 1298-1302.
- [20] H. Waetzig and C. Dette, *Fresenius' J. Anal. Chem.*, 345 (1993) 403.
- [21] H. Waetzig and C. Dette, *J. Chromatogr.*, 636 (1993) 31.
- [22] J.L. Beckers, F.M. Everaerts and M.T. Ackermans, *J. Chromatogr.*, 537 (1991) 407.
- [23] P. Jandik and G. Bonn, *Capillary Electrophoresis of Small Molecules and Ions*, VCH, New York, Weinheim, Cambridge, 1993.
- [24] O. Mharapara, *M.Sc. Thesis*, Comenius University, Bratislava, 1992.
- [25] J.C. Reijenga and E. Kenndler, *J. Chromatogr. A*, 659 (1994) 403.
- [26] F. Foret, M. Deml and P. Boček, *J. Chromatogr.*, 452 (1988) 601.
- [27] B.A. Bidlingmeyer and F.W. Waren, Jr., *Anal. Chem.*, 56 (1984) 1583A.
- [28] E. Kenndler and C. Schwer, *Anal. Chem.*, 63 (1991) 2499.
- [29] M.F. Nesterin and I.M. Skurikhin (Editors), *Khimicheskiei Sostav Pishchevykh Produktov*, Pischevaya Promyshlennost, Moscow, 1979.
- [30] J.C. Reijenga, G.V.A. Aben, Th.P.E.M. Verheggen and F.M. Everaerts, *J. Chromatogr.*, 260 (1983) 241.
- [31] W. Schuetzner and E. Kenndler, *Anal. Chem.*, 64 (1992) 1991.
- [32] D. Kaniansky and J. Marák, in preparation.
- [33] B.J. Wildman, P.E. Jackson, W.R. Jones and P.G. Alden, *J. Chromatogr.*, 546 (1991) 459.
- [34] D.L. Massart, B.G.M. Vandeginste, S.N. Deming, Y. Michotte and L. Kaufman, *Chemometrics: A Textbook*, Elsevier, Amsterdam, Oxford, New York, Tokyo, 1988, p. 113.
- [35] B.J. Wanders, *Thesis*, University of Technology, Eindhoven, 1993.
- [36] D. Kaniansky, J. Marák, V. Madajová and E. Šimuničová, *J. Chromatogr.*, 638 (1993) 137.



ELSEVIER

Journal of Chromatography A, 677 (1994) 186–191

JOURNAL OF
CHROMATOGRAPHY A

Short Communication

High-performance liquid chromatography of *cis*–*trans* isomers of proline-containing dipeptides

III. Comparative studies with different stationary phases

A. Wutte^a, G. Gübitz^{*,a}, S. Friebe^b, G.-J. Krauss^{*,b}

^aInstitute of Pharmaceutical Chemistry, Karl-Franzens-University of Graz, Universitätsplatz 1, A-8010 Graz, Austria

^bDepartment of Biochemistry and Biotechnology, Martin-Luther-University of Halle, Weinbergweg 16a, D-06120 Halle, Germany

First received 14 January 1994; revised manuscript received 19 April 1994

Abstract

Different stationary phases were compared for their capacity to separate *cis*–*trans* isomers of proline-containing dipeptides for equilibrium and isomerization studies. Both reversed-phase chromatography on an RP-18 or a graphitized carbon phase (Hypercarb S) and ligand-exchange chromatography on an L-proline–Cu(II) phase can be used effectively to separate the *cis*–*trans* isomers.

1. Introduction

Conformational changes of the peptide bond occurring in peptides with a C-terminal proline or N-alkylamino acids have been studied using different spectroscopic and kinetic methods [1–5]. Several approaches for the investigation of dynamic equilibria have been reported, including *cis*–*trans* isomerism of proline-containing peptides by high-performance liquid chromatography (HPLC). Melander et al. [6] and others described experiments to obtain quantitative data on the conformational changes of the peptidyl–proline imidic bond by low-temperature RP-HPLC. According to Melander et al. [6], differing hydrophobic interactions of the conformers

are responsible for the resolution. Recently, we introduced cyclodextrin-bonded silicas for the chromatographic separation of peptide-bond isomers [7,8]. The conformers of proline-containing di- and oligopeptides were resolved with high efficiency using steric discrimination by inclusion complexation. Even peptides with two peptidyl–proline bonds split into their conformer peaks. Similar results concerning dipeptides have been obtained when using an RP-8 phase and β -cyclodextrin as additive to the mobile phase [8].

This paper deals with comparative studies of different HPLC supports representing the reversed-phase mode (RP-18 phase and a graphitized carbon phase) and the ligand-exchange mode using an L-proline–Cu(II) bonded phase, previously developed for the resolution of enantiomers [9,10]. Further, the influence of β -

* Corresponding author.

cyclodextrin as an additive in combination with the graphitized carbon phase was studied.

2. Experimental

2.1. Materials

Optically pure dipeptides were purchased from Bachem Biochemica (Heidelberg, Germany) and β -cyclodextrin from Merck (Darmstadt, Germany). The separations were carried out on a 250×4 mm I.D. Separon SG \times RP-18 ($7 \mu\text{m}$) column from Tessek (Prague, Czech Republic) and a 100×4.6 mm I.D. Hypercarb S ($7 \mu\text{m}$) column from Shandon Scientific (Astmere, UK). The 250×4.6 mm I.D. L-proline-Cu(II) ligand-exchange chromatographic (LEC) column ($5 \mu\text{m}$) was prepared as reported previously [9,10].

2.2. Apparatus

HPLC separations were performed with a Merck-Hitachi HPLC system consisting of an L-6200 intelligent pump, an L-4000 UV detector and a computing integrator. A Lauda RM6 thermostat regulated cooling of the columns.

2.3. Chromatographic conditions

Chromatographic experiments were performed isocratically using phosphate buffer-acetonitrile eluents of different composition and pH. The analyte absorptions were monitored at 223 nm.

Peak splitting as a result of isomerization processes was verified by reinjection of the fractionated peaks, whereby the same retention time was obtained in this second separation for the peak collected.

3. Results and discussion

3.1. Separation on RP-18 phase

Efficient separations with significant α -values were obtained for Ala-Pro, Leu-Pro, Ile-Pro and Phe-Pro on the RP-18 phase at low temperature (Table 1). According to previous studies by Melander et al. [6] on an RP-8 phase, the elution order was interpreted to be *trans* before *cis*, owing to the stronger hydrophobic interactions of the larger hydrophobic surface of the *cis* isomer with the reversed phase. The absolute order of elution, however, was not determined either by Melander et al. or in this study.

The ratio of the *cis* and *trans* isomers in solution was found to be dependent on temperature, solvent composition and pH. This conforms with the investigations of Henderson and Horvath [11]. In an aqueous solution of Leu-Pro freshly prepared at 0°C , the first isomer eluted, postulated as *trans*, was significantly dominant, reflecting the presumed original ratio. After exposing the solution to room temperature, the equilibrium changed (Fig. 1). These observations were confirmed on the other phases used.

Table 1
 k' and α values for the *cis-trans* isomers of dipeptides on different phases

Dipeptide	Hypercarb S			RP-18			L-Proline-Cu(II)		
	k'_1	k'_2	α	k'_1	k'_2	α	k'_1	k'_2	α
Ala-Pro	3.4	6.6	1.9	3.7	4.7	1.2	6.0	7.6	1.2
Ile-Pro	5.2	11.4	2.1	6.0	12.5	2.0	7.5	10.3	1.3
Leu-Pro	5.0	12.8	2.6	5.7	9.0	1.5	7.3	10.5	1.4
Phe-Pro	16.0	67.0	4.1	9.5	38.3	4.0	15.6	48.3	3.1

Hypercarb S and RP-18: mobile phase, 0.05 M phosphate buffer (pH 6.2)-acetonitrile (92:8). L-Proline-Cu(II): mobile phase, 0.05 M phosphate buffer (pH 4.5)-acetonitrile (92:8). Temperature, 0°C ; flow-rate, 1 ml/min.

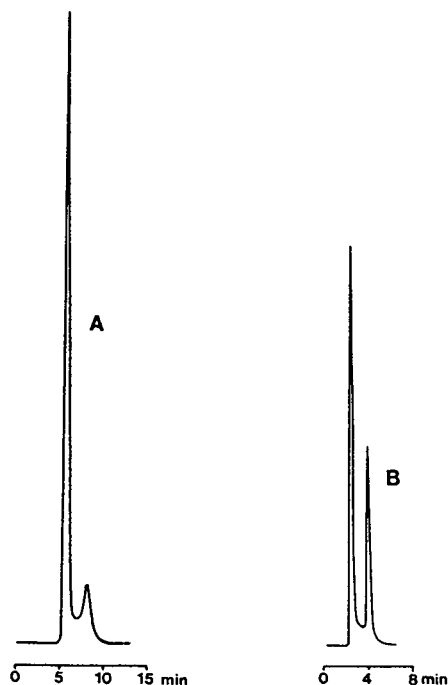


Fig. 1. Isomerization of Leu-Pro. Column, RP-18; mobile phase, 0.05 M phosphate buffer (pH 6.2)–acetonitrile (92:8); flow-rate, 1 ml/min. (A) Injection of an aqueous solution of Leu-Pro freshly prepared at 0°C; (B) isomerization after storage of the solution at room temperature.

3.2. Separation on Hypercarb S phase

All dipeptides show higher retention than with the octadecylsilica column (Table 1). The retention mechanism is assumed to be influenced by the layer structure of the graphite [12] and also by hydrophobic interactions.

Experiments using an acidic (pH 4.5) or a basic (pH 8) eluent resulted in extremely high retention values without peak splitting. An eluent of pH 6.2 was found to be most effective in separating the two isomers. To decrease the retention time of the second peak and so to reduce the plateau between the two peaks caused by relaxation of the molecules, a higher ionic strength of the buffer and an organic modifier were used. Fig. 2 demonstrates the influence of temperature and organic modifiers on the separation of the conformers of Leu-Pro.

Phe-Pro showed an extremely high retention

time with only two spikes and a marked plateau between them. In contrast to Ala-Pro, Leu-Pro and Ile-Pro, the peak ratio of the conformers of Phe-Pro was reversed. This peak ratio is analogous to that found on reversed phases. The retention time decreased and the resolution improved when β -cyclodextrin (β -CD) was added to the mobile phase (Fig. 3). This phenomenon can be explained by steric hindrance of isomer interconversion caused by the formation of an inclusion complex. The plateau observed between the isomer peaks in separations without β -CD was found to be significantly reduced. These results are in accordance with previous investigations using β -CD as a mobile phase additive in combination with reversed phases or by using chemically bonded β -CD phases [7,8].

To study peak splitting as a result of peptide bond isomerization, fractions collected from both peaks of Ile-Pro were reinjected. After exposure of the solution to ambient temperature for 45 min, relaxation to the original peak ratio was observed.

3.3. Separation by ligand-exchange chromatography

The third type of stationary phase investigated was a chemically bonded L-proline-Cu(II) phase, previously used for the resolution of enantiomers [9,10]. The idea was to obtain a discriminant steric fixation of the isomers by chelate complexation and the isomers were in fact resolved at low temperature. Without copper on the column there was no separation (Fig. 4).

Surprisingly, the peak ratio was the reverse of that on the RP-18 and Hypercarb S phases for all the dipeptides investigated, indicating a possibly reversed elution order due to a different separation mechanism (compare Fig. 1 with Fig. 4). A freshly prepared aqueous solution of Leu-Pro showed a dominant second peak, presumably the *trans* isomer. The same behaviour was observed for all dipeptides except Phe-Pro. Injection of a fraction of the second peak of Ile-Pro collected from RP-18 on to the L-proline column resulted in a dominant first peak (Fig. 5). By analogy, if a fraction of the first peak was collected and

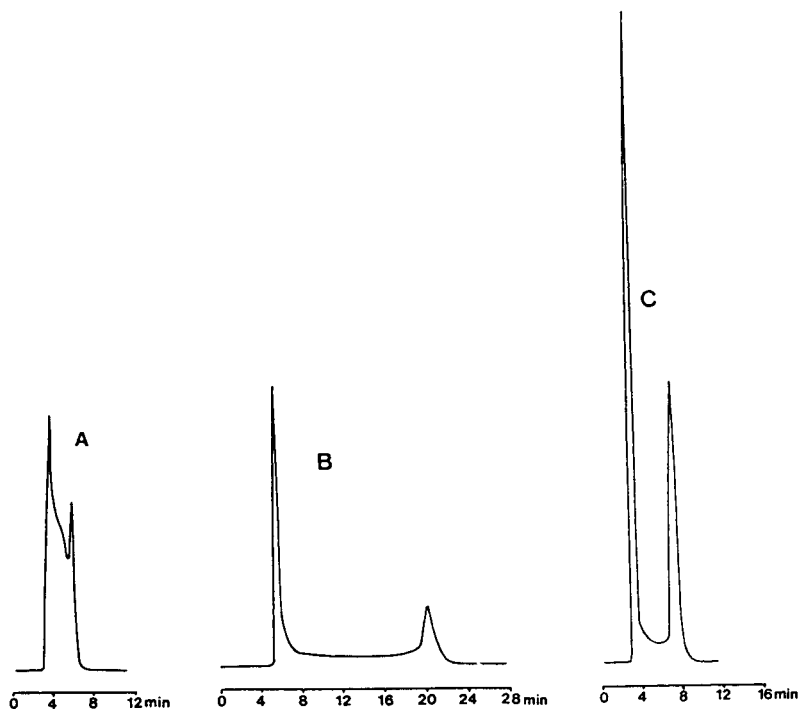


Fig. 2. Separation of the *cis-trans* isomers of Leu-Pro on Hypercarb S: influence of temperature and organic modifier on the resolution. (A) Temperature, 23°C; mobile phase, 0.05 M phosphate buffer (pH 6.2); flow-rate, 1 ml/min. (B) Temperature 5°C; mobile phase as in (A). (C) Temperature, 5°C; mobile phase, 0.05 M phosphate buffer (pH 6.2)–acetonitrile (92:8).

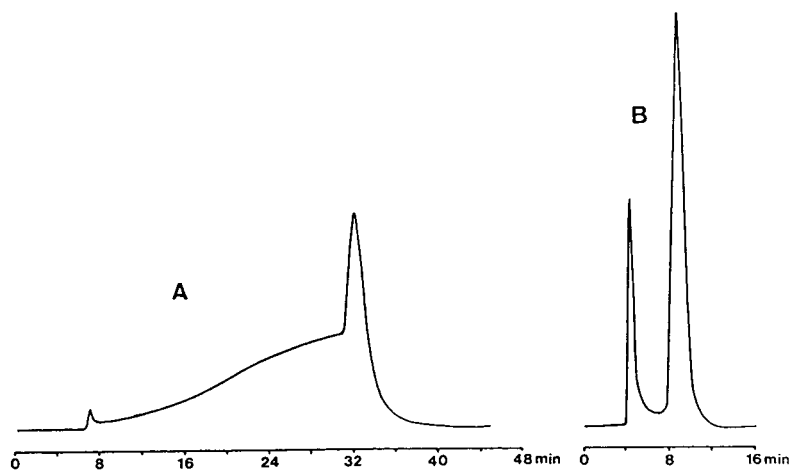


Fig. 3. Separation of the *cis-trans* isomers of Phe-Pro on Hypercarb S: influence of cyclodextrin addition. Temperature, 5°C; flow-rate, 1 ml/min. Mobile phase: (A) 0.05 M phosphate buffer (pH 6.2)–acetonitrile (90:10); (B) 0.05 M phosphate buffer (pH 6.2)–acetonitrile (90:10) + 0.01 M β -cyclodextrin.

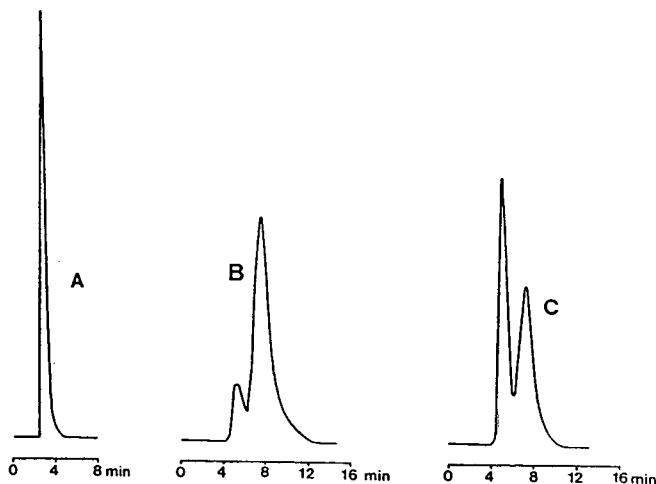


Fig. 4. Separation of the *cis-trans* isomers of Leu-Pro by ligand-exchange chromatography. Flow-rate, 1 ml/min; temperature, 0°C. (A) Column, L-proline without Cu(II); mobile phase, 0.05 M phosphate buffer (pH 4.5)–acetonitrile (92:8). (B) Injection of an aqueous solution of Leu-Pro freshly prepared at 0°C. Column, L-proline–Cu(II); mobile phase, 0.05 M phosphate buffer (pH 4.5) + 10⁻⁴ M copper(II) sulfate–acetonitrile (92:8). (C) Isomerization after storage of the solution at room temperature for 45 min. Conditions as in (B).

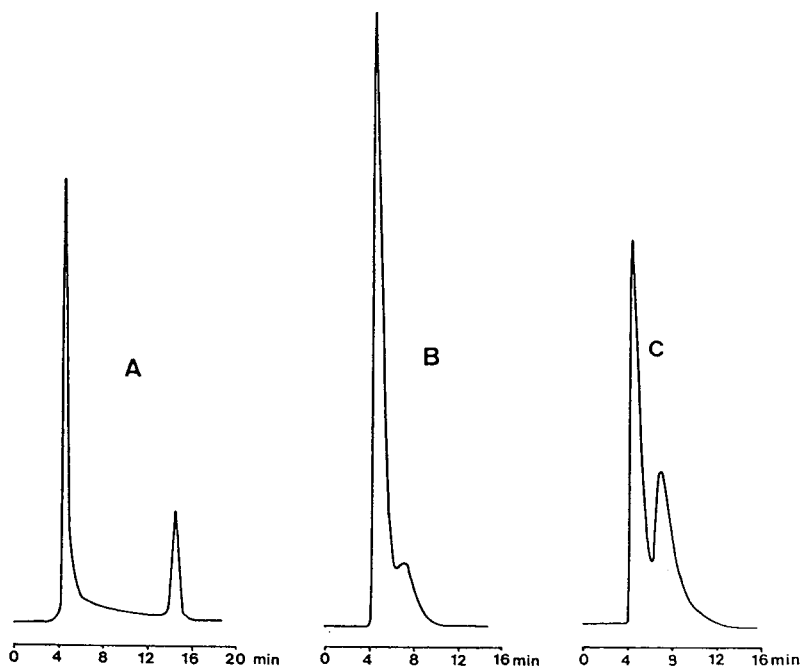


Fig. 5. Reinjection of a fraction of the second peak of Ile-Pro collected from the RP-18 column on to the L-proline–Cu(II) column. (A) Separation of an aqueous solution of Ile-Pro on the RP-18 column. Mobile phase, 0.05 M phosphate buffer (pH 4.5)–acetonitrile (98:2); temperature, 0°C; flow-rate, 1 ml/min. (B) Reinjection of a fraction of the second peak on to the L-proline–Cu(II) column. Conditions as in Fig. 4B. (C) Isomerization after storage of the fraction at room temperature for 45 min.

injected on to the L-proline column, the second peak was dominant. These results were confirmed in reverse by collecting fractions from the L-proline column and transferring them on to the RP-18 column.

4. Conclusions

Conformational changes of the peptide bond in proline-containing dipeptides were studied using HPLC with stationary phases utilizing different separation principles. It was shown that in addition to the conformer separations on reversed-phase and β -cyclodextrin-bonded silica described recently, a graphitized carbon phase and a chemically bonded L-proline–Cu(II) phase are additional tools for the investigation of *cis*–*trans* isomerism in proline-containing peptides. Based on the different discrimination mechanism, the elution order of the peptide conformers can change. The real elution order of the *cis* and *trans* forms can only be established by NMR analysis immediately after low-temperature isomer fractionation.

The composition of the mobile phase, pH, temperature and flow-rate are variables affecting the dynamic equilibrium and, accordingly, the

resolution of peptide conformers in the corresponding chromatographic system.

References

- [1] G. Fischer, H. Bang and C. Mech, *Biomed. Biochim. Acta*, 43 (1984) 1104.
- [2] D. Hübner, G. Fischer, D. Ströhl, E. Kleinpeter, B. Hartrodt and W. Brandt, *Fresenius' Z. Anal. Chem.*, 337 (1990) 131.
- [3] D. Hübner, T. Drakenberg, S. Forsen and G. Fischer, *FEBS Lett.*, 284 (1991) 79.
- [4] D. Hübner, B. Hartrodt, E. Kleinpeter, D. Ströhl, W. Brandt, H. Schinke, M. Wahab and G. Fischer, *Biochem. Biophys. Res. Commun.*, 177 (1991) 271.
- [5] J.T. Gerig, *Biopolymers*, 10 (1971) 2435.
- [6] W.R. Melander, J. Jacobson and C. Horvath, *J. Chromatogr.*, 234 (1982) 269.
- [7] S. Friebe, G.-J. Krauss and H. Nitsche, *J. Chromatogr.*, 598 (1992) 139.
- [8] S. Friebe, B. Hartrodt, K. Neubert and G.-J. Krauss, *J. Chromatogr. A*, 661 (1994) 7.
- [9] G. Gübitz, W. Jellenz and W. Santi, *J. Chromatogr.*, 203 (1981) 377.
- [10] G. Gübitz, W. Jellenz and F. Juffmann, *Chromatographia*, 16 (1982) 103.
- [11] D.E. Henderson and Cs. Horvath, *J. Chromatogr.*, 368 (1986) 203.
- [12] J.H. Knox, B. Kaur and G.R. Millward, *J. Chromatogr.*, 352 (1986) 3.

Short Communication

Separation of selenium analogues of sulphur-containing amino acids by high-performance liquid chromatography and high-resolution gas chromatography

Jaroslav Janák^{*a}, Hugo A.H. Billiet^b, Johannes Frank^b, Karel Ch.A.M. Luyben^b, Petr Hušek^c

^a*Institute of Analytical Chemistry, Academy of Sciences of the Czech Republic, Veveří 97, CZ-61142 Brno, Czech Republic*

^b*Kluyver Laboratory for Biotechnology, Julianalaan 67, 2628 BC Delft, Netherlands*

^c*Institute of Endocrinology, Narodní Avenue 8, CZ-11694 Prague, Czech Republic*

First received 21 February 1994; revised manuscript received 25 April 1994

Abstract

The historically conditioned adaptation of living organisms to chemically corresponding elements is influenced in nature by anthropogenic activities in many regions, the selenium–sulphur pair being one example of such a case. The separation of selenomethionine, selenoethionine and selenocystine was studied by HPLC and high-resolution GC. Ion-exchange chromatography followed by temperature-programmed GC gives the possibility of the analytical separation of trace amounts of selenomethionine in a complex mixture of common amino acids. Diastereoisomers of selenocystine were identified by HPLC in the AccQ-Tag mode.

1. Introduction

The anthropogenic influence in nature often causes specific variations of chemically related elements, which are able to change considerably the existing biological equilibrium based on the historically conditioned adaptation of living organisms to the ratio of these elements in the environment. Extensive industrial and agricultural activities carried out in different regions lead to substantial changes in the natural ratios of chemically corresponding elements, e.g., sulphur–selenium, phosphorus–arsenic and iodine–bromine.

Recently, considerable attention has been paid

to selenium as an element with a considerable biogenic function [1–3], since the recommended daily intake of selenium for a healthy human being is about 50–80 μg whereas a daily intake of more than ca. 800 μg is considered to be toxic. Selenium has a higher redox activity than sulphur, which positively influences the ability of certain enzymes, e.g., glutathione peroxidase, to scavenge unwanted oxygen-derived free radicals, which play a role in mutagenesis during the growth of living matter.

Although the determination of the absolute selenium content in biological materials by means of hydride (SeH_2) generation has been studied previously [4,5], it is more significant to speciate the selenium in the different chemical forms in which it occurs in food and which serve

* Corresponding author.

as intermediates in the biosynthesis of selenoprotein P and/or glutathione peroxidase [6]. The most relevant results have been obtained by the electrophoretic localization of selenium in individual protein fragments [6]. Wolf and co-workers tested ion-exchange chromatography for the separation and preparation of selenomethionine in a complex of common amino acids. They observed co-elution of selenomethionine with isoleucine and leucine and subsequently used a complicated chemical reaction with cyanogen bromide [7] and a microbiological assay [8] for the identification of selenomethionine. Owing to the relatively low resolving power of the system they used [7], in this work we investigated the potential of the separation of several selenium analogues of sulphur-containing amino acids by HPLC and high-resolution (HR) GC.

2. Experimental

2.1. Chemicals

The selenoamino acids seleno-D,L-ethionine (S-3750, Lot 116F-0171) and seleno-D,L-cystine (S-3625, Lot 108F-0321) were pure products from Sigma (St. Louis, MO, USA) and seleno-L-methionine (batch No. 561505, Lot 074491) was a pure product from Calbiochem (La Jolla, CA, USA).

2.2. Liquid chromatography

Chemicals for the Pico-Tag and AccQ-Tag system were purchased from Waters, Division of Millipore (Milford, MA, USA) according to their prescription.

The Waters Pico-Tag amino acid analysis system and procedure as described in the Waters operators' manual No. 88140 (July 1990, 9/86, 2/86, 5/84, revision 4) was used. The Waters Pico-Tag system is an automated gradient elution liquid chromatograph designed for the determination of amino acids by precolumn derivatization followed by reversed-phase HPLC. The precolumn derivatization is based on the reaction

of phenyl isothiocyanate to produce phenylthiocarbamoylamino acids. The total run time is 20 min.

The AccQ-Tag system is described in the Waters manual No. WAT052874, rev. 0, April 1993. The method is based on precolumn derivatization according to the method of Cohen and Michaud [9]. The gradient conditions were changed in order to be able to separate glutamine, asparagine, ornithine and tryptophan together with the amino acids present in acid protein hydrolysates. The gradient procedure is as follows. Mobile phase A contains 70 mM sodium acetate solution adjusted to pH 5 with phosphoric acid and mobile phase component B consists of 50% mobile phase A and 50% acetonitrile. The gradient profile is 98% A and 2% B at the start, then changed from 98 to 88% A in 26 min followed by a decrease to 54% A in 23 min. At that point, the column is purged with 100% B and re-equilibrated with 98% A for the next injection. The total run time is 65 min.

2.3. Gas chromatography

Derivatization was performed according to Ref. [10]. The selenoamino acids are mixed with ethyl chloroformate ester in aqueous solution [water–ethanol–pyridine (60:32:8)], after which relevant ethoxycarbonyl amino acid esters (EtOxC-AAEtEst) are formed in a few seconds. After extraction with chloroform, GC separation was performed [11] on a DB-1701 column (J & W Scientific, Folson, CA, USA) (5 m × 0.18 mm I.D., 0.4 μm thick film of 7% phenyl–7% cyanopropylpolydimethylsiloxane). A Shimadzu GC 14A gas chromatograph controlled by a Shimadzu C-R 18 Chromatopak was used with flame ionization detection using a hydrogen overpressure of 0.75 atm and temperature programming at 20°C/min from 120 to 300°C followed by an isothermal run for 5 min at 300°C.

3. Results and discussion

The retention data measured by the applied HRGC and HPLC systems are given in Table 1.

Table 1
Retention times (min) of the derivatized amino acids as measured by GC and HPLC

Derivatives of		GC	Pico-Tag	AccQ-Tag	IC [8]
Abbreviation ^a	Full name				
Ala	Alanine	0.55	8.81	27.65	
Gly	Glycine	0.68	6.97	18.42	
AAba	α -Aminobutyric acid	1.10	–	35.96	
Val	Valine	1.23	12.21	40.78	
Leu	Leucine	1.55	14.89	46.29	33.64
Ile	Isoleucine	1.59	14.57	46.00	32.46
Pro	Proline	1.85	9.14	33.30	
Thr	Threonine	1.99	8.59	25.03	
Ser	Serine	2.11	6.36	15.86	
Glu	Glutamic acid	2.11	3.47	17.56	
Asn	Asparagine	2.28	6.00	16.40	
Asp	Aspartic acid	2.66	3.17	14.25	
Met	Methionine	3.05	12.77	41.41	30.20
Hyp	Hydroxyproline	3.47	–	–	
Phe	Phenylalanine	3.55	16.32	47.47	
CysH	Cysteine	3.87	13.72	34.00	
I.S. ^b	Chlorophenylalanine	4.49	–	–	
Gln	Glutamine	4.92	6.66	19.64	
Orn	Ornithine	5.13	–	43.32	
Lys	Lysine	5.52	18.18	44.99	
His	Histidine	5.82	7.52	22.90	
Tyr	Tyrosine	6.24	11.18	40.33	
Trp	Tryptophan	7.02	16.75	48.77	
Cys	Cystine	7.88	–	38.80	32.40
NH ₃	Ammonia	–	–	24.04	
Arg	Arginine	–	8.23	28.31	
SeMet	Selenomethionine	3.36	13.80	43.49	33.09
SeEt	Selenoethionine	3.63	16.20	47.41	
SeCys ₁	Selenocystine (1)	8.38	13.80	40.30	
SeCys ₂	Selenocystine (2)	8.38	14.15	40.73	

^a Used in Figs. 1 and 2.

^b Internal standard.

To evaluate the separation possibilities and resolution problems with the studied seleno analogues of sulphur-containing amino acids in mixtures with naturally occurring amino acids, it is illustrative to compare the chromatograms of pure selenoamino acids and common amino acids under identical conditions obtained by GC and LC.

Fig. 1 shows the results of independent runs with an equimolar test mixture of common amino acids and selenoamino acids as EtOxC-AAEtEst separated by temperature-programmed GC. It is evident that selenomethionine is

well resolved from methionine and hydroxyproline and that selenoethionine is well separated from phenylalanine and cysteine. The selenocystine derivative forms a single peak eluting far behind the cystine peak.

In Fig. 2, liquid chromatograms of relevant derivatives of the investigated selenoamino acids are depicted for both the (A) Pico-Tag and (B) AccQ-Tag protocols. For selenomethionine, 89% of the total recorded peak areas, measured as the absorbance at 254 nm of the phenylthiocarbamoyl derivative, was found in the main peak. Similarly, the selenoethionine

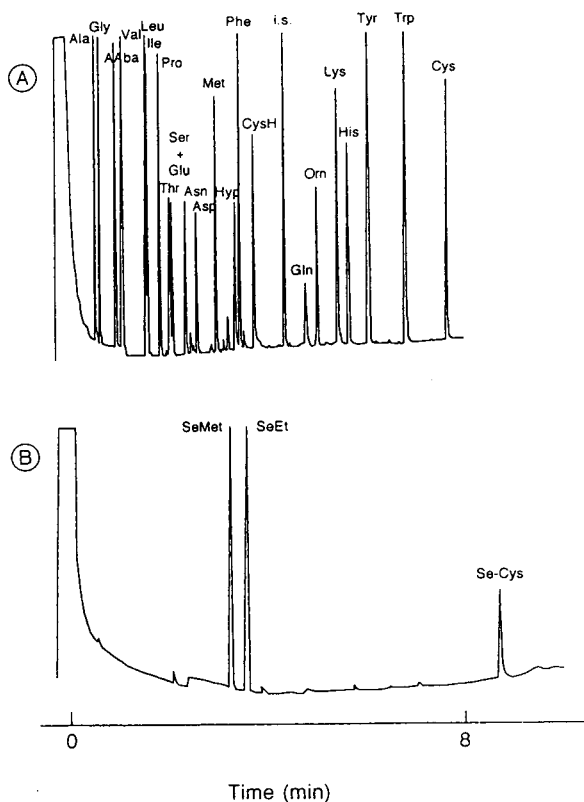


Fig. 1. GC separation of (A) a test mixture of common amino acids and (B) a mixture of the studied selenoamino acids, all as EtOx₂AAEtEst under identical conditions.

peak represents 78% and the double peak of selenocystine 85% of the total peak areas. It is remarkable that selenomethionine has the same retention as the first peak of selenocystine, in contrast to the large retention distance between selenomethionine and selenoethionine, which differ by only one CH₂ group.

To rule out of presence of selenomethionine in the selenocystine preparation, the samples were also analysed using the AccQ-Tag protocol. Virtually baseline resolution for the selenocystine double peak was obtained and selenomethionine was well separated from selenocystine. Here it appears that valine (see Table 1) co-elutes with the second peak of the selenocystine doublet, but as this amino acid is well resolved from selenocystine in the Pico-Tag chromatogram (see Table 1), the double peak is

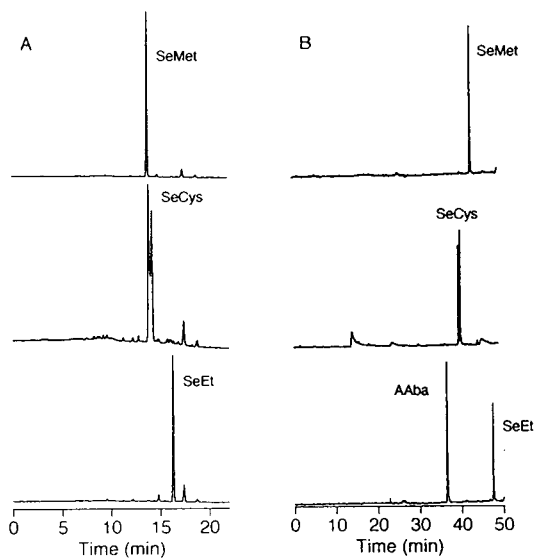


Fig. 2. Liquid chromatograms of selenoamino acid derivatives obtained using (A) the Pico-Tag and (B) the AccQ-Tag systems.

either due to another impurity or represents two different derivatives of selenocystine. Interestingly, GC reveals only a single peak and does not show the presence of valine or selenomethionine, in agreement with the results obtained by HPLC. Cystine and selenocystine have two optically active centres, giving rise to four possible diastereoisomers, DD, DL, LD and LL. It is clear that an achiral system is able to distinguish only between DD and LL diastereoisomers. A similar separation has been observed earlier for cystine diastereoisomers [12]. It is possible that the full separation of all isomers can be achieved by chiral chromatography.

The small differences in the peak heights of impurities in the HPLC traces are caused by the different detection modes used in the Pico-Tag (absorbance) and AccQ-Tag (fluorescence) protocols.

4. Conclusions

It can be concluded that optimal detection of trace amounts of selenomethionine in the presence of a large excess of the common amino

acids can be achieved in the following way. The sample is subjected to an ion-exchange separation according to Ref. [8] and the cysteine–isoleucine–leucine peak cluster (32–35 min) is collected and, after derivatization with chloroformate, subjected to GC. Temperature-programmed GC results in complete separation of the components of the mixture with the other amino acids eluting either well before (1.6 min) or after (3.85 min) the selenomethionine peak (3.38 min), thus permitting the detection of trace amounts of selenomethionine. A quantitative evaluation of the detection limit of trace amounts of selenomethionine among the excess of common amino acids based on the investigation of real samples will be published later.

Acknowledgements

The first author is indebted to Professor Wayne R. Wolf, US Department of Agriculture, Human Nutrition Research Center, Beltsville, MD, USA, for kindly supplying authentic samples of the selenoamino acids used in his research [7,8]. The authors also thank Ms. C.

Erkelens for the analysis of the (seleno)amino acids by the Pico-Tag and AccQ-Tag methods.

References

- [1] R.J. Shamberger, *Biochemistry of Selenium*, Plenum Press, New York, 1983.
- [2] J. Neve and A. Favier (Editors), *Selenium in Medicine and Biology*, Walter de Gruyter, Berlin, 1989.
- [3] K. Forchhammer and A. Buck, *Naturwissenschaften*, 78 (1991) 497.
- [4] W.T. Buckley, J.J. Budac, D.V. Godfrey and K.M. Koenig, *Anal. Chem.*, 64 (1992) 724.
- [5] M. Janghorbani and B.T.G. Ting, *Anal. Chem.*, 61 (1989) 701.
- [6] J.T. Deagen, J.A. Butler, B.A. Zachara and P.D. Whagner, *Anal. Biochem.*, 208 (1993) 176.
- [7] W.R. Wolf, D.E. LaCroix and M.E. Slagt, *Anal. Lett.*, 25 (1992) 2165.
- [8] E. Tschursin and W.R. Wolf, *Fresenius' J. Anal. Chem.*, 345 (1993) 243.
- [9] S.A. Cohen and D.P. Michaud, *Anal. Biochem.*, 211 (1993) 279.
- [10] P. Hušek, *J. Chromatogr.*, 522 (1991) 289.
- [11] P. Hušek and C.C. Sweely, *J. High Resolut. Chromatogr.*, 14 (1991) 751.
- [12] C.H.W. Hirs, S. Moore and W. Stein, W., *J. Am. Chem. Soc.*, 76 (1954) 6063.



ELSEVIER

Journal of Chromatography A, 677 (1994) 197–200

JOURNAL OF
CHROMATOGRAPHY A

Short Communication

Highly selective liquid crystalline polysiloxane stationary phase for gas chromatographic separation of isomers

G. Kraus^a, J.M. Thierfelder^a, L. Soják^{b,*}

^aInstitute of Analytical Chemistry, Martin-Luther Universität Halle, D-06120 Halle (Saale), Germany

^bChemical Institute, Faculty of Natural Sciences, Comenius University, 842 15 Bratislava, Slovak Republic

First received 29 December 1993; revised manuscript received 22 March 1994)

Abstract

The gas chromatographic isomeric selectivity (for *p*- and *m*-xylene) of six mesogenic monomers and polysiloxanes having various side-chains, degrees of polymerization and linking ester groups (–OOC– and –COO–) were investigated. The results indicate that the polymeric stationary phases had higher isomeric selectivities. The highest selectivity coefficient for *p*- and *m*-xylene, $\alpha = 1.21$, was obtained at 65°C for the polymeric stationary phase [4-octyloxy(4-allyloxyphenyl benzoate)]polymethylhydrogensiloxane (POBAP-20) with an optimized film thickness of 0.63 μm .

1. Introduction

Generally, liquid crystals are the most selective stationary phases for the gas chromatographic separation of isomers. The bonding of polysiloxanes with liquid crystalline compounds produces substances with interesting characteristics as stationary phases. Among liquid crystalline polymers, in this particular case mesogenic polysiloxane, are many substances useful as selective stationary phases for the separation of compounds additionally according to their molecular shape [1]. Capillary columns prepared from such polymers are generally more thermostable and often more efficient than columns coated with monomeric phases. By the selection of polysiloxane chains, namely of the correct composition and *n*-alkyl chain length,

and by the connection of the mesomorphic molecules to the polysiloxane backbone, liquid crystals can be obtained that are isotropic at temperatures exceeding 300°C. The melting points of these mesogenic polysiloxane (MEP-SIL)-type phases are in the range 90–140°C [2]. This limits their application in the gas chromatographic separation to the substances that have relatively low boiling points.

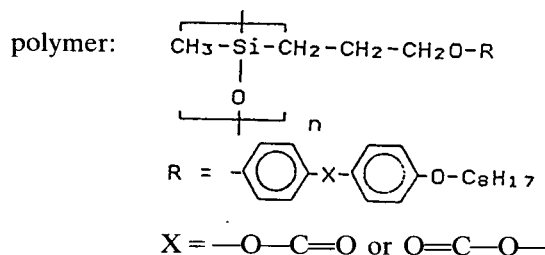
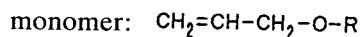
In previous work [3] the retention behaviour of MEPSIL with different lateral chains was studied. Relatively high selectivity for *p*- and *m*-xylene was observed in the smectic range of these stationary phases. Jin et al. [4] reported very high selectivity for *p*- and *m*-xylene measured on similar liquid crystalline polysiloxane phases. Based on these results, we focused our interest on selectivity studies with this type of polymeric liquid crystals. For this purpose, we synthesized monomers and polymers having dif-

* Corresponding author.

ferent side-chains, degrees of polymerization and linking ester functional groups ($-\text{OOC}-$ and $-\text{COO}-$) [3], and then investigated the gas chromatographic behaviour of these compounds with respect to their selectivity for the separation of isomers.

2. Experimental

The retention properties of six synthesized liquid crystalline stationary phases coated on glass capillary columns (columns 1–6 in Table 1) with different structures were studied:



The basic characteristics of phase transitions of the monomer [4-octyloxy(4-allyloxyphenyl benzoate)] (No. 1) and their polymers obtained by reaction with polymethylhydrogensiloxane (Nos. 2 and 3) and the monomer [4-allyloxy(4-octyloxyphenyl benzoate)] (No. 4) and their polymers (Nos. 5 and 6) are presented in Table

1. The phase transition temperatures were measured using a light-polarized microscopy and a DSC-7 calorimeter (Perkin-Elmer) (data were obtained from M. Müller, Halle University, Germany). These values are in a good agreement with gas chromatographic measurements. The film thickness of the stationary phases, coated on glass capillary columns ($30 \text{ m} \times 0.31 \text{ mm}$ I.D.) by the static method described by Grob et al. [5], were 0.31, 0.47, 0.63 and $1.00 \mu\text{m}$, respectively. The measurements were carried out with a Carlo Erba GI 452 gas chromatograph equipped with a flame ionization detector. Hydrogen was used as the carrier gas with a velocity of 27 cm/s . The efficiencies of the prepared glass capillary columns were within the limits published in a review [6] for other MEPSIL liquid crystalline phases.

3. Results and discussion

The selectivity coefficients α for *p*- and *m*-xylene of the six liquid crystalline phases coated on capillary columns were measured at several temperatures. The measurements were carried out in the mesogenic, crystalline and glassy states with heating and cooling of the columns.

Fig. 1 shows dependence of α on temperature with column heating for monomeric and polymeric MEPSIL columns with a stationary phases film thickness of $0.31 \mu\text{m}$. The curves indicate that the selectivity of polymeric phases is higher

Table 1
Phase transitions of the investigated monomeric and polymeric liquid crystalline stationary phases

No.	n^a	Name	Middle group	Monomer ^b	Polymer ^b
1	—	OBAP	$-\text{OOC}-$	Cr65(S_A 60)N87Is	
2	20	POBAP	$-\text{OOC}-$		Cr55CL134Is
3	36	POBAP	$-\text{OOC}-$		Cr67 S_B 82 S_A 156Is
4	—	ABOP	$-\text{COO}-$	Cr63N85Is	
5	20	PABOP	$-\text{COO}-$		Cr35CL98Is
6	36	PABOP	$-\text{COO}-$		G28S89N111Is

^a n = Average degree of polymerization.

^b Abbreviations: Cr = crystalline; G = glassy; S_A , S_B = smectic A and B; N = nematic; Is = isotropic liquid; CL = crystalline liquid state; the numbers are transition temperatures in $^\circ\text{C}$.

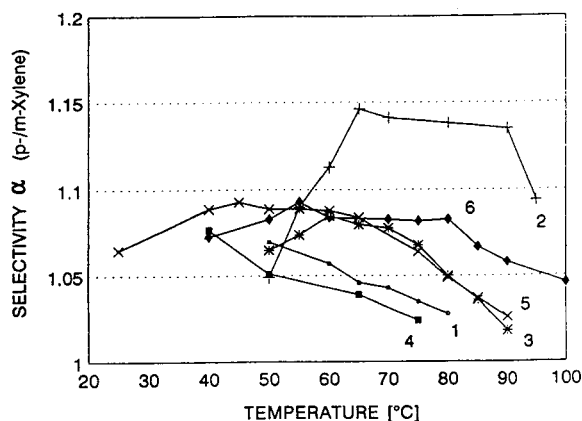


Fig. 1. Temperature dependence of selectivity coefficient of the investigated liquid crystalline stationary phases with film thicknesses $0.31 \mu\text{m}$ in the column heating mode. 1 = OBAP; 2 = POBAP-20; 3 = POBAP-36; 4 = ABOP; 5 = PABOP-20; 6 = PABOP-36.

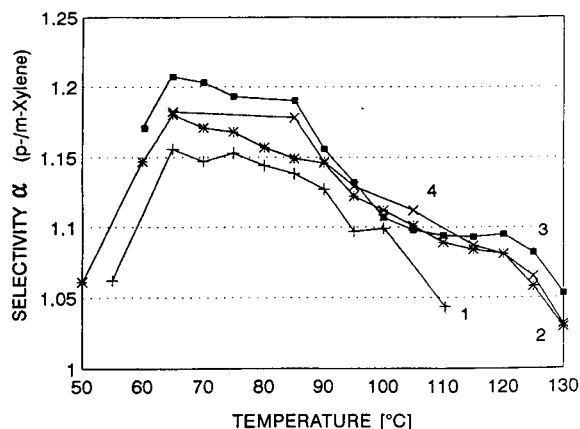


Fig. 2. Temperature dependence of selectivity coefficient on film thickness of POBAP-20 in the column cooling mode: 1 = $0.31 \mu\text{m}$; 2 = $0.47 \mu\text{m}$; 3 = $0.63 \mu\text{m}$; 4 = $1.00 \mu\text{m}$.

than that of monomeric phases. This result is contrary to the idea that the selectivity of liquid crystal polysiloxane stationary phases increases with increasing content of the mesogenic substituent in the polymeric molecule [7]. Moreover, the length of the Si chains (size of the molecule) influences the selectivity coefficient in different ways. For example, in the POBAP phase the α values for the polymer with $n = 20$ are generally higher than for the polymer with $n = 36$. Conversely, for the PABOP phases the polymer with $n = 36$ has a slightly higher selectivity than the polymer with $n = 20$ at temperatures exceeding 75°C , whereas at lower temperatures both polymers have similar α values. From the dependences in Fig. 1, it is evident that the highest selectivity coefficients were obtained in columns with a POBAP-20 stationary phase and with a film thickness of $0.31 \mu\text{m}$ at 65°C ($\alpha = 1.15$). A similar dependence of the α values on temperature was found also in measurements with cooling POBAP-20 capillary columns.

The column selectivity also depends on the film thickness of the liquid crystalline stationary phase [8]. In capillary columns maximum selectivity is obtained when an optimum film thickness of stationary phase is applied. Fig. 2 demonstrates the dependence of the α values on the

film thickness of POBAP-20 stationary phase in the column cooling mode. It appears that in the interesting temperature range $60\text{--}90^\circ\text{C}$, with increasing stationary phase film thickness from 0.31 to $0.63 \mu\text{m}$ the α value increase, but for a film thickness of $1.0 \mu\text{m}$ the selectivity coefficient is slightly lower. The highest value, $\alpha = 1.21$ for *p*- and *m*-xylene, was found on a POBAP-20 capillary column with a film thickness of $0.63 \mu\text{m}$ at 65°C .

A very high α value of 1.33 for *p*- and *m*-xylene at 70°C has been reported [4] for a similar liquid crystalline stationary phase to PABOP-20 (degree of polymerization $n = 19$). However, the authors subsequently reported that their experimental measurements were misinterpreted [9].

Values of selectivity coefficients for *p*- and *m*-xylene measured on liquid crystalline stationary phases were compiled by Mazur and Witkiewicz [6]. They reported the highest measured selectivity coefficient $\alpha = 1.19$ at 40°C [10]. Comparison of these data with our measurements shows that the stationary phase POBAP-20 has the highest selectivity coefficient for *p*- and *m*-xylene. Possible explanations for the high selectivity of POBAP-20 might include a favourable ratio of the mesogenic group, degree of polymerization, structure of lateral chains, packing of

the molecules and/or the film thickness of the MEPSIL phase in capillary columns. A computer program is in preparation to evaluate possible correlations between the molecular structure of liquid crystals and their isomeric selectivity.

Acknowledgements

The authors are indebted to Dr. B. Krücke for preparing the liquid crystalline compounds, M. Müller for the phase transition data and Dr. A. Kraus for suggestions regarding the manuscript (all from Halle University).

References

- [1] H. Finkelmann, R.J. Laub, W.L. Roberts and C.A. Smith, in M. Cooke, A.J. Dennis and G.L. Fisher (Editors), *Polynuclear Aromatic Hydrocarbons: Physical and Biological Chemistry*, Battelle Press, Columbus, OH, 1982, pp. 275–285.
- [2] G.M. Janini, G.M. Muschnik, H.J. Issaq and R.J. Laub, *Anal. Chem.*, 60 (1988) 1119.
- [3] F. Hahne, *Dissertation*, Martin-Luther-Universität, Halle, 1990.
- [4] Y. Jin, R. Fu, Z. Guan, J. Gong and B. Li, *J. Chromatogr.*, 483 (1989) 394.
- [5] K. Grob, Jr., G. Grob and K. Grob, *J. Chromatogr.*, 156 (1978) 1.
- [6] J. Mazur and Z. Witkiewicz, *LC · GC*, 3 (1990) 38.
- [7] S.A. Wise, L.C. Sander, K.H.C. Chang, K.E. Markides and M.L. Lee, *Chromatographia*, 25 (1988) 473.
- [8] R.R. Heath, J.R. Jordan and P.E. Sonnet, *J. High Resolut. Chromatogr. Chromatogr. Commun.*, 4 (1981) 328.
- [9] R. Fu, personal communication.
- [10] J. Mazur, Z. Witkiewicz and R. Dabrowski, *Biul. Wojsk. Akad. Tech.*, 37 (1988) 33.

Short Communication

Analysis of the petroleum components benzene, toluene, ethyl benzene and the xylenes in water by commercially available solid-phase microextraction and carbon-layer open tubular capillary column gas chromatography

Leonard P. Sarna^a, G.R. Barrie Webster^{a,*}, Marcia R. Friesen-Fischer^b,
Ramanathan Sri Ranjan^b

^aDepartment of Soil Science, University of Manitoba, Winnipeg, MB R3T 2N2, Canada

^bDepartment of Agricultural Engineering, University of Manitoba, Winnipeg, MB R3T 5V6, Canada

First received 3 November 1993; revised manuscript received 8 March 1994

Abstract

Extraction of the petroleum components benzene, toluene, ethyl benzene and the xylenes (BTEX) from water is described using a commercially available poly(dimethylsiloxane) solid-phase microextraction fibre assembly with separation and quantification by carbon-layer open tubular capillary column gas chromatography and flame ionization detection. All components of BTEX are resolved. No cryofocussing is required.

1. Introduction

Contamination of surface and ground water with hydrocarbon fuel is an increasing problem. In both the monitoring of such contamination and in determining the success of remediation methods, a straightforward and inexpensive analytical method is required. Benzene, toluene, ethyl benzene and the three isomers of xylene (*o*-, *m*- and *p*-) (BTEX) are common industrial solvents and fuel components and were used in this study in view of their importance as common contaminants of ground water [1] as well as their reported presence in landfill leachates [2]. Their presence may be due to incomplete combustion

of gasoline, leaking underground fuel-storage tanks, or accidental spills of gasoline or other types of hydrocarbon fuels, or industrial accidents.

Analytical methodology for these compounds usually involves liquid–liquid extraction [3,4], purge-and-trap [5,6] or headspace sampling [7] followed by capillary column gas chromatography (GC) using an appropriate detector, such as flame ionization detection (FID) or mass spectrometry (MS).

The new poly(dimethylsiloxane)-coated extraction fibre technique first reported by Belardi and Pawliszyn [8] has been successfully used to extract 2-naphthol from aqueous solution and further described in a series of recent papers [9–15]. Thermal desorption of the sorbed BTEX

* Corresponding author.

within the GC injector coupled with cryofocusing was used in conjunction with conventional capillary GC and FID, or ion-trap detection. The technique has also demonstrated potential application to the extraction of chlorobenzenes and polychlorinated biphenyls [9], caffeine and fragrances [11] and US Environmental Protection Agency priority pollutants [13]. In each case, cryotrapping has been utilized to focus the more volatile analytes on the capillary column prior to analysis.

Theoretical considerations of the solid-phase microextraction technique (SPME) have been discussed thoroughly in the literature [9,10] and need not be repeated here, except to say that the amount of analyte absorbed by the coated fibre in a given time has been shown to be affected by three major factors: (a) the distribution constant of the analyte, (b) the volume of the stationary phase and (c) the stirring of the solution (which has been shown to shorten equilibration time). In SPME, exhaustive extraction does not occur. An equilibrium is established between the aqueous and stationary phases and it has been demonstrated that a linear relationship exists between the amount of analyte sorbed to the stationary phase and the concentration of analyte in the sample. This relationship is mathematically described in Eq. 1

$$n = KV_s C_{aq} \quad (1)$$

where n = number of moles of analyte absorbed by the stationary phase, K = distribution constant of the analyte, V_s = volume of the stationary phase and C_{aq} = concentration of the analyte in the aqueous phase.

Conventional capillary GC of BTEX has usually been carried out using non-polar columns, e.g., DB-1 and DB-5 columns (Chromatographic Specialties, Brockville, Canada) [16–18]. As mentioned above, use of these columns for SPME analysis has required cryofocussing following thermal desorption in the GC injector. Recently, GC analysis of the BTEX contaminants split-injected in the conventional manner has been reported using the recently developed carbon-layer open tubular (CLOT) capillary column [19,20] from Supelco (Canada) (Oakvil-

le, Canada). We report a simple, new method for the analysis of BTEX from aqueous samples in which the convenience of solventless fibre extraction is mated with the separating power of the CLOT column without the need for cryofocussing.

2. Experimental

2.1. Standards

Conventional standard solutions of benzene, toluene, ethyl benzene and the xylenes (0.002%, v/v) were made up in dichloromethane. Injections of 1.7 to 170 ng/ μ l of each component were used to plot a standard curve.

A standard solution in methanol of benzene, toluene, ethyl benzene and *o*-, *m*- and *p*-xylene (0.002%, v/v) was prepared for use in spiking of water samples at levels from 35 to 850 ng component per ml.

2.2. Extraction

SPME extraction was performed using a Supelco No. 5-7300 manual 100- μ m poly(dimethylsiloxane) solid-phase microextraction fibre assembly. Aliquots of 10 ml of spiked water samples were placed in 12-ml screw-cap vials equipped with stir bars, fitted with silicone/PTFE septa, and clamped in place on a magnetic stir plate. The SPME assembly was clamped in place above and resting on the vial cap. The vial septum was pierced with the septum-piercing needle and the fibre was lowered into the solution so that the stainless-steel needle attachment was just below the meniscus (Fig. 1). After 2.0, 3.5 or 5.0 min extraction time, the fibre was retracted into the septum-piercing needle and the needle was withdrawn from the vial septum.

2.3. Injection

To determine the optimum depth of penetration for the fibre in the GC injection port, the needle/fibre assembly was compared to a normal 10- μ l GC syringe. The length comprising the

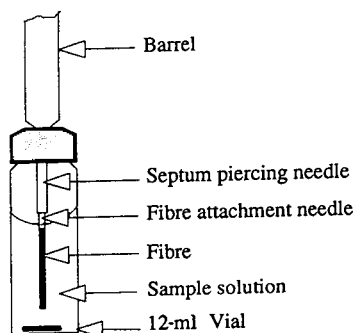


Fig. 1. Septum cap vial with SPME assembly illustrating position of fibre and septum-piercing needle during extraction. Small magnetic stir bar is shown.

stainless-steel septum-piercing needle plus the attachment needle and the silica fibre was adjusted to equal the length of a normal syringe needle. The SPME fibre assembly was adjusted to bring the top of the barrel to 3.4 cm on the scale on the fibre assembly.

The SPME fibre assembly was clamped upright over the GC injection port. The GC septum was pierced using the septum-piercing needle with the barrel of the fibre assembly resting on the GC injection port. The fibre was lowered into the injection port with the purge off. After 2 min desorption time, the fibre was retracted into the septum-piercing needle, the needle was withdrawn from the injection port, and the chromatography was begun.

The completeness of the thermal desorption was checked by carrying out "blank" runs of the previously desorbed fibre by GC using a thermal desorption time of 2 min.

2.4. Analysis

A Hewlett-Packard 5890 GC system equipped with FID and operating in the splitless mode was used for the analysis of the BTEX. Separations were conducted using a Supelco 30 m \times 0.32 mm I.D. CLOT column. The chromatographic conditions were as follows: injector, 220°C; column, 40°C for 2 min, 15°C/min to 180°C, hold 1 min; detector, 250°C; flow-rates: helium carrier, 1.8 ml/min; helium makeup, 30 ml/min; hydrogen, 30 ml/min; air, 150 ml/min. SPME samples from

BTEX solutions containing 35 to 850 ng/ml were analyzed and the FID responses related to the concentrations sampled.

3. Results and discussion

New analytical methodology based on a combination of the previously separately de-

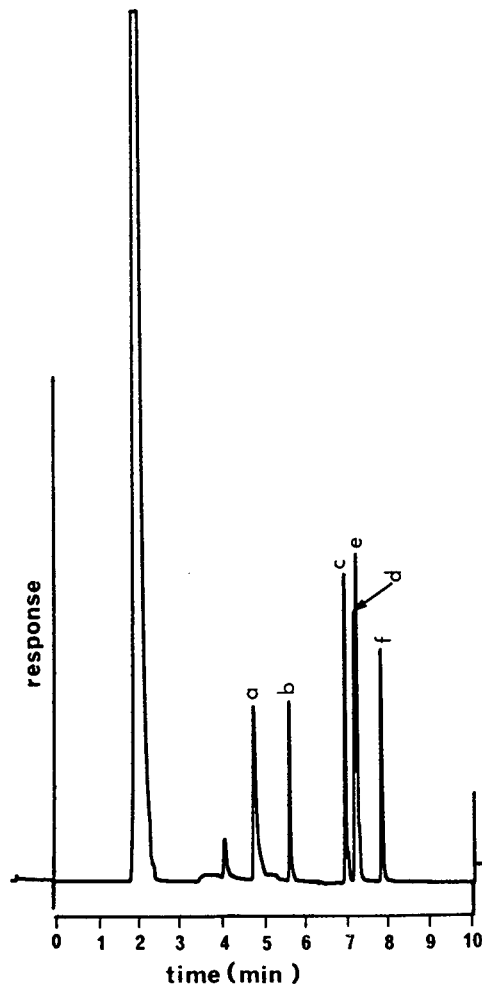


Fig. 2. Recovery of BTEX components from water sample spiked at 170 ng/ml by SPME-CLOT-GC-FID showing resolution of the *m*- and *p*-xylene isomers. Peak identities are given in Table 1. Unlabelled peaks prior to peak a, from the left, are methanol from the BTEX solutions used to spike the water, and an unknown. Total desorption and GC run time, 10 min.

scribed techniques of SPME and CLOT column capillary GC with FID has been successfully demonstrated to be feasible for the analysis of BTEX hydrocarbon contaminants in water. The apparatus for each of these techniques is now available "off the shelf".

Little difference in BTEX levels recovered was shown between the exposure times chosen, and is consistent with earlier reports [12,13]. While a 2-min extraction time was shown to be sufficient for BTEX from water followed by a 2-min thermal desorption time in the injection port of the GC, we chose 3.5 min exposure time for this work. Complete desorption after 2 min at 220°C was demonstrated. Total run time for a desorption and GC analysis was 10 min.

Fig. 2 demonstrates the recovery of BTEX components from a 10-ml aliquot spiked at 170 ng/ml per component. Two points are noteworthy. The first is that the chromatogram was generated without the need of the cryotrapping required for all previous work involving the use of SPME. Cryotrapping was previously required to minimize peak broadening associated with the relatively long desorption times involved in sample introduction by SPME. The second point is that the chromatogram clearly illustrates resolution of the *m*- and *p*-xylene isomers, not seen in earlier papers using either conventional or SPME analysis.

Since SPME relies on the partition of the BTEX from water into the polymer coating of

the extraction fibre, the response seen for each component will vary according to its partition coefficient. Table 1 presents data on the retention time and minimum detectable limit for each of the BTEX components. The linearity of the response for each of the component compounds compared to its concentration in the spiked water sample was determined. The r^2 values in Table 1 reflect the goodness of fit over the range of 36 to 860 ng/ml of BTEX components in water. The differences in minimum detectable limits for the BTEX components more closely reflect the trend in the octanol-water partition coefficients (K_{ow}) reported by Arthur et al. [12] than the distribution coefficients in their original study and support their premise that the K_{ow} values of analytes can be used to predict the linear range and limit of quantification in new method development using these fibres before any experimental work is begun. The current study used the commercially supplied SPME fibre; Arthur et al. used fibres prepared in their own laboratory.

4. Conclusions

Analysis of BTEX in water by SPME, thermal desorption in the injection port, and GC-FID was directly possible using the commercially available CLOT column with linear response demonstrated for water samples containing 35 to

Table 1

Retention relative to benzene, minimum detectable limit (MDL) by direct fibre introduction of individual BTEX components from fortified water, and linear regression results (coefficient of determination) for the BTEX components extracted from water by SPME and desorbed and analyzed by GC

Compound	Relative retention	MDL (ng)	Range of fortification (ng/ml)	
(a) Benzene	1.00	0.4	35–850	0.9507
(b) Toluene	1.34	0.4	35–850	0.9701
(c) Ethylbenzene	1.63	0.05	35–850	0.9930
(d) <i>p</i> -Xylene	1.68	0.2	35–850	0.9923
(e) <i>m</i> -Xylene	1.69	0.2	35–850	0.9904
(f) <i>o</i> -Xylene	1.81	0.1	35–350	0.9973

Benzene retention time was 4.18 min.

850 ng/ μ l. The previously prescribed cryofocusing of the desorbed BTEX is now unnecessary, making the SPME–CLOT column technique for BTEX readily usable by most analytical laboratories equipped with normal GC–FID instrumentation.

References

- [1] D.M. Mackay, P.V. Roberts and J.A. Cherry, *Environ. Sci. Technol.*, 19 (1985) 384.
- [2] J.F. Barker, *Water Pollut. Res. J. Canada*, 22 (1987) 33.
- [3] G.A. Eiceman, J.T. McConnon, M. Zaman, C. Shuey and D. Earp, *Int. J. Environ. Anal. Chem.*, 24 (1986) 143.
- [4] *Test Methods for Evaluating Solid Waste, Physical/Chemical Methods, SW-846*, US Environmental Protection Agency, 3rd ed., July 1992, method 3520A.
- [5] S.B. Hawthorne and R.E. Sievers, *Environ. Sci. Technol.*, 18 (1984) 483.
- [6] *Test Methods for Evaluating Solid Waste, Physical/Chemical Methods, SW-846*, US Environmental Protection Agency, 3rd ed., July 1992, method 5030A.
- [7] J.F. Pankow, *Environ. Sci. Technol.*, 25 (1991) 123.
- [8] R.P. Belardi and J. Pawliszyn, *Water Pollut. Res. J. Canada*, 24 (1989) 179.
- [9] C.L. Arthur and J. Pawliszyn, *Anal. Chem.*, 62 (1990) 2145.
- [10] D. Louch, S. Motlagh and J. Pawliszyn, *Anal. Chem.*, 64 (1992) 1187.
- [11] S.B. Hawthorne, D.J. Miller, J. Pawliszyn and C.L. Arthur, *J. Chromatogr.*, 603 (1992) 185.
- [12] C.L. Arthur, L.M. Killam, S. Motlagh, M. Lin, D.W. Potter and J. Pawliszyn, *Environ. Sci. Technol.*, 26 (1992) 979.
- [13] C.L. Arthur, D.W. Potter, K.D. Bucholtz, S. Motlagh and J. Pawliszyn, *LC·GC*, 10 (1992) 656.
- [14] D.W. Potter and J. Pawliszyn, *J. Chromatogr.*, 625 (1992) 247.
- [15] C.L. Arthur, L.M. Killam, K.D. Bucholtz, J. Pawliszyn and J.R. Berg, *Anal. Chem.*, 64 (1992) 1960.
- [16] P.V. Cline, J.J. Delfino and P.C.S. Rao, *Environ. Sci. Technol.*, 25 (1991) 914.
- [17] S.R. Hutchins, *Environ. Toxicol. Chem.*, 10 (1991) 1437.
- [18] S.R. Hutchins, G.W. Sewell, D.A. Kovacs and G.A. Smith, *Environ. Sci. Technol.*, 25 (1991) 68.
- [19] P.S. Spock, R.E. Long and L. Sidisky, *Supelco Reporter*, XI, No. 4 (1992) 23.
- [20] L.M. Sidisky and M.V. Robillard, *J. High Resolut. Chromatogr.*, 16 (1993) 116.



ELSEVIER

Journal of Chromatography A, 677 (1994) 206-207

JOURNAL OF
CHROMATOGRAPHY A

Book Review

Manual of Pesticide Residue Analysis, Vol. II, edited by H.-P. Thier and J. Kirchhoff, (translated by J. Edwards and C.A. Traedgold), DFG Deutsche Forschungsgemeinschaft, Pesticide Commission/VHC, Weinheim, 1992, XVI + 481 pp., price DM 168.00, ISBN 3-527-27017-5 (Weinheim), 0-89573-957-7 (New York).

Volume I of the *Manual of Pesticide Residue Analysis* in the English version was published in 1987 and this continuation Volume II appeared in 1992.

The first volume dealt with single analytical methods for the detection and determination of 23 individual pesticides, together with 17 multi-residue methods and 6 clean-up procedures. The general section of the book discussed the main problems of sample collection and preparation and limits of detection and determination. Some other micro methods were also mentioned.

In residue analysis there is an ever-increasing demand to improve the effectiveness of older methods, e.g., to lower the limit of detection, to avoid the disturbing effects of co-extracts and to broaden the application of the methods to different food materials and pesticides. With the development of new pesticides there is a lack of sensitive methods. Volume II contains not only updated, very effective multi-residue analytical methods but also new methods that will be most useful in the determination of newly developed pesticides.

The methods published in both volumes have been tested in one or more independent laboratories, so most of these methods are included in the list of Recommended Methods of Analysis issued by the Codex Committee on Pesticide

Residue of the FAO/WHO Codex Alimentarius Commission.

Volume II consists of six main parts. The first part gives the definition of limit of detection (LDC) and limit of determination (LDM). A useful guide is given of how to establish a calibration graph, and a new concept is given for deriving the LDC and LDM by the calibration technique. This part also lists the main fragment ions and the relative intensities of almost 160 pesticides. These data will be especially helpful in GC-MS studies of biological samples, when multiple ion detection is used.

Clean-up methods are dealt with in the second part. This chapter is also a continuation of that in Volume I. Gel permeation chromatography is applied in analyses for approximately 350 pesticides and 60 non-pesticidal compounds with an automated apparatus. The elution volume ranges of these compounds are listed. The limitation of this method is discussed; fifteen other pesticides are enumerated that cannot be measured by gel permeation chromatography. The other two clean-up procedures presented are both based on solid-phase extraction for collecting pesticides from water samples using disposable alkyl-modified silica gel columns. The procedures for conditioning the columns are different in the two methods.

The third part is devoted to the most up-to-date methods for 32 individual pesticides in numerous plant materials and environmental samples (soil and water) using gas chromatography (GC) and high-performance liquid chromatography (HPLC). The manual contains some important data on the individual compounds such as the IUPAC name, structural formula, molar mass, melting and boiling points, vapour pressure and solubility in water in acidic, neutral and alkaline media. It would have been very useful for users if some toxicological data had also been listed. These data have a decisive influence on how sensitive the residue analytical methods should be. The methods are carefully described and it is easy to follow them. Where necessary, the procedures contain instructions for the detection and determination of the metabolites, e.g., for carbofuran, chloridazon, diclofluanid, tolylfluanid, glyphosate and pyridazine.

Two updated multi-residue methods, described in the fourth part, give instructions for the detection and determination of organochlorine and organophosphorus insecticides, triazine herbicides, several other nitrogen-containing compounds and some other pesticides. Further, five new multi-residue methods presented will help in analyses for natural pyrethroids, piperonyl butoxide, pyrethroids, organotin compounds, methylcarbamate insecticides and phthalimide derivatives. This chapter gives the common names, IUPAC names and structural formulae of about 130 pesticides, chemically related compounds and metabolites that can be determined by the multi-residue methods described in this and the next two chapters.

determined by the multi-residue methods described in this and the next two chapters.

Part five contains multiple methods for water analysis. Residues of fungicides, organochlorine insecticides and phenoxyalkanoic acid herbicides (the latter after two different derivatizations) are determined by GC. Further, HPLC methods are presented for the determination of triazine herbicides and desalkyl metabolites of chlorotriazine herbicides.

In the parts of the manual covered so far, GC or HPLC was used as the final determination method in pesticide residue analysis. The last part of the book is devoted to multiple pesticide residue methods using the automated multiple development (AMD) technique of thin-layer chromatography (TLC). The final determination is based on the UV absorbance of pesticides at six different wavelengths in the TLC scanner. The German versions of these methods were published in 1991.

To summarize, Volume II of the *Manual of Pesticide Residue Analysis*, together with Volume I, provides a wealth of information on the achievements of modern analytical methods that will satisfy the needs of professionals working in this field. It should be available in any pesticide laboratory. Its only shortcoming is that numerous analytical methods in Volume II cannot be used without Volume I. The two volumes together are really helpful tools in modern pesticide residue analysis.

Katalin Fodor-Csorba

Budapest, Hungary



ELSEVIER

Journal of Chromatography A, 677 (1994) 208

JOURNAL OF
CHROMATOGRAPHY A

Book Review

Applications of Supercritical Fluids in Industrial Analysis, edited by J.R. Dean, Chapman & Hall, London, 1993, XIV + 224 pp., price £65.00, ISBN 0-7541-0057-2.

This text is a compilation of chapters provided by a variety of researchers and edited by J.R. Dean from the University of Northumbria in Newcastle, UK. The text follows a standard format with a brief introduction to theory, an overview of instrumentation (during the 1992 time frame) both for supercritical fluid extraction (SFE) and chromatography (SFC) equipment, followed by a variety of applications chapters which highlight the areas of food science, polymers, environmental applications and pharmaceuticals. The final chapter is a brief overview of future developments which more accurately brings the textbook up-to-date (1993) with new instrumentation advancements and applications.

The editor and authors of the text have written a comprehensive text on the application topics chosen. However, there are a wider variety of

applications for both SFC and SFE technology that may not be broad enough to warrant a full chapter of applications but do illustrate potential future uses of SFE and SFC which have been omitted.

The editor/authors of this text, perhaps are practitioners of supercritical fluid technologies, but do not appear to have a broad based comprehensive view of the overall current state of the technology. The information in this text is an update of the text by Markides and Lee issued in 1990, entitled *Analytical Supercritical Fluid Chromatography and Extraction*, but in no way is as comprehensive.

Mary Ellen P. McNally

Wilmington, DE, USA

Journal of Chromatography A

Request for Manuscripts

Susumu Honda will edit a special, thematic issue of the *Journal of Chromatography A* entitled

Chromatographic and Electrophoretic Analyses of Carbohydrates

Both reviews and research articles will be included.

Topics such as the following will be covered:

- Gas chromatography and gas chromatography–mass spectrometry of carbohydrates
- Supercritical fluid chromatography of carbohydrates
- Thin-layer chromatography of carbohydrates
- Liquid chromatography of carbohydrates
 - ◆ Separations based on various modes including adsorption, hydrophilic interaction, hydrophobic interaction, ion exchange, ligand exchange, size exclusion, bioaffinity, etc.
 - ◆ Derivatization
 - ◆ Preparative liquid chromatography
 - ◆ High-performance liquid chromatography–mass spectrometry
- Electrophoresis of carbohydrates
 - ◆ Gel electrophoresis
 - ◆ Capillary zone electrophoresis
 - ◆ Micellar electrokinetic capillary chromatography
 - ◆ Ultrasensitive detection
 - ◆ Derivatization
 - ◆ Capillary electrophoresis–mass spectrometry
- Chromatography and electrophoresis in glycobiology
 - ◆ Release of carbohydrates from glycoconjugates
 - ◆ Monosaccharide composition analysis
 - ◆ Oligosaccharide mapping
 - ◆ Oligosaccharide sequencing
 - ◆ Automated analysis of carbohydrates

Potential authors of reviews should contact Roger Giese, Editor, prior to any submission.
Address: Mugar Building Rm 122, Northeastern University, Boston, MA 02115, USA;
tel.: (+1-617) 373-3227; fax: (+1-617) 373-8720.

The deadline for receipt of submissions is **November 15, 1994**. Manuscripts submitted after this date can still be published in the Journal, but then there is no guarantee that an accepted article will appear in this special, thematic issue. Four copies of the manuscript, citing this issue, should be submitted to the Editorial Office, *Journal of Chromatography A*, P.O. Box 681, NL-1000 AR Amsterdam, The Netherlands. All manuscripts will be reviewed and acceptance will be based on the usual criteria for publishing in the *Journal of Chromatography A*.

Send your article on floppy disk!

All articles may now be submitted on computer disk, with the eventual aim of reducing production times and improving the reliability of proofs still further. Please follow the guidelines below.



With revision, your disk plus one final, printed and exactly matching version (as a printout) should be submitted together to the editor. It is important that the file on disk to be processed and the printout are identical. Both will then be forwarded by the editor to Elsevier.



The accepted article will be regarded as final and the files will be processed as such. Proofs are for checking typesetting/editing: only printer's errors may be corrected. No changes in, or additions to the edited manuscript will be accepted.



Illustrations should be provided in the usual manner and, if possible, on a separate floppy disk as well.



Please follow the general instructions on style/arrangement and, in particular, the reference style of this journal as given in the "Guide for Authors".



The preferred storage medium is a 5¼ or 3½ inch disk in MS-DOS or Macintosh format, although other systems are also welcome.



Please label the disk with your name, the software & hardware used and the name of the file to be processed.

For further information on the preparation of compuscripts please contact:

Elsevier Science B.V.
Journal of Chromatography A
P.O. Box 330
1000 AH Amsterdam, The Netherlands
Phone: (+31-20) 5862 793 Fax: (+31-20) 5862459



ELSEVIER
SCIENCE

Fundamentals of Adsorption

Proceedings of the Fourth International Conference, Kyoto, Japan, 17–22 May 1992

Edited by **M. Suzuki**

Studies in Surface Science and Catalysis Volume 80

Fundamentals of Adsorption contains 2 plenary lectures and 96 selected papers from the IVth International Conference, Kyoto, May, 1992. The topics cover a wide range of studies from fundamentals to applications: characterization of porous adsorbents, molecular simulation, adsorption isotherms, diffusion in adsorbents, breakthrough detection, chromatography, pressure swing operation, etc. Model studies on adsorption, surface characterization, microporosimetry, molecular simulations of equilibrium and diffusion, computer simulation of adsorption beds, and many theoretical studies are also included. Special attention is given to: bulk gas separation and purification, solvent recovery, bioproduct separation, environmental pollution control, methane storage, adsorption cooling and resources recovery.

Contents: Plenary Lecture: Novel applications of adsorption technology (S. Sircar). **Plenary Lecture:** Roles of capillary condensation in adsorption (M. Okazaki). Simulated counter-current chromatographic bioreactor-separators (P.E. Barker *et al.*). Diffusion in zeolite adsorbents: measurement, modelling and structure-performance relation (G.V. Baron *et al.*). Computer simulation studies of the adsorption of Kr in a pore of triangular cross-section (M.J. Bojan, W.A. Steele). Evaluation of adsorbents for volatile organic chemicals (P.C. Chiang *et al.*). Molecular simulation of adsorption and diffusion in VPI-5 and other aluminophosphates (R.F. Cracknell, K.E. Gubbins). Adsorption and desorption dynamics of hydrocarbons, SO₂ and CO₂ onto activated carbon: rate mechanisms (D.D. Do *et al.*). PSA for air purification: experiments and modeling (D.K. Friday *et al.*). Sorption of ethene and propane and their binary mixtures in zeolites (J.A. Hampson, L.V.C. Rees). A new method for investigation of sorption kinetics of volatile

multi-component mixtures on porous solids (J. Hille *et al.*). Hydrogen sulfide removal with pressure swing adsorption from process off-gas (J. Izumi *et al.*). Dynamic behavior in the diffusion of adsorbed molecules in the micropore of zeolites as investigated by molecular dynamics and computer graphics (M. Kubo *et al.*). Competitive adsorption of polymer chains at fractal surfaces (N. Kurata *et al.*). Chromatographic study of liquid phase adsorption of p-tert-octylphenol on octadecylsilyl-silica gel (K. Miyabe, M. Suzuki). Thermodynamic and kinetics data of sorption in zeolites determined by FTIR (W. Nießen *et al.*). Adsorption of water vapour on activated alumina (D.M. Ruthven *et al.*).



**ELSEVIER
SCIENCE**

Prediction of high pressure multicomponent adsorption equilibria (W. Sievers, A. Mersmann). An overview of adsorptive storage of natural gas (O. Talu). Author Index. Keyword Index.

© 1993 818 pages Hardbound
Price: Dfl. 575.00 (US\$ 328.50)

ISBN 0-444-98658-8

Co-edition with and distributed in
Japan by Kodansha Scientific Ltd.

ORDER INFORMATION

ELSEVIER SCIENCE B.V.

P.O. Box 330
1000 AH Amsterdam
The Netherlands
Fax: (+31-20) 5862 845

For USA and Canada
P.O. Box 945
Madison Square Station
New York, NY 10159-0945
Fax: (212) 633 3680

US\$ prices are valid only for the USA & Canada and are subject to exchange rate fluctuations; in all other countries the Dutch guilder price (Dfl.) is definitive. Customers in the European Union should add the appropriate VAT rate applicable in their country to the price(s). Books are sent postfree if prepaid.

PUBLICATION SCHEDULE FOR THE 1994 SUBSCRIPTION

Journal of Chromatography A and *Journal of Chromatography B: Biomedical Applications*

MONTH	1993	J-M	J	J	A	
Journal of Chromatography A	652-657	658-669	670/1 + 2 671/1 + 2 672/1 + 2	673/1 673/2 674/1 + 2 675/1 + 2 676/1	676/2 677/1 677/2 678/1	The publication schedule for further issues will be published later.
Bibliography Section		681/1	681/2			
Journal of Chromatography B: Biomedical Applications		652-655	656/1 656/2	657/1 657/2	658/1 658/2	

INFORMATION FOR AUTHORS

(Detailed *Instructions to Authors* were published in *J. Chromatogr. A*, Vol. 657, pp. 463-469. A free reprint can be obtained by application to the publisher, Elsevier Science B.V., P.O. Box 330, 1000 AH Amsterdam, Netherlands.)

Types of Contributions. The following types of papers are published: Regular research papers (full-length papers), Review articles, Short Communications and Discussions. Short Communications are usually descriptions of short investigations, or they can report minor technical improvements of previously published procedures; they reflect the same quality of research as full-length papers, but should preferably not exceed five printed pages. Discussions (one or two pages) should explain, amplify, correct or otherwise comment substantively upon an article recently published in the journal. For Review articles, see inside front cover under Submission of Papers.

Submission. Every paper must be accompanied by a letter from the senior author, stating that he/she is submitting the paper for publication in the *Journal of Chromatography A* or *B*.

Manuscripts. Manuscripts should be typed in **double spacing** on consecutively numbered pages of uniform size. The manuscript should be preceded by a sheet of manuscript paper carrying the title of the paper and the name and full postal address of the person to whom the proofs are to be sent. As a rule, papers should be divided into sections, headed by a caption (e.g., Abstract, Introduction, Experimental, Results, Discussion, etc.). All illustrations, photographs, tables, etc., should be on separate sheets.

Abstract. All articles should have an abstract of 50-100 words which clearly and briefly indicates what is new, different and significant. No references should be given.

Introduction. Every paper must have a concise introduction mentioning what has been done before on the topic described, and stating clearly what is new in the paper now submitted.

Experimental conditions should preferably be given on a *separate* sheet, headed "Conditions". These conditions will, if appropriate, be printed in a block, directly following the heading "Experimental".

Illustrations. The figures should be submitted in a form suitable for reproduction, drawn in Indian ink on drawing or tracing paper. Each illustration should have a caption, all the *captions* being typed (with double spacing) together on a *separate sheet*. If structures are given in the text, the original drawings should be provided. Coloured illustrations are reproduced at the author's expense, the cost being determined by the number of pages and by the number of colours needed. The written permission of the author and publisher must be obtained for the use of any figure already published. Its source must be indicated in the legend.

References. References should be numbered in the order in which they are cited in the text, and listed in numerical sequence on a separate sheet at the end of the article. Please check a recent issue for the layout of the reference list. Abbreviations for the titles of journals should follow the system used by *Chemical Abstracts*. Articles not yet published should be given as "in press" (journal should be specified), "submitted for publication" (journal should be specified), "in preparation" or "personal communication".

Vols. 1-651 of the *Journal of Chromatography*; *Journal of Chromatography, Biomedical Applications* and *Journal of Chromatography, Symposium Volumes* should be cited as *J. Chromatogr.* From Vol. 652 on, *Journal of Chromatography A* (incl. Symposium Volumes) should be cited as *J. Chromatogr. A* and *Journal of Chromatography B: Biomedical Applications* as *J. Chromatogr. B*.

Dispatch. Before sending the manuscript to the Editor please check that the envelope contains four copies of the paper complete with references, captions and figures. One of the sets of figures must be the originals suitable for direct reproduction. Please also ensure that permission to publish has been obtained from your institute.

Proofs. One set of proofs will be sent to the author to be carefully checked for printer's errors. Corrections must be restricted to instances in which the proof is at variance with the manuscript.

Reprints. Fifty reprints will be supplied free of charge. Additional reprints can be ordered by the authors. An order form containing price quotations will be sent to the authors together with the proofs of their article.

Advertisements. The Editors of the journal accept no responsibility for the contents of the advertisements. Advertisement rates are available on request. Advertising orders and enquiries can be sent to the Advertising Manager, Elsevier Science B.V., Advertising Department, P.O. Box 211, 1000 AE Amsterdam, Netherlands; courier shipments to: Van de Sande Bakhuyzenstraat 4, 1061 AG Amsterdam, Netherlands; Tel. (+31-20) 515 3220/515 3222, Telefax (+31-20) 6833 041, Telex 16479 els vi nl. UK: T.G. Scott & Son Ltd., Tim Blake, Portland House, 21 Narborough Road, Cosby, Leics. LE9 5TA, UK; Tel. (+44-533) 753 333, Telefax (+44-533) 750 522. USA and Canada: Weston Media Associates, Daniel S. Lipner, P.O. Box 1110, Greens Farms, CT 06436-1110, USA; Tel. (+1-203) 261 2500, Telefax (+1-203) 261 0101.

Capillary Electrophoresis

Principles, Practice and Applications

by S.F.Y. LI, National University of Singapore, Singapore

Journal of Chromatography Library Volume 52

Capillary Electrophoresis (CE) has had a very significant impact on the field of analytical chemistry in recent years as the technique is capable of very high resolution separations, requiring only small amounts of samples and reagents. Furthermore, it can be readily adapted to automatic sample handling and real time data processing. Many new methodologies based on CE have been reported. Rapid, reproducible separations of extremely small amounts of chemicals and biochemicals, including peptides, proteins, nucleotides, DNA, enantiomers, carbohydrates, vitamins, inorganic ions, pharmaceuticals and environmental pollutants have been demonstrated. A wide range of applications have been developed in greatly diverse fields, such as chemical, biotechnological, environmental and pharmaceutical analysis.

This book covers all aspects of CE, from the principles and technical aspects to the most important applications. It is intended to meet the growing need for a thorough and balanced treatment of CE. The book will serve as a comprehensive reference work and can also be used as a textbook for advanced undergraduate and graduate courses. Both the experienced analyst and the newcomer will find the text useful.

Contents:

1. Introduction. Historical Background. Overview of High Performance CE. Principles of Separations. Comparison with Other Separation Techniques.
2. Sample Injection Methods. Introduction. Electrokinetic

Injection. Hydrodynamic Injection. Electric Sample Splitter Split Flow. Syringe Injection System. Rotary Type Injector. Freeze Plug Injection. Sampling Device with Feeder. Microinjectors. Optical Gating. **3. Detection Techniques.** Introduction. UV-Visible Absorbance Detectors. Photodiode Array Detectors. Fluorescence Detectors. Laser-based Thermooptical and Refractive Index Detectors. Indirect Detection. Conductivity Detection. Electrochemical Detection. Mass Spectrometric Detection. **4. Column Technology.** Uncoated Capillary Columns. Coated Columns. Gel-filled Columns. Packed Columns. Combining Packed and Open-Tubular Column. **5. Electrophoretic Media.** Electrophoretic Buffer Systems. Micellar Electrokinetic Capillary Chromatography Inclusion Pseudophases. Metal-complexing Pseudophases. Other Types of Electrophoretic Media. **6. Special Systems and Methods.** Buffer Programming. Fraction Collection. Hyphenated Techniques. Field Effect Electroosmosis. Systematic Optimization of Separation. **7. Applications of CE.** Biomolecules. Pharmaceutical and Clinical Analysis. Inorganic Ions. Hydrocarbons. Foods and Drinks. Environmental Pollutants. Carbohydrates. Toxins. Polymers

and Particles. Natural Products. Fuel. Metal Chelates. Industrial Waste Water. Explosives. Miscellaneous Applications. **8. Recent Advances and Prospect for Growth.** Recent Reviews in CE. Advances in Injection Techniques. Novel Detection Techniques. Advances in Column Technology. Progress on Electrolyte Systems. New Systems and Methods. Additional Applications Based on CE. Future Trends.

References. Index.

1992 608 pages Hardbound US\$ 225.75 / Dfl. 395.00

ISBN 0-444-89433-0

1993 608 pages Paperback Price: US\$ 114.25 / Dfl. 200.00
ISBN 0-444-81590-2

"Everything seems to be there, every detection system you have ever dreamed of, any capillary coating, enough electrolyte systems to saturate your wits, and more..."

"...by far the most thorough and comprehensive book in the field yet to appear."

P.G. Righetti, Milan

ORDER INFORMATION

For USA and Canada
ELSEVIER SCIENCE INC.

P.O. Box 945
Madison Square Station
New York, NY 10160-0757
Fax: (212) 633 3880

In all other countries
ELSEVIER SCIENCE B.V.

P.O. Box 330
1000 AH Amsterdam
The Netherlands
Fax: (+31-20) 5862 845

US\$ prices are valid only for the USA & Canada and are subject to exchange rate fluctuations; in all other countries the Dutch guilder price (Dfl.) is definitive. Customers in the European Community should add the appropriate VAT rate applicable in their country to the price(s). Books are sent postfree if prepaid.



**ELSEVIER
SCIENCE B.V.**



0021-9673(19940812)677:1;1-M

0 0 0 2537